MECHANISMS OF BACTERIA – MEDIATED LIPID DROPLET FORMATION IN MACROPHAGES

Thesis submitted for the degree of

Doctor of Philosophy

at the University of Leicester

by

Giovanna Nicolaou BSc, MSc

Department of Cardiovascular Sciences

University of Leicester

July 2013

STATEMENT OF ORIGINAL AUTHORSHIP

I certify that the work presented here is entirely my own and that the use of material from other sources have been properly and fully acknowledged in the text.

I am aware of the University's definition of plagiarism and I understand the consequences if proven that I have committed plagiarism.

ABSTRACT

Mechanisms of bacteria-mediated lipid droplet formation in macrophages -

Giovanna Nicolaou

Atherosclerosis is a chronic inflammatory disease of the arteries that represents the root cause of the majority of heart attacks and strokes. The accumulation of lipid droplets (LDs) in macrophages and their subsequent transformation into foam cells is one of the key steps in the development of atherosclerotic lesions. It has been traditionally thought that this process is largely dependent on the accumulation of oxidised low-density lipoprotein (OxLDL) via uptake by macrophage scavenger receptors. However, as DNA signatures from a wide array of bacterial species have been identified in human atherosclerotic lesions, this project aimed to investigate whether and by which mechanisms these organisms may modulate macrophage foam cell formation, with a particular emphasis on the potential roles played by Toll-like receptor (TLR) signalling.

The present findings establish that exposure of murine or human macrophages to diverse heat-killed atheroma-associated bacteria, or stimulants of any TLR, leads to the accumulation of cholesterol ester and foam cell formation. This process is dependent on TLR signalling, particularly TLR2 and TLR4, but independent of lipoprotein oxidation or scavenger receptor uptake, and although it is dose-dependently potentiated by LDL, it can also occur in the absence of LDL supplementation. TLR-dependent lipid accumulation is not due to enhanced pinocytosis or LDL receptor-dependent LDL uptake. Instead, the results indicate both reduced cholesterol efflux to HDL and increased *de novo* lipid synthesis, via TLR-dependent modulation of key proteins of the two pathways, the ABCA1/G1 cholesterol efflux proteins, and 3-hydroxy-3-methylglutatyl CoA reductase (HMGCR), respectively.

Taken together, the results point towards a novel mechanism of foam cell formation that begins in circulating monocytes exposed to bacteria or their products before they are recruited to developing lesions. Novel therapies for the prevention of atherosclerosis could be developed to target the mechanisms of crosstalk between the TLR and lipid regulatory pathways identified by the current project.

ACKNOWLEDGEMENTS

First and foremost, I would like to thank my supervisor Dr. Clett Erridge for his precious help and advice in and out of the laboratory, as well as his limitless patience and support throughout the project.

I would also like to thank my co-supervisor Professor Alison H. Goodall for her help and support.

Special thanks to Ms. Tina James, Dr. Hassan Hamali, and Mr. Mohammed Alsahli for their help and advice on flow cytometry, Mr. Jasbir Moore for his help with western blot analysis, Dr. Veryan Codd and Dr. Andrea Koekemoer for their valuable help with the cholesterol efflux studies, as well as the use of radiolabelled reagents, Dr. Natalie Garton from the Department of Infection, Immunity, and Inflammation for the demonstration and advice on thin layer chromatography, and Dr. Tasos C. Christofides from the Department of Mathematics and Statistics (University of Cyprus) for his valuable advice on data analysis. Many thanks to those participating in the high-fat meal study, and to everyone who donated blood for experimental use, as well as to the phlebotomists for their valuable help in the collection of blood.

A big thank you to my lovely friend and colleague Evi for all the support.

Last but not least, many thanks to my parents, my brother, my family, and my friends for their unconditional love and support throughout the whole journey. I wouldn’t be able to get through it without you.

Dedicated to them, and especially to my granddads.

CONTENTS

LIST OF TABLES AND ILLUSTRATIVE MATERIALS

TABLES

FIGURES

Chapter 1 - Introduction

Chapter 2 – Materials and Methods

Chapter 3 - Results

Chapter 5 – Results

Chapter 6 – Results

ABBREVIATIONS

- ABC: ATP-binding cassette
- ACAT: Acyl-Coenzyme A: Cholesterol acyltransferase
- ADRP: Adipocyte differentiation-related protein
- Apo-E: apolipoprotein E
- BHT: butylated hydroxytoluene
- CAMs: cell adhesion molecules
- CD36: cluster of differentiation 36
- CE: cholesterol ester
- CETP: cholesterol ester transfer protein
- CRP: C-reactive protein
- CVD: cardiovascular disease
- DGAT: diglyceride acyltransferase
- DMEM: Dulbecco's Modified Eagle's Medium
- ER: endoplasmic reticulum
- FAs: fatty acids
- FC: free cholesterol
- FCS: foetal calf serum
- GM-CSF: Granulocyte-macrophage-colony stimulating factor
- HDL: High-density lipoprotein
- HL: hepatic lipase
- HMG-CoA: 3-hydroxy-3-methylglutaryl-CoA
- HMGCR: HMG-CoA reductase
- HSL/Lipe: hormone sensitive lipase
- HSP: heat-shock protein
- ICAM-1: intercellular adhesion molecule-1
- IFN-γ: interferon-gamma
- IKK: IκB kinase kinase
- IL-1: interleukin-1
- IL-1R: interleukin-1 receptor
- IRAK: IL-1 receptor-associated kinases
- IRF: Interferon regulatory factor
- LBP: LPS-binding protein
- LCAT: Lecithin: cholesterol acyltransferase
- LD: Lipid droplet
- LDL: Low-density lipoprotein
- LDLR: Low-density lipoprotein receptor
- LOX-1: Lectin-like OxLDL receptor-1
- LPS: lipopolysaccharide
- LRRs: Leucine-rich repeats
- LXRs: Liver-X receptors
- MAPK: Mitogen-activated protein kinase
- MCP-1: monocyte chemoattractant protein-1
- M-CSF: macrophage-colony stimulating factor
- MD-2: myeloid differentiation factor-2
- mmLDL: minimally-modified LDL

- MMPs: matrix metalloproteinases
- MyD88: myeloid differentiation factor 88
- nCEH: neutral cholesterol ester hydrolase
- NF-κB: Nuclear factor kappa-B
- Nox: NADPH oxidase
- OxLDL: oxidised LDL
- OxPAPC: oxidised 1-palmitoyl-2-arachidonyl-sn-glycerol-3-phosphocholine
- PAMPs: Pathogen-associated molecular patterns
- PBS: phosphate buffer saline
- PIA: polyinosinic acid
- PLTP: phospholipid transfer protein
- PMB: polymyxin B
- PPARs: Peroxisome proliferator-activated receptors
- PRRs: Pattern recognition receptors
- RCT: Reverse cholesterol transport
- ROS: Reactive oxygen species
- ScRs: Scavenger receptors
- SMCs: smooth muscle cells
- SR-A: Scavenger receptor-A
- SR-B1: Scavenger receptor class B1
- SREBP: Sterol regulatory element binding protein
- TGs: triglycerides
- TGF-β: transforming growth factor-beta
- TIP-47: Tail-interacting protein of 47 kDa
- TIR: Toll/IL-1R/Resistance
- TIRAP: TIR domain-containing adaptor protein
- TLRs: Toll-like receptors
- TNF-α: tumour necrosis factor-alpha
- TRIF: TIR domain-containing adaptor-inducing interferon beta
- VCAM-1: vascular cell adhesion molecule-1
- VLDL: very low-density lipoprotein

1. INTRODUCTION

Cardiovascular disease (CVD) is a term given to describe a group of diseases affecting the heart and blood vessels, which includes, among others, coronary heart disease, cerebrovascular disease, peripheral arterial disease, cardiomyopathies, as well as congenital heart diseases.

Data from the World Health Organisation (WHO) (http://www.who.int/mediacentre/factsheets/fs317/en/index.html) suggest that an estimated 17.3 million people died from CVDs in 2008, a number that represented around 30% of global deaths. Of these, approximately 7.3 million were caused by coronary heart disease. More than 80% of CVD deaths occur in low to middle-income countries. It is estimated that by 2030, nearly 23.3 million people will die annually from CVD.

Atherosclerosis is the key process underpinning the majority of CVDs. It is considered a chronic, inflammatory disease affecting the large and medium-sized arteries, usually at sites of disturbed blood flow, such as at vessel bifurcations, branches, and curvatures (Tobias and Curtiss 2007; Erridge *et al.* 2008a; Tsompanidi *et al.* 2010). The main characteristics of this pathological process are the deposition of lipids, as well as the infiltration and accumulation of immune cells and extracellular matrix components in the subendothelial space; events that lead to vessel wall thickening and subsequently, the narrowing of the vessel lumen (Libby *et al.* 2002; Tobias and Curtiss 2007; Renko *et al.* 2008; He *et al.* 2009; Ye *et al.* 2009; Xu *et al.* 2010).

Despite advances in the management of coronary risk factors, atherosclerotic cardiovascular disease is the major cause of morbidity and mortality in industrialized countries (Van Eck *et al.* 2005; Okazaki *et al.* 2008; Tabas 2010; Xu *et al.* 2010).

1.1. Plaque biology

Atherosclerotic disease can be divided into three stages: initiation, progression, and complications, and each of these stages has its own distinct events with their own cellular and molecular characteristics (Pasterkamp *et al.* 2004). The lesions themselves are classified as fatty streaks, fibrous plaques and complex lesions (Jialal and Devaraj 1996) (Figure 1.1).

Fatty streaks, considered the "precursors of lesions", begin to develop during the first decade of life and are small, asymptomatic, and therefore, clinically silent (Tabas 2010). The first event in the initiation of a fatty streak is traditionally thought to be the extracellular accumulation of lipids, mainly low-density lipoprotein (LDL), and their retention in the intima layer of the artery, mainly by proteoglycan molecules. Modification of the trapped lipoprotein particles leads to the activation of the endothelium (Libby *et al.* 2002).

The endothelium is a dynamic organ system important in the preservation of the arterial wall integrity and vascular tone (den Dekker *et al.* 2010; Jackson *et al.* 2012). It exhibits both anti-adhesive and anti-coagulant properties, and a healthy endothelium generally resists adhesive interactions with blood cells. In case of tissue injury, however, or after feeding animals an atherogenic diet, the endothelium becomes activated, and begins to express on its surface various cell adhesion molecules (CAMs), which mediate the binding of circulating leukocytes and platelets to its surface (Libby *et al.* 2002; Tall *et al.* 2008; Tsompanidi *et al.* 2010). The adherence of monocytes to the activated endothelium is the first step in the formation of an atherosclerotic lesion, and it is mediated by the interaction between CAMs expressed on both the endothelium and the monocytes (Hodgkinson and Ye 2003; Chinetti *et al.* 2006; Xu *et al.* 2010).

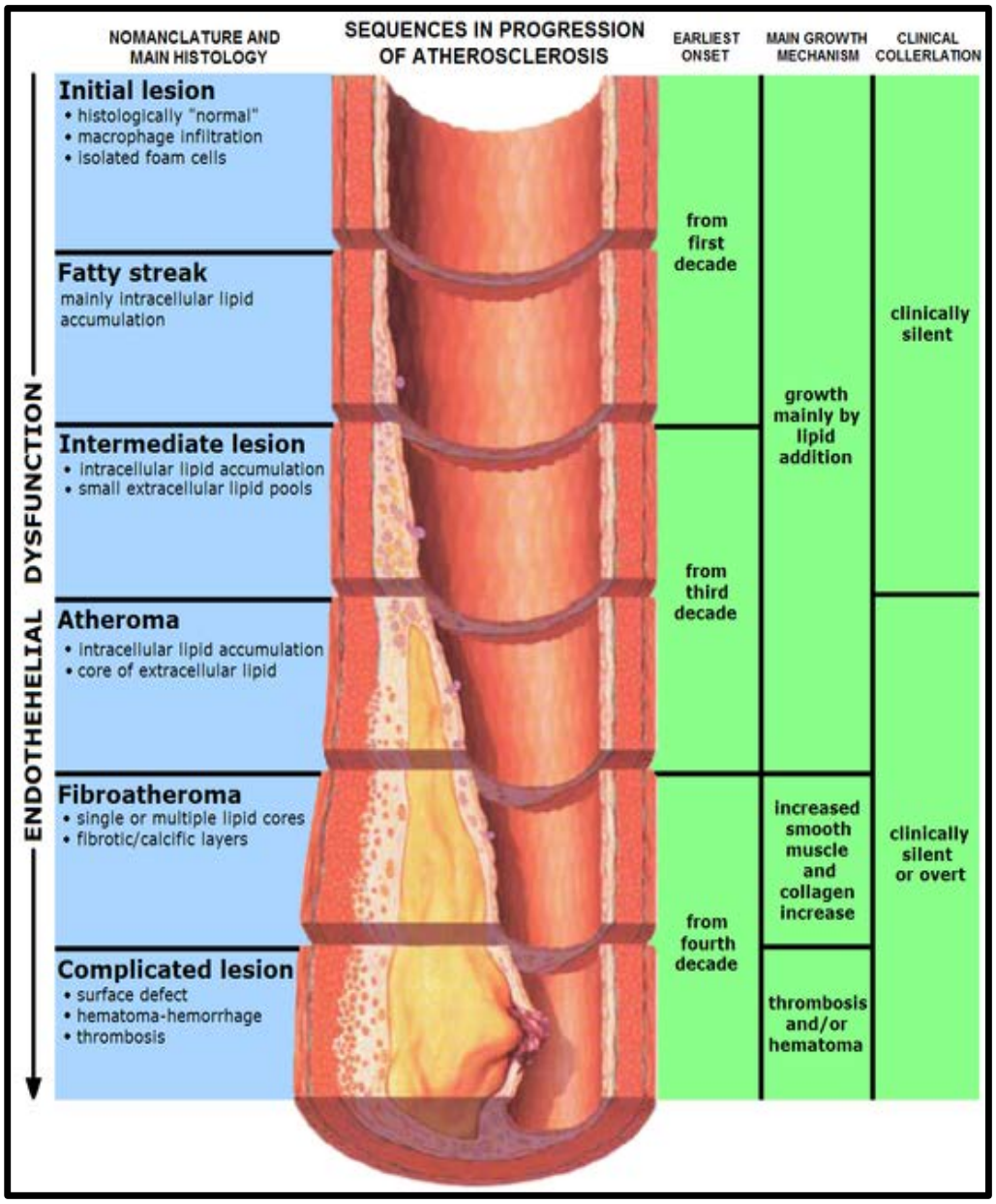

Figure 1.1. Sequences in the progression of atherosclerosis.

One of the first events in the early stages of the disease is the intracellular accumulation of lipids and the formation of a fatty streak. This progresses towards an atheroma in the intermediate stages and a more complex lesion with outward remodelling of the artery in the advanced stages [Taken from: http://en.wikipedia.org/wiki/Atherosclerosis].

Leukocyte extravasation is comprised of four steps: rolling, activation, arrest and adhesion, and trans-endothelial migration of a leukocyte. Rolling is mediated by a group of CAMs of the selectin family. E- and P-selectin molecules on the endothelium interact with mucin-like CAMs expressed on the monocyte membrane (Kindt and Kuby 2007). The process of rolling facilitates the interaction of the monocyte with chemokines present on the endothelial surface. This leads to the activation of the monocytes which begin to express on their surface a set of CAMs known as integrins. Firm attachment of monocytes to the endothelium is mediated by the interaction of integrins with CAMs of the immunoglobulin superfamily, such as vascular cell adhesion molecule-1 (VCAM-1) and intercellular adhesion molecule-1 (ICAM-1) (Libby *et al.* 2002; Burger and Wagner 2003).

The final step is the transmigration of the adherent monocyte into the intima of the artery (Libby *et al.* 2002; Burger and Wagner 2003; Hodgkinson and Ye 2003; Larigauderie *et al.* 2004; Xu *et al.* 2010), a process thought to be mediated by monocyte chemoattractant protein-1 (MCP-1) (Libby *et al.* 2002; Tsompanidi *et al.* 2010). Once inside the vessel wall, exposure to cytokines, chemokines, and growth factors leads to further activation and differentiation of monocytes into macrophages (Libby *et al.* 2002; Hodgkinson and Ye 2003; Serri *et al.* 2004; Larigauderie *et al.* 2004; Tobias and Curtiss 2007; Sorrentino *et al.* 2010; Xu *et al.* 2010). Uptake of modified lipoproteins by monocyte-derived macrophages results in their transformation into foam cells (Libby *et al.* 2002; Hodgkinson and Ye 2003; Tobias and Curtiss 2007; Tall *et al.* 2008; Tsompanidi *et al.* 2010; Sorrentino *et al.* 2010; Xu *et al.* 2010; van Tits *et al.* 2011).

The accumulation of lipid-laden macrophages in the subendothelial space is the main characteristic of a fatty streak (Ball *et al.* 1995; Jialal and Devaraj 1996; Rahaman *et al.* 2006; Rigamonti *et al.* 2008; Xu *et al.* 2010), and at this stage, the lesion is

reversible (Jialal and Devaraj 1996; Tsompanidi *et al.* 2010). Alternatively, it may progress to become a fibrous plaque, a characteristic of advanced lesions (Jialal and Devaraj 1996; Tsompanidi *et al.* 2010).

Mediators secreted by macrophage foam cells, such as cytokines, and chemokines, promote the recruitment of T-lymphocytes into the intima (Libby *et al.* 2002; Hodgkinson and Ye 2003; Castrillo *et al.* 2003; Tsompanidi *et al.* 2010), which along with resident vascular wall cells begin to secrete cytokines and growth factors that stimulate the migration of smooth muscle cells (SMCs) from the underlying media into the intima layer, and their subsequent proliferation (Libby *et al.* 2002; Hodgkinson and Ye 2003; Rigamonti *et al.* 2008; de Souza *et al.* 2008; Tsompanidi *et al.* 2010). SMCs secrete various extra-cellular matrix macromolecules, such as collagen, proteoglycans, elastin fibres etc., which eventually form a structure known as the fibrous cap, which stabilises the plaque (Jialal and Devaraj 1996; Tsompanidi *et al.* 2010; den Dekker *et al.* 2010). An advanced atherosclerotic plaque may remain stable or it may further progress to a more mature, complex phenotype, with complications such as calcification, necrosis, intra-plaque haemorrhage, and thrombosis (Ball *et al.* 1995; Jialal and Devaraj 1996; den Dekker *et al.* 2010).

Sustained activation of leukocytes and SMCs can change the stability of the plaque. Activated T-lymphocytes secrete interferon-gamma (IFN-γ), a cytokine that was shown to inhibit the production of collagen by SMCs (Libby *et al.* 2002). Activated macrophages in the atheroma secrete various proteolytic enzymes, such as matrix metalloproteinases (MMPs), whose activity was shown to modulate the turnover of extracellular matrix in the arterial wall, promoting its degradation (Libby *et al.* 2002; Kruth *et al.* 2002; Chinetti *et al.* 2003; Segers *et al.* 2008; de Souza *et al.* 2008; den Dekker *et al.* 2010). Their expression was shown to be increased in advanced plaques,

and MMP9 was shown to facilitate the migration of SMCs into the intima, and the infiltration of immune cells (Hodgkinson and Ye 2003; Segers *et al.* 2008; de Souza *et al.* 2008).

Increased degradation of extracellular matrix components in combination with reduced collagen synthesis eventually leads to weakening of the fibrous cap, rendering the plaque unstable and vulnerable to rupture (Segers *et al.* 2008; Randolph 2008; de Souza *et al.* 2008; den Dekker *et al.* 2010). The main features of a vulnerable atherosclerotic plaque include a thin fibrous cap (<65 μm), few SMCs, a large number of macrophage foam cells, and the presence of a large lipid-rich necrotic core (Wang *et al.* 1999; Tall *et al.* 2008; Tsompanidi *et al.* 2010; den Dekker *et al.* 2010).

A well-known characteristic of a necrotic core is the presence of an acellular lipid core beneath the fibrous cap, which, as the term indicates, contains mainly lipids and very few cells (Ball *et al.* 1995). It was first proposed that the lipid core was a result of excessive lipid deposition; however, it was later shown that dead macrophage foam cells were the main contributors of the lipid material (Ball *et al.* 1995; Wang *et al.* 1999). Immunohistological analysis of advanced atherosclerotic lesions showed that the lipid core stained positively for the CD68 macrophage marker, proving the implication of macrophages in this process (Ball *et al.* 1995; Kuchibhotla *et al.* 2008). CD68 reactivity was shown to be weaker and in some cases, almost absent towards the centre of the lipid core. No actin-positive SMCs were found at the lipid core (Ball *et al.* 1995). The areas surrounding the lesion were shown to contain variable proportions of macrophage foam cells and SMCs (Ball *et al.* 1995).

Different modes of cell death have been proposed, including apoptosis, autophagy and necrosis (Ball *et al.* 1995; Yuan *et al.* 2010; Le Goff and Dallinga-Thie 2011). It is now clear that the formation of a lipid-rich necrotic core is a result of a combination of

increased cell death, and the failure to remove these dead cells from the plaque (Witztum and Steinberg 1991; Ball *et al.* 1995; Jialal and Devaraj 1996; Tsompanidi *et al.* 2010).

Rupture of the unstable plaque results in the release of the highly thrombogenic necrotic core, which promotes the production of tissue factor from macrophages, the formation of a thrombus and eventually, the occlusion of the artery (Libby *et al.* 2002; Kruth *et al.* 2002; Tobias and Curtiss 2005; Tsompanidi *et al.* 2010; den Dekker *et al.* 2010). Clinical complications associated with artery occlusion include myocardial infarction and stroke (Tobias and Curtiss 2005; Tsompanidi *et al.* 2010).

1.2. Risk factors for atherosclerosis

The common risk factors and characteristics that contribute to CVD were identified in an ambitious health project that began in 1948, known as the Framingham Heart study. This project followed the development of CVD in three generations of participants over a long period of time, and provided useful information on the effects and the contribution of major risk factors in the development of the disease (http://www.framinghamheartstudy.org).

Traditional risk factors for atherosclerosis include: age, gender, LDL, HDL, blood pressure, diabetes, smoking, and genetics (Castrillo *et al.* 2003; Chinetti *et al.* 2006; Tobias and Curtiss 2007; Vikatmaa *et al.* 2009; Tsompanidi *et al.* 2010; Perk *et al.* 2012).

The risk of CVD increases with increasing age, and it is more common in men. Dyslipidaemia, characterised by abnormal levels of lipids in the blood, is the major "classical" risk factor contributing to atherosclerotic disease (Björkbacka *et al.* 2004; Tobias and Curtiss 2007; Persson *et al.* 2008; Tsompanidi *et al.* 2010; Perk *et al.* 2012). Elevated HDL-cholesterol levels have been inversely associated with the risk of CVD; however, recent studies showed that people with genetically high levels of HDL are not at less risk of developing CVD (Voight *et al.* 2012).

A common outcome between these risk factors is the initiation of intimal inflammatory responses and the progression of the atherosclerotic process (Libby *et al.* 2002; Björkbacka *et al.* 2004; Dasu *et al.* 2008).

1.3. Evidence that inflammation drives atherosclerosis

The recognition of exogenous or modified endogenous molecules triggers the activation of the immune system and the subsequent initiation of the inflammatory cascade. Mutual activation of innate and adaptive immunity is a prerequisite for optimal clearance of pathogens (Segers *et al.* 2008).

Each arm of the immune system is served by a specific group of cells. Monocytes, macrophages, dendritic cells (DCs), and granulocytes are the main types of cells involved in innate immunity. T-lymphocytes and B-lymphocytes are the main types of cells comprising the adaptive arm of the immune system (Segers *et al.* 2008). Monocyte-derived macrophages and T-lymphocytes are the two cell types most commonly associated with the pathogenesis of atherosclerosis (Segers *et al.* 2008; Paul *et al.* 2008; Kleemann *et al.* 2008; Lu and Daugherty 2009; Kadl *et al.* 2011). Cytokines such as interleukin-1 (IL-1), IL-6, IL-8, tumour necrosis factor-alpha (TNF-α), and IFN-γ secreted by both macrophages and T-lymphocytes are considered to be pro-inflammatory, and therefore, atherogenic (Segers *et al.* 2008; Kleemann *et al.* 2008) (Figure 1.2).

Increasing evidence suggests that inflammation characterises every stage of the atherosclerotic disease. Several human association studies have documented the association of atherosclerosis risk with the presence of inflammatory markers in the plasma. Elevated plasma levels of C-reactive protein (CRP), IL-1, IL-6, IL-8, have been associated with elevated risk of CVD in apparently healthy individuals, independently of traditional risk factors (Berk *et al.* 1990; Greaves and Channon 2002; Boekholdt *et al.* 2004; Brånén *et al.* 2004; Rocha and Libby 2009).

The presence of inflammatory markers and their receptors was demonstrated in atheromata, and their expression was shown to be up-regulated in human atherosclerotic

lesions (Erridge 2008; Persson *et al.* 2008; Kleemann *et al.* 2008). Of interest, inhibition or genetic deletion of almost any pro-inflammatory gene leads to a great reduction in atherosclerotic lesions in both murine models of atherosclerosis, the Apo-E$^{-/-}$ and LDLr$^{-/-}$ mice (Boekholdt *et al.* 2004; Erridge 2008; Segers *et al.* 2008; Cignarella 2011).

IL-1 is produced mainly by macrophages and dendritic cells, and exists in two forms, IL-1α and IL-1β, both of which have similar, but not overlapping functions. They signal through the IL-1 receptor (IL-1R), and induce the production of cytokines and chemokines, as well as the expression of cell adhesion molecules on endothelial cells. IL-1 also contributes to vascular injury by stimulating the release of matrix-degrading enzymes, such as MMPs (Kleemann *et al.* 2008; Cignarella 2011). Genetic deficiency of IL-1β in atherosclerosis-prone Apo-E$^{-/-}$ mice led to reduction in atherosclerosis, and the progression of the disease was reduced in Apo-E$^{-/-}$ mice lacking a functional IL-1R, even under conditions known to aggravate the disease (Chi *et al.* 2004; Kleemann *et al.* 2008; Cignarella 2011).

TNF-α is a pro-inflammatory cytokine predominantly expressed by monocytes and macrophages, which is also considered an inflammatory marker, as elevated plasma levels have been associated with CVD events (Zhou *et al.* 2008; Kleemann *et al.* 2008; de Souza *et al.* 2008). TNF-α deletion in Apo-E$^{-/-}$ mice resulted in reduced atherosclerosis, even after the administration of a high fat diet (Brånén *et al.* 2004).

Similarly to IL-1 and TNF-α, genetic deletion of MCP-1 or IFN-γ or their receptors in atherosclerosis-prone mice was shown to decrease lesion formation and its composition, with plaques consisting of fewer macrophages and higher degrees of collagen and fibrosis (Boring *et al.* 1998; Greaves and Channon 2002; Boekholdt *et al.* 2004; Rocha and Libby 2009).

Apart from cytokines, CAMs have also been associated with early atherosclerosis development. Studies using VCAM-1 or ICAM-1 knock-out mice crossed with Apo-$E^{-/-}$ or $LDLr^{-/-}$ mice showed decreased atherosclerosis development (Davies and Gordon 1993; Collins *et al.* 2000; Dansky *et al.* 2001; Greaves and Channon 2002). Similarly, Apo-$E^{-/-}$ mice deficient in P- or E-selectin were shown to have significantly smaller lesions than Apo-$E^{-/-}$ mice expressing these CAMs (Collins *et al.* 2000; Dansky *et al.* 2001; Burger and Wagner 2003). Studies showed the existence of a positive association between plasma concentrations of soluble CAMs and atherosclerosis, suggesting that they could be used as possible serum markers for pre-clinical atherosclerosis (Rohde *et al.* 1998; Collins *et al.* 2000).

The balance between pro- and anti-inflammatory cytokines is an important factor determining lesion development and progression (Jackson *et al.* 2012). It has been suggested that enhancement of anti-inflammatory responses might offer therapeutic opportunities for atherosclerosis by promoting the resolution of inflammation. Both macrophages and T-lymphocytes are capable of producing anti-inflammatory cytokines, such as IL-4, IL-10, IL-13, and transforming growth factor-beta (TGF-β), all of which are considered atheroprotective (Rocha and Libby 2009).

Inflammation is initiated via activation of a series of Pattern Recognition Receptors (PRRs) (Page *et al.* 2009). One of the major family of PRRs is the Toll-Like Receptor (TLR) family, which detects both tissue damage and invading microorganisms (Tobias and Curtiss 2007; Segers *et al.* 2008; Page *et al.* 2009).

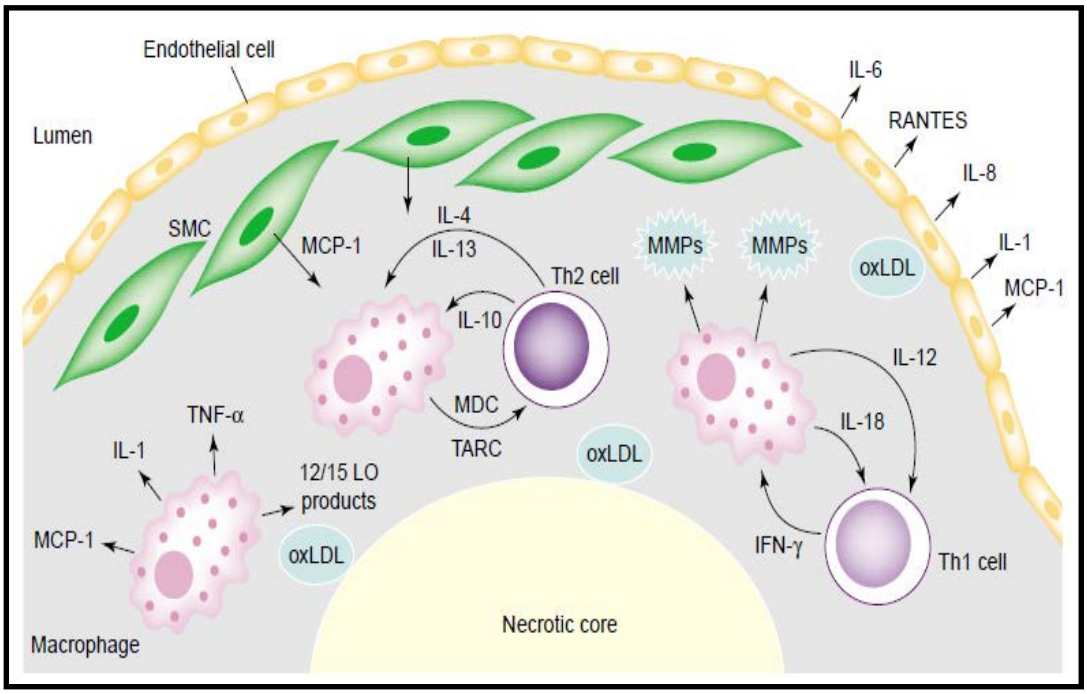

Figure 1.2. Inflammatory signals during the process of atherogenesis

The interactions between inflammatory cells and various arterial wall components mediate the production of pro-inflammatory mediators and the progression of an atherosclerotic plaque to a more complex phenotype. Abbreviations: interleukin (IL), interferon-gamma (IFN-γ), monocyte chemoattractant protein-1 (MCP-1), matrix metalloproteinases (MMPs), oxidised LDL (OxLDL), Type 1 and Type 2 helper T cells, respectively (Th1 / Th2 cell), tumour necrosis factor-alpha (TNF-α).

[Taken from: Greaves and Channon (2002) Inflammation and Immune responses in atherosclerosis. *Trends in Immunology*, 23(**11**):535-541].

1.4. Toll-like Receptors

The Toll protein is a receptor found on the cell surface of *Drosophila melanogaster*, which is required for the establishment of the dorso-ventral axis as well as the immune response of the fruit fly (Adachi *et al.* 1998; Takeuchi *et al.* 1999; Tobias and Curtiss 2007; den Dekker *et al.* 2010). In 1996, Jules Hoffmann and Bruno Lemaitre observed that flies carrying mutations in the Toll gene were highly susceptible to a lethal infection caused by a fungus, *Aspergillus fumigatus*, to which wild type flies were immune (Adachi *et al.* 1998; Takeuchi *et al.* 2000; Tobias and Curtiss 2007; Kumagai *et al.* 2008; Hoshino *et al.* 2010; den Dekker *et al.* 2010).

The first evidence for the existence of a mammalian homologue of the *Drosophila* Toll protein was obtained in 1994 (Tobias and Curtiss 2007). Demonstration of a functional role of this mammalian homologue came in 1997, when Ruslan Medzhitov and Charles Janeway showed that a chimeric protein composed of the intracellular domain of the human Toll homologue and the extracellular domain of mouse CD4 was able to activate the expression of immune response genes when transfected into a human cell line (Medzhitov *et al.* 1997; Tobias and Curtiss 2007). Subsequently, a whole family of mammalian Toll-like receptors (TLRs) was identified (Tobias and Curtiss 2007; Kumagai *et al.* 2008). This constituted the first evidence that fruit flies and humans share a conserved immune response pathway (Hoshino *et al.* 2010).

TLRs belong to the family of germ line-encoded PRRs, responsible for the recognition of microbe-related molecules, also known as Pathogen-Associated Molecular Patterns (PAMPs) (Takeuchi *et al.* 2001; Saitoh *et al.* 2004; Patole *et al.* 2006; Tobias and Curtiss 2007; Takashima *et al.* 2009; Stewart *et al.* 2010; Sorrentino *et al.* 2010). PAMPs represent highly conserved, non-self molecules derived from bacteria, viruses, or yeast, and their recognition by PRRs triggers the activation of the

immune system (Castrillo *et al.* 2003; Erridge 2008; Lee *et al.* 2008; Almeida *et al.* 2009; Lin *et al.* 2010). Their expression has been demonstrated in many different types of cells, including macrophages, dendritic cells, endothelial cells and SMCs (Lorenz *et al.* 2002; Lee *et al.* 2008; Lin *et al.* 2010; Feingold *et al.* 2010; den Dekker *et al.* 2010).

Ten functional human TLRs have been identified so far, each recognising a specific spectrum of PAMPs (Lorenz *et al.* 2002; Pålsson-McDermott and O'Neill 2004; Schoneveld *et al.* 2005; Kazemi *et al.* 2005; Tobias and Curtiss 2007; Erridge 2009; Page *et al.* 2009; Gu *et al.* 2010). TLRs recognising extracellular ligands – TLR1, 2, 4, 5, 6 – are found on the cell surface, whereas, TLR 3, 7, 8 and 9, that recognise phagocytosed or intracellular ligands, are found in intracellular compartments, such as endosomes or lysosomes (Patole *et al.* 2006; Tobias and Curtiss 2007; Page *et al.* 2009; den Dekker *et al.* 2010). The ligand recognition domain of intracellular TLRs is found on the inside of the endosomal compartment, while their signal transduction domain is located in the cytoplasm (Kumagai *et al.* 2008).

1.4.1. TLR ligands

TLRs exert their activity by forming dimers, either homodimers or heterodimers. The ligand specificity of the receptors depends on the dimer formed (Pasterkamp *et al.* 2004). TLR2 can dimerise with two other members of the TLR family – TLR1 and TLR6 (Erridge 2008). The TLR1/TLR2 heterodimer recognises triacylated lipoproteins, as well as cell wall components from Gram-positive bacteria, such as lipoteichoic acid (LTA) (Takeuchi *et al.* 2000; Ihendyane *et al.* 2004; Tobias and Curtiss 2007; Tanigawa *et al.* 2008; Erridge 2009). The dimerisation of TLR2 with TLR6 allows the recognition of bacterial diacylated lipoproteins (Tobias and Curtiss 2007; Erridge 2009). TLR3 is responsible for the recognition of viral double-stranded RNA (dsRNA). The TLR4 homodimer recognises lipopolysaccharide (LPS) from Gram-negative bacteria.

Bacterial flagellin is the only ligand of TLR5. TLRs 7 and 8 recognise viral single-stranded RNA (ssRNA), and TLR9 detects viral or bacterial unmethylated CpG-containing DNA (Takeuchi *et al.* 2001; Lorenz *et al.* 2002; Castrillo *et al.* 2003; Patole *et al.* 2006; Kawamoto *et al.* 2008; Kumagai *et al.* 2008; Takashima *et al.* 2009). The molecular specificity of TLR10 is still under investigation, although its structural similarity to TLR1 and TLR6 suggests possible dimerisation with TLR2, and lipopeptides as a possible ligand (Beutler *et al.* 2006; Erridge *et al.* 2008a).

1.4.2. Structural features of TLRs

All TLRs share a common structure related to the lectin group of proteins. These receptors are single membrane-spanning proteins with ectodomains mainly composed of leucine-rich repeats (LRRs), and an intracellular Toll/IL-1R/Resistance (TIR) domain, named after the similarity between the cytoplasmic domain of TLR and the similar region of the IL-1 receptor (Takeuchi *et al.* 2000; Pacheco *et al.* 2002; Pålsson-McDermott and O'Neill 2004; Beutler *et al.* 2006; Tobias and Curtiss 2007; Kumagai *et al.* 2008; Stewart *et al.* 2010; den Dekker *et al.* 2010). Human TLRs have around 18-27 LRRs. X-ray crystallography revealed that these repeats form a sickle-shaped extracellular domain (Beutler *et al.* 2006). The dimeric TLR protein consists of two horseshoe-shaped subunits situated side by side, interacting with each other. Part of the extracellular domain makes up the ligand-binding region of TLRs (Beutler *et al.* 2006; Dasu *et al.* 2009).

The LRRs are followed by a sequence forming a single trans-membrane helix, and then by a cytoplasmic domain comprising the TIR domain. This domain is responsible for the recruitment of adaptor proteins that initiate the TLR signal transduction pathways through protein-protein interactions (Tobias and Curtiss 2007; Kawamoto *et al.* 2008). TIR domains have a compact, globular structure and they consist of three

regions which are highly conserved among the TIR family called boxes 1, 2 and 3 (den Dekker *et al.* 2010). These regions serve as binding sites for the adaptor proteins that participate in the signalling pathway (Dasu *et al.* 2009). No interaction between adjacent TIR domains from dimeric TLR has been reported (Beutler *et al.* 2006).

1.4.3. TLR signal transduction pathways

Signal transduction pathways of TLRs lead to the initiation of an inflammatory or anti-viral response (Björkbacka *et al.* 2004). The pattern of the TLR that will be activated upon stimulation depends on the identity of the pathogen encountered. Each activated TLR controls the production of a particular set of pro-inflammatory molecules (Dalpke *et al.* 2005), although the majority of TLRs share the same signal transduction pathway. This pathway is known as the Nuclear Factor-kappa B (NF-κB) pathway (Schoneveld *et al.* 2005; Lee *et al.* 2008; Page *et al.* 2009; Ye *et al.* 2009) (Figure 1.3).

Binding of the ligand to the receptor complex leads to dimerisation and activation of the receptor (Dasu *et al.* 2008; Kawamoto *et al.* 2008). Dimerisation results in conformational changes in the cytoplasmic TIR domains of the dimer, a step required for the recruitment of adaptor proteins and the initiation of the signal cascade (Kawamoto *et al.* 2008).

Protein-protein interactions are mediated by modular homophilic domains present in TLRs and are essential for linking the receptor to the downstream signalling molecules (Tobias and Curtiss 2007; De Nardo *et al.* 2009; Takashima *et al.* 2009). Typical examples of these TIR domain-containing adaptor proteins are Myeloid Differentiation Factor-88 (MyD88) and TIR domain-containing Adaptor Protein (TIRAP), also known as Mal, which act as a complex (Takeuchi *et al.* 2000; Castrillo *et al.* 2003; Takashima *et al.* 2009; Stewart *et al.* 2010). The C-terminal domain of the MyD88 protein binds to TLR via the cytoplasmic TIR domain (Adachi *et al.* 1998; Pålsson-McDermott and

O'Neill 2004). The N-terminal domain is a death-domain (DD) module, which mediates the interaction with other DD-containing proteins (Adachi *et al.* 1998; Pålsson-McDermott and O'Neill 2004; Kumagai *et al.* 2008). Binding of this complex to the TIR domain of the receptor promotes the association of a second complex formed by two protein kinases, the IL-1 Receptor-Associated Kinases (IRAK)-1 and -4 (Pålsson-McDermott and O'Neill 2004; Kawamoto *et al.* 2008; Takashima *et al.* 2009).

IRAK-1 is phosphorylated by its protein kinase partner IRAK-4 (Kumagai *et al.* 2008; De Nardo *et al.* 2009; den Dekker *et al.* 2010). The attached phosphate creates a docking site on IRAK-1 for TNF Receptor-Associated Factor-6 (TRAF-6) (Pålsson-McDermott and O'Neill 2004; Kumagai *et al.* 2008; Page *et al.* 2009). IRAK-1 and TRAF-6 then dissociate from this complex forming an intermediate IRAK-1/TRAF-6 complex which binds to a second complex composed of Transforming growth factor-*β*-Activated Kinase (TAK-1) and TAK-1 binding proteins-1 and -2 (TAB-1/2), resulting in the activation of the TAK-1 kinase activity (Kumagai *et al.* 2008; den Dekker *et al.* 2010).

TAK-1 activation leads to the phosphorylation and activation the I*κ*B Kinase (IKK) complex, also known as the signalosome, through several intermediate steps (Pålsson-McDermott and O'Neill 2004; Kumagai *et al.* 2008; De Nardo *et al.* 2009; den Dekker *et al.* 2010). The IKK*γ* subunit of the complex, the transcription factor NF-*κ*B Essential Modulator (NEMO), modulates the complex's kinase activity (Pålsson-McDermott and O'Neill 2004).

Assembly of the IKK complex is a key step in the activation of the NF-*κ*B pathway (Pålsson-McDermott and O'Neill 2004). NF-*κ*B is a powerful gene regulatory protein. Its activity is inhibited by a second protein, the I*κ*B*α*, which is an unphosphorylated cytoplasmic protein. NF-*κ*B bound to the unphosphorylated I*κ*B*α* is kept in the

cytoplasm (den Dekker *et al.* 2010). Phosphorylation of the I*κ*B*α* protein by the IKK complex leads to the ubiquitination and degradation of the former, and to the release of active NF-*κ*B, which translocates from the cytoplasm to the nucleus (Pålsson-McDermott and O'Neill 2004; Dasu *et al.* 2009; den Dekker *et al.* 2010). There, it initiates the transcription of genes that promote innate and inflammatory responses, like TNF-*α*, IL-1, IL-6 (Takeuchi *et al.* 2000; Schoneveld *et al.* 2005; Kumagai *et al.* 2008; Erridge *et al.* 2008a; Chávez-Sánchez *et al.* 2010).

1.4.3.1. TRIF-dependent TLR signalling

Evidence suggests the existence of an alternative signalling pathway for the activation of NF-*κ*B, also known as MyD88-independent pathway, used only by TLR3 and TLR4 (Dasu *et al.* 2009). This pathway is responsible for the delayed activation of NF-*κ*B, as well as the activation of a different set of transcription factors known as Interferon Regulatory Factors (IRF)-3 and -7 (Castrillo *et al.* 2003; Pålsson-McDermott and O'Neill 2004; Kawamoto *et al.* 2008; den Dekker *et al.* 2010) (Figure 1.3).

The adaptor proteins participating in this pathway are TRAM/TIR-containing Adaptor Molecule-2 (TICAM2) and TRIF, also known as TICAM1 (Pålsson-McDermott and O'Neill 2004; Dalpke *et al.* 2005; Erridge 2008; Takashima *et al.* 2009). TRAM is only used in the TLR4 signalling pathway and has a similar role to TIRAP/Mal, acting as a bridge between TLR and TRIF (Pålsson-McDermott and O'Neill 2004; Kawamoto *et al.* 2008; Takashima *et al.* 2009). The latter can interact with TRAF6 protein via several TRAF-binding domains found on the N-terminal of the protein, eventually leading to the activation of NF-*κ*B, IRF-3 and IRF-7 (Pålsson-McDermott and O'Neill 2004; Kawamoto *et al.* 2008; Wiesner *et al.* 2010).

TRIF is also used by TLR3 in a pathway involving different protein kinase complexes (Chen *et al.* 2009). TRIF was shown to bind to a complex composed of IKK*ε*

and TANK-binding kinase-1 (TBK-1) (Pålsson-McDermott and O'Neill 2004). The complex phosphorylates and activates IRF-3 and IRF-7, which migrate to the nucleus and initiate the transcription of type I interferon genes (Castrillo *et al.* 2003; Pålsson-McDermott and O'Neill 2004; Page *et al.* 2009; Sorrentino *et al.* 2010).

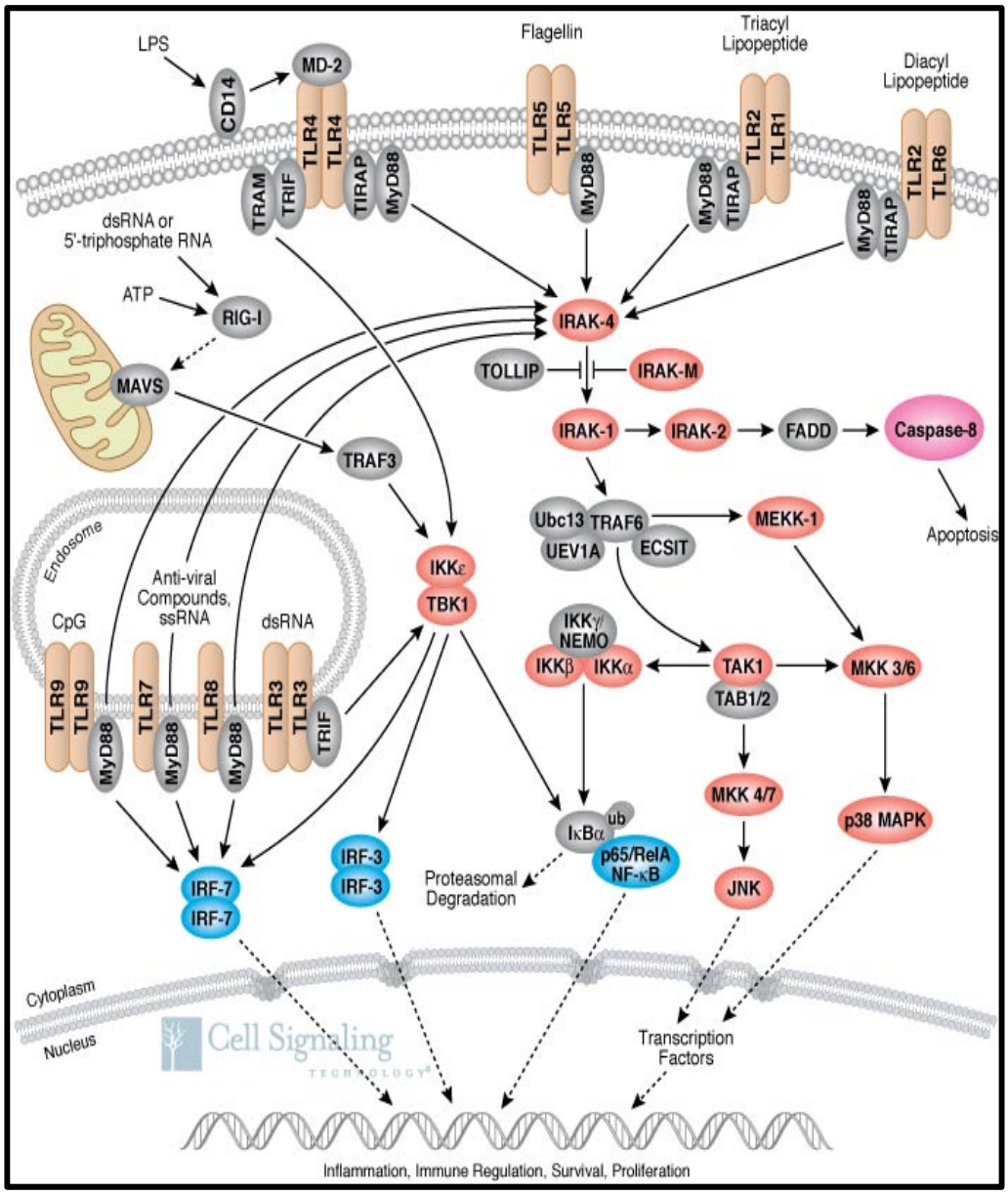

Figure 1.3. TLR signalling pathway

Binding of the ligand to the extracellular domain of the receptor induces dimerisation of the receptor and the recruitment of adaptor proteins in the cytoplasm. Interaction of these proteins with the cytoplasmic domain of these receptors leads to the activation of downstream kinases, which induce the activation of the transcription factor NF-*κ*B and its translocation into the nucleus, where it initiates the transcription of genes involved in innate and inflammatory responses. Abbreviations: cluster of differentiation 14 (CD14), inhibitor of kappa light polypeptide gene enhancer in B-cells inhibitor, alpha (I*κ*B*α*),

inhibitory-binding protein κB kinase (IKK), IL-1 receptor-associated kinase (IRAK), interferon regulatory factor (IRF), c-Jun N-terminal kinase (JNK), lipopolysaccharide (LPS), myeloid differentiation factor-2 (MD-2), myeloid differentiation factor-88 (MyD88), NF-κB essential modulator (NEMO), Nuclear factor-κB (NF-κB), TAK-binding protein (TAB), Transforming growth factor-β-activated kinase (TAK), TANK-binding kinase (TBK), Toll/Interleukin 1 receptor (TIR) domain containing adaptor protein (TIRAP), Toll-like receptor (TLR), TNF receptor-associated factor-6 (TRAF6), TRIF-related adaptor molecule (TRAM), TIR-containing adaptor molecule (TRIF). [Taken from: http://www.cellsignal.com].

1.4.4. Toll-like receptor 4 (TLR4)

TLR4, originally named human Toll (hToll), was the first TLR receptor to be characterised in humans (Pålsson-McDermott and O'Neill 2004). TLR4 is well known as the "LPS receptor" as studies regarding its function showed that, stimulation of the receptor with LPS led to the up-regulation of inflammatory mediators through the activation of the NF-κB signalling pathway (Lorenz *et al.* 2002). Its importance in the biological response to LPS was also demonstrated by both gene targeting and positional cloning studies (Takeuchi *et al.* 1999).

The first evidence demonstrating that TLR4 activation was linked to LPS came from the identification of a remarkable phenotype in mice by Poltorak *et al.* (1998) and Qureshi *et al.* (1999) (Takeuchi *et al.* 1999). Mice of the C3H/HeJ strain were found to be hyporesponsive to LPS, even at lethal doses (Takeuchi *et al.* 2000; Pålsson-McDermott and O'Neill 2004). This phenotype was found to result from a single point mutation occurring in a residue present in the BB loop of the cytoplasmic TIR domain of the receptor (Pålsson-McDermott and O'Neill 2004). This mutation causes the

substitution of the amino acid histidine for proline at position 712 (P712H), and it inhibits the signal transduction cascade (Beutler *et al.* 2006; Hoshino *et al.* 2010).

Furthermore, mice of the strains C57Bl/10ScCr and C57Bl/10ScN, having a null mutation on the *Tlr4* gene, were shown to be non-responsive to LPS (Pålsson-McDermott and O'Neill 2004). The single gene locus where these mutations were found was named *Lps* (Takeuchi *et al.* 1999; Beutler *et al.* 2006; Hoshino *et al.* 2010). This locus is mapped on chromosome 4 in mice; in the human genome the corresponding region is on chromosome 9q32-33 (Hoshino *et al.* 2010).

NF-κB reporter assays showed that TLR4 displays greater constitutive activity compared to the other members of the TLR family (Kawamoto *et al.* 2008). Activation of the signalling pathway is strictly dependent on dimerisation of the receptor, which was shown to be mediated by LPS binding (Saitoh *et al.* 2004; Dasu *et al.* 2008; Kawamoto *et al.* 2008).

The first component of the LPS receptor complex to be identified was a specific member of the innate immune system called CD14, which was shown to have a high affinity for LPS (Lohmann *et al.* 2007). It exists in two forms – soluble (sCD14), which can be found in the plasma; and membrane-bound (mCD14), which is anchored to the cell membrane via a glycosyl-phosphatidylinositol tail and lacks a trans-membrane domain (Lynn and Golenbock 1992; Kutuzova *et al.* 2001; Pålsson-McDermott and O'Neill 2004; Lohmann *et al.* 2007). It was initially thought that CD14 was the functional LPS receptor. However, after the discovery of TLR4, studies focusing on the role of CD14 in the TLR4 signalling pathway showed that this protein is not able to transduce a signal across the membrane (Kutuzova *et al.* 2001), and it mainly participates in the binding of LPS and its subsequent presentation to the MD-2/TLR4 complex (Saitoh *et al.* 2004; Pålsson-McDermott and O'Neill 2004; Kawamoto *et al.*

2008; Erridge *et al.* 2008b). Later studies using CD14-knockout mice showed that this molecule is not required for TLR4 signalling (Pålsson-McDermott and O'Neill 2004).

Myeloid Differentiation factor-2 (MD-2) is a secreted glycoprotein that binds to the TLR4 ectodomain and acts as an adaptor protein in the activation of the receptor by LPS (Kutuzova *et al.* 2001; Saitoh *et al.* 2004; Pålsson-McDermott and O'Neill 2004; Lohmann *et al.* 2007; Tobias and Curtiss 2007; Kawamoto *et al.* 2008). This protein is of great importance for LPS response, as studies in mice showed that mutations in the MD-2 protein completely prevented LPS signalling and TLR4 dimerisation, and that responsiveness to LPS was restored in cells expressing TLR4 but lacking MD-2 by wild type MD-2, suggesting a role in mediating ligand recognition and the subsequent dimer formation (Saitoh *et al.* 2004; Pålsson-McDermott and O'Neill 2004).

The interaction between LPS and CD14 occurs via a plasma shuttle-protein known as LPS-Binding Protein (LBP) (Kawamoto *et al.* 2008). This acute phase protein is produced in the liver and it is found in the circulation, where it binds LPS with high affinity (Lynn and Golenbock 1992; Pålsson-McDermott and O'Neill 2004; Vikatmaa *et al.* 2009). LBP can transfer LPS to plasma lipoproteins in a process intended to lower LPS toxicity threshold and to prevent inflammatory responses by activated cells (Parker *et al.* 1995; Vreugdenhil *et al.* 2001). Binding of LPS to LBP is followed by the formation of an LPS/LBP/CD14 complex, which enables the transfer of LPS to the TLR4/MD-2 complex for activation (Lynn and Golenbock 1992; Takeuchi *et al.* 1999; Saitoh *et al.* 2004; Pålsson-McDermott and O'Neill 2004).

1.4.4.1. LPS

LPS, also known as endotoxin, is the major constituent of the outer membrane of Gram-negative bacteria (Parker *et al.* 1995; Rose *et al.* 1995; Takeuchi *et al.* 2000; Saitoh *et al.* 2004; Pålsson-McDermott and O'Neill 2004; Almeida *et al.* 2009).

Exposure of bacteria to the blood leads to the release of LPS from the bacterial surface as membrane fragments or blebs, alone or in complex with bacterial phospholipids and proteins (Parker *et al.* 1995; Pålsson-McDermott and O'Neill 2004; Vikatmaa *et al.* 2009). Activation of cells by LPS via TLR4 stimulation triggers the production of pro-inflammatory mediators such as IL-1, IL-6 and TNF-*α*, chemokines, (Takeuchi *et al.* 1999; Kutuzova *et al.* 2001; Pacheco *et al.* 2002; Pålsson-McDermott and O'Neill 2004) as well as the expression of CAMs on both endothelial cells and monocytes (Loppnow *et al.* 1990; Lynn and Golenbock 1992; Funk *et al.* 1993; Vreugdenhil *et al.* 2001; Baranova *et al.* 2002; Kollipara and Perumal 2010).

The structure of LPS was shown to be crucial for the induction of LPS responses by activated cells (Pålsson-McDermott and O'Neill 2004). LPS consists of lipid A, which anchors it to the bacterial membrane, a covalently attached core polysaccharide and frequently, an extensive O-polysaccharide chain composed of repeating saccharide units (Lynn and Golenbock 1992; Baranova *et al.* 2002; Saitoh *et al.* 2004; Hoshino *et al.* 2010; Le Brun *et al.* 2013) (Figure 1.4). The toxic effects of LPS have been attributed to its lipid A moiety (Flegel *et al.* 1993; Rose *et al.* 1995; Lee *et al.* 2001; Saitoh *et al.* 2004; Lohmann *et al.* 2007). Changes in the number of fatty acids (FAs) composing the lipid A portion, as well as their position, their chain lengths and phosphate content were shown to be associated with the loss of toxicity of the lipid A moiety (Loppnow *et al.* 1990; Lee *et al.* 2001; Baranova *et al.* 2002).

Neutralisation of LPS can be achieved by its sequestration by plasma lipoproteins; chylomicrons, VLDL, LDL and HDL are able to bind LPS in the circulation (Parker *et al.* 1995; Vreugdenhil *et al.* 2001; Vikatmaa *et al.* 2009). Binding to lipoproteins prolongs LPS's half-life in the bloodstream, as unbound LPS is rapidly removed from the circulation (Flegel *et al.* 1993; Parker *et al.* 1995). The interactions between LPS

and the lipoproteins are, however, of low affinity, and they depend on the concentration of LPS in the plasma; it has to be low enough so that the concentration of the unbound LPS is below the threshold that could trigger cell activation (Flegel *et al.* 1993).

Among the plasma lipoproteins, LDL and VLDL have been shown to be the most effective in inducing LPS inactivation (Flegel *et al.* 1993; Vreugdenhil *et al.* 2001). LBP was shown to be bound to Apo-B-containing lipoproteins in the circulation (Vreugdenhil *et al.* 2001). The interaction between the LPS/LBP complex and the lipoprotein is thought to occur via a specific binding site present on Apo-B (Vreugdenhil *et al.* 2001). Both LBP and Apo-B were shown to compete for LPS, which they bind with high affinity (Flegel *et al.* 1993; Vreugdenhil *et al.* 2001).

It is proposed that LPS binds to the lipoproteins in the same way that it is bound to the bacterial membrane – the fatty acyl chains of the lipid A domain are inserted in the monolayer of phospholipids that surrounds the lipoprotein particle (Parker *et al.* 1995). In this way, the immunostimulatory activity of LPS is reduced, and interactions between LPS and its receptors are prevented (Flegel *et al.* 1993; Parker *et al.* 1995; Vreugdenhil *et al.* 2001).

Analysis of the expression pattern of the genes induced during LPS stimulation showed that the majority of the genes that were up-regulated were associated with inflammation (IL-1β, TNF), signal transduction pathways (IL-1, NF-κB) and immunity (Wong *et al.* 2008).

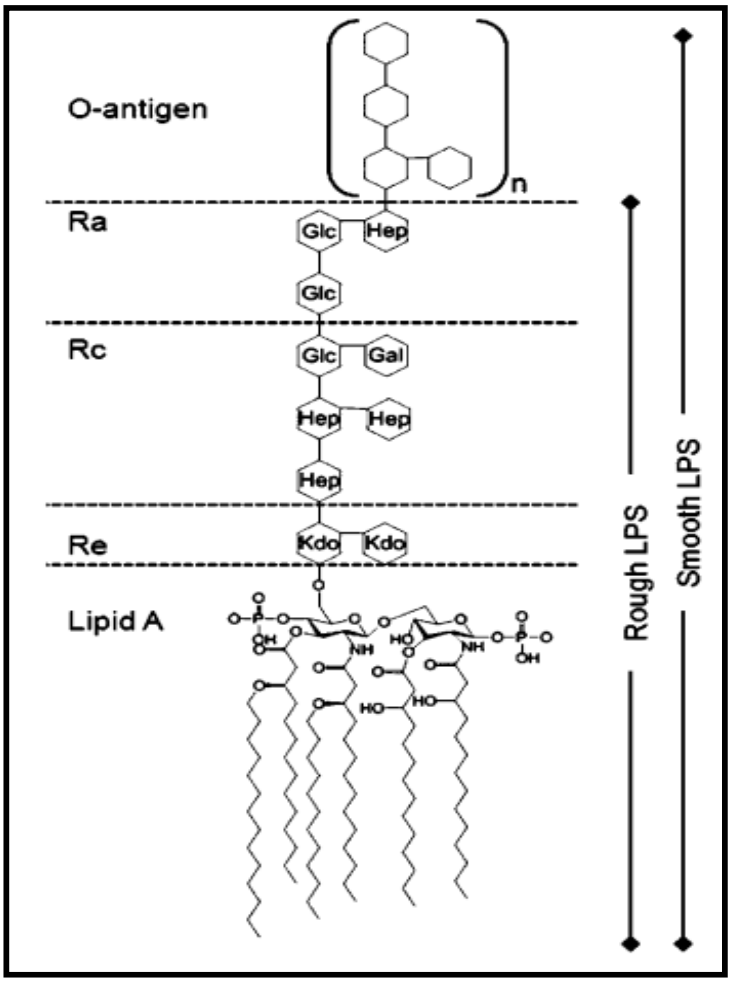

Figure 1.4. Structure of *E. coli* LPS.

Schematic representation of the LPS component of the Gram-negative bacterium *Escherichia coli*. LPS is usually composed of a lipid A portion which is covalently attached to a core polysaccharide. Smooth LPS has an additional O-polysaccharide chain, or O-antigen, attached to the core polysaccharide. Abbreviations: galactose (Gal) glucose (Glc), L-glycero-D-manno heptose (Hep), 2-keto-3-deoxyoctonoic acid (Kdo). [Taken from: Le Brun *et al.* (2013) Structural characterization of a model Gram-negative bacterial surface using lipopolysaccharides from rough strains of *Escherichia coli*. *Biomacromolecules*, 14(**6**):2014–2022].

1.4.5. TLRs and atherosclerosis

There is now much evidence to support a key role for TLR signalling in the mechanisms connecting inflammation, infection, and atherosclerosis (Cao *et al.* 2007; Erridge *et al.* 2008a; Sorrentino *et al.* 2010; Gu *et al.* 2010). Macrophages were shown to express all of the TLRs and to be responsive to all the TLR ligands under normal conditions (Erridge 2009). TLR1, 2, 4, and 5 were shown to have the highest expression levels (Schoneveld *et al.* 2005; Cao *et al.* 2007; Lee *et al.* 2008; Lundberg and Hansson 2010) and bacterial PAMPs that might directly stimulate these receptors, such as bacterial lipopeptides, LPS, or flagellin have been detected in atheromata (Schoneveld *et al.* 2005; Erridge 2009).

Among TLRs, TLR2 and TLR4 are the most studied receptors in the context of initiation and progression of atherosclerosis in both human and animal models (Dasu *et al.* 2008; Lin *et al.* 2010; Sorrentino *et al.* 2010; Gu *et al.* 2010). The development of atherosclerotic lesions was impaired in both TLR2/LDLr and TLR2/Apo-E double knockout mice (Tobias and Curtiss 2007; Schoneveld *et al.* 2008; Dasu *et al.* 2009). Deficiency of TLR2 led to a decrease in lipid accumulation (Lin *et al.* 2010) and lesion size (Cao *et al.* 2007; Choi *et al.* 2009), as well as in the expression of MMPs during plaque formation (Schoneveld *et al.* 2005; Monaco *et al.* 2009).

One of the first indications regarding the role of TLR4 in atherosclerosis came from the work of Michelsen *et al.* (2004) where it was shown that TLR4/Apo-E double knockout mice developed less atherosclerosis compared to Apo-$E^{-/-}$ control mice (Michelsen *et al.* 2004b; Schoneveld *et al.* 2008; Kawamoto *et al.* 2008; Choi *et al.* 2009; den Dekker *et al.* 2010; Sorrentino *et al.* 2010). Complete absence of TLR4 in these mice was shown to be associated with a decrease in lesion size, lipid content and macrophage infiltration (Tobias and Curtiss 2007; Lee *et al.* 2008; Lee *et al.* 2009).

Other components of the pathway have also been shown to play a role in atherogenesis. Reduced chemokine expression and subsequent reduction of macrophage activation and recruitment, and lesion formation was observed in Apo-$E^{-/-}$ mice, after deletion of the adaptor protein MyD88, suggesting a role of this protein in the normal recruitment of monocytes to inflamed atherosclerotic sites (Björkbacka *et al.* 2004; Tobias and Curtiss 2007; Schoneveld *et al.* 2008; Stewart *et al.* 2010; Sorrentino *et al.* 2010). CD14 deficiency did not seem to have any effect in disease development (Tobias and Curtiss 2007).

Enhanced expression of activated NF-κB and its target genes, which include chemokines, CAMs, and cytokines, was detected by immunohistochemical or immunofluorescent techniques in atherosclerotic lesions but not in a healthy artery (Baranova *et al.* 2002), and was found to co-localise with cells expressing TLRs (Edfeldt *et al.* 2002).

Stimulation of TLR2 by a selective ligand (Pam_3CSK_4) was shown to be pro-atherogenic, as it increased vascular intimal hyperplasia, and atherosclerotic plaque formation in both Apo-$E^{-/-}$ and $LDLr^{-/-}$ mice (Schoneveld *et al.* 2005; Cao *et al.* 2007; Tobias and Curtiss 2007; Monaco *et al.* 2009; Sorrentino *et al.* 2010). Activation of TLR2 in adventitial fibroblasts was shown to increase the expression of pro-inflammatory mediators, such as IL-1α, IL-1β, IL-6, IL-8, and MCP-1, agents known to influence leukocyte activation, proliferation and migration (Schoneveld *et al.* 2005; Tobias and Curtiss 2007; Chávez-Sánchez *et al.* 2010).

Similar to TLR2, activation of TLR4 by LPS mediates the expression of pro-inflammatory cytokines and chemokines implicated in the initiation of the inflammatory response, as well as several molecules involved in atherogenesis, such as VCAM-1, ICAM-1 and MCP-1 (Sorrentino *et al.* 2010). TLR4 activation has also been associated

with increased intimal lesion formation (Castrillo *et al.* 2003; Sorrentino *et al.* 2010), arterial outward remodelling (Schoneveld *et al.* 2005; Tobias and Curtiss 2007), as well as plaque destabilisation (den Dekker *et al.* 2010). LPS-mediated TLR4 activation was shown to induce the production of proteolytic enzymes, specifically MMP-9, predisposing the plaque to rupture (den Dekker *et al.* 2010), an observation further supported by evidence showing that TLR4 is expressed at sites of plaque rupture in patients with acute MI (Lin *et al.* 2010).

Increased expression of TLR2 and TLR4 has been detected on the major cell types of an atherosclerotic lesion, such as endothelial cells, macrophages and vascular SMCs (Castrillo *et al.* 2003; den Dekker *et al.* 2010; Chávez-Sánchez *et al.* 2010). In Apo-$E^{-/-}$ mice, the mRNA levels of these two receptors were shown to be up-regulated in advanced atherosclerotic lesions (Dasu *et al.* 2009; Lin *et al.* 2010). TLR2 expression was shown to be up-regulated in $LDLr^{-/-}$ mice, after administration of a high fat diet, and it was more pronounced on endothelial cells at sites exposed to disturbed blood flow (Tobias and Curtiss 2007; Lin *et al.* 2010).

Patients with CVD or acute coronary syndrome (ACS) were shown to have increased levels of TLR2 and TLR4 on circulating monocytes compared to controls (Ashida *et al.* 2005; Methe *et al.* 2005; Schoneveld *et al.* 2008; Choi *et al.* 2009; Kuwahata *et al.* 2010). Also, the risk of CVD was shown to be increased in patients with chronic infections or current or ex-smokers, who are characterised by elevated levels of plasma endotoxin (Wiedermann *et al.* 1999; Pussinen *et al.* 2007).

Many studies have been conducted in order to investigate the role of one of the most common TLR4 polymorphisms, Asp299Gly, in atherosclerosis. Kiechl *et al.* (2002) reported that this polymorphism was associated with decreased carotid artery atherosclerosis (Kazemi *et al.* 2005; Tobias and Curtiss 2007; Feingold *et al.* 2010) and

reduced intima media thickness (Schoneveld *et al.* 2005), as well as greater cardiovascular protection in carriers compared to non-carriers (Castrillo *et al.* 2003; den Dekker *et al.* 2010). The single point mutation in the *Tlr4* region on chromosome 9 impairs receptor signalling (Feingold *et al.* 2010), and individuals carrying the Asp299Gly allele were shown to be hyporesponsive to LPS (den Dekker *et al.* 2010) and to have lower levels of circulating pro-inflammatory mediators in response to this PAMP (Kiechl *et al.* 2001). Other case-control studies also confirmed these results. Several larger population studies however, yielded conflicting results, as the presence of the polymorphism could not be related to predisposition or evolution of the atheroma (Yang *et al.* 2003; den Dekker *et al.* 2010).

1.4.6. Endogenous TLR ligands

It has been proposed that TLR activation in atherosclerotic lesions could be induced by the presence of endogenous TLR ligands (Lin *et al.* 2010). At least twenty endogenous TLR ligands have been proposed in the past ten years, mostly for TLR2 and/or TLR4. Among the suggested ligands are heat-shock proteins (HSPs), hyaluronic acid fragments, fibronectin extracellular domain A (EDA), as well as saturated fatty acids, minimally modified LDL (mmLDL), and oxidised phospholipids (Tobias and Curtiss 2005; Schoneveld *et al.* 2008; Takashima *et al.* 2009).

The expression of these molecules was shown to be up-regulated in atherosclerotic lesions of atherosclerosis-prone mice (Tobias and Curtiss 2005; den Dekker *et al.* 2010). Data from early reports suggested that HSPs could contribute to atherosclerosis development via TLR4 (den Dekker *et al.* 2010). Fibronectin-EDA was shown to activate TLR4 in primary cells *in vitro*, and deletion of either TLR2 or TLR4 or fibronectin-EDA was shown to decrease atherosclerosis in Apo-$E^{-/-}$ mice (Schoneveld *et al.* 2008; den Dekker *et al.* 2010; Chávez-Sánchez *et al.* 2010).

Modified and/or oxidised lipoproteins and their products have also been considered endogenous TLR ligands, with the ability to initiate a sustained PRR-mediated inflammatory response (Schoneveld *et al.* 2008; Choi *et al.* 2009). Oxidised LDL (OxLDL) was shown to induce the expression of TLR4 in cultured human monocyte-derived macrophages (Xu *et al.* 2001). However, the role of oxidised lipids as endogenous ligands remains controversial as Erridge *et al.* (2009) showed that neither oxysterols, nor oxidised phospholipids or OxLDL activate TLRs in different human cell systems.

There is now evidence suggesting that the majority of currently proposed endogenous TLR ligands are not really TLR ligands, as it was shown that they did not induce the "classical" TLR signalling markers, such as NF-κB or p38 MAPK activation, or their transcription products, when used in their pure, clean form (Tobias and Curtiss 2005). Their stimulatory capacity observed in studies was related to the use of recombinant proteins which were shown to be contaminated with bacterial TLR2 or TLR4 ligands (Tobias and Curtiss 2005; Erridge 2010).

It is not clear what the stimuli responsible for triggering TLR signalling in atherosclerosis may be, and little is known about the effects that TLR signalling may have on macrophage lipid regulation.

1.5. Monocyte and macrophage biology

The mononuclear phagocytic system consists of monocytes, which circulate in the blood, and macrophages, found in tissues (Ricardo *et al.* 2008). Monocyte development starts in the bone marrow. A hematopoietic stem cell (HSC) is differentiated into a myeloid progenitor cell, known as the granulocyte/macrophage colony-forming unit (GM-CFU), which can be further differentiated into a granulocyte colony-forming unit (G-CFU) or a macrophage colony-forming unit (M-CFU) (Ma *et al.* 2003; Gordon and Taylor 2005). Monocytes derive from M-CFU, and precursors include monoblasts, and pro-monocytes (Ma *et al.* 2003; Gordon and Taylor 2005). The process is driven by colony-stimulating factors, such as GM-CSF and M-CSF, and leads to the generation of around 5 x 10^9 monocytes daily. Monocytes are released into the bloodstream, where they circulate for several days before settling into tissues. Mature monocytes found in the circulation represent ~ 5-10% of the peripheral blood leukocytes, and they are morphologically heterogeneous, with varied sizes and nuclear morphology, as well as different degrees of granularity (Gordon and Taylor 2005; Brochériou *et al.* 2011).

In 1939, Ebert and Florey reported that circulating monocytes were able to migrate from the blood into tissues, where they would differentiate into macrophages (Gordon and Taylor 2005). The specific phenotype acquired by these differentiated macrophages depends on the microenvironment they are in, i.e. alveolar macrophages are found in the lungs, Kupffer cells in the liver, osteoclasts in the bone (Ma *et al.* 2003; Gordon and Taylor 2005; Ricardo *et al.* 2008; Brochériou *et al.* 2011). Resident tissue macrophages can proliferate thus contributing to the maintenance of the tissue macrophage populations (Ma *et al.* 2003; Gordon and Taylor 2005).

1.5.1. Monocyte heterogeneity in humans and mice

The identification of monocytes was initially based on the presence of the antigenic marker CD14. Identification of an additional marker, CD16, allowed the division of monocytes into two subsets: the "classical" monocyte expressing $CD14^{hi}CD16^{-}$, and the $CD14^{+}CD16^{+}$ subset of cells, which also expressed CD32 and major histocompatibility complex (MHC) class II molecules. These cells display many similarities with resident tissue macrophages. Further characterisation of the two subtypes was based on the expression of specific chemokine receptors: classical monocytes expressed the CC-chemokine receptor 2 (CCR2), whereas the $CD14^{+}CD16^{+}$ subset expressed CCR5. A common characteristic of the two subsets was their ability to differentiate into DCs when cultured with IL-4 and GM-CSF. When used in an *in vitro* trans-endothelial migration model, monocytes were shown to be able to migrate across the endothelium and to differentiate into macrophages, which remained in the sub-endothelial matrix. Alternatively, monocytes differentiated into DCs with the ability to migrate back across the endothelium. Of the two subsets, $CD14^{hi}CD16^{-}$ cells were less likely to differentiate into DCs than was the $CD14^{+}CD16^{+}$ subset, suggesting that the $CD14^{+}CD16^{+}$ subset, under the right conditions, might act as a precursor of DCs (Gordon and Taylor 2005). The presence of CD64 led to the identification of an additional subset of monocytes which seemed to have characteristics of both monocytes and DCs, as shown by the expression of both CD68 and HLA-DR molecules ($CD14^{+}CD16^{+}CD64^{-}$ and $CD14^{+}CD16^{+}CD64^{+}$) (Gordon and Taylor 2005).

Similarly to humans, mouse monocytes, first identified by the presence of $F4/80^{+}$ $CD11b^{+}$, were subdivided into two groups according to the expression of CCR2, CD62L, and the CX_3C-chemokine receptor 1 (CX_3CR1). Based on the expression levels of these markers, the two subsets were defined as $CCR2^{+}CD62L^{+}CX_3CR1^{low}$ or $CCR2^{-}CD62L^{-}$

CX_3CR1^{hi}. The first subset is known as the "inflammatory" subset because of the involvement of the expressed receptors in chemokine binding and leukocyte recruitment at sites of inflammation (Gordon and Taylor 2005). Later, Ly6C was identified by Geissmann *et al.* (2003) as an additional marker for the "inflammatory" monocyte subset. Studies examining the development and function of these subsets suggested that circulating monocytes, with the $CCR2^{+}CD62L^{+}CX_3CR1^{low}$ phenotype, can modify their phenotypic and functional characteristics in the absence of an inflammatory stimulus (Geissmann *et al.* 2003; Gordon and Taylor 2005). The new intermediate phenotype is defined as $CCR2^{+}CCR7^{+}CCR8^{+}Ly6C^{mid}$. Both subsets are responsive to inflammatory stimuli, and can migrate to tissues, where they differentiate into macrophages and DCs. Alternatively, in the absence of inflammation, the "intermediate" monocytes can alter their phenotype into "resident" monocytes, with the $CCR2^{-}CD62L^{-}CX_3CR1^{hi}Ly6C^{-}$ phenotype, which can replenish the macrophage and DC pools, once in the tissues (Gordon and Taylor 2005; Ricardo *et al.* 2008).

A comparison of the mouse monocyte subsets with the monocyte subsets found in humans indicated that the $CCR2^{+}CD62L^{+}CX_3CR1^{low}Ly6C^{+}$ subset corresponded to the "classical" human monocyte subset $CD14^{hi}CD16^{-}$, which was also shown to be $CCR2^{+}CX_3CR1^{low}$. The second murine subset, $CCR2^{-}CD62L^{-}CX_3CR1^{hi}Ly6C^{-}$, corresponded to the $CD14^{+}CD16^{+}CD64^{-}$ human subset, which also expressed CX_3CR1. This suggested for the first time that mice could be used as an *in vivo* system to study human monocyte heterogeneity (Geissmann *et al.* 2003; Gordon and Taylor 2005).

1.5.2. Macrophages

Macrophages serve the innate arm of the immune system, which is considered the first line of defence against pathogens (Pacheco *et al.* 2002; Ma *et al.* 2003; Kazemi *et*

al. 2005; Lin *et al.* 2010; Kollipara and Perumal 2010). This heterogeneous cell population plays a critical role in maintaining tissue homeostasis and remodelling, as well as in regulating immune responses (Gordon and Taylor 2005; Ricardo *et al.* 2008; Rigamonti *et al.* 2008; de Souza *et al.* 2008; De Nardo *et al.* 2009; van Tits *et al.* 2011).

The phenotype and function of macrophages are determined by the microenvironment of the tissue in which they reside (Gordon and Taylor 2005; Ricardo *et al.* 2008; Kadl *et al.* 2011). Macrophages exhibit both pro- and anti-inflammatory properties mediating the initiation as well as the resolution of an inflammatory response, and their activation state depends on the inflammatory stimuli they encounter (Funk *et al.* 1993; Ricardo *et al.* 2008; Rigamonti *et al.* 2008; Kadl *et al.* 2011). Recognition of invading pathogens is achieved through specific receptors expressed either on the cell surface or intracellularly, such as PRRs, and scavenger receptors (ScRs) (Pacheco *et al.* 2002; Ma *et al.* 2003; Gordon and Taylor 2005; Kollipara and Perumal 2010; Feng *et al.* 2010). Clearance of dead cells via phagocytosis triggers the initiation of intracellular cascades and the induction of anti-inflammatory mediators, as well as the activation of the adaptive immunity, events that eventually result in resolution of acute inflammatory responses and the restoration of homeostasis (Funk *et al.* 1993; Pacheco *et al.* 2002; Ma *et al.* 2003; Rigamonti *et al.* 2008; De Nardo *et al.* 2009; Kollipara and Perumal 2010; Feng *et al.* 2010). Sustained activation of inflammatory responses can be detrimental and therefore it is important that these responses are tightly regulated (Rigamonti *et al.* 2008).

1.5.3. Macrophage activation

Activation of macrophages has been divided into four main stages: priming, classical type I activation, alternative type II activation, and deactivation (Ma *et al.* 2003; Gordon and Taylor 2005; Ricardo *et al.* 2008; Tabas 2010).

Macrophages in peripheral tissues receiving survival signals, such as M-CSF and GM-CSF, have the ability to differentiate and become activated in response to inflammatory cues (Ma *et al.* 2003; Brochériou *et al.* 2011). These cells might undergo priming before becoming activated. This is achieved by exposing macrophages to an initial stimulus, which "prepares" them for subsequent secondary stimulus. At this stage, a primed macrophage does not exhibit a fully activated phenotype, so it is not able to produce any pro-inflammatory mediators. IFN-γ at low doses is the major priming stimulus and priming is mediated by the interaction of IFN-γ with its receptor IFN-γ-R through the Janus kinase / Signal Transducer and Activator of Transcription (JAK/STAT) signalling pathway (Ma *et al.* 2003).

The classical type I activation is triggered by exposure of macrophages to Th1 cytokines, such as IL-1β, IFN-γ, or TNF, or LPS from Gram-negative bacteria and GM-CSF, and leads to the differentiation of macrophages towards an aggressive, pro-inflammatory phenotype (Ma *et al.* 2003; Gordon and Taylor 2005; Ricardo *et al.* 2008; Rigamonti *et al.* 2008; Kadl *et al.* 2011; Brochériou *et al.* 2011; van Tits *et al.* 2011). So-called M1 macrophages exhibit increased antigen presentation capacity, and enhanced microbicidal activity, triggering Type I inflammation and Th1 responses (Funk *et al.* 1993; Ma *et al.* 2003; Gordon and Taylor 2005; van Tits *et al.* 2011). M1 polarised macrophages also express MHC class II antigens, and are characterised by the production of pro-inflammatory cytokines, such as IL-1, IL-2, IL-12, IL-23, TNF-α, as well as reactive oxygen and nitrogen species (Ricardo *et al.* 2008; Kadl *et al.* 2011;

Brochériou *et al.* 2011; van Tits *et al.* 2011). M1 polarisation is thought to be associated with the activation of the NF-κB and Activator Protein-1 (AP-1) signalling pathways (Ma *et al.* 2003; Kadl *et al.* 2011).

Resolution of inflammation can be mediated by macrophages activated through the alternative type II activation pathway, termed M2 macrophages (Ricardo *et al.* 2008; Tabas 2010; van Tits *et al.* 2011). This is mainly induced by Th2 cytokines, such as IL-4 and IL-13, and these cells exhibit an anti-inflammatory phenotype (Ma *et al.* 2003; Gordon and Taylor 2005; Ricardo *et al.* 2008; Rigamonti *et al.* 2008; Tabas 2010; Kadl *et al.* 2011; Brochériou *et al.* 2011). Contrary to the M1 polarisation, this pathway is thought to be regulated by members of a nuclear superfamily of receptors known as Peroxisome Proliferator-Activated Receptors (PPARs) (Ricardo *et al.* 2008; Tabas 2010; Kadl *et al.* 2011). M2 macrophages express high levels of mannose receptors and arginase-1, and are involved in tissue repair by promoting cell growth and collagen synthesis (Ma *et al.* 2003; Gordon and Taylor 2005; Ricardo *et al.* 2008; Kadl *et al.* 2011; van Tits *et al.* 2011). Their immunoregulatory properties are mediated by decreased secretion of pro-inflammatory cytokines, increased endocytic capacities, as well as the production of anti-inflammatory cytokines, such as IL-10 and TGF-β (Gordon and Taylor 2005; Ricardo *et al.* 2008; Brochériou *et al.* 2011; van Tits *et al.* 2011).

The presence of a third type of activated macrophages, named Mox, was suggested by Kadl *et al.* (2011). This phenotype is thought to occur in microenvironments enriched in oxidised phospholipids, where the levels of oxidative stress-inducing agents are high (Kadl *et al.* 2011). The research was based on previous observations made by the group that oxidised phospholipids were capable of inducing the recruitment of macrophages *in vivo*, in a process dependent on CCR2R (Kadl *et al.* 2011). Mox

macrophages had a specific gene expression pattern, which was shown to be different from that of M1 or M2 phenotypes, and included genes regulating the synthesis of antioxidant enzymes, as well as genes induced in response to oxidative stress. Of interest, the glutathione/oxidised glutathione ratio (GSH/GSSG) was increased in Mox macrophages, suggesting an increased capacity of these cells to cope with oxidative stress (Kadl *et al.* 2011). The role of these cells in redox regulation was further supported by the identification of Nuclear Factor (erythroid-derived)-like 2 (Nrf2) as an important mediator of the Mox phenotype. Nrf2 is a redox-sensitive transcription factor and it was found to regulate the gene expression of the Mox phenotype specifically (Kadl *et al.* 2011).

When compared to both M1 and M2 macrophages, Mox showed decreased phagocytic capacity which could result in the accumulation of cell debris, apoptotic cells, and tissue-damaging material that might contribute to an ongoing inflammatory state (Kadl *et al.* 2011). The up-regulation of several pro-inflammatory genes, such as IL-1β and COX2 indicated that these cells exhibited a pro-inflammatory phenotype, although to a reduced extent when compared to M1 macrophages (Kadl *et al.* 2011).

The last step in macrophage activation is the deactivation of activated cells, which is achieved with anti-inflammatory cytokines, such as IL-10 and TGF-β, or glucocorticosteroids (Ma *et al.* 2003; Gordon and Taylor 2005; Ricardo *et al.* 2008). Glucocorticosteroids inhibit the production of pro-inflammatory prostaglandins (PGs) and leukotrienes (LTs) by down-regulating the production of arachidonic acid. During the stage of resolution, anti-inflammatory variants of these two mediators, termed cyclopentenone prostaglandins (cyPGs) and lipoxins, down-regulate the pro-inflammatory signals mediated by NF-κB, AP-1, and STAT (Ma *et al.* 2003; Gordon and Taylor 2005).

There is evidence suggesting that macrophages are not limited to a single activation state, and when the proper stimuli are present, they may switch from a pro-inflammatory phenotype to an anti-inflammatory or resting phenotype (Ricardo *et al.* 2008; Kadl *et al.* 2011; Brochériou *et al.* 2011). Further recruitment of polarised macrophages or the effects of variable local factors on these cells can change the balance between the different macrophage phenotypes in a tissue (Kadl *et al.* 2011).

1.5.4. Macrophages and atherosclerosis

Monocyte-derived macrophages play a crucial role in the development of atherosclerosis, as it is one of the main types of cells involved in atherogenesis and plaque formation (Serri *et al.* 2004; Schmitz and Grandl 2009; Ye *et al.* 2009; Feng *et al.* 2010; van Tits *et al.* 2011). Their role in the development of the disease has been demonstrated in studies were monocyte deficiency in mouse atherosclerosis models led to a 4-fold reduction in lesion formation (de Villiers *et al.* 1998; Rajavashisth *et al.* 1998; Kleemann *et al.* 2008).

Mediators of both the classical and alternative activation phenotypes, such as IL-12 and IL-4, were shown to elicit the accumulation of macrophages and the initiation of inflammatory responses in atherosclerotic plaques (Kadl *et al.* 2011). Macrophages with different activation phenotypes were shown to be present in established lesions, and the extent of inflammation depends on the balance between the M1 and M2 phenotypes (Ricardo *et al.* 2008). The fact that atherosclerosis is considered to be a chronic inflammatory disease, and that inflammation characterises all stages of the disease suggests that the M1 phenotype dominates over the M2 phenotype, which leads to impaired resolution of inflammatory responses (Tabas 2010).

One of the most important features of macrophages is their ability to be transformed into foam cells, which is the hallmark of atherosclerosis (Castrillo *et al.* 2003; Van Eck *et al.* 2005; Forcheron *et al.* 2005; Rigamonti *et al.* 2008; Paul *et al.* 2008; Chen *et al.* 2009; Buers *et al.* 2009; Choi *et al.* 2009; Rosenblat *et al.* 2010; van Tits *et al.* 2011).

1.6. Foam cells

During the early phase of atherosclerotic lesion development, monocytes recruited in the intima layer of the artery differentiate into macrophages, and after excessive lipoprotein accumulation, they are transformed into foam cells, the main type of cell found in early atherosclerotic lesions (Henriksen *et al.* 1981; Funk *et al.* 1993; Steinberg 2005; Chinetti *et al.* 2006; Cao *et al.* 2007; Buono *et al.* 2007; Persson *et al.* 2008; He *et al.* 2009; Schmitz and Grandl 2009; Feng *et al.* 2010). Lesional endothelial cells and vascular SMCs can also be transformed into foam cells, although to a lesser extent (Steinberg 2005).

A characteristic of these cells is the cytosolic accumulation of lipid-rich vacuoles, which give the cytoplasm a foam-like appearance (D'Avila *et al.* 2008; Chen *et al.* 2009) (Figure 1.5). It is thought that the uptake of extracellular lipids by macrophages, and their transformation into foam cells might have protective effects as potentially harmful lipids are removed from the arterial wall (Witztum and Steinberg 1991; Paul *et al.* 2008).

The main lipid types found in lesional foam cells are cholesterol esters (CEs) and triglycerides (TGs), with CEs being the most abundant (Steinberg 2005; Forcheron *et al.* 2005; Chinetti *et al.* 2006; Cao *et al.* 2007; Persson *et al.* 2008; Buers *et al.* 2009; von Hodenberg *et al.* 2010; Feingold *et al.* 2010). Plasma lipoproteins are thought to be the main source of CEs in foam cells (Kita *et al.* 1990).

It is believed that the process of foam cell formation is a result of an imbalance between lipid uptake and efflux (Castrillo *et al.* 2003; Forcheron *et al.* 2005; Paul *et al.* 2008; Schmitz and Grandl 2009; Xue *et al.* 2010). Changes in the expression pattern of cholesterol metabolism genes observed in lesions suggest that the process of lipoprotein uptake is up-regulated, whereas the cellular efflux is down-regulated (Forcheron *et al.* 2005; Cao *et al.* 2007).

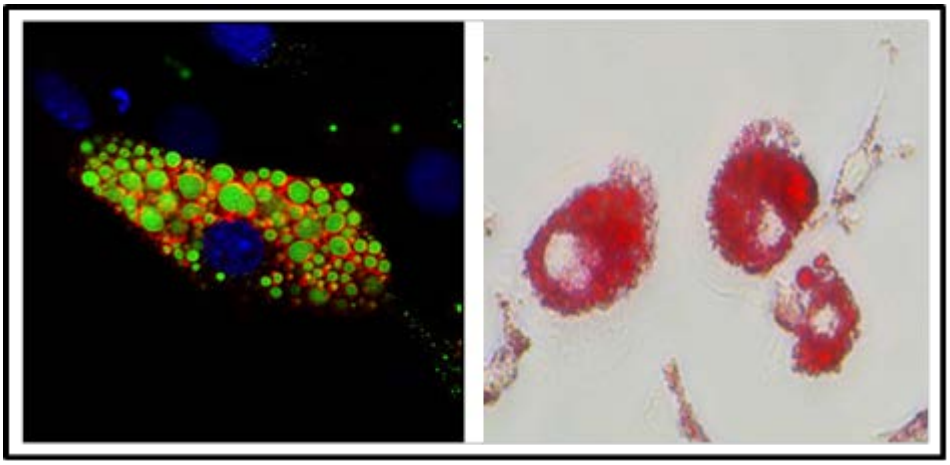

Figure 1.5. Adipocyte and human monocyte foam cells.

Cytoplasmic lipid inclusions in 3T3-L1 adipocyte (left) stained with BODIPY (green). In blue the nucleus labelled with DRAQ5 fluorescent dye, and in red the cytoplasm labelled with phospho-HSL antibody. Cytoplasmic lipid inclusions in human monocytes (right) stained with the lipophilic dye Oil Red-O.

[Image of adipocyte taken from: http://www.cellsignal.com/products/4139.html].

For many years it has been widely assumed that in order for lipoproteins to be taken up by macrophages, they had to be somehow modified (den Dekker *et al.* 2010), as it was shown that in these cells, the uptake of native unmodified LDL *in vitro* occurred at rates too low to be able to explain the excessive accumulation of lipids observed in foam cells *in vivo* (Goldstein *et al.* 1979; Steinbrecher *et al.* 1984; Lee *et al.* 2008).

Chemically modified lipoproteins proposed to be responsible for the formation of foam cells are oxidised LDL (OxLDL), minimally modified LDL (mmLDL), and acetylated LDL (AcLDL) (Xu *et al.* 2010). Of these forms, OxLDL has received the most attention (Jialal and Devaraj 1996; Persson *et al.* 2008; den Dekker *et al.* 2010; Xu *et al.* 2010) and became the focus of the "oxidative modification hypothesis of atherosclerosis".

1.7. Traditional View of Foam Cell Formation

The traditional view of foam cell formation suggests that this process is dependent on a particular form of modified lipoprotein, namely OxLDL, which can be taken up by a variety of mechanisms, including receptor-mediated uptake through ScRs, and can lead to the excessive accumulation of CEs (Kruth *et al.* 2002; Larigauderie *et al.* 2006).

This type of modified lipoprotein received much attention when, in 1979, Goldstein and Brown observed that patients with homozygous familiar hypercholesterolemia (FH) lacking a functional LDL receptor accumulated CE-rich foam cells in their arteries in a similar way to hypercholesterolaemic patients with normal LDL receptors (Goldstein *et al.* 1979; Kita *et al.* 1990; Jialal and Devaraj 1996; Steinberg 2005). Based on previous experiments showing that the rate of native LDL uptake by mouse peritoneal macrophages was too slow to induce foam cell formation, they suggested that modification of LDL was essential for the formation of foam cells, and that the process was dependent on an alternative receptor pathway different from the classical LDL receptor pathway (Goldstein *et al.* 1979; Witztum and Steinberg 1991; Jialal and Devaraj 1996; Steinberg 2005).

Through a number of experiments they showed that LDL particles treated with acetic anhydrite led to the formation of a modified form of LDL that was able to bind to macrophages with high affinity and specificity (Witztum and Steinberg 1991; Steinberg 2005). These particles were rapidly taken up and degraded by macrophages, resulting in cholesterol and CE accumulation. The “new” macrophage receptor responsible for this uptake was termed the “acetyl-LDL receptor” (Goldstein *et al.* 1979; Witztum and Steinberg 1991; Steinberg 2005).

Later studies by different groups showed that incubation of LDL with endothelial cells or SMCs in culture could lead to a modified form of LDL recognised with high

affinity by macrophages (Henriksen *et al.* 1981; Steinbrecher *et al.* 1984; Kita *et al.* 1990; Witztum and Steinberg 1991; Steinberg 2005). This new form of LDL was characterised by a higher average density and exhibited greater mobility on agarose gel electrophoresis, when compared to unmodified LDL from controls (Henriksen *et al.* 1981). Its uptake by macrophages was thought to be mediated by the acetyl-LDL receptor previously identified by Goldstein and Brown (Henriksen *et al.* 1981; Kita *et al.* 1990; Witztum and Steinberg 1991). This new form of LDL was shown to be induced by oxidation, and this discovery of OxLDL set the base of the so-called "oxidative modification hypothesis of atherosclerosis" (Witztum and Steinberg 1991; Steinberg 2005).

This hypothesis was supported by studies showing that oxidation of LDL could be induced *in vitro* by co-culture with the majority of cells found in the arterial wall, such as endothelial cells, SMCs and macrophages, which suggested that this process could occur in the artery wall (Witztum and Steinberg 1991; Jialal and Devaraj 1996; Steinberg 2005). LDL oxidation was also induced in cell-free cultures by heavy metal ions such as copper or iron (Witztum and Steinberg 1991; Jialal and Devaraj 1996).

The oxidation process begins with the formation of mmLDL, the result of mild oxidation of the LDL particle (Jialal and Devaraj 1996). This form of LDL was shown to be able to induce the expression of CAMs on endothelial cells and the secretion of monocyte chemoattractant molecules, such as MCP-1 and M-CSF, which can promote the recruitment of monocytes in the intima (Witztum and Steinberg 1991; Jialal and Devaraj 1996). Differentiation of monocytes into macrophages promotes further modification of mmLDL into OxLDL (Witztum and Steinberg 1991; Jialal and Devaraj 1996). Oxidation is considered a gradual process involving the formation of lipid

peroxides and their subsequent degradation, the products of which can form complexes with other proteins and lipids (Witztum and Steinberg 1991; Wiesner *et al.* 2010).

Lipid peroxidation is thought to be initiated by ROS, such as superoxide anions, generated intracellularly (Witztum and Steinberg 1991; Jialal and Devaraj 1996; Lee *et al.* 2008). ROS can be derived from various sources *in vivo*, such as mitochondria, cytochrome P450 monoxygenases, as well as NADPH oxidases (Nox), located on the surface of activated phagocytes (Steinbrecher *et al.* 1984; Jialal and Devaraj 1996; Lee *et al.* 2009). Lipoxygenases, such as 15-lipoxygenase (15-LO), are also thought to be involved in this process, as deficiency of 12/15-LO in Apo-$E^{-/-}$ or $LDLr^{-/-}$ mice was shown to reduce atherosclerosis (Witztum and Steinberg 1991; Jialal and Devaraj 1996; Steinberg 2005).

Evidence of *in vivo* existence of OxLDL particles further supported this hypothesis. The presence of OxLDL in plasma and in atherosclerotic lesions of experimental animals and humans was demonstrated with immunocytochemical techniques, and these particles resembled the *in vitro*-generated OxLDL, both physicochemically and biologically (Witztum and Steinberg 1991; Jialal and Devaraj 1996; Steinberg 2005). Various oxidised phospholipids found within the OxLDL particle are thought to be the main epitopes recognised by OxLDL auto-antibodies (Jialal and Devaraj 1996; Steinberg 2005). These antibodies were found to be present at high levels in patients with atherosclerotic disease, and both OxLDL and its antibodies have been correlated with the progression of the disease (Witztum and Steinberg 1991; Jialal and Devaraj 1996; Steinberg 2005). However, the therapeutic effects of such antibodies *in vivo* remain to be determined (Feng *et al.* 2010).

Many of the biological properties exhibited by OxLDL are thought to be pro-atherogenic. Oxidised phospholipids were shown to be able to cause the recruitment of

monocytes and macrophages *in vivo*, and to inhibit their escape from the tissues, trapping them in the intima (Witztum and Steinberg 1991). They are also able to enhance their cytotoxic effects by triggering the production of pro-inflammatory mediators, and the expression of MMPs (Jialal and Devaraj 1996; Wang *et al.* 1999; Libby *et al.* 2002; Larigauderie *et al.* 2006; Wiesner *et al.* 2010; Kadl *et al.* 2011). Gene expression patterns of vessel wall cells were also reported to be changed by OxLDL (Witztum and Steinberg 1991; Chawla *et al.* 2001a). Several reports have also suggested the implication of OxLDL in platelet aggregation and stimulation of pro-coagulant activity on the surface of macrophages in humans (Witztum and Steinberg 1991).

1.7.1. Scavenger receptors

Cellular uptake of cholesterol is usually mediated through the classical pathway involving the LDL receptor. This pathway is regulated by cholesterol via a feedback inhibition mechanism, and therefore it has traditionally been considered to be unlikely to be involved in the process of foam cell formation (Jialal and Devaraj 1996). The uptake and internalisation of modified lipoproteins, known to cause CE accumulation and foam cell formation, was proposed to be instead mediated by a group of specific plasma membrane receptors termed “scavenger receptors” (Witztum and Steinberg 1991; Jialal and Devaraj 1996; de Villiers and Smart 1999; Buono *et al.* 2007; Lee *et al.* 2008; Schmitz and Grandl 2009; Choi *et al.* 2009; van Tits *et al.* 2011). These receptors were considered good candidates as they were shown to have broad ligand specificity, they were able to bind their ligands with high affinity, and most importantly, unlike the LDL receptor, their activity was not down-regulated by the intracellular cholesterol content (Jialal and Devaraj 1996; Steinberg 2005; Segers *et al.* 2008).

The main ScRs implicated in OxLDL binding are the class A scavenger receptor SR-A, the class B scavenger receptor CD36, and the class E scavenger receptor lectin-like OxLDL receptor-1 (LOX-1) (Haraguchi *et al.* 2003; Steinberg 2005; Segers *et al.* 2008; Kuchibhotla *et al.* 2008; Lee *et al.* 2008; Schmitz and Grandl 2009; Feng *et al.* 2010). These membrane receptors are expressed on different cell types, including the main cell types implicated in the development of atherosclerosis – endothelial cells, vascular SMCs, and monocyte-derived macrophages (Schmitz and Grandl 2009; Feng *et al.* 2010; Xue *et al.* 2010). They bind to a wide array of ligands, including apoptotic cells, anionic phospholipids as well as long chain fatty acids, suggesting a possible role in fatty acid transport (de Villiers and Smart 1999; Steinberg 2005; Rahaman *et al.* 2006; Kuchibhotla *et al.* 2008; Schmitz and Grandl 2009). However, these receptors are better known for their role in the uptake of modified LDL, mainly OxLDL or AcLDL, by differentiated macrophages in atherosclerotic lesions (Lee *et al.* 2008). The expression of SR-A and CD36 was shown to be regulated by Liver-X-Receptors (LXRs) and PPARs, of which OxLDL and its constituent modified lipids are known ligands (de Villiers and Smart 1999; Haraguchi *et al.* 2003). Binding of modified LDL to the receptors is mediated by the recognition of altered molecular patterns present on the LDL particle, such as oxidised phospholipids (Li and Glass 2002; Haraguchi *et al.* 2003; Larigauderie *et al.* 2004; Rahaman *et al.* 2006; Lee *et al.* 2008; Manning-Tobin *et al.* 2009; Schmitz and Grandl 2009; Feng *et al.* 2010).

SR-A and CD36 were reported to account for almost 90% of OxLDL accumulation in macrophages cultured *in vitro* (de Villiers and Smart 1999; Steinberg 2005; Manning-Tobin *et al.* 2009). Of the two, more than 50% of OxLDL uptake is attributed to CD36, mainly due to higher ligand affinity (Rahaman *et al.* 2006; Choi *et al.* 2009; Xue *et al.* 2010). Their role in atherogenesis and foam cell formation was studied in

mouse models by different groups. Experiments using ScR-knockouts in either Apo-$E^{-/-}$ or $LDLr^{-/-}$ mice showed improvement of the atherosclerosis severity (Steinberg 2005; Kuchibhotla *et al.* 2008). In the absence of one or both of these receptors, a 30-40% decrease in macrophage recruitment was observed (Kuchibhotla *et al.* 2008). Further experiments indicated that SR-A or CD36 deficiency led to reduced lipid uptake and decreased lipid accumulation, as well as decreased secretion by macrophages of pro-inflammatory cytokines and ROS, suggesting a pro-atherogenic role of these receptors (Kuchibhotla *et al.* 2008). Most of the studies regarding the role of CD36 yielded consistent results; however, this was not the case when SR-A was studied, as both pro- and anti-atherogenic properties have been suggested for this receptor (de Villiers and Smart 1999; Manning-Tobin *et al.* 2009).

1.7.2. Lectin-like OxLDL receptor-1 (LOX-1)

LOX-1 is another receptor involved in the uptake of OxLDL (de Villiers and Smart 1999; Lee *et al.* 2008). This receptor was originally identified on endothelial cells, and was later shown to be also expressed on SMCs and macrophages, albeit at relatively low levels (de Villiers and Smart 1999; Lee *et al.* 2008; Ishiyama *et al.* 2010). LOX-1 has been detected in atherosclerotic lesions (Lee *et al.* 2008). Similar to SR-A and CD36, this receptor was shown to be up-regulated by pro-inflammatory cytokines, such as IL-1β and TNF-α (de Villiers and Smart 1999; Lee *et al.* 2008). Recognised ligands include, apart from OxLDL, apoptotic cells, bacteria and LPS (Lee *et al.* 2008). Upon OxLDL binding, LOX-1 was shown to induce the activation of intracellular signalling pathways associated with protein kinases and transcription factors implicated in the regulation and the expression of genes involved in atherosclerosis (Ishiyama *et al.* 2010). LOX-1

deficiency was shown to decrease atherosclerotic lesion formation (Lee *et al.* 2008; Ishiyama *et al.* 2010).

1.8. Antioxidant controversies.

Although acetyl-LDL was shown to promote excessive lipid accumulation in macrophages *in vitro*, this reagent, created by chemical modification of LDL, was not considered a naturally occurring biological product as its presence has never been reported *in vivo* (Henriksen *et al.* 1981; Steinberg 2005). However, it was soon proposed that similar forms of modified LDL could be generated *in vivo* if some mechanism existed by which the LDL particle could become oxidised by ROS. This hypothesis became popular as it was believed that the process of LDL oxidation could occur in the vessel wall, where antioxidants were present at low concentrations (Steinbrecher *et al.* 1984; Jialal and Devaraj 1996). Many groups then sought to investigate the attractive hypothesis that atherosclerosis could be prevented or reduced by treatment with anti-oxidants in animal models of the disease (Steinbrecher *et al.* 1984; Kita *et al.* 1990; Witztum and Steinberg 1991; Jialal and Devaraj 1996).

The main antioxidants used in these studies were probucol, butylated hydroxytoluene (BHT), N, N'-diphenylphenylenediamine (DPPD), vitamin E, *β*-carotene, and ascorbic acid. The first antioxidant to be tested was probucol, a lipid-soluble agent, which was shown to have protective effects both *in vitro* and *in vivo* by decreasing the oxidation process (Jialal and Devaraj 1996; Steinberg 2005). It was also shown to ameliorate atherosclerosis in hypercholesterolaemic rabbits (Witztum and Steinberg 1991). However, clinical studies in human volunteers showed that treatment with probucol could lower HDL cholesterol levels, an effect that limited the use of this agent as an antioxidant in the clinical setting (Jialal and Devaraj 1996).

Vitamin E was shown to inhibit the *in vitro* oxidation of LDL mediated by endothelial cells, and had atheroprotective effects when used as a supplement in the diets of Apo-$E^{-/-}$ mice (Steinbrecher *et al.* 1984; Steinberg 2005). However, vitamin E

supplementation yielded conflicting results when used in rabbit models of atherosclerosis (Steinberg 2005).

Large-scale, placebo-controlled clinical trials have also been conducted to investigate the potential benefit of anti-oxidant supplementation with respect to cardiovascular risk in man, particularly through supplementation with *β*-carotene, vitamin C and vitamin E (Steinberg and Witztum 2002). However, meta-analysis of the data obtained from such trials has revealed that these antioxidants conferred no beneficial or protective effect against CVD at the doses used (50-400 mg/ day), and in fact could cause a significant increase in cardiovascular mortality (Steinberg and Witztum 2002; Steinberg 2005; Dotan *et al.* 2009).

DPPD and BHT have also been used in antioxidant studies where they inhibited the process of LDL oxidation (Steinbrecher *et al.* 1984; Witztum and Steinberg 1991). However, they have only been used in one study each, as they were shown to have toxic effects, which limited their use in humans (Jialal and Devaraj 1996; Steinberg 2005).

Probucol and ascorbic acid were shown to inhibit the oxidation of LDL induced *in vitro* by transition metal ions, such as copper and iron (Kita *et al.* 1990; Jialal and Devaraj 1996). However, these forms of modified LDL have not been reported to be present *in vivo* (Jialal and Devaraj 1996; Libby *et al.* 2002).

Another mechanism considered to be responsible for the oxidation of LDL is the production of ROS from oxidases, present on the surface of activated phagocytes (Kirk *et al.* 2000; Brennan *et al.* 2001). Studies on myeloperoxidase (MPO)/LDLr$^{-/-}$ or Nox/Apo-E$^{-/-}$ mice showed no change in the extent of the atherosclerotic lesion, and in the case of MPO$^{-/-}$, lesions were even larger than control mice (Kirk *et al.* 2000; Brennan *et al.* 2001). These data suggests that reaction products generated by these

enzymes do not promote atherosclerosis and that they may have a protective role instead (Brennan *et al.* 2001).

Further evidence supporting the idea that oxidation of LDL might not be involved in the process of foam cell formation came from studies where even highly oxidised forms of LDL failed to induce excessive cholesterol accumulation in macrophages (Kruth *et al.* 2002). These cells were characterised by enlarged lysosomes containing trapped OxLDL (Kruth *et al.* 2002; Schmitz and Grandl 2009). This was explained by the fact that OxLDL impaired the process of CE hydrolysis and the subsequent esterification of free cholesterol (FC) by cholesterol esterases (Kruth *et al.* 2002; Schmitz and Grandl 2009). Furthermore, analysis of the different types of modified lipids and proteins extracted from human atherosclerotic lesions indicated that these modifications did not correspond to the changes that could be induced by *in vitro* oxidation (Libby *et al.* 2002). Similar results were obtained from *in vitro* experiments where LDL isolated from the culture medium after incubation with stimulated macrophages had the same electrophoretic mobility as native LDL, indicating that no oxidation took place (Ye *et al.* 2009).

More conflicting results were obtained when the absence of ScRs was studied. Based on previous results suggesting pro-atherogenic roles for CD36 and SR-A, it was thought that a combined deficiency of both receptors would confer protection greater than either alone (Kuchibhotla *et al.* 2008). Whereas absence of both receptors significantly suppressed lesional inflammation, as well as the apoptotic rate of lesional macrophages and plaque progression in Apo-$E^{-/-}$ mice, it had no effect on foam cell formation, lesion development or the progression of the disease, indicating that alternative ScR-independent lipid uptake mechanisms, existed *in vivo* (Moore *et al.* 2005; Steinberg 2005; Kuchibhotla *et al.* 2008; Manning-Tobin *et al.* 2009).

Studies in humans further supported the anti-atherogenic role of CD36, as deficiency of this receptor was associated with increased atherosclerosis (Masuda *et al.* 2009; Yuasa-Kawase *et al.* 2012). CD36-deficient patients were characterised by higher levels of plasma lipids, as well as insulin resistance and high blood pressure, which are all known major CVD risk factors (Masuda *et al.* 2009; Yuasa-Kawase *et al.* 2012).

Natural autoantibodies against OxLDL, termed EO6, which have been described in plasma and atherosclerotic lesions of several species (Watson *et al.* 1997), were shown to recognise phosphorylcholine on oxidised-phosphatidylcholine present on the surface of OxLDL (Shaw *et al.* 2000; Chang *et al.* 2002; Miller *et al.* 2011). The use of these antibodies in immunohistochemistry experiments forms the strongest evidence of existence of OxLDL in plaques. However, it has been recently discovered that these antibodies bind also to cells undergoing apoptosis, as well as bacterial membranes, which are enriched in these epitopes (Shaw *et al.* 2000; Chang *et al.* 2002; Binder *et al.* 2003; Chang *et al.* 2004; Miller *et al.* 2011).

So, although many of the biological properties of OxLDL are considered atherogenic and were shown to influence atherosclerosis progression (Kruth *et al.* 2002), the conflicting results obtained from various studies raised doubts about the importance of OxLDL as a causative agent of foam cell formation, and the relevance of the oxidative modification hypothesis in the context of human atherosclerosis (Steinberg 2005).

1.9. Evidence of alternative mechanisms of foam cell formation

Alternative mechanisms of foam cell formation have been proposed by various groups, including exposure of macrophages to such stimuli as aggregated LDL, *β*-VLDL, and immune complexes (Kruth *et al.* 2002; Steinberg 2005; Larigauderie *et al.* 2006; Rahaman *et al.* 2006; Buers *et al.* 2009). Aggregation of LDL, which can be achieved by vortexing or incubation with lipases, was shown to promote rapid lipid accumulation in a process involving phagocytosis and the LDL receptor (Khoo *et al.* 1988; Kruth *et al.* 2002; Steinberg 2005; Larigauderie *et al.* 2006). Complexes of LDL with antibodies or glycosaminoglycans were shown to be able to bind to macrophages, promoting the uptake of LDL via an endocytosis-dependent mechanism (Kruth *et al.* 2002; Larigauderie *et al.* 2006).

Other classes of lipoproteins have also been shown to cause lipid accumulation and foam cell formation *in vitro*. Culture of macrophages with TG-rich lipoproteins, such as chylomicrons, hypertriglyceridaemic VLDL or free FA-albumin complexes was shown to cause a rapid lipid accumulation (Haraguchi *et al.* 2003; Larigauderie *et al.* 2006; von Hodenberg *et al.* 2010), in a process also thought to involve the LDL receptor (Haraguchi *et al.* 2003).

Treatment of cells with cytokines was also shown to induce foam cell formation (Lee *et al.* 2009). Both IL-1*β* and TNF-*α* were shown to mediate the uptake and retention of lipids, specifically cholesterol and TGs, in a dose-dependent manner, in both control and aggregated-LDL-treated cells (Persson *et al.* 2008). Similarly, treatment of J774 macrophages with OxLDL in the presence of TNF-*α* was shown to induce foam cell formation, in a process dependent on the up-regulation of MAPK pathways, which in turn led to increased expression of macrophage ScR SR-A (Hsu and Twu 2000). Inhibition of NF-*κ*B activation was shown to reduce the formation of foam

cells in OxLDL-treated cultured human macrophages (Ferreira *et al.* 2007). This was accompanied by increased expression of CD36, the transcription factors PPAR-γ and LXR-α, as well as of cholesterol transporter proteins (Ferreira *et al.* 2007).

Recent studies reported the existence of an alternative mechanism for foam cell formation that was independent of modified lipoproteins or receptor-mediated uptake (Kruth *et al.* 2002; Buono *et al.* 2007; Anzinger *et al.* 2010). Accumulation of native LDL in M-CSF-differentiated macrophages or phorbol myristate acetate (PMA) - activated macrophages was shown to be induced via receptor-independent, fluid-phase pinocytosis (Kruth *et al.* 2002; Buono *et al.* 2007). Lipid uptake was suggested to occur via either micro- or macro-pinocytosis, in a process thought to be either constitutive or protein kinase C (PKC)-dependent (Buono *et al.* 2007; Anzinger *et al.* 2010). The regulation of this process was thought to be achieved via LXRs, since activation of these transcription factors by their agonists was shown to inhibit pinocytosis of native LDL, preventing its accumulation (Buono *et al.* 2007).

Choi *et al.* (2009) also reported that mmLDL was able to stimulate macro-pinocytosis with subsequent uptake of both native and modified LDL, in a process that depended on TLR4 activation. The different oxidised lipid moieties and the CE hydroperoxides within the mmLDL particle were thought to be responsible for the activation of TLR4, by acting as ligands for this receptor. The signalling pathway was shown to involve binding of mmLDL to CD14 and a subsequent interaction of the intracellular domain of TLR4 with Syk tyrosine kinase. Activation of the intracellular signalling cascade led to re-arrangements of the cell cytoskeleton, characteristic of pinocytosis (Choi *et al.* 2009).

Foam cell formation has also been documented to occur in the presence of bacteria or their products, and evidence suggests the contribution of TLRs in bacteria-dependent

foam cell formation (Sorrentino *et al.* 2010; Nicolaou *et al.* 2012). Funk *et al.* (1993) observed that, in the absence of exogenous lipoproteins, stimulation of RAW 264.7 macrophages with LPS led to a significant increase in intracellular TG levels, along with modest increases in FC, in a process shown to be dose-dependent. Similar results were also observed by Kazemi *et al.* (2005). Later studies reported that LPS-induced lipid accumulation in macrophages was TLR4-dependent, as TLR-deficient cells were not able to be transformed into foam cells upon stimulation with specific TLR ligands, with the greatest effect observed in $TLR2^{-/-}$ and $TLR4^{-/-}$ cells (Erridge 2008; Sorrentino *et al.* 2010).

C. pneumoniae infection was shown to increase the accumulation of CEs and the subsequent formation of foam cells in LDL-treated cells, via a mechanism initially thought to be dependent on the LDL receptor (Kalayoglu and Byrne 1998). Later studies, however, revealed a role for TLR2 in the process of *C. pneumoniae*-induced foam cell formation, as lipid accumulation was prevented in $TLR2^{-/-}$ macrophages infected with the bacterium (Cao *et al.* 2007; Chen *et al.* 2009).

The accumulation of lipids and the subsequent foam cell formation in macrophages infected with *Mycobacterium bovis* bacillus Calmette-Guérin was also shown to be dependent on the activation of TLR2 (D'Avila *et al.* 2006; Wan *et al.* 2007). Other members of the TLR family, mainly TLR1 and TLR6, as well as TLR4 have also been implicated in the recognition of mycobacterial antigens (D'Avila *et al.* 2006; Bozza *et al.* 2007).

Activation of TLR3, 4 and 9 was shown to up-regulate the expression of SR-A, Macrophage Receptor with Collagen structure (MARCO), and LOX-1 on macrophages, receptors known to be implicated in the formation of foam cells at the early stages of the disease (de Villiers and Smart 1999; Lee *et al.* 2008; Lundberg and Hansson 2010).

In the presence of LDL, activation of TLR9 by its ligand CpG DNA was shown to induce the formation of foam cells through a mechanism involving the p38-MAPK-mediated up-regulation of LOX-1 and Nox-1 expression (Lee *et al.* 2008; Sorrentino *et al.* 2010; Gu *et al.* 2010). Other TLR ligands, such as the synthetic ligands Pam_3CSK_4 and FSL-1, LPS, and flagellin were also shown to induce the expression of LOX-1 and Nox1 (Lee *et al.* 2008; Lee *et al.* 2009).

Of note, LOX-1 and CD36 were shown to act as co-receptors for the TLR2/TLR6 complex. CD36 was shown to bind to polyanionic ligands of bacterial and self-origin, such as apoptotic cells, FAs, and to assist the complex in the recognition of bacterial diacylglycerols, such as LTA (Schoneveld *et al.* 2005; Cao *et al.* 2007; Tobias and Curtiss 2007; Schoneveld *et al.* 2008; Lundberg and Hansson 2010; Stewart *et al.* 2010).

Apart from potentiating lipid uptake by cells, TLRs seem to have an effect on lipid efflux as well. Activation of TLR3 or TLR4 by their ligands was shown to inhibit cholesterol efflux, by mainly inducing the down-regulation of genes involved in the efflux process, such as cholesterol export proteins (Baranova *et al.* 2002; Kazemi *et al.* 2005; Feingold *et al.* 2010; Nicolaou *et al.* 2012). Down-regulation of these genes is thought to be dependent on the inhibition of the LXR pathway by the IRF3 signalling pathway activated by the two TLRs (Castrillo *et al.* 2003).

The exact mechanism promoting the formation of foam cells is still not well understood, and improved understanding of how these cells form may benefit from consideration of the lipid regulation pathways in macrophages.

1.10. Macrophage Lipid Regulation

The two main forms in which cholesterol is present in all tissues are cholesterol esters (CEs) and free cholesterol (FC). Cholesterol is a major constituent of plasma membranes, and the precursor of steroid hormones, such as testosterone and progesterone. It can be acquired either by *de novo* synthesis in the cell or from the diet (Forcheron *et al.* 2005).

The acetyl-CoA used as the carbon atom backbone in the *de novo* synthesis reaction is obtained from the oxidation of FAs (Berg *et al.* 2007). Cholesterol biosynthesis takes place in the liver, in a process that can be divided into three stages (Berg *et al.* 2007). The process begins with the formation of 3-hydroxy-3-methylglutaryl-CoA (HMG-CoA) from acetyl-CoA and acetoacyl-CoA, and its conversion into mevalonate (Berg *et al.* 2007) (Figure 1.6). This irreversible reaction is the rate-limiting step in cholesterol biosynthesis, and it is catalysed by an ER-located enzyme, HMG-CoA reductase. Mevalonate is then converted into isopentenyl pyrophosphate, which is the key building block of cholesterol (Berg *et al.* 2007).

Through a series of condensation reactions, squalene (C_{30}) is formed by six molecules of isopentenyl pyrophosphate (C_5). The third and last stage consists of the cyclisation of squalene and the subsequent formation of lanosterol, which is then converted into cholesterol (Figure 1.6). This last step takes place in the membranes of the ER (Berg *et al.* 2007).

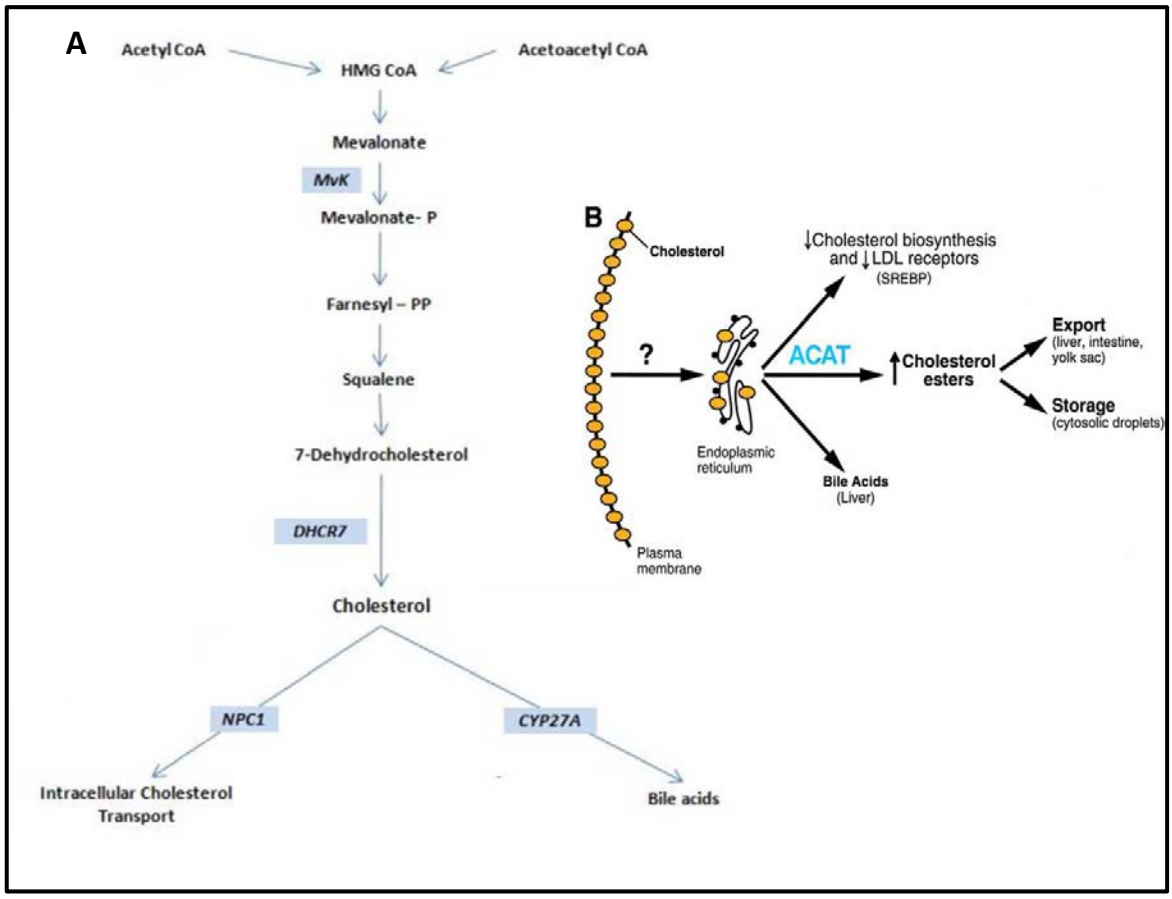

Figure 1.6. Synthesis and esterification of cholesterol.

Free cholesterol generated by *de novo* biosynthesis (A) or from the diet is converted into cholesterol esters by ACAT, and it is either removed from the cell or stored inside the cell (B). Abbreviations: Acyl-Coenzyme A: cholesterol acyltransferase (ACAT), sterol 27-hydroxylase (CYP27A), 7-dehydrocholesterol reductase (DHCR7), 3-hydroxy-3-methylglutaryl-CoA (HMG CoA), mevalonate kinase (MvK), Niemann Pick type C-1 (NPC1).

Taken from: http://www.ohsu.edu/xd/health/services/doernbecher/research-education/research/research-labs/steiner-lab-current-projects.cfm and http://www.ej2hosting.com/gilmarcomuniones.es/cholesterol-esterification.

Alternatively, the cell can acquire free cholesterol by the transport of cholesterol in the form of CEs, from the periphery to the various tissues, by LDL. The LDL particle is taken into the cell, via LDL receptor-mediated endocytosis (Goldstein *et al.* 1979; Brown *et al.* 1980; Ye *et al.* 2009) (Figure 1.7). Binding of the LDL particle to its receptor is mediated by its apolipoprotein component, Apo-B100. The LDL receptor is situated on the plasma membrane, at sites coated with clathrin, which mediate the formation of endocytic vesicles and the internalisation of the LDL-receptor complex. Once inside the cell, vesicles fuse with lysosomes where they are degraded by Lysosomal Acid Lipase (LAL); both its apolipoprotein component (Apo-B100) and the transported CEs are hydrolysed, and FC is generated (Li and Glass 2002; Forcheron *et al.* 2005; Bozza *et al.* 2007; Paul *et al.* 2008; Chinetti-Gbaguidi and Staels 2009).

Although required for viability, excessive concentrations of FC generated either by *de novo* synthesis or the LDL degradation reaction can be toxic to the cell (Forcheron *et al.* 2005). Protection is conferred mainly by re-esterification of cholesterol to CEs, which is the most common form of cholesterol storage found in tissues (Brown *et al.* 1980; Li and Glass 2002; Chinetti *et al.* 2003; Forcheron *et al.* 2005; Okazaki *et al.* 2008). The enzyme responsible for this conversion is known as Acyl-Coenzyme A:Cholesterol AcylTransferase (ACAT), found in the ER (Brown *et al.* 1980; Li and Glass 2002; Chinetti *et al.* 2003; Forcheron *et al.* 2005; Bozza *et al.* 2007; Rigamonti *et al.* 2008; Paul *et al.* 2008; He *et al.* 2009) (Figure 1.6), which drives the combination of free cholesterol with long chain fatty acids.

Alternatively, excess FC can be removed from cells via a process known as reverse cholesterol transport (RCT). This pathway was originally proposed by Glomset (1968) and it describes the removal of cholesterol from tissues and its transportation by HDL or other lipoproteins to the liver for elimination (de Villiers and Smart 1999; Sviridov and

Nestel 2002; Khovidhunkit *et al.* 2003; Van Eck *et al.* 2005; Chinetti-Gbaguidi and Staels 2009; Tsompanidi *et al.* 2010). Three different pathways of RCT have been described: diffusive or passive efflux which is associated with Apo-E secretion, active efflux carried out by specific trans-membrane transport proteins of the ATP-Binding Cassette Transporter superfamily (ABC-transporter), and SR-BI-mediated efflux (Baranova *et al.* 2002; Chen *et al.* 2007; Tall *et al.* 2008; de la Llera-Moya *et al.* 2010; Xue *et al.* 2010).

The process of RCT begins with the intracellular hydrolysis of CEs in the lysosomes, which leads to the generation of FC (Forcheron *et al.* 2005; Bozza *et al.* 2007; Chinetti-Gbaguidi and Staels 2009; Sekiya *et al.* 2009; von Hodenberg *et al.* 2010). Hydrolysis reactions can be carried out by specific CE hydrolases, such as Hormone Sensitive Lipase (Lipe/HSL) in murine macrophages, and neutral cholesterol ester hydrolase (nCEH) in humans (Forcheron *et al.* 2005; Bozza *et al.* 2007; Okazaki *et al.* 2008; Sekiya *et al.* 2009). Accumulation of CEs and subsequent foam cell formation was shown to be inhibited after overexpression of these enzymes (Sekiya *et al.* 2009).

Non-esterified FC is transported to the plasma membrane by a specific set of proteins known as Niemann Pick type C-1/2 (NPC1 and 2) for efflux (Chinetti *et al.* 2003; Forcheron *et al.* 2005; Rigamonti *et al.* 2008). Efflux is mediated by various members of the ABC-transporter family of proteins, the main ones being ABCA1 and ABCG1/G4 (Tall *et al.* 2008; Rigamonti *et al.* 2008; Lammers *et al.* 2009; Kim *et al.* 2009; Khera *et al.* 2011). These proteins exert their activity by using ATP as an energy source (Van Eck *et al.* 2005).

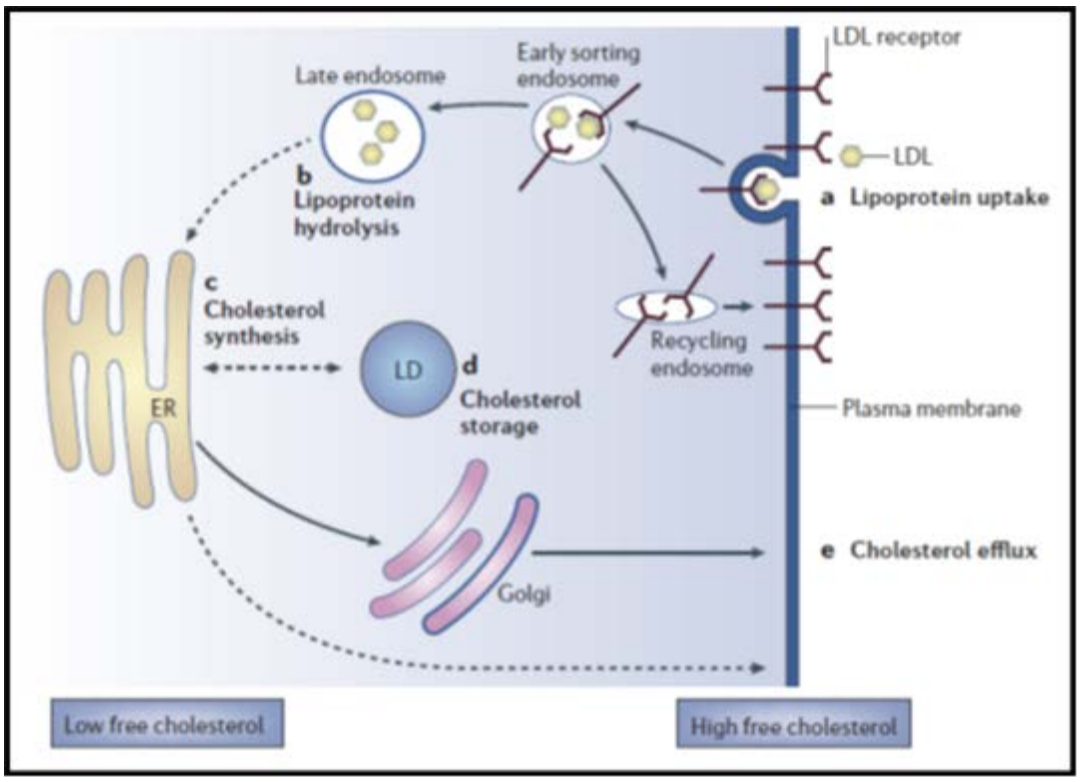

Figure 1.7. Regulation of intracellular cholesterol levels.

Binding of the LDL particle to the LDL receptor leads to the formation of endocytic vesicles (a) and the internalisation of the complex. Fusion of these vesicles with lysosomes leads to the hydrolysis of the lipoprotein particle (b) and the generation of free cholesterol, which, along with cholesterol synthesised by *de novo* synthesis in the ER (c), can be either esterified and stored in cytoplasmic lipid droplets (d) or removed from the cell via cholesterol efflux pathways (e).

[Taken from: Martin and Parton (2006) Lipid droplets: a unified view of a dynamic organelle. *Nature Review – Molecular Cell Biology*, 7:373-378].

ABCA1 is highly expressed in lung, brain, adrenal glands, liver, as well as in macrophages (Van Eck *et al.* 2005; Chen *et al.* 2007). *Abca1* was identified as the mutated gene in Tangier disease, a rare disorder characterised by very low plasma HDL levels, increased numbers of macrophage foam cells and premature atherosclerosis

development (Chawla *et al.* 2001b; Baranova *et al.* 2002; Ni *et al.* 2007; Xue *et al.* 2010). Overexpression of ABCA1 in Apo-$E^{-/-}$ mice was shown to induce an increase in the levels of HDL cholesterol in the serum, as well as a reduction in atherosclerosis susceptibility (Van Eck *et al.* 2005).

ABCA1 is thought to mediate the efflux of phospholipids and cholesterol mainly to lipid-poor apo-A1, a plasma cholesterol acceptor bound to the transporter (Chinetti *et al.* 2003; Van Eck *et al.* 2005; Tall *et al.* 2008; Sekiya *et al.* 2009; Tsompanidi *et al.* 2010; Yvan-Charvet *et al.* 2010) (Figure 1.8). Apo-A1 is found on the small discoidal form of HDL, termed pre-β1-HDL (Sviridov and Nestel 2002; Chinetti-Gbaguidi and Staels 2009; Tsompanidi *et al.* 2010). It has been suggested that the affinity of apo-A1 for ABCA1 might be reduced upon accumulation of lipids (Van Eck *et al.* 2005). The particle acquires its final spherical shape (α-HDL) after esterification of the accumulated cholesterol into cholesteryl esters by Lecithin:Cholesterol AcylTransferase (LCAT) (Sviridov and Nestel 2002; Tsompanidi *et al.* 2010).

During HDL remodelling, cholesterol is transferred from the large α-HDL particles to Apo-B-containing lipoproteins. Cholesterol ester transfer protein (CETP) catalyses the exchange of CEs in HDL for TGs in VLDL/LDL particles for later catabolism (Sviridov and Nestel 2002; Tall *et al.* 2008; Tsompanidi *et al.* 2010). A variety of lipases, such as hepatic lipase (HL), mediate the hydrolysis of phospholipids and TGs, and phospholipids are transferred from VDLD/LDL to HDL through the action of phospholipid transfer protein (PLTP) (Sviridov and Nestel 2002; Tsompanidi *et al.* 2010) (Figure 1.8). At this stage, lipid-poor apo-A1 is generated, which can be used again in the first stages of RCT (Sviridov and Nestel 2002; Tall *et al.* 2008). The concentration and activity of CETP and HL are thought to be rate-limiting, since small changes in these two enzymes could lead to the formation of dysfunctional HDL

particles, which decrease the efficiency of the RCT process (Sviridov and Nestel 2002; Tall *et al.* 2008).

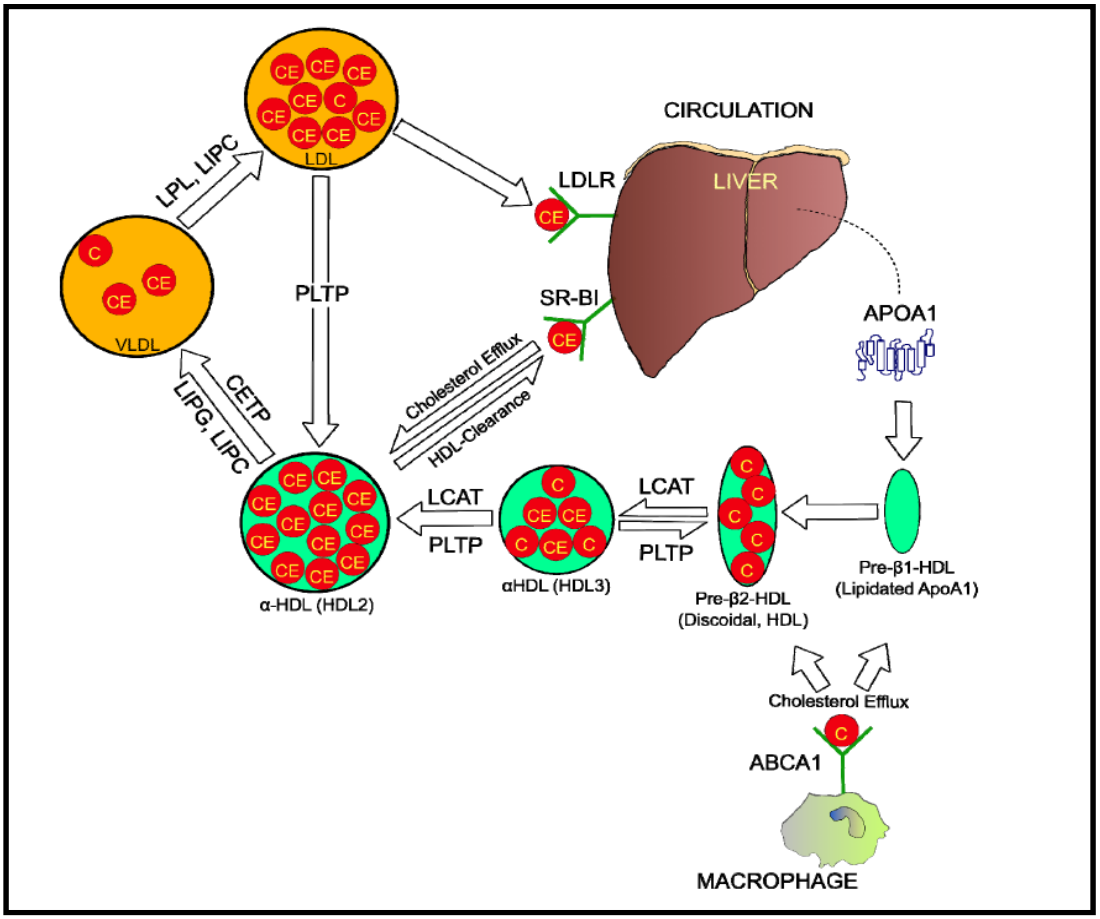

Figure 1.8. Reverse cholesterol transport (RCT) pathway.

Abbreviations: alpha-high-density lipoprotein, (*α*-HDL), ATP-binding cassette A1 (ABCA1), apolipoprotein-A1 (Apo-A1), cholesterol (C), cholesterol ester (CE), cholesterol ester transfer protein (CETP), lecithin:cholesterol Acyltransferase (LCAT), low-density lipoprotein receptor (LDLR), hepatic lipase (LIPC), endothelial lipase (LIPG), lipoprotein lipase (LPL), phospholipid transfer protein (PLTP), scavenger receptor-B1 (SR-B1).

[Taken from: Daniels *et al.* (2009) Lipoproteins, cholesterol homeostasis and cardiac health. *International journal of Biological Sciences*, 5(**5**):474-488].

Contrary to ABCA1, ABCG1 mediates cholesterol efflux to mature HDL particles, as well as other lipoprotein particles, such as LDL (Ni *et al.* 2007; Tall *et al.* 2008; Lammers *et al.* 2009; Yvan-Charvet *et al.* 2010; Xue *et al.* 2010; Ji *et al.* 2011). Its expression was detected in most tissues, including the lungs, spleen, and brain, and it is primarily expressed in macrophages, lymphocytes and endothelial cells (Ni *et al.* 2007). Several reports suggested that ABCG1 proteins were localised in sub-cellular compartments, and that upon up-regulation, they were re-distributed to the plasma membrane (Ni *et al.* 2007; Kim *et al.* 2009).

These proteins were shown to have complementary activity, and in the absence of one transporter, the other compensates for the lost activity (Tall *et al.* 2008; Yvan-Charvet *et al.* 2010). Combined deficiency of the two transporters severely impairs cholesterol efflux to cholesterol acceptors (Tall *et al.* 2008; Sekiya *et al.* 2009; Yvan-Charvet *et al.* 2010). Mice deficient in ABCA1 or ABCG1 were characterised by increased foam cell formation in various tissues due to decreased cellular cholesterol efflux, as well as increased inflammatory cell accumulation and macrophage-specific inflammatory responses, which resulted in accelerated atherosclerosis (Baranova *et al.* 2002; Ni *et al.* 2007; Yvan-Charvet *et al.* 2010; Khera *et al.* 2011; Le Goff and Dallinga-Thie 2011).

Both transporters are regulated by LXRs (Chawla *et al.* 2001b; Chen *et al.* 2007; Tall *et al.* 2008; Sekiya *et al.* 2009; Yvan-Charvet *et al.* 2010). Expression was also shown to be up-regulated by cholesterol loading of cells (Ni *et al.* 2007; Tall *et al.* 2008). There is evidence suggesting that PPAR agonists, such as Pioglitazone, are also able to induce the expression of these transporters, in an LXR-dependent manner (Haraguchi *et al.* 2003; Ni *et al.* 2007; Khera *et al.* 2011). Endotoxin and cytokines, such as IL-1β and TNF-α, on the contrary, were shown to down-regulate both mRNA

and protein levels of the two transporters, and subsequently, cholesterol efflux (Chen *et al.* 2007; Kim *et al.* 2009).

In the last stage of RCT, specific lipoprotein receptors mediate the uptake of HDL by the liver (Sviridov and Nestel 2002) (Figure 1.8), where hepatic enzymes catalyse the degradation of cholesterol into bile acids, which are then excreted into the bile (Baranova *et al.* 2002; Khovidhunkit *et al.* 2003; Chen *et al.* 2007; Ni *et al.* 2007). One such receptor with important roles in RCT is the second member of the class B scavenger receptors, SR-B1 (de Villiers and Smart 1999; Li and Glass 2002; Sviridov and Nestel 2002; Haraguchi *et al.* 2003; Ni *et al.* 2007; Rigamonti *et al.* 2008). It was first isolated and characterised as a lipoprotein receptor in murine tissues (Constantineau *et al.* 2010). Similar to CD36, SR-B1 is a membrane glycoprotein found to be expressed in various tissues and cells, with high expression levels seen in the liver, the adrenal glands, the ovaries, as well as in atherosclerotic lesions of Apo-$E^{-/-}$ mice (Baranova *et al.* 2002; Van Eck *et al.* 2005; Constantineau *et al.* 2010). It selectively binds to HDL and mediates the uptake of CEs from the HDL particle, as well as the bi-directional efflux of FC between HDL and SR-B1-expressing cells (de Villiers and Smart 1999; Li and Glass 2002; Sviridov and Nestel 2002; Van Eck *et al.* 2005; Schmitz and Grandl 2009; Constantineau *et al.* 2010; Ji *et al.* 2011). SR-B1 is also involved in the removal of Apo-B-containing lipoproteins, such as VLDL and LDL (Van Eck *et al.* 2005).

SR-B1 knockout mice displayed elevated plasma cholesterol levels due to accumulation of large HDL particles (Sviridov and Nestel 2002; Van Eck *et al.* 2005). Complete disruption of its function was associated with reduced hepatic uptake of CEs from HDL, and their subsequent biliary secretion (Van Eck *et al.* 2005). Modest overexpression of this protein was shown to have atheroprotective effects, due to

enhanced flow of cholesterol through the RCT pathway (Sviridov and Nestel 2002; Tsompanidi *et al.* 2010). However, high overexpression of SR-B1 is considered to be pro-atherogenic, since it results in decreased levels of both Apo-B-containing lipoproteins and HDL from plasma, which has a negative effect on the rate of RCT (Sviridov and Nestel 2002; Van Eck *et al.* 2005).

Passive or diffusional cholesterol efflux represents a large part of the efflux process in non-loaded macrophages (Yvan-Charvet *et al.* 2010). Its main mediator is apolipoprotein E (Apo-E) (Yvan-Charvet *et al.* 2010). This protein is mainly involved in the metabolism and clearance of atherogenic lipoproteins, such as chylomicron remnants and VLDL, from the circulation (Tsompanidi *et al.* 2010). Both *in vitro* and *in vivo* studies showed that Apo-E bound to lipoproteins is recognised by the LDL receptor, which mediates the removal of these lipoproteins (Tsompanidi *et al.* 2010). Apo-E was shown to interact with ABCA1 and to mediate the formation of discoidal pre-β1-HDL particles and later large α-HDL particles, in ways similar to apo-A1 (Van Eck *et al.* 2005; Tsompanidi *et al.* 2010). The secretion of Apo-E by macrophages was shown to facilitate the process of cholesterol efflux from the cells both in the absence or presence of extracellular cholesterol acceptors (Lammers *et al.* 2009). Cholesterol efflux potential was shown to be reduced when Apo-E was depleted from the HDL fraction, and this was accompanied by a marked increase in VLDL and LDL levels (Björkbacka *et al.* 2004; Tall *et al.* 2008). Similar results were observed in Apo-E-deficient macrophages; a reduction in ABCG1 expression was also observed in these macrophages, suggesting that these two proteins might have an additive role in the process of cholesterol efflux (Lammers *et al.* 2009).

The process of cholesterol efflux can be considered to be beneficial with respect to atherosclerosis, as it is thought to protect macrophages from apoptosis induced by LDL

accumulation (Tall *et al.* 2008; Khera *et al.* 2011). Most of its beneficial effects have been associated with HDL itself. This particle adopts a variety of lipoprotein compositions and it exists in either a discoidal or a spherical form, depending on its lipid composition (Tsompanidi *et al.* 2010; de la Llera-Moya *et al.* 2010). The main apolipoprotein component is apo-A1 (Flegel *et al.* 1993; Sviridov and Nestel 2002; Tsompanidi *et al.* 2010). Apo-A1 is organised into amphipathic α-helices, which are responsible for its lipid-binding properties (Tsompanidi *et al.* 2010). Two apo-A1 molecules are thought to be wrapped around the discoidal particle. Subsequent esterification of cholesterol leads to the formation of a larger, spherical particle, and the apo-A1 component is re-arranged to adjust on the spherical surface (Tsompanidi *et al.* 2010).

Epidemiological studies have documented an inverse relationship between plasma HDL levels and CVD, and it is therefore considered to have atheroprotective properties (Sviridov and Nestel 2002; Khovidhunkit *et al.* 2003; Van Eck *et al.* 2005; Tsompanidi *et al.* 2010; de la Llera-Moya *et al.* 2010). Apart from its participation in RCT, the apo-A1 component of the HDL particle is thought to have antioxidant properties, which might limit the oxidative modification of lipoproteins (Van Eck *et al.* 2005; Tsompanidi *et al.* 2010; de la Llera-Moya *et al.* 2010; Khera *et al.* 2011). HDL was also shown to be an effective scavenger of LPS, and to improve endothelial function by stimulating the production of endothelial NOS, suggesting that it might also have anti-inflammatory properties (Van Eck *et al.* 2005; Tsompanidi *et al.* 2010; Yvan-Charvet *et al.* 2010; de la Llera-Moya *et al.* 2010).

It is now clear, however, that raised levels of circulating HDL-cholesterol are not always associated with efficient RCT (Ni *et al.* 2007). What seems to be more important is the functionality of HDL-cholesterol particles during RCT (de la Llera-Moya *et al.*

2010). Studies on the capacities of human sera to promote cholesterol efflux suggest that the concentration of pre-β1-HDL is a better predictor of the efficiency of serum to promote efflux via ABCA1, since the concentration of pre-β1-HDL was shown to correlate well with three steps of the RCT pathway: apo-A1 lipidation, the conversion of the pre-β1-HDL particle into larger HDL particles, and the subsequent remodelling of HDL (Sviridov and Nestel 2002; de la Llera-Moya *et al.* 2010).

Cholesterol synthesis and uptake depend on the cellular cholesterol levels, and both processes are subject to feedback regulation mainly related to the amount and activity of HMG-CoA reductase or the LDL receptor (Ye *et al.* 2009). Intracellular depletion of cholesterol is sensed by proteins of the basic helix-loop-helix-leucine-zipper family of transcription factors called Sterol Regulatory Element Binding Proteins-1 and -2 (SREBPs) (Wang *et al.* 1994; Schmitz and Grandl 2009; Ye *et al.* 2009; Kotzka *et al.* 2010). The proteins are synthesised as high molecular weight precursors, bound to the ER membrane and the nuclear envelope (Ye *et al.* 2009). In sterol depleted cells, the precursor is proteolytically cleaved to generate the mature form of the protein, which translocates to the nucleus where it binds to specific sequences termed sterol-responsive elements (SREs) on target genes, and acts as a transcription factor regulating the expression of genes such as LDL-R, HMG-CoA reductase, and fatty acid synthesis genes, in order to increase sterol levels (Wang *et al.* 1994; Schmitz and Grandl 2009; Ye *et al.* 2009; Kotzka *et al.* 2010).

Both LDL-R and HMG-CoA reductase translation rates are inhibited in situations where there is too much cholesterol in the cell, either in the form of oxysterols, or transferred in LDL (Wang *et al.* 1994). In the case of HMG-CoA reductase, high levels of intracellular sterols were shown to reduce the activity of the enzyme by mechanisms involving degradation, as well as phosphorylation of the enzyme (Berg *et al.* 2007).

Accumulated cholesterol can also promote the RCT pathway, by means dependent on the activation of LXRs and PPARs.

1.11. Lipid Droplets

Excessive lipid accumulated within cells is usually stored in lipid-rich cytoplasmic inclusions termed lipid bodies or lipid droplets (LDs) (Larigauderie *et al.* 2006; Persson *et al.* 2008; Paul *et al.* 2008; Almeida *et al.* 2009). These non-membrane bound organelles consist of a monolayer of phospholipids and associated proteins, and a central core of neutral lipids, including triacylglycerols, diacylglycerols, retinyl esters, FC and CEs at different ratios (Larigauderie *et al.* 2006; Robenek *et al.* 2006; Bozza *et al.* 2007; Wan *et al.* 2007; Tavian and Colombo 2007; Buers *et al.* 2009; Schmitz and Grandl 2009).

LD biogenesis was shown to be stimulus- and cell type-dependent (Bozza *et al.* 2009). However, the mechanisms of LD biogenesis are yet not clearly understood. At least three hypothetical models regarding the LD formation have been proposed. Despite the subtle differences between these models, all suggest that LDs are somehow derived from the ER and are related with it in different ways (Wang *et al.* 1999; Bozza *et al.* 2007; Wan *et al.* 2007; Schmitz and Grandl 2009). LD-ER interactions are thought to facilitate lipid exchange between the two organelles and LD growth (Robenek *et al.* 2006; Bozza *et al.* 2007).

The first model is known as the “budding model”. According to this model, lipid metabolism enzymes accumulate between the two leaflets of the ER membrane bilayer, where they catalyse the synthesis of neutral lipids from FAs and cholesterol (Martin and Parton 2006; Robenek *et al.* 2006). When a certain critical concentration is reached, the membrane of the cytoplasmic leaflet of the ER is distended and the droplet buds off the ER into the cytoplasm. The formed LD is surrounded by a monolayer of phospholipids derived from the ER membrane, and contains ER resident proteins (Martin and Parton 2006; Robenek *et al.* 2006; Wan *et al.* 2007) (Figure 1.9 – a).

A slightly different model of LD formation was proposed by Robenek *et al* (2006). In this model, termed the "egg cup model", LDs are formed alongside and not inside the ER, in ER cups formed by both leaflets of the ER membrane, enclosing the LD in a way resembling an egg cup (ER) holding an egg (LD). This interaction favours the growth of the droplet, and the transfer of LD-associated proteins and lipids from the ER into the droplets. The transfer of lipids is thought to be mediated by LD-associated proteins which can be found at high concentrations in the ER cups, at the sites closest to the LD (Martin and Parton 2006; Robenek *et al.* 2006) (Figure 1.9 – b).

The first two models provide a good explanation regarding the monolayer of phospholipids surrounding LDs, but it does not provide evidence to support the presence of ER membrane-associated and LD-associated proteins, as well as ribosomes inside the LD core (Wan *et al.* 2007). The third model, known as the "engulfing model", was proposed by Wan *et al.* (2007) and was later supported by other groups. This model suggests that multiple loops deriving from the ER membrane are incorporated into the LD during formation, allowing the incorporation of ER proteins into the LD core (Wan *et al.* 2007; Bozza *et al.* 2009).

Most of our understanding on lipid droplet biology comes from studies in adipocytes, the main regulator of lipid and glucose homeostasis, where LDs serve as sites of cholesterol and FA storage, energy generation, steroid and eicosanoid mediator synthesis during inflammation, as well as synthesis of membrane components (Pacheco *et al.* 2002; Meadows *et al.* 2005; Wan *et al.* 2007; Guilherme *et al.* 2008; Schmitz and Grandl 2009).

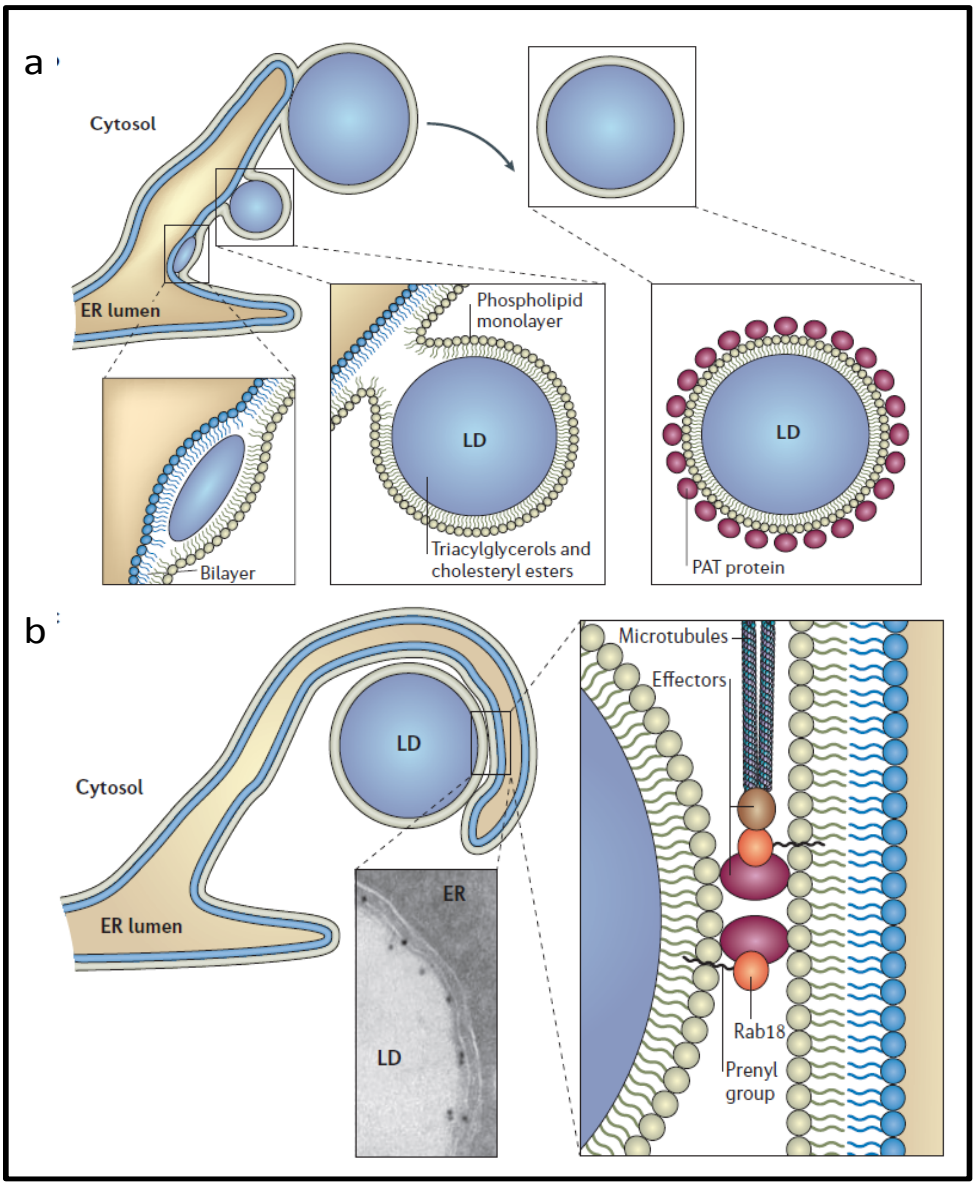

Figure 1.9. Suggested hypothetical models for lipid droplet formation.

Illustration of two of the models proposed for the formation of cytoplasmic lipid droplets in cells: the "budding model" (a) and the "egg cup model" (b). Abbreviations: endoplasmic reticulum (ER), lipid droplet (LD), Perilipin/Adipophilin/TIP47 protein (PAT), Ras-associated binding protein (Rab)

[Taken from: Martin and Parton (2006) Lipid droplets: a unified view of a dynamic organelle. *Nature Reviews – Molecular Cell Biology*, 7:373-378].

Expansion or depletion of LDs in adipocytes depends on the expression pattern of various components such as specific receptors, and the availability of their selective ligands (D'Avila *et al.* 2006), various transport proteins (i.e. ABC-transporters), enzymes involved in metabolic activities, structural and regulatory proteins, and transcription factors, such as PPAR*α*, *β/δ*, *γ,* and SREBP-1 (Schmitz and Grandl 2009). The process of lipolysis in adipocytes is under hormonal regulation (Guilherme *et al.* 2008). Insulin increases the levels of TGs by blocking intracellular cyclic AMP, and subsequently HSL, the enzyme responsible for lipolysis, leading to LD formation during fed conditions. On the contrary, during fasting states, catecholamines, signalling via GPCRs, or the lack of insulin, result in increased cyclic AMP levels, activation of HSL via phosphorylation of the enzyme, and enhanced lipolysis, leading to the release of FAs and glycerol and LD depletion (Guilherme *et al.* 2008).

LDs can be found in all organisms, in different sizes and numbers (Bozza *et al.* 2009). Leukocytes in their resting state contain only a small number of sparse LDs or none at all; however, upon leukocyte activation by a variety of stimuli or different pathological conditions, the number of LDs can increase rapidly (Pacheco *et al.* 2002; Meadows *et al.* 2005; Bozza *et al.* 2007; Bozza *et al.* 2009; Almeida *et al.* 2009). Increases in the size and the number of LDs are usually associated with the accumulation of neutral lipids in their core. Any morphological differences are related to the composition of lipids and their ratios within the LD (D'Avila *et al.* 2006). An increased number of LDs within leukocytes is usually associated with inflammatory responses to infections or other pathological conditions (Pacheco *et al.* 2002; Wan *et al.* 2007).

LDs were first believed to be sites of fatty acid and cholesterol storage and metabolism (Pacheco *et al.* 2002; Meadows *et al.* 2005; Wan *et al.* 2007; Schmitz and

Grandl 2009). However, it has now become clear that LDs have functions beyond mere lipid storage; they are considered to be specialised, inducible, metabolically active cytoplasmic organelles with roles in cell signalling and activation, lipid metabolism regulation, membrane trafficking, and the synthesis and secretion of various inflammatory mediators (D'Avila *et al.* 2006; Robenek *et al.* 2006; Bozza *et al.* 2007; Wan *et al.* 2007; Tavian and Colombo 2007; Almeida *et al.* 2009).

Immunolocalisation studies also showed that LDs are enriched in phospholipid-esterified arachidonate, eicosanoid-forming enzymes, and their regulatory kinases and phosphatases, such as cyclooxygenase (COX), lipoxygenase (LO), phospholipase-A_2 (PLA_2), mitogen-activated protein kinase (MAPK) etc. (Wang *et al.* 1999; Pacheco *et al.* 2002; Larigauderie *et al.* 2004; D'Avila *et al.* 2006; Bozza *et al.* 2007; Wan *et al.* 2007; Schmitz and Grandl 2009; Mattos *et al.* 2010). Also, increased number of LDs in leukocytes has been associated with enhanced generation and release of prostaglandins and leukotrienes (Wang *et al.* 1999; Pacheco *et al.* 2002; Wan *et al.* 2007). All these findings support the multifunctional role of LDs.

1.11.1. Lipid Droplet-Associated Proteins

The main structural proteins associated with LDs, belong to the PAT domain-containing protein family (Buers *et al.* 2009), and include Perilipin, Adipophilin or Adipose Differentiation-Related Protein (ADRP), and Tail-Interacting Protein of 47 kDa (TIP47) (Guilherme *et al.* 2008; Paul *et al.* 2008; Bozza *et al.* 2009; Schmitz and Grandl 2009; Mattos *et al.* 2010; Gu *et al.* 2010). PAT proteins can be found both on the surface and the lipid core of LDs (Robenek *et al.* 2006; Bozza *et al.* 2007; Wan *et al.* 2007; Bozza *et al.* 2009; Mattos *et al.* 2010). Under basal conditions, these proteins reside on the plasma membrane of lipid-accumulating cells, and they were shown to relocate on the plasma membrane at sites close to the forming LD when lipid

accumulation is stimulated (Robenek *et al.* 2006). Apart from roles in the formation and assembly of LDs (Robenek *et al.* 2006; Paul *et al.* 2008; Schmitz and Grandl 2009), these proteins were also shown to be involved in lipid metabolic processes, such as lipolysis and lipogenesis (Wan *et al.* 2007; Gu *et al.* 2010).

Perilipin is mainly expressed in adipocytes, macrophages, and steroidogenic cells (Larigauderie *et al.* 2004; Forcheron *et al.* 2005; Tanigawa *et al.* 2008; Buers *et al.* 2009). As an LD-coating phosphoprotein, it is found on the LD surface (Larigauderie *et al.* 2004; Meadows *et al.* 2005; Forcheron *et al.* 2005). Its expression on cells is thought to be regulated by lipids, specifically FAs, via the activation of PPAR-γ (Forcheron *et al.* 2005; Guilherme *et al.* 2008).

There is evidence suggesting that perilipin is involved in hydrolysis of TGs, and that its activity can be modified by phosphorylation (Larigauderie *et al.* 2004; Meadows *et al.* 2005; Forcheron *et al.* 2005; Guilherme *et al.* 2008). In the basal state, non-phosphorylated perilipin was shown to suppress lipolysis of TGs by blocking the access of HSL to the surface of LDs (Larigauderie *et al.* 2004). When lipolysis is stimulated, the phosphorylated perilipin allows the access of activated HSL to the surface, allowing lipolysis to take place (Meadows *et al.* 2005; Forcheron *et al.* 2005; Guilherme *et al.* 2008).

ADRP, initially described in adipocytes, is ubiquitously expressed and it is considered to be a marker for LDs and lipid accumulation (Wang *et al.* 1999; Hodgkinson and Ye 2003; Larigauderie *et al.* 2006; Bozza *et al.* 2007; Tanigawa *et al.* 2008). It is the most prominent LD-associated protein expressed in macrophages and it is found both at the LD surface and within its lipid core (D'Avila *et al.* 2006; Wan *et al.* 2007; Buers *et al.* 2009; Almeida *et al.* 2009; Gu *et al.* 2010). Neutral lipid staining and ADRP immunolabelling were shown to co-localise, with ADRP forming a ring around

the lipid core (Robenek *et al.* 2006), suggesting that ADRP might have a role in protecting the LDs from the action of cholesterol esterases such as HSL (Larigauderie *et al.* 2004; Wan *et al.* 2007).

ADRP has been implicated in the uptake and transport of FAs, binding of FAs and cholesterol, and storage of neutral lipids (Meadows *et al.* 2005; Robenek *et al.* 2006; Bozza *et al.* 2007; Paul *et al.* 2008; Feingold *et al.* 2010). The protein is thought to induce the accumulation of TGs by promoting the incorporation of Acyl-CoA into TGs, and by inhibiting the FA *β*-oxidation (Larigauderie *et al.* 2006). It is therefore considered to have a rate-limiting role in the process of TG accumulation in cells (Larigauderie *et al.* 2006). In human macrophages, the expression and stability of this protein was shown to be up-regulated by modified forms of LDL, such as OxLDL and AcLDL, as well as synthetic agonists of PPAR-*γ* and PPAR-*δ* (Hodgkinson and Ye 2003; Larigauderie *et al.* 2006; Guilherme *et al.* 2008; Paul *et al.* 2008).

The third protein of the PAT family, TIP47, was first described as a cytosolic protein interacting with the cytoplasmic domains of the cation-independent and cation-dependent mannose-6-phosphate receptors (Buers *et al.* 2009; Gu *et al.* 2010). Later studies showed that the protein was not restricted to the cytosol, and like ADRP, could also be found at the surface and the core of LDs in a variety of cells, including macrophages (Wan *et al.* 2007; Buers *et al.* 2009). The C-terminal PAT domain of ADRP and TIP47 is highly conserved, suggesting a possible role of TIP47 in binding lipids (Buers *et al.* 2009).

This protein was shown to act as a lipid cargo protein, involved in the binding and transport of FAs and the subsequent accumulation of TGs (Gu *et al.* 2010), as overexpression of TIP47 led to increased TG levels, whereas suppression of TIP47 expression was accompanied by a decrease in the cellular TG content (Buers *et al.*

2009). A protein responsible for the final step of TG biosynthesis, Diglyceride Acyltransferase (DGAT), was found to co-localise with TIP47 on the LD monolayer, suggesting cooperation of these two proteins during the process of TG accumulation and LD formation (Buers *et al.* 2009).

TIP47 was also shown to replace ADRP on the LD surface after lipid loading of ADRP-knockdown macrophages, and this was followed by an increase in cellular TG levels, suggesting that TIP47 might compensate for the lack of ADRP (Buers *et al.* 2009).

1.11.2. Lipid Droplets and Foam Cell Formation

It is believed that PAT proteins play an important role in the storage of lipids in LDs, and therefore could contribute to the transformation of macrophages into foam cells (Forcheron *et al.* 2005). The expression of perilipin and ADRP was shown to be increased after loading of human monocytes-macrophages with lipids, such as OxLDL or AcLDL (Forcheron *et al.* 2005; Paul *et al.* 2008; Buers *et al.* 2009). On the contrary, OxLDL was shown to have no effect on the expression of TIP47 (Gu *et al.* 2010).

Overexpression of either ADRP or perilipin in THP-1 macrophages was related to increased TG and CE accumulation and storage (Meadows *et al.* 2005; Forcheron *et al.* 2005; Larigauderie *et al.* 2006; Tanigawa *et al.* 2008). This was shown to inhibit the efflux of cholesterol from cells, since less FC was available for efflux (Larigauderie *et al.* 2004; Feingold *et al.* 2010). Absence of ADRP in THP-1 macrophages almost abolished foam cell formation *in vitro*, mainly because of decreased CE and TG accumulation (Paul *et al.* 2008; Tanigawa *et al.* 2008; Buers *et al.* 2009; Feingold *et al.* 2010).

Both perilipin and ADRP were detected in the arterial wall, and their expression was shown to be up-regulated in atherosclerotic lesions, mainly in macrophage foam cells

(Wang *et al.* 1999; Forcheron *et al.* 2005; Paul *et al.* 2008; Tanigawa *et al.* 2008; Feingold *et al.* 2010). ADRP deficiency was shown to inhibit atherosclerosis development in Apo-$E^{-/-}$ mice (Gu *et al.* 2010).

Even though LD-associated proteins have been closely related to the formation of foam cells, little is known about the exact mechanism by which these proteins promote this process. Given their roles in LD biology, it could be assumed that these proteins might be involved in the transport of lipids and their subsequent storage in LDs, as well as the regulation of lipolysis by protecting LDs from active lipases (Forcheron *et al.* 2005; Guilherme *et al.* 2008).

The expression of LD-associated proteins was also shown to be partly regulated by TLRs. Activation of TLR4 by LPS was shown to induce the expression of ADRP, both *in vitro* and *in vivo*, and the formation of numerous LDs (Schmitz and Grandl 2009) which correlated with enhanced generation of pro-inflammatory mediators (Pacheco *et al.* 2002; Gu *et al.* 2010). Other known TLR ligands, such as zymosan and Poly I:C were also shown to induce the expression of ADRP, although to a lesser extent (Feingold *et al.* 2010). TIP47 expression was shown to be up-regulated by TLR9, through the c-Jun N-terminal kinase (JNK) and Phosphatidylinositide 3-kinase (PI3K) pathways (Gu *et al.* 2010).

Both mRNA and protein expression of ADRP and perilipin where shown to be increased after infection of THP-1 macrophages with *Mycobacterium leprae*. This was accompanied by the formation of LDs, which are thought to be used by the infective agent as a source of nutrients for intracellular survival (D'Avila *et al.* 2006; Tanigawa *et al.* 2008). The process of LD formation induced by mycobacteria was later shown to be independent of pathogen ingestion, and was linked to pathogen- and ligand-initiated receptor-mediated pathways (D'Avila *et al.* 2006; Wan *et al.* 2007).

The potential roles that LD synthesis pathways play in the formation of foam cells are little studied, and the stimuli that promote their formation are poorly understood.

1.12. Contribution of bacteria to atherosclerosis

Reports suggesting that infectious agents could play a role in the development of CVDs have existed for more than 100 years ago. Hektoen, in the late 1800s, described how infection of the arterial wall and subsequent degenerative changes, including the formation of lesions, could occur following infection with tuberculosis (Hektoen 1896). After the turn of the 20th century, the co-existence of tuberculosis and atherosclerosis was reported by Sir. William Olser (Michelsen *et al.* 2004a). More recently, several epidemiological studies have shown that subjects with chronic infections, such as those caused by *Helicobacter pylori*, Epstein-Barr virus (EBV), Cytomegalovirus (CMV), Human Immunodeficiency virus (HIV), Herpes Simplex virus 1 and 2 (HSV1/HSV2), or hepatitis B or C had a significantly higher risk of developing atherosclerosis compared to subjects with no chronic infections (Boekholdt *et al.* 2003; Ott *et al.* 2006; Rigamonti *et al.* 2008; Vikatmaa *et al.* 2009; Feng *et al.* 2010; Wang *et al.* 2011).

The idea that infectious agents could be related to the development of CVD received renewed interest when in 1988, Saikku *et al.* identified the presence of the obligate intracellular Gram-negative bacterium *Chlamydia pneumoniae*, in human coronary atherosclerotic lesions (Michelsen *et al.* 2004a; Vikatmaa *et al.* 2009). Since then, a number of human and animal studies have confirmed the seroepidemiological link between *C. pneumoniae* and atherosclerotic disease (Funk *et al.* 1993; Baranova *et al.* 2002; Bulut *et al.* 2002; Kazemi *et al.* 2005; Cao *et al.* 2007; Chen *et al.* 2009).

Many studies have reported the detection of *C. pneumoniae* within atherosclerotic lesions but not in healthy, adjacent tissue, by a variety of techniques including PCR, immunostaining, ELISA, and electron microscopy (Libby *et al.* 2002; Castrillo *et al.* 2003; Cao *et al.* 2007; Vikatmaa *et al.* 2009). Suggested important virulence factors include chlamydial LPS (cLPS) and chlamydial heat-shock proteins (cHSPs), the

presence of which has been reported in both serum and atherosclerotic lesions (Xu *et al.* 2001; Libby *et al.* 2002; Vikatmaa *et al.* 2009).

C. pneumoniae can infect and survive in endothelial cells, circulating monocytes and macrophages, as well as SMCs (Chen *et al.* 2009). It is thought that circulating monocytes or infected macrophages from sites of chronic infection could transport *C. pneumoniae* to the developing lesion through the endothelium, triggering endothelial dysfunction, and production of pro-inflammatory mediators (Castrillo *et al.* 2003; Kazemi *et al.* 2005; He *et al.* 2009; Wiesner *et al.* 2010).

However, although inoculation with *C. pneumoniae* was shown to promote atherosclerosis in animal models (Blessing *et al.* 2001; Engelmann *et al.* 2006), and that this could be reversed by anti-chlamydial agents (Muhlestein *et al.* 1998), the results obtained from human clinical trials of antibiotic treatments for coronary artery disease failed to show a beneficial effect (Liu and Waters 2005; Segers *et al.* 2008; Wang *et al.* 2011).

Studies in germ-free hyperlipidaemic mice showing that micro-organisms were not necessary for the development of atherosclerotic lesions in mice raised further doubt as to the potential of infection to modulate atherosclerosis (Wright *et al.* 2000). However, it has been suggested that these trials most likely failed because the antibiotics employed targeted only one type of microorganism, while evidence suggests that diverse forms of infection may promote atherogenesis, and that lifetime exposure to overall infectious burden is a more relevant contributor to cardiovascular risk than infection with individual organisms (Mayr *et al.* 2000; Kiechl *et al.* 2001; Segers *et al.* 2008; Renko *et al.* 2008).

Chronic dental infections, such as periodontitis, are also considered as a risk factor for the development of CVDs (Ott *et al.* 2006), since they have been associated with

acute myocardial infarction and infective endocarditis (Funk *et al.* 1993; Lockhart *et al.* 2008; Koren *et al.* 2011). Studies in Apo-$E^{-/-}$ mice showed that infection with *Porphyromonas gingivalis,* a Gram-negative bacterium implicated in periodontal disease, increased atherosclerosis (Tobias and Curtiss 2005; Renko *et al.* 2008; Feng *et al.* 2010).

The pro-atherogenic changes reported in subjects with periodontitis are thought to be mediated by the bacterial LPS, whose serum levels were shown to be elevated during the infection (Feingold *et al.* 2010). *P. gingivalis*-induced acceleration of atherosclerosis is thought to be linked to the activation of TLRs, mainly TLR2, and the subsequent induction of the NF-κB pathway, via a MyD88-p38 MAPK pathway (Lin *et al.* 2010; Yu *et al.* 2010).

The presence of bacterial signatures in atherosclerotic plaques has been reported by different groups via broad range 16S rDNA PCR, which utilises primers recognising conserved sequences of bacterial genes encoding ribosomal RNA (Erridge *et al.* 2008a; Renko *et al.* 2008; Koren *et al.* 2011). Remarkably, a broad spectrum of different bacterial genera has been identified in human atheroma using such techniques, including common pathogens, environmental organisms and commensal bacteria (Ott *et al.* 2006; Renko *et al.* 2008; Koren *et al.* 2011). For example, frequently identified sequences are derived from *Staphylococcus* species, *Streptococcus* species, *Klebsiella pneumoniae* and *Proteus vulgaris* (Ott *et al.* 2006; Koren *et al.* 2011). Crucially, however, these DNA signatures appear to reflect bacterial remnants, and do not indicate active infection of the artery wall, as viable organisms are only very rarely cultivable from isolated plaque material (Meijer *et al.* 2000; Liu and Waters 2005). These data supports the “pathogen burden hypothesis” whereby more than one specific pathogen might be involved in the process of atherogenesis (Ott *et al.* 2006; Renko *et al.* 2008).

Bacterial products have been considered attractive candidates with roles in promoting atherosclerosis and inducing inflammation. Such molecules are shed by all growing and dividing bacteria, including commensals, and a number of these retain inflammatory and atherogenic properties independently of bacteria viability. Experimental administration of purified PAMPs or heat-killed bacteria to animal models of atherosclerosis was shown to result in increased lesion formation (Lehr *et al.* 2001; Mullick *et al.* 2005; Westerterp *et al.* 2007; Madan and Amar 2008). A variety of bacterial antigens have been detected in human atherosclerotic lesions by immunohistochemistry, further supporting the notion that bacterial PAMPs rather than live bacteria themselves might have a more significant impact in the process of atherogenesis (Laman *et al.* 2002)

Many recent clinical and experimental studies have highlighted the importance of transient, low grade bacteraemia in the context of atherosclerosis development (Wiesner *et al.* 2010). Apart from infections, other factors such as cigarette smoking, obesity, and type II diabetes can increase exposure to endotoxin (Erridge 2008). Transient bacteraemia is common after local infections, surgical procedures, as well as after common everyday procedures such as tooth brushing (Lockhart *et al.* 2008). In health, circulating levels of endotoxin are low (< 1 pg/ ml), but can be significantly increased in subjects at risk of, or harbouring, CAD (Wiedermann *et al.* 1999; Pussinen *et al.* 2007).

The occurrence of transient bacteraemia after vigorous tooth brushing was reported in a study conducted by Bhanji *et al.* (2002). Later, in a study performed by Lockhart *et al.* (2008), it was reported that the overall incidence of bacteraemia after tooth brushing was 32%, with around 9% of the subjects being bacteraemic as long as 60 minutes after the procedure. Taking into account the professional guidelines recommending tooth

brushing at least two times a day, it has been suggested that the risk of bacteraemia after tooth brushing is similar to that occurring after dental extraction (Lockhart *et al.* 2008).

Increasing evidence suggests the contribution of commensals in the induction of low grade endotoxaemia. The human intestinal flora is a diverse ecosystem which confers benefits on the host by aiding digestion, synthesising vitamins and protecting against pathogen invasion (Wang *et al.* 2011). The tight epithelial junctions, in conjunction with mucous flow serve as a filtering system to limit the entry of gut-derived bacterial products into the circulation. However, there is evidence to suggest that a small proportion of these biologically active bacterial products can translocate into the circulation (Ghoshal *et al.* 2009; Wiesner *et al.* 2010), particularly following ingestion of high-fat meals (Erridge *et al.* 2007; Ghoshal *et al.* 2009; Ghanim *et al.* 2010; Harte *et al.* 2012).

Although infections alone do not seem to be sufficient to cause atherosclerosis, the presence of certain microbial agents might be significant in aggravating or activating lesions (Edfeldt *et al.* 2002; Koren *et al.* 2011). Circulating endotoxins and inflammatory cytokines produced during chronic extra- and intra-vascular infections could provide inflammatory stimuli that influence and enhance atherosclerosis (Libby *et al.* 2002; Feng *et al.* 2010; Wiesner *et al.* 2010).

It remains unclear what effect bacteria commonly found in plaques might have on macrophage lipid metabolism and foam cell formation. This study was performed in order to examine whether or not these human atheroma-associated bacteria or their related products could promote the transformation of murine or human macrophages into foam cells, and if so, the potential mechanisms involved in this process. We particularly focused on TLR signalling and the transcriptional regulation of pathways involved in lipid droplet formation and lipid metabolism.

PROJECT AIMS

The main aims of this project were:

1. To determine whether or not bacteria commonly associated with human atheroma can promote the formation of foam cells in human or mouse macrophages.
2. To develop a high throughput, automated method for the quantification of foam cell formation in cultured human and murine macrophages.
3. To establish the cellular and molecular mechanisms by which bacteria or their products promote the accumulation of lipids in macrophages.

2. MATERIALS & METHODS

Reagents

Unless otherwise stated, all reagents were supplied by Sigma-Aldrich, Poole, Dorset.

2.1. Maintenance and culture of cell-lines

The murine J774A.1 and RAW 264.7 macrophage cell lines were purchased from the European Collection of Cell Cultures (Cat nos. 91051511 and 91062702, respectively). L929 fibroblast (Cat no. 85011425), and HEK-293 epithelial (Cat no. 85120602) cell lines were also from ECACC. Virally transformed primary mouse macrophages from TLR2- and TLR4-deficient mice were kind gifts of Dr. Clare E. Bryant (University of Cambridge).

J774A.1 and RAW 264.7 macrophage cell lines were maintained in Dulbecco's Modified Eagle's Medium (DMEM) supplemented with 10% foetal calf serum (FCS), L-glutamine (1%) and plasmocin (0.01%) (Invivogen) at 37 ˚C, in a humidified incubator containing 5% CO_2. Cells were subcultured at 85% - 90% confluence by dislodging with sterile plastic scrapers (Greiner), transferred into 25 ml universal tubes and centrifuged at 400 g for 5 minutes. The cell pellet was resuspended in 10 ml of fresh culture medium and one twelfth of the suspension was removed to seed a new T75 flask (referred to hereafter as splitting at 1:12). Remaining cells were plated in 6-, 24- or 96-well plates at various densities as described in subsequent sections.

The HEK-293 epithelial cell line and L929 fibroblast cell lines were maintained in DMEM supplemented with 10% FCS, L-glutamine (1%) and plasmocin (0.01%). Both cell lines were kept at 37 ˚C (5% CO_2). Cells were washed once with sterile PBS, and subcultured at 85% - 90% confluence by treating with trypsin/EDTA (0.25%) for 2 minutes. Complete detachment of cells was achieved by gently tapping the flask on the

sides, after which they were transferred into 25 ml universal tubes and centrifuged at 400 g for 5 minutes. The cell pellet was resuspended in 10 ml of fresh culture medium and a new T75 flask was seeded by spitting at 1:12.

Phosphate buffer saline (PBS) was prepared by dissolving 1 PBS buffer tablet (Oxoid) per 100 ml of distilled water. PBS used for cell culturing was sterilised by autoclaving (20 min, 120˚C). The solution was kept at room temperature (RT).

All handling of cells and related reagents was performed using strict sterile technique in a class II cell culture safety cabinet.

2.2. Cryopreservation and resuscitation of cell lines

A total of 5 T75 flasks were prepared for the process of cell line cryopreservation. Cells were subcultured at ~90% confluence by scraping or trypsin treatment, transferred into 3 50 ml tubes and centrifuged at 400 g for 5 minutes. The cell pellet in one tube was resuspended in 15 ml of freezing medium (90% FCS + 10% dimethyl sulphoxide – DMSO), after which the whole suspension was transferred into the next tube, and used to resuspend the cell pellet. The procedure was repeated until all three cell pellets were resuspended and collected into one single tube. The cell suspension was carefully divided into 15 cryovials (1 ml/ tube), and stored overnight at -80 ˚C in a cell freezer box to promote slow freezing and to avoid damage of cells by formation of ice crystals. The aliquots were then stored in liquid nitrogen.

For the resuscitation of cells, 25 ml of culture medium were transferred into a 50 ml tube and placed in a 37 ˚C waterbath for 30 minutes. The thawing procedure should be carried out quickly to optimize recovery of cells and to ensure a high proportion of cell survival. An aliquot of the stored stock cells was removed from liquid nitrogen and was immediately transferred into a 37 ˚C waterbath, until the cell suspension started to

defrost (< 1 minute). The tube was then transferred into a cell culture safety cabinet, and 500 μl of warm culture medium was slowly added to completely defrost the cell suspension. The defrosted aliquot was transferred into the remaining warm medium, and after gentle mixing, the content was transferred into a T75 flask, which was incubated overnight at 37 ˚C (5% CO_2). The medium was carefully removed the next day, and replaced with fresh culture medium. The flask was kept in the incubator until the cells were confluent enough to split them.

2.3. Isolation of mouse primary bone marrow-derived macrophages

C57BL/6 mice (male or female, age 10-12 weeks) were sacrificed and immediately immersed in 75% ethanol (EtOH) to sterilize external surfaces. Skin and tissue were removed from the legs and the lower part of the body, and the femoral bones were isolated from the rest of the body. All tissue and muscles were carefully dissected from the femoral bones, which were then immersed in 75% EtOH for 5 minutes, before being transferred to sterile PBS for 5 minutes and then RPMI-1640 supplemented with 1% penicillin / streptomycin until the next step. Bone scissors were used to carefully remove the knuckles from the ends of each bone, and bone marrow cells were isolated by flushing bone marrow growth medium (RPMI-1640 / 1% Pen / Strep / 5% heat-inactivated FCS / 10% L929-cell conditioned medium*) through the bone using a 27 gauge needle and a 1 ml syringe. Cells were plated in 6-well plates (2 ml / well) or 24-well plates (400 μl / well), and incubated at 37 ˚C (5% CO_2) for 3 days, after which the medium was changed and replaced with BMM “phi” growth medium (RPMI-1640 / 1% Pen / Strep / 10% heat-inactivated FCS / 10% L929-cell conditioned medium*). The medium was carefully changed every other day, and the cells were used for experiments on day 7.

*L929-cell conditioned medium was obtained by culturing L929 cells at an initial confluence of 50% for 5 days in RPMI-1640 supplemented with 10% FBS that had been heat-inactivated by a 30 minute incubation at 50 ˚C. The medium was then collected and filtered through a 0.22 μm filter, and stored in aliquots at -20 ˚C (Weischenfeldt and Porse 2008).

2.4. Culture of primary human monocytes and generation of primary human macrophages

Recruited human volunteers were asked to sign a consent form with approval from the University of Leicester Research Ethics Committee. On the day of the experiment, blood was collected from a vein of the forearm by an experienced phlebotomist into citrate-containing vacutainer blood collection tubes (Bunzl), and a vacutainer with no additives for the collection of serum from each individual (autologous serum). The citrated blood was used for the isolation of peripheral blood mononuclear cells (PBMCs), which include lymphocytes, monocytes, and phagocytes.

Citrated blood was diluted in an equal volume of sterile PBS, and PBMCs were separated by density gradient centrifugation at 800 g for 25 minutes at 21 ˚C (acc: 5 / dec: 2, with Beckman Coulter Allegra X-22R) using Histopaque-1077 (polysucrose, 5.7 g/ dl, and sodium diatrizoate, 9.0 g/ dl). With this technique, red blood cells (RBCs) and granulocytes form a pellet at the bottom of the tube. PBMCs were carefully collected from the PBMC-containing interphase located between the plasma (top) and the Histopaque layer (bottom) into clean tubes, washed twice in sterile PBS by centrifuging at 300 g for 5 minutes (21 ˚C; acc: 9 / dec: 9), and cell pellets were resuspended in RPMI-1640 medium (no serum). Cells were plated at a density of 1 x 10^6 cells per well of 96-well plates or 3 x 10^6 cells per well of 24-well plates or 6-well plates, and

incubated for 2 hours at 37 ˚C. Non-adherent cells were removed by several gentle washes with RPMI-1640. The last wash was replaced with RPMI-1640 supplemented with 5% autologous serum*, and cells were incubated at 37 ˚C (5% CO_2), where they were kept untouched for three days. The medium was then carefully changed every 2-3 days, trying not to disturb the cell monolayer. Monocytes were kept in culture for a week, after which monocyte-derived macrophages were used in our experiments.

*Blood collected into the vacutainer with no additives was centrifuged at 800 g for 25 minutes at 21 ˚C (acc: 5 / dec: 2). The layer of serum formed on top of the clotted blood was carefully collected into clean Eppendorf tubes, and kept at -20 ˚C.

2.5. Preparation of heat-killed bacteria

A panel of bacteria was selected for study based on earlier reports of the presence of these organisms in human atherosclerotic lesions (Ott *et al.* 2006; Erridge *et al.* 2008a; Renko *et al.* 2008), as summarised in Table 2.1. Cultures of each type of bacteria were grown in Luria broth (LB) overnight in a shaking incubator (160 rpm) at 37 ˚C. An aliquot of each bacterial culture was then plated on LB-agar plates and cultured overnight at 37 ˚C to ensure growth of the correct bacteria.

Bacteria were then washed by supplementation with PBS to 15 ml and centrifuged at 800 g for 20 minutes. The bacterial pellet was resuspended in PBS and washed again under the same conditions. The pellet was then resuspended in 5 ml PBS and aliquoted into 1.5 ml Eppendorf tubes. Bacterial cells in these aliquots were then heat-killed using a heat block at a temperature of 100 ˚C for 15 minutes, and allowed to cool before storage at -20 ˚C. To quantify the bacterial cell concentration in each preparation, the optical density (OD) of each sample was measured at 600 nm, and background-corrected against PBS (used as blank). These data were then used to calculate the

amount needed for preparing stock aliquots using the established approximation of 1 absorbance unit at 600 nm being equivalent to 10^9 bacteria / ml. Stocks of each bacterium were prepared in sterile PBS at a final concentration of 10^8 bacteria / ml and stored at -20 °C before use in experiments.

Table 2.1. List of the bacteria used in the experiments.

BACTERIA	
Gram-positive	**Gram-negative**
Staphylococcus aureus (Sa)	*Acinetobacter baumannii* (Ab)
Staphylococcus epidermidis (Se)	*Escherichia coli* (Ec)
Streptococcus salivarius (Ss)	*Klebsiella pneumoniae* (Kp)
	Proteus vulgaris (Pv)
	Pseudomonas aeruginosa (Pa)
	Pseudomonas diminuta (Pd)

2.6. Challenge of monocytes or macrophages for assay of foam cell formation

To examine how bacteria or PAMPs promote cellular accumulation of lipid droplets, J774A.1 macrophages were plated in either 96-well plates (0.5 - 1 x 10^5 cells / ml, depending on required culture time) or 24-well plates (1 - 4 x 10^5 cells/ml, depending on required culture time), incubated overnight, and then treated with different heat-killed bacteria, or purified bacterial PAMPs, at concentrations as described in the relevant results chapters. In most experiments, cells were exposed to PAMPs or bacteria in DMEM / 10% FCS without LDL supplementation. In some experiments (as indicated subsequently), medium was supplemented with native LDL (nLDL) (Biomedical Technologies - BTI) at 5-30 μg/ ml. The culture medium was removed from each well before the challenge preparations were added to the cells. Gram-negative bacterial preparations were used at 10^4 or 10^5 bacteria / ml, and Gram-positive bacteria at 10^5 or 10^6 bacteria / ml, since pilot experiments revealed that higher concentrations of bacteria induced cell death and detachment. PAMPs were used at concentrations ranging from

0.01 - 1000 ng/ ml, with the exception of Poly I:C and CpG DNA which were used at 0.1- 10,000 ng/ ml. The PAMPs used in these studies were sourced from Invivogen and are listed in Table 2.2. Cells were incubated at 37 ˚C in 5% CO_2 for 24, 48 or 72 hours prior to quantification of foam cell formation by light microscopy or flow cytometry as described in sections 2.7 and 2.8 respectively.

For treatment of mouse primary BMDM, cells were treated with medium alone, acetylated LDL (AcLDL) or oxidised LDL (OxLDL) (30 μg/ ml) for 24 hours, or 10^5 *E. coli* / ml for 24, 48, and 72 hours in RPMI-1640 containing 5% FCS, and stained with Oil Red-O for examination by light microscopy, as described in section 2.7.

To measure foam cell formation from monocytes in human whole blood, citrated venous human blood was collected from healthy human volunteers, as described in section 2.4. 3 ml aliquots of whole blood were treated with 1 μg/ ml of selective PAMPs, or 10^6 *K. pneumoniae* or *S. salivarius* / ml for 30 minutes at 37 ˚C. PBMCs were then prepared immediately from the treated blood as described in section 2.4. Plated monocytes were incubated overnight (18 hours) in RPMI-1640 / 5% autologous serum at 37 ˚C (5% CO_2), and foam cell formation was quantified by light microscopy of Oil Red- O stained monocytes, as described below.

Table 2.2. List of the PAMPs used in the experiments.

PAMPs	
Pam_3CSK_4	TLR1/TLR2 agonist – Synthetic triacylated lipoprotein
FSL-1	TLR2/TLR6 agonist – Synthetic diacylated lipoprotein
Poly I:C	TLR3 agonist - Polyinosine-polycytidylic acid – synthetic analogue of dsRNA
LPS	TLR4 agonist – Lipopolysaccharide from *E. coli* (O111:B4)
Flagellin	TLR5 agonist – Flagellin from *S. typhimurium*
CpG DNA	TLR9 agonist – bacterial CpG-containing DNA

2.7. Quantification of foam cell formation by light microscopy

Macrophage lipid content was visualised by staining cells with the lipophilic stain Oil Red-O. Oil Red-O working solution was prepared by mixing Oil Red-O stock solution (500 mg Oil Red-O powder in 100 ml isopropanol, stored at RT in the dark) with H_2O (3:2 vol:vol), followed by a 10 minute incubation in the dark and 0.22 μm filtration. Cells were washed in PBS, fixed with 4% w/vol paraformaldehyde (PFA) in PBS for 10 minutes at 4 ˚C, after which they were washed twice with PBS, and incubated with Oil Red-O working solution for 30 minutes in the dark. The cells were then washed three times in PBS and examined at 40x magnification on a Nikon Eclipse TE2000-E inverted microscope. The Volocity Acquisition software (PerkinElmer) was used to acquire and analyse images. Alternatively, the EVOS xl light microscope (AMG) was used. A minimum of five images were captured per well, and total cells per field and foam cells, defined as those cells containing equal to or more than ten Oil Red-O positive lipid droplets (≥10) per cell, were counted manually. When primary cells, such as mouse BMDMs or human monocytes, were stained, an additional fixing step was performed before the first PBS wash, by adding an equal volume of 4% w/vol PFA directly into the medium for 10 minutes, after which the normal protocol was followed, reducing the two in between washing steps down to one and two times respectively.

2.8. Quantification of foam cell formation by flow cytometry

Foam cell formation was also quantified by flow cytometry, which is a technique most commonly employed for the sorting, counting, and phenotypic examination of particles, such as cells, within a heterogeneous suspension. It involves the analysis of the light scatter and fluorescence properties of these particles as they pass through a laser within a narrow stream of fluid termed the laminar flow. Cells are injected into a

flowing stream of sheath fluid, and the stream is compressed to approximately one cell diameter through a process known as hydrodynamic focusing, which allows single cells to be passed through the path of a focussed laser beam. Flow cytometers are equipped with lasers producing a fixed, single wavelength for excitation. Light scatter properties are analysed using two parameters: the forward angle light scatter (FS) and the right angle light scatter or side scatter (SS). FS is measured at a narrow angle (<10˚) from the laser beam direction, and it is used to give an indication of particle size. SS is measured at a right angle (90˚ deflection) to the laser beam, and allows a measure of cellular granularity or complexity, thereby serving to aid separation by cell structure or type. The emitted individual fluorescent signals are separated by dichroic lenses and emission filters and collected through optical or electronic detectors or photomultiplier tubes (PMTs). They are then converted into electrical pulses and processed by a series of linear and log amplifiers. Based on the fluorescence intensity originally detected by the PMT's, each event is assigned a channel number on either a one or two parameter histogram, and it is individually correlated for all the parameters of interest. The obtained data is displayed as events on histograms or dot plots using Multiparameter Acquisition and Display software platforms. Each of these histograms can be analysed statistically to calculate the percentages of negative and/or positive staining cells, as well as the mean fluorescence intensity. It is also possible to apply gates on a histogram for further sub-population analysis.

Flow cytometric quantification of foam cell formation was performed using the lipophilic fluorescent dye Nile Red (9-diethylamino-5H-benzo[α]phenoxazine-5-one or Nile Blue oxazone), a red benzophenoxazone dye. The emission spectra of Nile Red depend on the polarity of the solvent it is dissolved into, and can range from golden-yellow to deep red. Because of its ability to stain neutral lipids such as cholesterol esters

or triglycerides, it is widely used as a lipophilic dye for the detection of intracellular cytoplasmic lipid droplets. Nile Red stock solution was prepared by dissolving 10 mg of Nile Red powder in 10 ml acetone for a 1 mg/ ml stock solution.

After being fixed with 4% w/vol PFA (as above), cells were stained with 10 μg / ml Nile Red (1:100 dilution of 1 mg/ ml stock solution) in PBS for 20 minutes in the dark. Cells were washed twice in PBS and resuspended by gentle agitation with the rubber end of a 1 ml syringe plunger. Fluorescence of cells was measured using a Coulter Epics MCL-XL flow cytometer (Beckman Coulter). Cells cultured in medium alone were assigned 2% positivity by adjustment of the threshold of positivity on the FL1 FITC channel. Percentages of positive cells along with mean fluorescence intensity (MFI) were recorded.

2.9. Three-colour fluorescence microscopy of macrophages

In some experiments, co-localisation of cellular lipid droplets, actin and nuclear DNA were visualised by three-colour fluorescence microscopy. Medium was removed and cells were gently washed with PBS before fixation with 4% PFA / PBS for 10 minutes as described above. After a gentle washing step the cells were permeabilized with 0.4% saponin in PBS for 15 minutes at RT, incubated with 0.5% BSA in PBS for 20 minutes at RT, and actin was stained by addition of 1/50th volume of working FITC-Phalloidin stock (500 μg/ ml in DMSO – 100x stock) and incubation for 1.5 hours at RT in the dark. After the incubation, the cells were washed 3x with 0.5% BSA / PBS and 1x with PBS and counterstained with Nile Red (1:100 of stock solution) and 4',6-diamidino-2-phenylindole (DAPI) (1:8,000) (1 mg/ ml in H_2O) for 30 minutes in the dark at RT. The cells were then washed 3x with 0.5% BSA / PBS and 1x with PBS and kept in the dark at 4 ˚C until visualisation using an EVOS xl light microscope (AMG) at

20x - 40x magnification. Three images were captured for each field, corresponding to actin (FITC-channel, green), Nile-red (red fluorescent protein (RFP)-channel, red), and DAPI (ultraviolet-channel, blue). Merged images were then prepared from the three independent images of the same field using the EVOS microscope software.

2.10. Biochemical assay of macrophage cholesterol content

Quantification of cholesterol content was performed using the Amplex Red Cholesterol assay kit (Invitrogen – Molecular Probes). The assay is based on an enzyme-coupled reaction, which enables the detection of both free cholesterol and cholesterol esters. Cholesterol esters present in a sample are hydrolysed by cholesterol esterase into cholesterol, which is then oxidised to the corresponding ketone (cholest-4-en-3-one) and hydrogen peroxide (H_2O_2) by the enzyme cholesterol oxidase. The produced H_2O_2 is detected using a very sensitive and stable probe for H_2O_2 termed 10-acetyl-3,7-dihydroxyphenoxazine (Amplex Red reagent). The reaction of the Amplex Red reagent with H_2O_2 takes place in the presence of HRP and results in the production of a highly fluorescent compound called resorufin (absorption: 571 nm; fluorescence emission: 585 nm).

To measure cellular cholesterol content, J774A.1 macrophages plated at a density of 4 x 10^5 cells/ well of a 24-well plate were challenged with medium alone or different concentrations of *E. coli* (10^3 - 10^5/ ml), or TLR stimulants (100 ng/ ml), in the presence of 30 μg/ ml nLDL for 48 hours prior to assay. The cells were then washed once with PBS and fixed with 0.5% PFA / PBS for 10 minutes at 4 ˚C. After two further washes with PBS, 160 μl of absolute ethanol was added to each well, and the plate was placed on a rocker at 4 ˚C for 30 minutes for the extraction of cellular lipids. Lipid extracts were transferred into Eppendorf tubes and stored at -20 ˚C or used immediately.

The cholesterol assay was carried out according to the manufacturer's instructions. Briefly, a cholesterol standard curve was prepared in a clear bottom, opaque walled luminometer plate (Greiner) by mixing 250 μl of 20% ethanol in 1x reaction buffer (RB) (0.5 M potassium phosphate, pH 7.4, 0.25 M NaCl, 25 mM cholic acid, 0.5% Triton X-100) with 1 μl of cholesterol standard, for a starting concentration of 8 μg/ ml (20 μM). 2-fold serial dilutions of this were then performed over a further 10 wells in 1x RB / 20% ethanol. A negative control containing no cholesterol (1x RB / 20% ethanol only) was also included. Total cholesterol (TC) and free cholesterol (FC) content were measured for each sample in two designated halves of the measurement plate (section 1 and 2 respectively). In each case, 10 μl of cellular lipid extracts in 100% ethanol were diluted in 40 μl of 1x RB. Amplex Red working solution (300 μM 1x Amplex Red reagent, 2U/ ml 1x HRP, 2U/ ml 1x cholesterol oxidase) containing 2U/ ml of 1x cholesterol esterase was added to the standard curve and sample section 1; while Amplex Red working solution containing no cholesterol esterase was added to sample section 2. The plate was incubated at 37 ºC in the dark for 30 minutes. Fluorescence was then measured with a NOVOstar microplate reader (BMG Labtech) using excitation at 560 nm and detection at 590 nm. The data was background corrected by subtracting the value derived from the negative control. The cholesterol content of each sample was determined using the equation obtained from the standard curve and was normalised to protein content measured as described below.

2.11. Protein Quantification by Bicinchoninic Acid (BCA) assay

In several experiments results were required to be normalised to cellular protein content. After the extraction of lipids, cell lysates were extracted in lysis buffer (0.1 M NaOH, 0.1% SDS in H_2O) for 30 minutes at RT before using a syringe plunger to

scrape remaining cellular residue into the lysis buffer. Protein was then measured in these extracts using the BCA protein assay kit (Thermo Scientific – Pierce). This assay is based on bicinchoninic acid (BCA), which allows the colorimetric detection and quantification of total protein in a sample. Copper (Cu^{+2}) present in the working reagent is reduced to Cu^{+} by protein in an alkaline medium (biuret reaction). The resulting cuprous cation interacts with two molecules of BCA resulting in the production of a purple-colored product, which exhibits a strong absorbance at 562 nm. Serial dilutions of known concentrations prepared from a common protein, such as bovine serum albumin (BSA), are used to determine the protein concentration of each unknown sample.

Standard curves were prepared from 2-fold serial dilutions of BSA in lysis buffer at a starting concentration of 2 mg/ ml in a 96-well plate. 25 μl of each cell extract was then transferred into empty wells on the same 96-well plate. The BCA working reagent was prepared by mixing 50 parts of BCA reagent A (sodium carbonate, sodium bicarbonate bicinchoninic acid, sodium tartrate in 0.1 M sodium hydroxide) with 1 part of BCA reagent B (4% cupric sulphate) (50:1, Reagent A:B). 200 μl of working reagent were then added to the standards and the samples in each well, and the plate was incubated for 30 minutes at 37 ºC. Absorbance was measured at 562 nm using the ELx800 absorbance microplate reader (BioTek) and protein concentrations were calculated relative to the standard curve prepared on the same plate.

2.12. TLR inhibition studies

To examine the effects of TLR inhibition on foam cell formation, J774A.1 macrophages were treated with 10^5 *K. pneumoniae*/ ml in DMEM / 10% FCS without LDL supplementation in the absence or presence of the specific TLR4 inhibitors

polymyxin B (PMB) (10 μg/ ml), TAK-242 (1 μg/ ml) or the TLR2 and TLR4 inhibitor oxidised 1-palmitoyl-2-arachidonyl-*sn*-glycero-3-phosphatidyl choline (OxPAPC, prepared as described below, 30 μg/ ml) for 24 hours at 37 ˚C. Alternatively, cells were treated for 72 hours at 37 ˚C (5% CO_2) with 10^6 *K. pneumoniae*/ ml in DMEM / 10% FCS in the presence of 3 μg/ ml of mouse monoclonal antibodies against TLR2 (T2.5) or TLR3 (TLR3.7) (Hycult Biotechnology). Foam cell formation was quantified by flow cytometry, as described in section 2.8.

The oxidation of the phospholipid 1-palmitoyl-2-arachidonyl-*sn*-glycero-3-phosphatidyl choline (PAPC) in air leads to the generation of a mixture of oxidised lipid species termed OxPAPC (Erridge *et al.* 2008b). OxPAPC was prepared by aliquoting 100 μl of 10 mg/ ml PAPC stock (stored at -80 ˚C in teflon top glass tubes) into a clean glass vial wrapped in aluminium foil. Aliquoted lipid was then dried to a uniform film under slow nitrogen passage. PAPC films were allowed to auto-oxidise in air at RT in the dark for 4 days, after which they were resuspended in 500 μl of chloroform ($CHCl_3$) to yield a stock OxPAPC solution of 2 mg/ ml, and stored as PAPC as described above. OxPAPC is a defined inhibitor of TLR2 and TLR4, but not other TLRs (Erridge *et al.* 2008b; Miller *et al.* 2011).

2.13. Scavenger receptor and antioxidant studies

To examine the contribution of LDL oxidation and scavenger receptor-dependent uptake of modified LDL particles in foam cell formation, J774A.1 macrophages were treated with Pam_3CSK_4 or LPS (1 ng/ ml), or 10^4 *E. coli*/ ml or 10^6 *S. epidermidis*/ ml in DMEM / 10% FCS in the absence of LDL supplementation, with or without the antioxidant butylated hydroxytoluene (BHT, 50 μM) or the scavenger receptor blocker

polyinosinic acid (PIA, 20 μg/ ml) for 72 hours at 37 ˚C (5% CO_2). Foam cell formation was quantified by flow cytometry, as described in section 2.8.

2.14. Measurement of foam cell formation in TLR-deficient macrophages

To test the hypothesis that TLRs might be involved in foam cell formation, we performed experiments using macrophages lacking TLR2 or TLR4, as previous studies conducted in Apo-$E^{-/-}$ or $LDLr^{-/-}$ mice lacking components of the TLR signalling pathway or the receptor itself showed resistance to foam cell formation even in the presence of specific TLR ligands (Björkbacka *et al.* 2004; Michelsen *et al.* 2004b; Schoneveld *et al.* 2008).

Virally transformed $TLR2^{-/-}$ and $TLR4^{-/-}$ macrophages from mouse macrophage cell-lines, each being immortalised lines from peritoneal macrophages derived from TLR2- or TLR4-deficient mice, were cultured in DMEM supplemented with 10% FCS, 1% L-glutamine and plasmocin, and subcultured as described for J774A.1 macrophages in section 2.1. Cells were plated at a density of 1 x 10^5 per well of 24-well plates and challenged with medium alone, nLDL (30 μg/ ml), and 10^5 *E. coli*/ ml with or without nLDL supplementation. The plates were incubated for 72 hours prior to Oil Red-O staining and light microscopy examination, as described in section 2.7.

2.15. Whole blood *E. coli* time-course experiment

To investigate the kinetics of bacteria-induced foam cell formation in human monocytes, we carried out a time-course experiment in whole blood in an attempt to determine a time point at which droplets begin to form. A total of three tubes of citrated venous blood were collected from healthy donors, as described in section 2.4. Blood was aliquoted into 12 wells of a 24-well plate, each containing 1 ml of blood, and

challenged with 10^6 *E. coli/* ml for 0, 1, 2, 3, 4, and 5 hours at 37 ˚C. The blood was then processed for analysis by Nile Red staining and flow cytometry. Briefly, 2 ml of BD FACS lysing solution (BD Biosciences) was mixed with 18 ml of distilled H_2O to prepare a 1x working stock. 200 μl of treated blood were mixed with 4 ml of 1x lysing solution in a 25 ml universal tube and incubated at RT in the dark for 10 minutes. PBS was used to top up the tubes to 25 ml and the samples were centrifuged at 300 g for 5 minutes. The cell pellets were resuspended in 1 ml of 1% PFA / PBS and fixed for 10 minutes at RT. Cells were then washed with PBS by centrifuging at 300 g for 5 minutes. The cell pellets were resuspended in 1 ml PBS and 500 μl of each sample were transferred into a second universal tube for staining. 2.5 μl of Nile Red stock solution was added into each tube, and the tubes were incubated for 20 minutes at RT in the dark. Cells were washed in PBS at 300 g for 5 minutes. The cell pellets were resuspended in 1 ml of PBS and were analysed by flow cytometry.

Sample analysis: A total of two (2) samples per person (unstained and stained) were analyzed on a Coulter Epics MCL-XL flow cytometer. The gate was set to cover and include the monocyte population based on characteristic forward and side scatter patterns (Figure 2.1). 2% positivity was assigned to unstained and Nile Red-stained samples from the 0 hour time point by gate adjustment of the FL1 FITC channel.

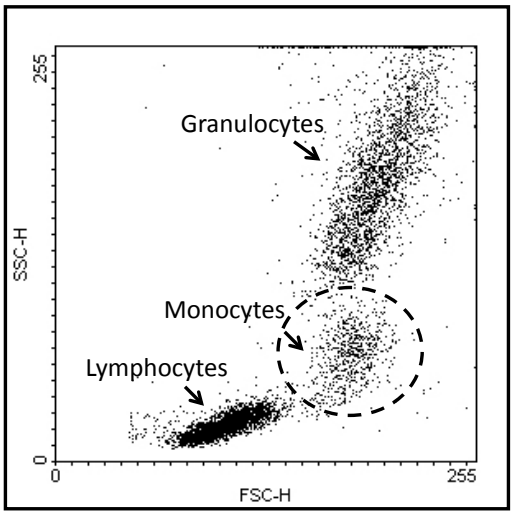

Figure 2.1. Light scatter diagram of white cell population from whole blood.

Separation of white cell populations from whole blood by size (Forward scatter - FS) and granularity (Side scatter - SS). Gate application on the histogram allows further sub-population analysis [Taken from: "Flow cytometry Workshop" – University of Leeds].

2.16. Quantification of LDL uptake by macrophages

As part of the experiments performed for the identification of the mechanisms of TLR-dependent lipid accumulation in macrophages, we investigated the effect of PAMPs on the LDL uptake by macrophages.

J774A.1 macrophages plated at a density of 3 x 10^5 cells per well of a 24-well plate were challenged with medium alone or Pam_3CSK_4 or LPS (1 μg/ ml) for 24 hours at 37 ˚C (5% CO_2). The following day the cells were incubated with 20 μg/ ml of the cell marker DiI-LDL (LDL labelled with 1,1'-dioctadecyl-3,3,3',3'-tetramethyl-indocarbocyanine perchlorate) (Biomedical Technologies - BTI) for 4 hours at 37 ˚C (5% CO_2). Foam cell formation was assessed with flow cytometry, as mentioned in section 2.8.

2.17. Quantification of cellular cholesterol efflux

It is believed that the process of reverse cholesterol transport (RCT) is decreased during the process of foam cell formation, contributing to the accumulation of lipids inside the cell (Forcheron *et al.* 2005; Rigamonti *et al.* 2008; Chinetti-Gbaguidi and Staels 2009; Lundberg and Hansson 2010). We therefore aimed to determine if TLR stimulants might have an effect on the RCT process. To address this, J774A.1 macrophages were plated at a density of 3 x 10^5 cells per well of 24-well plates (Day 1), and were left to attach for 7 hours at 37 ˚C (5% CO_2) before they were used for the experiment.

Radiolabelling: The ^{3}H-cholesterol aliquot needed for the experiment was prepared by mixing 60 μl of ^{3}H-cholesterol (1 mCi/ ml, Perkin-Elmer) with 1 ml of 100% EtOH into a 15 ml tube. The tube was placed into a heat block at 50 ˚C for 20 minutes and the sample was concentrated by drying it to a uniform film under slow nitrogen passage. Once dry, 50 μl of ethanol were added to the bottom of the tube, the tube was sealed with parafilm and placed in a 50 ˚C waterbath for 30 minutes.

Preparation of labelling medium: The labelling medium was prepared by resuspending the ^{3}H-cholesterol aliquot prepared above with 3 washes of 1 ml RPMI-1640 / 0.5% gentamicin / 1% FBS, and adding each wash to a second tube containing RPMI-1640 / 0.5% gentamicin / ACAT inhibitor CP113,818 (2 μg/ ml) (Sigma). The mixture was placed in a 37 ˚C waterbath for 15 minutes.

After the 7 hour incubation, the medium was removed from the plates and 0.5 ml of labelling media (RPMI-1640 / 0.5% gentamycin / 1% FBS / ACAT inhibitor (2 μg/ ml)/ ^{3}H-cholesterol (2 μCi/ ml)) was gently added to the cells. The plate was then incubated overnight at 37 ˚C.

On day 2, the labelling media was removed and the cells were washed with 0.5 ml warm wash buffer (DMEM / 14 mM HEPES). The wash buffer was then replaced with 0.5 ml of equilibration media (RPMI-1640 / 0.5% gentamicin / 0.2% BSA / ACAT inhibitor (2 μg/ ml) / cAMP (0.3 mM)). The plate was incubated for about 8 hours at 37 ˚C prior challenging the cells with 1 μg/ ml of Pam_3CSK_4 or LPS. All treatments were performed in duplicates. The plate was kept at 37 ˚C for a total of 24 hours.

On day 3, Apo-B-depleted serum was prepared from pooled human AB serum by precipitation of the Apo-B-containing lipoproteins with a polyethylene glycol solution (PEG 8000MW in glycine buffer) under sterile conditions. Briefly, human AB serum (100 μl) was incubated for 20 minutes at RT with 40 μl of 20% PEG solution. The samples were centrifuged for 30 minutes at 10,000 rpm at 4 ˚C, and the supernatant was carefully collected into clean tubes. Efflux medium containing Apo-B-depleted serum was prepared by aliquoting 1.25 ml of efflux medium (MEM-HEPES (no HCO_3^-) / ACAT inhibitor (2 μg/ ml) / cAMP (0.15 mM)) per sample and adding 35 μl of Apo-B-depleted serum to each aliquot. The remaining Apo-B-depleted serum was stored in a clean tube at 4 ˚C.

The equilibration medium was removed, the cells were washed with 0.5 ml warm wash buffer, and the wash buffer was then replaced with 0.5 ml of efflux medium containing the Apo-B-depleted serum. Efflux medium with no serum supplementation was used for T0 (measure of radiolabelled cholesterol taken up by the cell) and MEM (measure of passive efflux - fractional cholesterol efflux) background wells. The plate was incubated for 4 hours at 37 ˚C (no CO_2). After the incubation, 300 μl of media from each well was transferred to a 96-well microscreen filter plate (Merck Millipore) and the samples were filtered using a vacuum manifold unit. The rest of the media was removed from the wells and the cells were lysed in 0.5 ml 0.2 M NaOH / 0.1 % SDS for

30 minutes on a rocker at RT. 200 μl of filtered media were transferred into scintillation vials containing 5 ml of scintillation fluid (Scintiverse (TM) BD Cocktail, Fisher). The lysate from cells cultured in efflux media only was used for the T0 reading. Radioactivity was measured using a Packard 1500 Tri-Carb Liquid Scintillation Counter (Packard Instrument Co.) under the correct protocol. Measurements were recorded as counts per minute (CPM). Cholesterol efflux to HDL was calculated using the following formula:

$$\frac{\text{(Sample average – MEM average)}}{\text{T0 average}}$$

2.18. Measurement of cellular rate of pinocytosis

Pinocytosis is defined as the uptake of soluble molecules by a cell. To measure pinocytosis, horseradish peroxidase (HRP) was used as a fluid phase marker in this study. This compound requires H_2O_2 as an oxidising agent, and it is commonly used in immunohistochemistry, ELISA assays, or as antibody conjugates due to its colour-changing properties upon interaction with specific substrates. The concentration of HRP in a sample is proportional to the absorbance exhibited by the sample.

J774A.1 macrophages plated at a density of 4 x 10^5 cells per well of 24-well plates were washed once in PBS and challenged with 10^6 bacteria/ ml or different concentrations of Pam_3CSK_4 or LPS (0.1 – 1000 ng/ ml) in RPMI-1640 / 10% FCS. 5 μl of soluble Type II HRP (200 μg/ ml) were added into each well and the cells were incubated for 6 hours at 37 ˚C (5% CO_2). The baseline pinocytic capacity of the cells was also assessed by a 6-hour treatment with HRP alone in the absence of bacteria or PAMPs. Following the incubation, the cells were washed 4x with PBS and lysed in 250 μl of 0.1% SDS in dH_2O. Cells were scraped in the well and the lysates was passed

through a 0.9 mm needle. In a separate 96-well plate, 10-fold dilutions in PBS were performed to prepare an HRP standard curve with a starting concentration of 1 ng/ ml. 10 μl of a 1:10 dilution of the lysates in PBS were added to 90 μl of TMB substrate solution (1:1 mixture of H_2O_2 and Tetramethylbenzidine) in clean wells. The reaction was immediately stopped by adding 50 μl of 2% H_2SO_4. Absorbance was measured at 450 nm using the ELx800 absorbance microplate reader (BioTek).

An aliquot of the lysate was used for the BCA protein assay, as described in section 2.11, and the HRP concentration of each sample was calculated using the standard curve as a reference, and was normalised to the protein content.

2.19. TLR transfection assays for PAMP profiling

To examine the hypothesis that TLRs might be involved in bacteria-mediated accumulation of lipids in macrophages, we performed transfection assays in order to establish which types, if any, of TLR stimulants might be expressed by bacteria commonly found in atherosclerotic plaques. The assay is based on the luciferase assay system and makes use of specific enzymes belonging to the oxidative class of enzymes termed luciferases. In particular, “Firefly luciferase” derived from the firefly *Photinus pyralis,* was used for our experiments.

The chemical reaction catalysed by this enzyme consists of two steps. In the first step, luciferase induces the adenylation of the substrate D-luciferin by MgATP; this reaction leads to the formation of luciferyl adenylate and pyrophosphate. In the second step, luciferyl adenylate is oxidised by molecular oxygen and forms oxyluciferin and AMP. The formed oxyluciferin is in an electronically excited state, and transition to the ground state leads to the release of a light photon.

Because of this property, the enzyme is widely used in biological research. It is commonly used as a reporter gene to measure the activity of transcription factors in cells as a response to specific stimuli. The NF-κB-dependent luciferase reporter plasmid used in our experiments (pELAM-Luc) is composed of a luciferase gene which is under the control of an NF-κB-inducible ELAM-1 (endothelial leukocyte adhesion molecule-1) promoter. Transfection was achieved via the formation of vesicles termed liposomes. These vesicles are composed of a phospholipid bilayer with a region of aqueous solution in the middle, which enables them to carry both hydrophobic and hydrophilic substances. They are capable of delivering any encapsulated material inside the cell by fusion with the cell membrane. Human embryonic kidney cells (HEK-293) was the cell type preferred for this experiment not only because they are TLR-deficient, but also because they transfect readily with high efficiency.

Cell transfection: HEK-293 cells were maintained in DMEM supplemented with 10% FCS, 1% glutamine and plasmocin, and cultured as described in section 2.1. Transfection mixtures containing the NF-κB reporter plasmid pELAM-Luc, pCD14, and human plasmid constructs for TLR2, TLR4 (co-expressing MD-2), or TLR5 (Invivogen) were prepared in DMEM with no serum. GeneJuice (Merck) was used as the transfection reagent. DMEM / 0% serum was mixed briefly with Genejuice (1:27.6) by vortexing, and the mixtures were incubated at RT for 5 minutes to allow for liposome formation that would facilitate transfection. The plasmid constructs were defrosted in a 37 ˚C waterbath, and aliquoted into four tubes. Each tube contained 10 ng of the NF-κB reporter plasmid pELAM and 30 ng of plasmid encoding human CD14 per well, and one of the three human TLR plasmid constructs. pTLR2 was added at 10 ng per well; pTLR4/MD-2 and pTLR5 were added at 30 ng per well. The transfection mixtures were mixed by gentle pipetting, and used after approximately 10-40 minutes.

On the day of the experiment, HEK-293 cells were trypsinised, centrifuged at 400 g for 5 minutes, and the pellet was resuspended in 10 ml DMEM / 10% FCS. An aliquot was used to seed new flasks and the remaining cells were resuspended to a concentration of 3 x 10^5 cells/ ml. A 12 ml aliquot of this cell suspension was added into each transfection mixture tube prepared earlier. After mixing well, each mixture was plated at 100 μl per well in 96-well plates. The plates were incubated at 37 ˚C for 3 days before they were used for the experiments.

Sample plating: All the bacteria and PAMPs used in the experiment are shown in Table 2.1 and Table 2.2 respectively. DMEM supplemented with 1% FCS and 1% glutamine (D1) was used to prepare the challenge preparations. Bacteria were used at a final concentration of 10^6/ ml; PAMPs were used at a final concentration of 10 ng/ ml. Under sterile conditions in a class II cell culture safety cabinet, the challenge preparations were added to the cells (100 μl per well in triplicates), after the growth medium was carefully removed from each well. Control wells contained medium only. The plate was then incubated for 18 hours before analysis.

Cell lysis and luminometry: After the overnight incubation, the cells were lysed using a luminometry lysis buffer (25 mM Tris, 8mM $MgCl_2.6H_2O$, 1 mM DTT, 1% Triton X-100, glycerol, in H_2O – pH adjusted to 7.8 with phosphoric acid). The cells were then scraped into the wells using a pipette tip, and 40 μl of the lysed samples were transferred into clean clear-bottom luminometry plates (Greiner) with opaque wall wells. Luminescence was measured using a NOVOstar microplate reader (BMG Labtech), after it was primed with a luminometry firefly reagent (luminometry lysis buffer, 1 mM ATP, 0.25 mM Luciferin, 1% BSA).

Data Analysis: The results obtained were calculated as fold induction of the NF-κB reporter compared to cells cultured in medium alone (control).

2.20. Ribonucleic acid (RNA) extraction from cultured cells

For RNA extraction, human monocytes, isolated as described in section 2.4, were plated at a density of 3 x 10^6 cells per well of 6-well plates in RPMI-1640. After a 2 hour incubation, the cells were washed with RPMI-1640, and the remaining adherent monocytes were cultured in RPMI-1640 supplemented with 5% autologous serum. Medium was changed on the 3rd day, after which it was replaced every two days. On day 7, monocyte-derived macrophages were treated with medium alone, Pam_3CSK_4 or LPS (100 ng/ ml) in RPMI-1640 / 5% autologous serum for 24 or 48 hours, after which time total RNA was extracted. Alternatively, J774A.1 macrophages were plated at 3 x 10^5 cells/ well of 6-well plates and treated with medium alone, Pam_3CSK_4 or LPS (1 μg/ ml). Total RNA was extracted from cells at 0, 6, 24, or 48 hours using the RNeasy RNA miniprep kit (Qiagen) according to the manufacturer's instructions. The procedure involves the lysis and homogenisation of the cell samples with the use of a highly denaturing buffer that contains guanidine-thiocyanate. The buffer helps to inactivate RNases present in the lysate, resulting in purification of intact RNA. The added ethanol provides the appropriate binding conditions so when the sample is applied to an RNeasy Mini spin column, total RNA binds to the silica-based membrane where it is retained, while contaminants and smaller RNAs (< 200 nucleotides) are washed away during various centrifugation steps. The membrane-bound RNA can then be eluted in RNase-free water. Extracted RNA was quantified using a NanoDrop spectrophotometer.

2.21. Reverse transcription of RNA and cDNA preparation.

The extracted RNA was reverse transcribed to single-stranded cDNA using SuperScript-III Reverse Transcriptase (Invitrogen – Molecular Probes), according to the manufacturer's instructions. Briefly, for each sample a 20 μl reaction mix containing 1

μl Oligo-dT_{20} (2.5 µM final concentration), 1 μl 10 mM deoxyribonucleotide triphosphate (dNTP) mix (dATP, dTTP, dCTP, dGTP, 10 mM each, Promega), 10 pg - 5 μg total RNA (typically 8 μl) and 4 μl RNAse-free water was set up. The reaction mix was heated to 65 ˚C for 5 minutes using a heat block, and then incubated immediately on ice for 1 minute. 4 μl of 5x first strand buffer (250 mM Tris-HCl (pH 8.3), 375 mM KCl, 15 mM $MgCl_2$) were added to each reaction mix, together with 1 μl of 0.1 M Dithiothreitol (DTT), and 1 μl of SuperScript-III enzyme (200 U / μl). After a gentle mix, each tube was incubated at 50 ˚C for 1 hour to allow the reverse transcription reaction to take place. A second incubation at 70 ˚C for 15 minutes was then performed to inactivate the reaction enzymes. The resulting cDNA template was either stored at -20 ˚C, or used immediately in PCR reactions.

2.22. Real - Time Polymerase Chain Reaction (RT- PCR)

Real-time PCR is a variation of the standard PCR technique developed to improve the semi-quantitative results obtained by normal PCR. It can be used to quantify DNA or, when coupled with reverse transcription, mRNA in a sample, and it makes use of sequence-specific primers. Quantification is achieved by measuring the amount of product amplified at each stage during the PCR cycle, and it is based on the principle that DNA or RNA derived from genes with higher copy numbers will produce detectable product after fewer PCR cycles. Amplified products are quantified using fluorescent reporter probes or fluorescent dyes, such as SYBR green. This dye produces a fluorescent signal after binding non-selectively to double-stranded DNA, which can be measured by specialised thermal cycling machines.

The results obtained are plotted on either a linear or a logarithmic scale. Cycle number is shown on the X-axis; arbitrary fluorescence units (ΔRn) are represented on

the Y-axis. Data plotted on a linear scale produces a sigmoidal curve that exhibits an exponential and plateau phase. When plotted on a logarithmic scale, a straight line is produced. An additional horizontal line known as the threshold line has to be set in each plot. In a logarithmic scale, the threshold line is usually set half way up the linear part of the curve. When the data is plotted in a linear scale, the threshold line is set towards the bottom of the plot, at the beginning of the upturn of the curve. The point at which each curve crosses the threshold line determines the Ct value, and it defines the number of the cycle at which the fluorescent signal produced by that reaction crosses the threshold line (Figure 2.2). Ct values are inversely proportional to the amount of target DNA or RNA product present in the reaction mix. Together with the samples of interest, a negative and a positive control are usually included on the same plate. A negative control contains no template, and it is used to determine background fluorescence. A positive control or loading control is usually a housekeeping gene that is expressed in all cells at the same levels, and whose expression levels do not change upon treatment. Commonly used loading genes are GAPDH, β-actin, or 18S rRNAs. DNA or mRNA quantification is performed by comparing the results obtained from the unknown samples to a standard curve produced by serial dilutions of a sample containing the DNA target of interest.

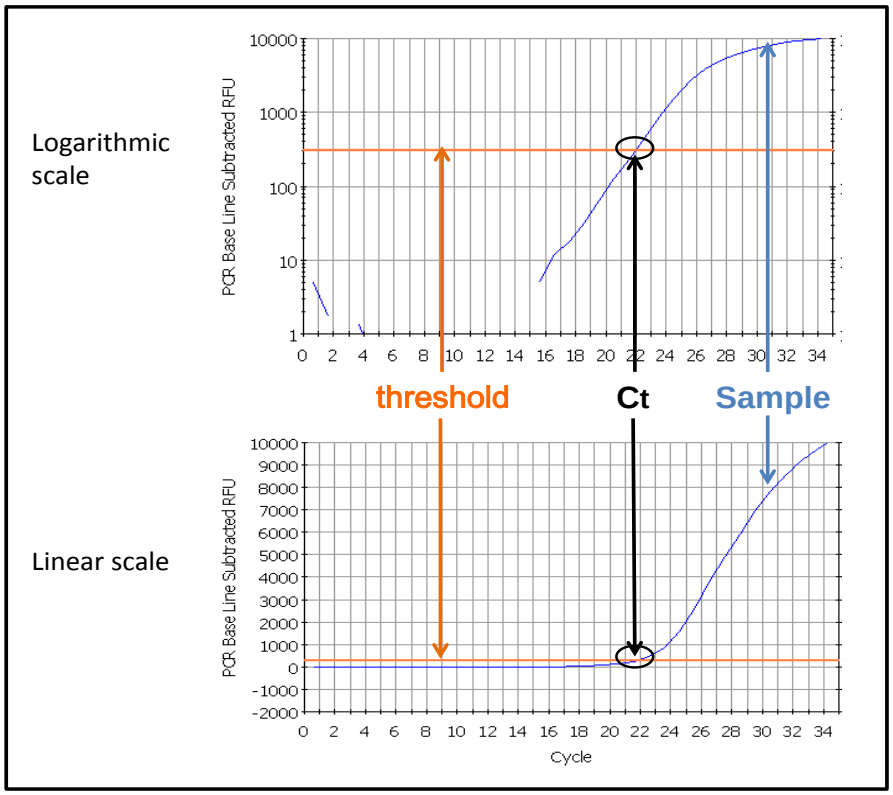

Figure 2.2. Real-time PCR plots.

[Taken from: "Real Time PCR Online Tutorial" by Dr. Margaret Hunt – University of South Carolina - http://pathmicro.med.sc.edu/pcr/realtime-home.htm].

Quantitative gene expression analysis of genes involved in inflammation, cholesterol uptake and efflux, fatty acid metabolism, and cholesterol *de novo* synthesis was performed using the ABI 7900 HT Fast Real-Time PCR system (Applied Biosystems, CA, USA) with the Sequence Detection System (version 2.1) or a Rotor-Gene Q RT-PCR cycler (Qiagen), and was based on SYBR green signal detection. Primers used in RT-PCR were designed using Primer-3 Input (version 0.4.0) and Primer-BLAST (NCBI) primer design software, or were identified from the literature and confirmed to bind targets specifically at the sequence level. The parameters taken into consideration during the design process are shown in Table 2.3. Human and murine primer sequences are listed in Table 2.4 and Table 2.5 respectively.

Table 2.3. Key parameters for primer design

Primer parameters	
Primer size	18-22 bp
Primer Tm	52 - 60 ˚C
Primer GC content (%)	40-60%
Max. GC in primer 3' end	3
Amplicon Length	~ 100 bp
Database	Refseq mRNA

β-actin was used as the loading control gene. For each gene examined, a standard curve was generated by preparing 5-fold dilutions of cDNA in duplicate wells of a 96-well RT-PCR-plate. A negative control with no template (NTC) was also included on each plate. Each reaction contained 1 μl of template cDNA, 1.5 μl of mixed double primer, 12.5 μl of SensiMix SYBR kit (Bioline), and 10 μl of Milli-Q H_2O. The final volume of each reaction was 25 μl per well. Once the plate was loaded onto the RT-PCR machine, the plate layout was defined using the associated software according to the content of each well (i.e. standard with concentration, unknown or NTC). The thermal profile used in the reaction was composed of three stages: **stage 1** at 50 ˚C for 2 minutes; **stage 2** at 95 ˚C for 10 minutes; **stage 3** at 95 ˚C for 0.15 minutes followed by 1 minute at 60 ˚C, repeated for 50 cycles.

Results analysis: Once the run was finished, a graph was obtained by selecting the wells containing the standard curve. Arbitrary fluorescence values (ΔRn) were plotted on the Y-axis that was set to a linear scale. The threshold line was set where the rate of change was highest. Values were exported to Excel for further analysis. Relative expression levels obtained for the unknowns were compared to the values obtained from

the corresponding standard curve and were normalised to the expression of *β*-actin. An example of a standard curve is shown in Figure 2.3.

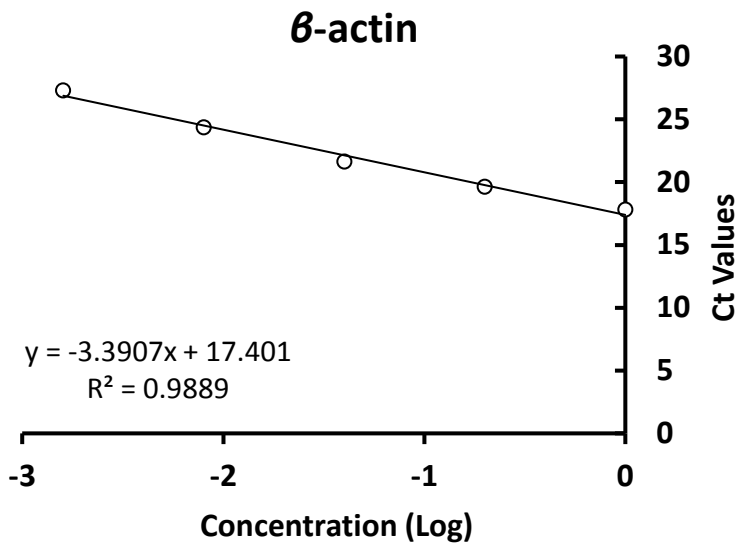

Figure 2.3. Real Time-PCR standard curve.

Example of a real-time PCR standard curve for the loading control gene *β*-actin, obtained by plotting the Ct values for each dilution against the log of the concentration in each well.

Table 2.4. List of human primer sequences used in RT-PCR.

Gene Name	NCBI ref. seq.	Sense (5'→3')	Antisense (5'→3')	Tm (˚C)	Prod. Size
Actin B – ***ACTB***	NM_001101.3	gacgaggcccagagcaagaga	gggtgttgaaggtctcaaaca	75/69	225
ATP -Binding Cassette A1 - **ABCA1**	NM_005502.3	caggaggtgatgtttctgacca	ttggctgttctccatgaaggtc	71/71	447
Diacylglycerol O-Acyltransferase 1 – **DGAT1**	NM_012079.4	ccttgagatgctgttcttca	atgagccagatgaggtgatt	66/66	162
Fatty Acid Synthase - **FASN**	NM_004104.4	ctctggttcatctgctctgg	catcaaaggtgctctcgtct	70/68	169
3-hydroxy-3-methylglutaryl-CoA reductase - **HMGCR**	NM_000859.2	taccatgtcaggggtacgtc	caagcctagagacataatcatc	70/68	247
Interleukin 1- beta - **IL-1B**	NM_000576.2	atggcagaagtacctaagctcgc	acacaaattgcatggtgaagtcagtt	66/68	802
Low Density Lipoprotein Receptor - **LDLR**	NM_000527.4	caatgtctcaccaagctctg	tctgtctcgaggggtagctg	68/72	258
Stearoyl-CoA Desaturase - **SCD**	NM_005063.4	ttcttctctcacgtgggttg	gaaaccaggatattctcccg	68/68	335
Sterol Regulatory Element-binding transcription factor 2 - **SREBF2**	NM_004599.2	atccccaaggccctggaagt	gtatgctgggcggaagctgt	72/72	375

Table 2.5. List of murine primer sequences used in RT-PCR.

Gene Name	NCBI ref. seq.	Sense (5'→3')	Antisense (5'→3')	Tm (˚C)	Prod. Size
Actin B – ***Actb***	NM_007393.3	ttctttgcagctccttcgttgccg	tggatggctacgtacatggctggg	75.3/74.1	458
ATP -Binding Cassette A1 - ***Abca1***	NM_013454.3	caactacaaagccctctttg	cttggctgttctccatgaag	59/62.4	301
ATP -Binding Cassette G1 – ***Abcg1***	NM_009593.2	gaagacctgcactgcgacatc	gttgcattgcgttgcgttagtc	67.2/68.5	908
Acetyl-Coenzyme-A Acetyltransferase 1 - ***Acat1***	NM_144784.3	ccattgatctattcccttgtcc	gagtccttgggtagttgtctcg	63.2/63.8	301
Diacylglycerol O-acyltransferase 1 - ***Dgat1***	NM_010046.2	tcgcgagtacctgatgtctg	agggggcg aaaccaatatac	64.1/63.5	323
Fatty Acid Synthase – ***Fasn***	NM_007988.3	tgccttcggttcagtctctt	tctgctctcgtcatgtcacc	63.9/64.2	391
Glucokinase – ***Gck***	NM_010292.4	aaagatgttgcccacctacg	ccacgatgttgttcccttct	63.7/63.8	383
3-hydroxy-3-methylglutaryl-CoA reductase - ***Hmgcr***	NM_008255.2	cttgtggaatgccttgtgattg	agccgaagcagcacatgat	66.4/66	76
Hormone Sensitive Lipase – ***Lipe (Hsl-1)***	NM_010719.5	gctggtgcagagagacac	gaaagcagcgcgcacgcg	59.7/75.9	409
Interleukin 1-beta - ***IL-1β***	NM_008361.3	gcctcgtgctgtcggacc	tgtcgttgcttggttcttccttg	69.7/68.4	114
Low Density Lipoprotein Receptor – ***Ldlr***	NM_010700.3	aggctgtgggctccatagg	tgcggtccagggtcatct	66.4/67	72

Table 2.5. List of murine primer sequences used in RT-PCR (continued).

Gene Name	NCBI ref. seq.	Sense (5'→3')	Antisense (5'→3')	Tm (°C)	Prod. Size
Phosphoenolpyruvate Carboxykinase 1 - ***Pck1***	NM_011044.2	aactgttggctggctctc	gaacctggcgttgaatgc	60.6/64.3	171
Perilipin 1 – ***Plin1***	NM_175640.2	cctggccaacactctttctc	gatggtgttccggagagtgt	63.7/64	379
Perilipin 2 – ***Plin2***	NM_007408.3	gaagagaagcatcggctacga	gtcaggttgcgggcgata	65.6/67.2	90
Perilipin 3 – ***Plin3***	NM_025836.3	ctaagccagagcaggtggag	tcccttcaggggttttctct	64.0/63.7	348
Peroxisome Proliferator - Activated Receptor γ – ***Pparg***	NM_001127330.1	cactcgcattcctttgac	cccacagactcggcactc	59.3/64.8	264
Stearoyl-CoA desaturase 1 - ***Scd1***	NM_009127.4	gcttccagatcctccctacc	gcccatgtctctggtgtttt	63.8/63.9	342

2.23. Quantification of IL-6 and TNF-*α* in cell culture supernatants by ELISA

Quantification of a specific antigen in a sample can be achieved using the enzyme-linked immunosorbent assay (ELISA). Two of the main types of ELISA are the indirect ELISA and the Sandwich ELISA. Sandwich ELISA is used to detect the presence of an antigen in a sample. The main difference between the two assays is that the well is coated with an antibody termed capture antibody, which is specific for a target antigen. If that antigen is present in the added sample, then it will bind to it. Both assays use specific secondary antibodies recognising the target antibody or antigen. These antibodies, termed detection antibodies, are covalently linked to an enzyme that leads to the production of a coloured product upon reaction with a colourless substrate. The rate of colour formation is proportional to the amount of the specific antibody or antigen in the sample (Berg *et al.* 2007) (Figure 2.4).

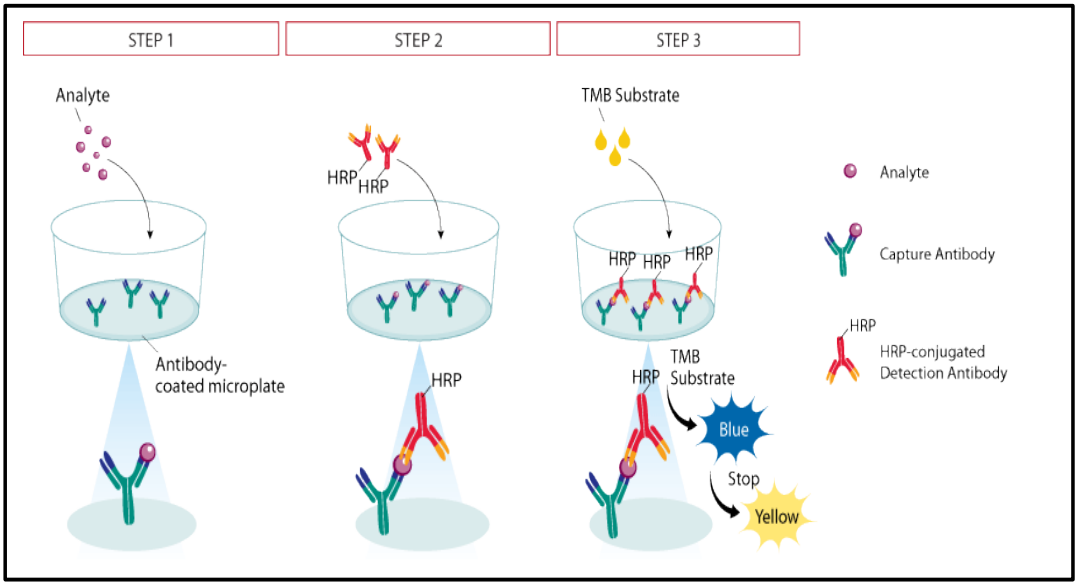

Figure 2.4. Sandwich ELISA

[Taken from: http://www.rndsystems.com/product_detail_objectname_quantikineelisaassayprinciple.aspx]

Sandwich ELISAs were used to quantify interleukin-6 (IL-6) and tumour necrosis factor-α (TNF-α) (R&D systems) in plasma samples collected from treated whole human blood. Briefly, whole blood collected as described in section 2.4 was transferred into 96-well plates (200 μl/ well), and was treated with Pam_3CSK_4 or LPS (0.01-1000 ng/ ml), or 10^6 heat-killed bacteria/ ml for 6 hours at 37 ˚C (5% CO_2). Standard curves were prepared for each treatment. Plasma from each treatment was separated by centrifugation (300 g for 5 minutes at 21 ˚C; acc: 7 / dec: 5), collected and stored at -80 ˚C.

The assay was carried out according to the manufacturer's instructions. Briefly, the capture antibody specific for each cytokine was diluted in sterile PBS (1:180) and 100 μl were added to each well of a high protein binding 96-well plate (Nunc Maxisorp). Following an overnight incubation at RT, the plate was washed 3x with wash buffer (PBS), and blocked with reagent diluent (RD - 1% BSA in PBS) for a minimum of 1 hour. The plate was then washed 3x with wash buffer as previously, and 100 μl of sample diluted in RD (1:10) were added to each well. Standard curves were prepared by performing 2-fold dilutions of each cytokine standard in RD (starting concentration for IL-6 35 ng/ ml; for TNF-α 320 ng/ ml). A well containing only RD was also included as blank for background correction. The plate was incubated for 2 hours at RT, after which it was washed with wash buffer. 100 μl of detection antibody diluted in RD (1:180) was added to each well, and the plate incubated for another 2 hours. Following a washing step, 100 μl of Streptavidin-HRP solution diluted in RD was added to each well, and the plate was incubated for 20 minutes at RT in the dark. After the incubation, a washing step was repeated and 100 μl of TMB substrate solution (1:1 mixture of H_2O_2 and Tetramethylbenzidine) was added to each well. The plate was incubated for 20 minutes at RT in the dark. To stop the reaction, 50 μl of stop solution (2N H_2SO_4) was added to

each well, and the OD of each well was determined at 450 nm using the ELx800 absorbance microplate reader (BioTek). The data obtained was background-corrected, and the concentration of each sample was calculated using the equation generated by plotting data from the standard curve.

2.24. Western blots

Western blotting allows the detection of a protein of interest in a complex mixture. Proteins in a sample are separated from one another according to their size by electrophoresis on an SDS-polyacrylamide gel. Proteins are then transferred from the gel to a membrane – made either of nitrocellulose or polyvinylidene fluoride (PVDF) - by applying an electrical current which encourages the movement of the proteins to the membrane, where they adhere, making them more accessible for reaction. The membrane is then probed with an antibody specific to the protein of interest. Detection is achieved by probing the membrane with a secondary antibody- usually HRP-conjugated- specific for the first, which generates a signal when an enhanced chemiluminescence (ECL) substrate is added to the membrane. The membrane can then be exposed to an X-ray film (autoradiogram) where the protein of interest appears as a dark band or bands on the film, or digital imaging machines where the signal is transformed into a digital image that can be further analyzed using the software provided by the machine (Berg *et al.* 2007).

J774A.1 macrophages plated at a density of 4 x 10^5 cells per well of 6-well plates were challenged with medium alone, or 1 μg/ ml LPS. Protein lysates from treated cells were prepared at 0, 2, 4, 6, 24, and 48 hours. Briefly, cells were washed once with PBS and resuspended in lysis buffer (3.05 g Tris, 0.375 g Sodium Pyrophosphate ($Na_4P_2O_7$), 0.58 g EDTA, 8 g SDS, 0.028 g bromophenol blue, 40 ml glycerol made up to 200 ml

with dH_2O) by scraping cells thoroughly in the well. Lysates were passed through a 29 gauge syringe needle 5 times to shear genomic DNA, transferred into Eppendorf tubes kept on ice, and 1:10 volume of 1M DTT was added into each tube. The protein samples were heated at 100 ˚C for 2 minutes and stored immediately at -20 ˚C.

For electrophoresis, cell lysates were loaded alongside a protein ladder (SeeBlue Plus2 pre-stained molecular weight standard – Invitrogen) on a 12% SDS-gel (1.5 M Tris-HCl, 0.5 M HCl, 10% SDS, 30% acrylamide, 10% APS, TEMED) or a 7.5% SDS-gel, and separated by gel electrophoresis at 170 volts for 1.5 hours. Proteins from the gel were transferred to a nitrocellulose membrane (Whatman Protran BA85) using a wet tank system apparatus (Figure 2.5). Transfer was performed at 260 mA for 2 hours in transfer buffer (0.3% Tris, 1.44% glycine in 20% methanol : 80% distilled water).

To ensure that the transfer was successful, the membrane was immersed in Ponceau S Red solution for 1 minute, after which it was washed in distilled water until the protein lanes were visible. The membrane was then completely destained in NATT wash buffer (0.26% Tris, 0.88% NaCl, 0.05% Tween-20 in dH_2O, pH adjusted to 7.4 with HCl) for 10 minutes at 4 ˚C on a rocking platform. A blocking step was performed by incubating the membrane in 2% BSA/ NATT buffer for 2 hours at 4 ˚C on a rocking platform. The membrane was then probed with primary antibody (rabbit polyclonal α-tubulin at 1:500 (Abcam), or rabbit polyclonal α-HMG-CoA reductase (HMGCR) at 1:200 (H-300 – Santa Cruz Biotechnology), or rabbit polyclonal α-Fatty Acid synthase (FASN) at 1:500 (#3189 – Cell Signalling Technology) overnight in 0.2% BSA / NATT at 4 ˚C on a rocking platform.

The following day, the membrane was washed with NATT (4 x 15 minutes / wash) at 4 ˚C on a rocker, and then probed with secondary antibody (HRP-conjugated goat anti-rabbit IgG, Santa Cruz Biotechnology, at 1:6,000) for 2 hours in 0.2% BSA /

NATT at 4 ˚C on a rocker. The membrane was then washed with NATT buffer as previously mentioned, and incubated in a chemiluminescence substrate solution (SuperSignal West Pico Chemiluminescence substrate solution kit – Thermo Scientific – Pierce) (Figure 2.6).

Membranes were exposed to a light sensitive film (Fuji) for several minutes and the film was developed using a film developer (Agfa). Alternatively, the membrane was visualised using an ImageQuant LAS 4000 chemiluminescent imager (General Electric).

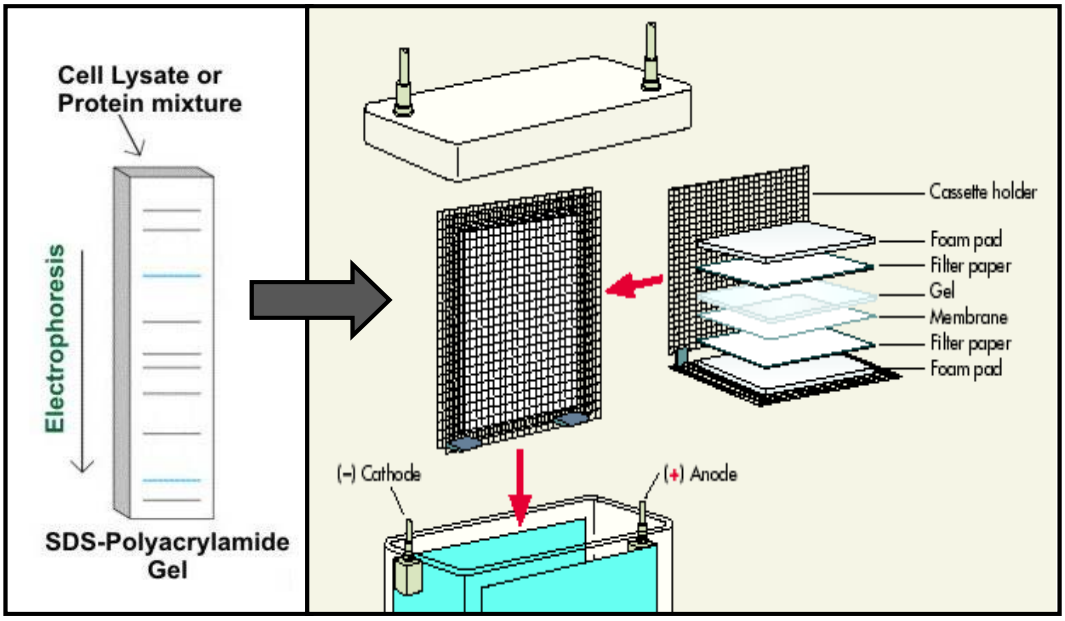

Figure 2.5. Gel electrophoresis and membrane transfer technique.

Protein samples are separated by SDS-Polyacrylamide gel electrophoresis and transfer of the proteins from the gel to a nitrocellulose membrane can be achieved using a wet tank system apparatus.

[Taken from: “The secrets of western blotting” Seminar – Merck Millipore].

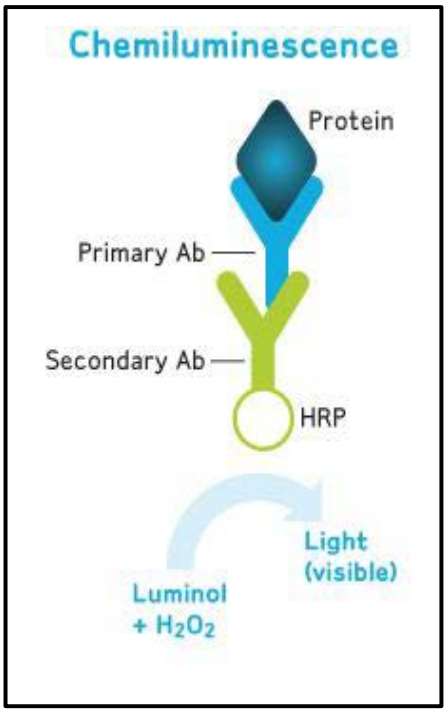

Figure 2.6. Chemiluminescence protein detection method.

This method is based on the use of a primary antibody that detects a protein epitope, and an HRP-conjugated secondary antibody that detects the primary antibody. Addition of a substrate solution containing H_2O_2 leads to light production, which can be detected by exposure of the membrane to an X-ray film or by digital imaging machines.

[Taken from: "The secrets of western blotting" Seminar – Merck Millipore].

2.25. Measurement of cellular *de novo* lipogenesis

To examine if TLR signalling may regulate cellular lipid synthesis, J774A.1 macrophages plated at a density of 1 x 10^6 cells per well of a 6-well plate were challenged with medium alone or Pam_3CSK_4 or LPS (100 ng/ ml) for 21 hours, after which 10 μCi/ ml of ^{14}C-acetate (200 μCi/ ml stock) (Perkin-Elmer) were added for the final 3 hours of culture. The cells were then washed with PBS and fixed for 10 minutes with 4% w/vol PFA / PBS. Cellular lipids were extracted after incubating the cells with 100% ethanol for 30 minutes at 4 ˚C on a rocker. Protein was also extracted after lysing

the cells with 0.1M NaOH / 0.1% SDS. 100 μl of each lipid extract was added to 5 ml of scintillation fluid, and the radioactivity of each sample was measured using a Packard 1500 Tri-Carb Liquid Scintillation Counter (Packard Instrument Co.). Measurements were recorded as counts per minute (CPM).

2.26. Thin-Layer Chromatography of lipid extracts

Thin layer chromatography (TLC) is a simple and convenient method widely used for lipid analysis. Individual or complex mixtures of lipids can be separated, identified and further characterised. Separation occurs on a "stationary phase", which is usually a silica gel plate. This is achieved due to differences in polarity between the TLC plate and the analytes; the "stationary phase" is usually polar, whereas the "mobile phase", which is the solvent system used, is quite non-polar.

The solvent system is placed into a chromatography chamber, which is usually a glass container with a lid (Figure 2.7). A piece of absorbent paper, similar in size to the chamber wall, is placed in the chamber; serving to improve the quality of the chromatography by creating a chamber environment that is uniformly saturated by the solvent vapors. Solvent is then poured into the chamber to a level that covers the bottom of the silica gel plate, but does not contact the sample origins. Once the samples have been separated, lipids can be visualised by staining the silica plate with specific dyes that bind to the separated samples producing coloured spots. Different staining reagents can be used, depending on the composition of the separated lipids (Schuh 2002; Fuchs *et al.* 2011).

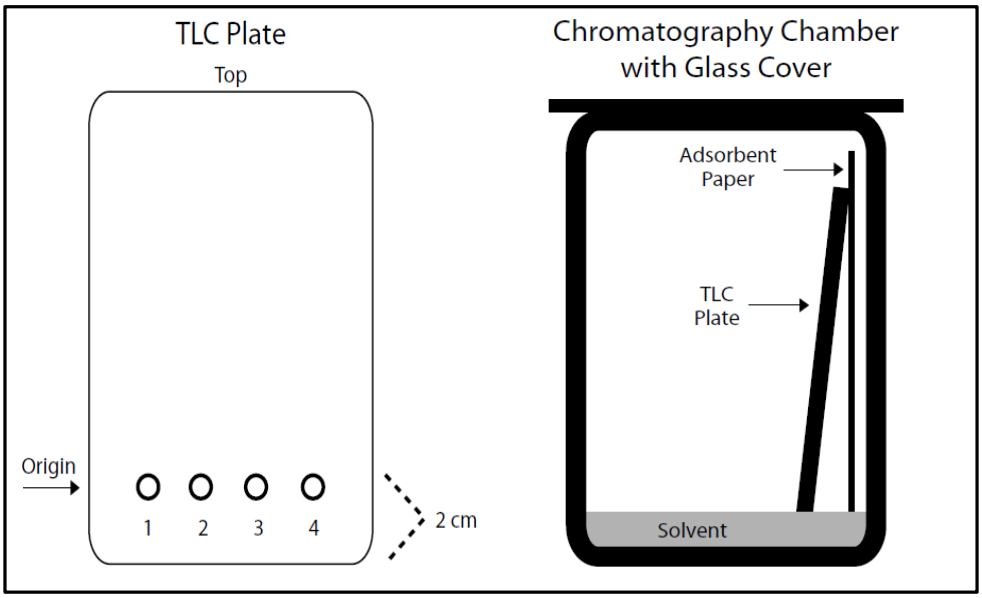

Figure 2.7. Thin layer chromatography (TLC) plate and chromatography chamber.

[Taken from: Schuh (2002) An introduction to lipid analysis in the cell biology laboratory. *The American Biology Teacher*, 64(**2**):122-129].

Preliminary experiments were performed using standards of the major lipid classes associated with *de novo* lipid synthesis, and included cholesterol (1 mg/ ml), cholesterol ester (1 mg/ ml), and triglyceride (5 mg/ ml) standards in $CHCl_3$, as well as a mixture of the three. Each of these lipid groups would move a specific distance on the silica plate, when the right solvent system is used. Different combinations of petroleum ether 60-80 ˚C and ethyl acetate (Fisher) were tested in order to identify the right solvent system that would lead to a good separation of the lipid groups examined.

5 μl of each lipid standard were loaded onto the TLC aluminium silica plates (Merck Millipore) by pipetting 1 μl at a time, allowing the spot to dry in between applications, to origins placed approximately 2 cm from the bottom of the plate and spaced approximately 1 cm apart. Once the application spots had dried, the TLC plate was placed in the chromatography chamber with the bottom immersed in the solvent

(petroleum ether 60-80 ˚C: ethyl acetate at 12:1 or 8:1 or 6:1 or 4.8:1 vol:vol). Optimal separation was achieved when the running solvent was used at 6:1 or 4.8:1. The remaining TLC experiments were performed using a running solvent at 6:1.

After the solvent front had migrated to approximately 1 cm from the top of the plate, the plate was removed from the chamber and left to air dry. Once dry, the plate was incubated with 5% phosphomolybdic acid hydrate in ethanol for 2 minutes, and then treated with a heat gun until the sample spots turned blue. The retardation factor (RF) value for each sample was then calculated using the formula:

$$RF = \frac{\text{migration distance of substance}}{\text{migration distance of solvent front}}$$

To quantify *de novo* lipid synthesis in PAMP - ^{14}C-acetate - treated cells (section 2.25), 5 μl of each lipid extract in EtOH were loaded onto silica plates, and TLC was performed as mentioned above. The plates, once dry, were placed into an X-ray cassette where they were exposed to a light sensitive film (Fuji) for two weeks. The films were developed using a film developer (Agfa). Based on the film, the zones of interest from each silica plate were scraped with a syringe needle into vials containing 5 ml scintillation fluid, and the radioactivity of each sample was measured as mentioned in section 2.25. The zones of interest included polar lipids (PL), cholesterol (CHO), diacylglycerides (DAG), free fatty acids (FFAs), triglycerides (TAG) and cholesterol esters (CE).

Densitometry was performed on a scanned image of the developed film using the Gene Snap and Gene Tools software (Synoptics Ltd).

2.27. Effect of HMG-CoA reductase inhibition on TLR2 and TLR4-dependent foam cell formation

In order to further investigate the possible link between TLR-induced foam cell formation and *de novo* cholesterol biosynthesis, we performed a series of experiments using statins, a group of drugs known to inhibit 3-hydroxy-3-methylglutaryl-CoA reductase (HMG-CoA reductase), the key enzyme involved in cholesterol synthesis. For these experiments, J774A.1 macrophages plated at a density of 2 x 10^5 cells per well of a 24-well plate were challenged with medium alone, 100 ng/ ml of Pam_3CSK_4 or 100 ng/ ml LPS, in the presence of DMSO, which served as a vehicle only control, or simvastatin (25 μM) for 48 hours at 37 ˚C (5% CO_2). Foam cell formation was assessed by flow cytometry, as mention in section 2.8.

2.28. High fat meal study

To investigate the effects that a fatty meal could have on white blood cell lipid content *in vivo*, a total of six healthy volunteers were recruited to take part in a small dietary intervention study. Each volunteer was given a document with detailed information regarding the study several days before the experiment, and was invited to sign a consent form approved by the Research Ethics Committee of the University of Leicester before taking part in the study.

Subjects were asked to fast for 12 hours prior the experiment. The meal consisted of a MacDonald's double sausage and egg McMuffin (34 g fat, 565 kCal) plus a hash brown (9 g fat, 140 kCal), (43 g fat, 705 kCal total), with a bottle of mineral water. Subjects refrained from eating a large or high-fat lunch. Two tubes of blood - one containing EDTA, one citrate - were collected twice from each individual, one set before the fatty meal, and one set 6 hours after the meal. Their heart rate, blood pressure

and temperature were also recorded before the fatty meal, at 3.5 hours and 6 hours after the meal. Whole blood cell counts were measured and recorded for each individual from the EDTA tubes collected before and after the meal using a Beckman Coulter AcT Diff II Haematology Analyser. Blood from the citrated tubes was processed for Nile red staining and flow cytometric analysis, as described in section 2.15.

Sample analysis: A total of four (4) samples per donor (unstained and stained for before and after) were analysed on a Coulter Epics MCL-XL flow cytometer as described in section 2.15.

2.29. Data analysis.

All experiments were performed at least three times in triplicates, unless otherwise stated. All the data obtained from the experiments was analysed in Microsoft Office Excel 2007. The results are reported as means ± SD or SEM. Statistical analysis was carried out using GraphPad Prism 5. ANOVA was performed with either Dunnett's or Tukey's post-tests. Additional tests used include the student's t-test with Bonferroni correction, and the non-parametric Kruskal-Wallis with Dunns post-test. Pearson correlation was used for the comparison of foam cell quantification methods. Differences were considered significant at $p < 0.05$.

3. RESULTS – EFFECTS OF ATHEROMA-ASSOCIATED BACTERIA ON LIPID ACCUMULATION IN MURINE MACROPHAGES

For many years, studies investigating a potential link between atherosclerosis and infections had focused on the bacterium *Chlamydia pneumoniae,* as it was the first bacterium to be identified in human atheroma (Saikku *et al.* 1988; Kuo *et al.* 1993). It was later shown that this organism has the potential to promote the formation of lipid droplets (LDs) in both human and murine macrophages (Cao *et al.* 2007), and to promote atherosclerosis in rodent models of the disease (Blessing *et al.* 2001; Engelmann *et al.* 2006), driving further interest in this particular organism. However, the notion that *C. pneumoniae* might alone be responsible for the promotion of atherosclerosis in man has recently been reconsidered, as later studies showed that treatment with antibiotics specifically targeting *C. pneumoniae* had little impact on cardiovascular risk (Liu and Waters 2005), while more sensitive analytical techniques revealed that bacterial DNA signatures of a wide variety of microorganisms are present in human atherosclerotic lesions (Erridge *et al.* 2008a; Renko *et al.* 2008). As little is known about the effect these organisms may have on macrophage lipid metabolism, we aimed to investigate the potential of these microorganisms to modulate the accumulation of lipid and foam cell formation in macrophages.

3.1. Foam cell formation in mouse primary macrophages.

To determine if a model bacterium could modulate lipid accumulation in primary macrophages, mouse bone marrow-derived macrophages (mBMDMs) matured for 7 days in growth medium were challenged with medium alone or 30 μg/ ml of acetylated LDL (AcLDL) or OxLDL for 24 hours, or 10^5 *E. coli* / ml for 24, 48 and 72 hours. Foam cell formation was assessed by Oil Red-O staining and light microscopy. *E. coli*

was selected as the model organism for this experiment, as organisms of this group are among the most commonly found in atherosclerotic lesions, and it is also part of the normal gut microbiota.

All AcLDL or OxLDL - treated macrophages became foam cells, as indicated by the intense red staining of numerous intracellular lipid droplets, and the process of foam cell formation occurred within 24 hours of treatment (Figure 3.1 – b, c). In contrast, treatment of cells with *E. coli* led to foam cell formation only at a later time point (72 hours), but not at 24 or 48 h (Figure 3.1 – d-f). Even then, not all *E. coli*-treated cells were Oil Red-O positive. The droplets formed in these cells were larger, covering only part of the cytoplasm, and had a more defined structure compared to the droplets in the AcLDL or OxLDL – treated cells, where only the area of the nucleus was not covered by Oil Red-O positive droplets.

Because primary cells are not easy to maintain in culture, and since the number of cells obtained from each animal is normally sufficient only for a small number of experiments, we decided to repeat the experiment using the J774A.1 murine macrophage cell line to establish whether or not this could be used as a practical model system for more comprehensive experimentation.

Treatment of these cells with AcLDL or OxLDL (30 μg/ ml) or 10^6 *E. coli*/ ml for 24 hours showed similar results to those obtained using mouse BMDMs. The majority of cells treated with AcLDL or OxLDL were Oil Red-O positive when examined by light microscopy (Figure 3.2 – b, c). OxLDL - treated cells exhibited a diffuse intense red colour that covered most of the cytoplasmic area, but no distinct droplets could be seen. Cells treated with AcLDL showed a similar pattern, but the droplets were clearly defined and larger in size. In contrast to primary mouse macrophages, treatment with *E. coli* for as little as 24 hours resulted in droplet formation in most of the cells. The

droplets were of varying sizes, and generally slightly smaller compared to those obtained in mouse macrophages at 72 hours.

Additionally, J774A.1 cells were treated with native LDL (nLDL) (30 μg/ ml) alone, or with both *E. coli* and nLDL. nLDL was not a strong inducer of lipid droplet formation, as only a few cells had positive stained droplets compared to cells treated with medium alone, AcLDL or OxLDL. Cells treated with both *E. coli* and nLDL had slightly more positive stained droplets compared to cells treated with *E. coli* alone, but overall the average number of droplets per cell was quite similar between the two treatments (Figure 3.2 – e, f).

Since the results obtained with J774A.1 macrophages were similar to those observed using mouse primary cells and since these cells are easy to culture and intermediate in extent of bacteria-induced foam cell formation between human and mouse macrophages (as discussed later), we continued to use the J774A.1 cell line as a model cell line for most subsequent experiments.

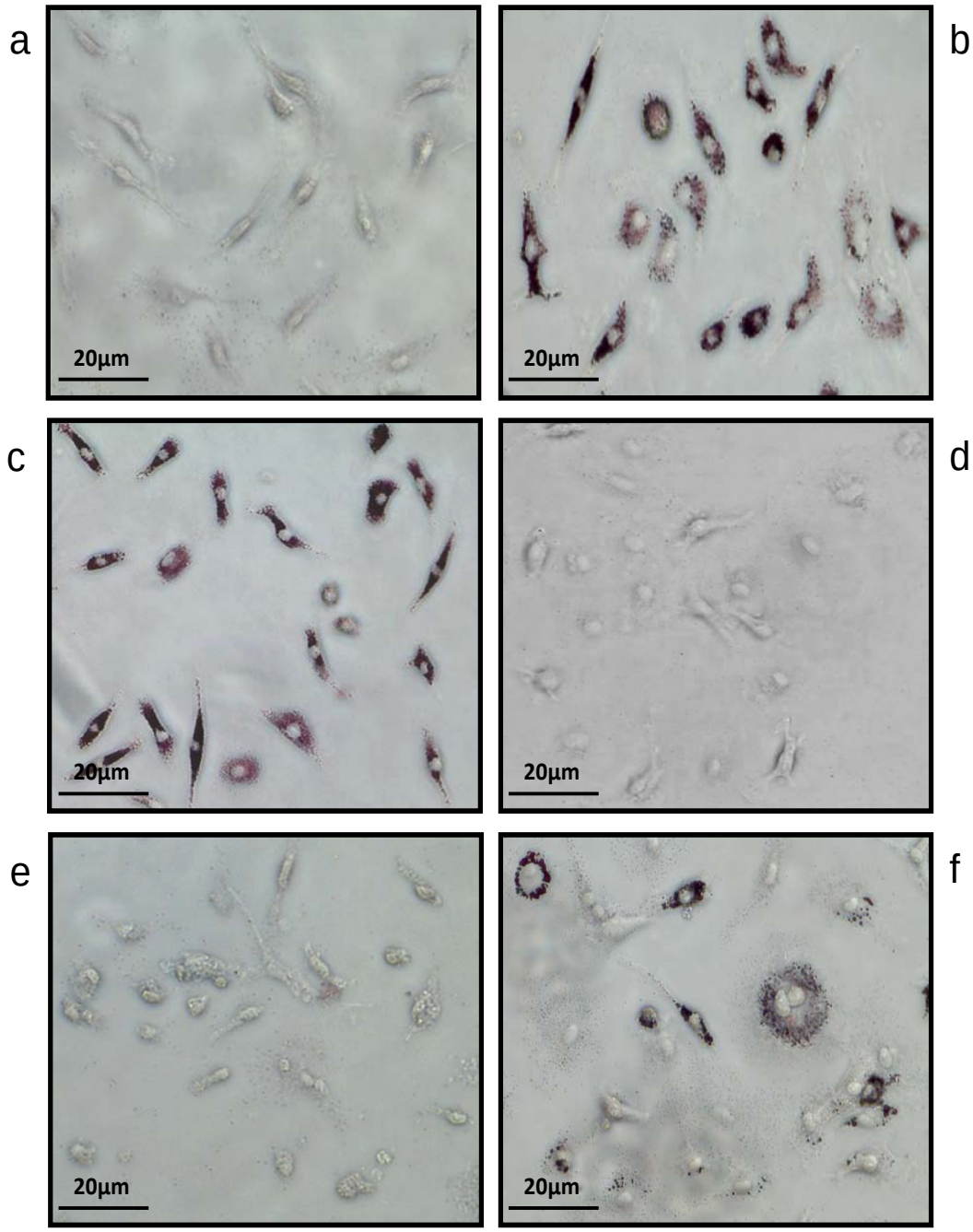

Figure 3.1. Foam cell formation in mouse bone marrow-derived macrophages.

Light microscopy (40x) images of Oil Red-O stained mouse bone marrow-derived macrophages (BMDMs) challenged with medium alone (a), acetylated LDL (30 μg/ ml) (b), oxidised LDL (30 μg/ ml) (c) for 24 hours, and 10^5 *E. coli* / ml without LDL supplementation for 24 hours (d), 48 hours (e), and 72 hours (f).

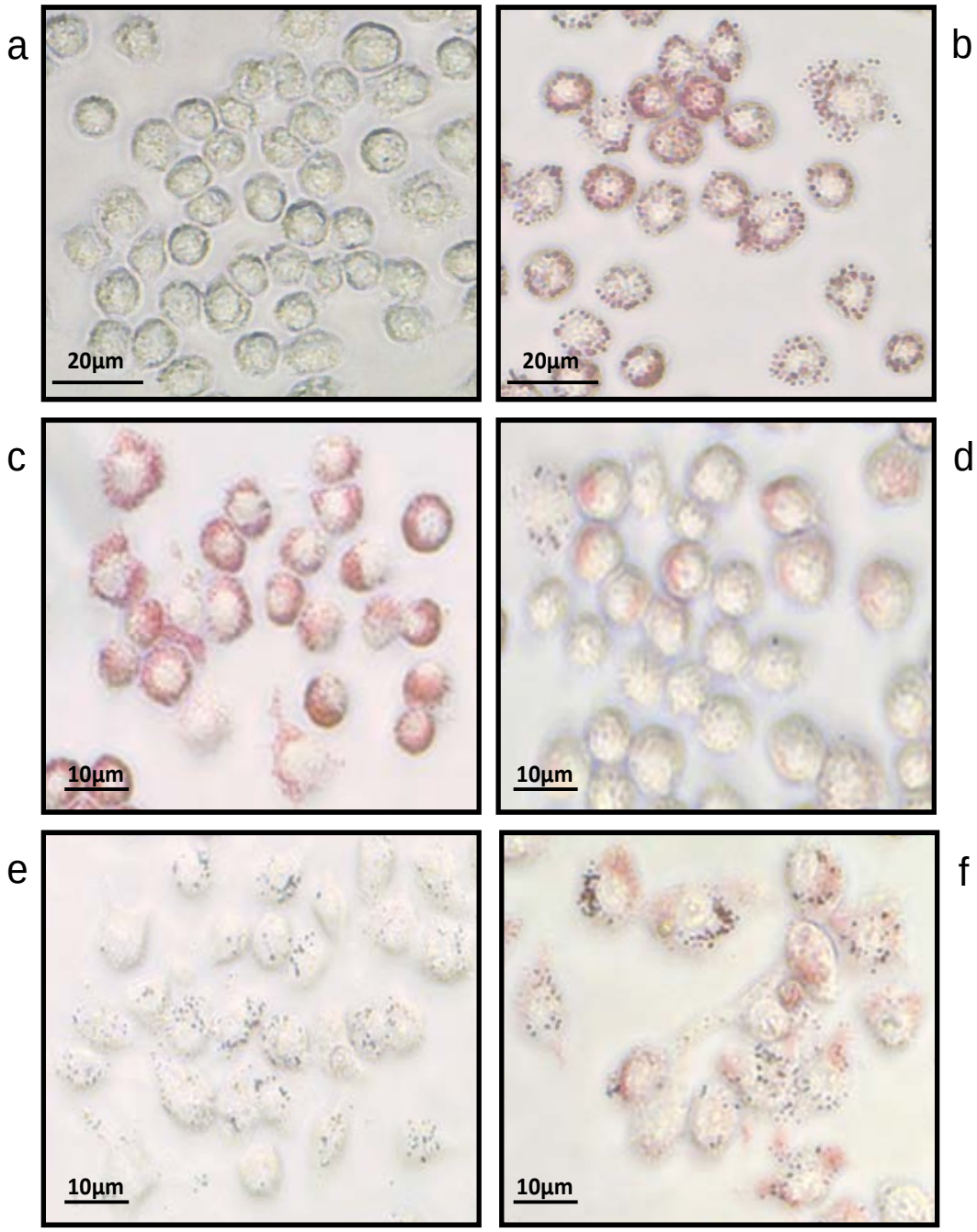

Figure 3.2. Foam cell formation in the J774A.1 macrophage cell line.

Light microscopy (40x) of Oil Red-O stained J774A.1 macrophages challenged for 24hrs with medium alone (a), acetylated LDL (30 μg/ ml) (b), oxidised LDL (30 μg/ml) (c), native LDL (30 μg/ml) (d), and 10^6 *E. coli* / ml alone (e) or with native LDL (30 μg/ ml) supplementation (f).

3.2. Nile Red staining and fluorescent microscopy.

Lipid droplet formation upon treatment with *E. coli* was also confirmed by fluorescent microscopy of Nile Red-stained J774A.1 macrophages. Nile Red is a dye which fluoresces brightly across a broad spectrum when it intercalates with neutral lipid. Cells were treated with medium alone, nLDL, AcLDL, or OxLDL at 30 μg/ ml, 10^6 *E. coli*/ ml or LPS (100 ng/ ml). LPS was used to test whether or not this major bioactive component of Gram-negative bacteria was sufficient to induce foam cell formation in the absence of other bacterial components. Cells were stained with Nile Red (to reveal lipid droplets), and counterstained with DAPI (nucleus) and FITC-phalloidin (actin).

As observed by fluorescence microscopy, all the stimuli used led to the formation of lipid droplets that appeared as red/ orange or gold yellow-coloured when merged with the other two colours (DAPI - blue; FITC - phalloidin - green) (Figure 3.3).

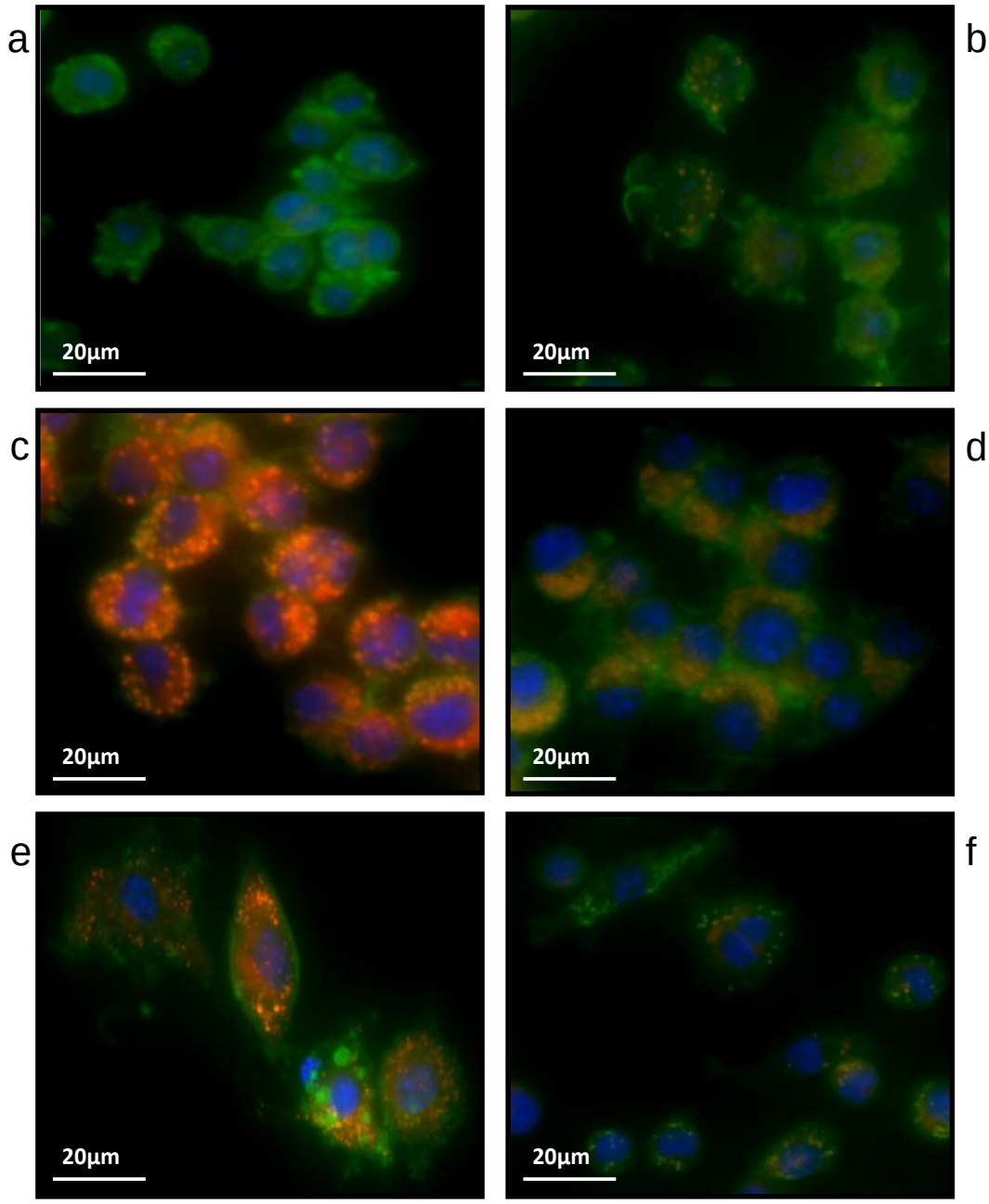

Figure 3.3. Fluorescent microscopy of Nile Red stained J774A.1 macrophages.

J774A.1 macrophages were treated for 72 hours with medium alone (a), native LDL (30 μg/ ml) (b), acetylated LDL (30 μg/ ml) (c), oxidised LDL (30 μg/ ml) (d), 10^6 *E. coli*/ ml (e), or 100 ng/ ml LPS (f). Cells were stained with FITC - phalloidin (actin; green), DAPI (nucleus; blue), and Nile Red (lipid droplets; red/ orange). Magnification: 40x.

3.3. Kinetics of bacteria-induced foam cell formation.

Since previous experiments showed that lipid droplets could be formed within 24 hours of treatment with specific stimuli, we performed a time-course experiment aiming to determine the earliest time point at which lipid droplets might begin to form. J774A.1 macrophages were treated with 10^6 *E. coli*/ ml for 0, 6, 24, 48, and 72 hours, and foam cell formation was assessed by Oil Red-O staining and light microscopy. Quantification was performed by manual counting of Oil Red-O positive lipid droplets, and the data was presented as average number of lipid droplets per cell at each time point.

Casual observation suggested that the process of droplet formation appeared to begin within 6 hours post-treatment (Figure 3.4). However, rigorous quantification of lipid droplets per cell revealed that only after 72 hours were the average number of lipid droplets per cell significantly higher than those counted in control cells treated with medium alone (*E. coli* 72 hours: 53 droplets/ cell *vs*. control: 1 droplet/ cell; $p<0.05$) (Figure 3.5). Nevertheless, the process appeared to be clearly time-dependent, as the number of droplets per cell was directly proportional to the time of treatment (Figure 3.5). The cells treated for 48 hours or longer acquired a more elongated, stretched-out shape, characteristic of activated macrophages. Of note, the number of cells per field was decreased as treatment time was increased, presumably due to increased rates of cell death or reduced attachment at later time points.

A convention widely adopted in the literature is that a foam cell can be defined as the cell bearing equal to or more than ten (≥10) lipid droplets (Cao *et al.* 2007). Based on this definition, all cells at the late time points were considered to be foam cells. The droplets formed at 48 and 72 hours looked slightly bigger than those obtained at 6 or 24 hours post-treatment, but this could be the result of nearby lipid droplets merging

together. Most of the cytoplasmic area was covered in droplets in the majority of the cells.

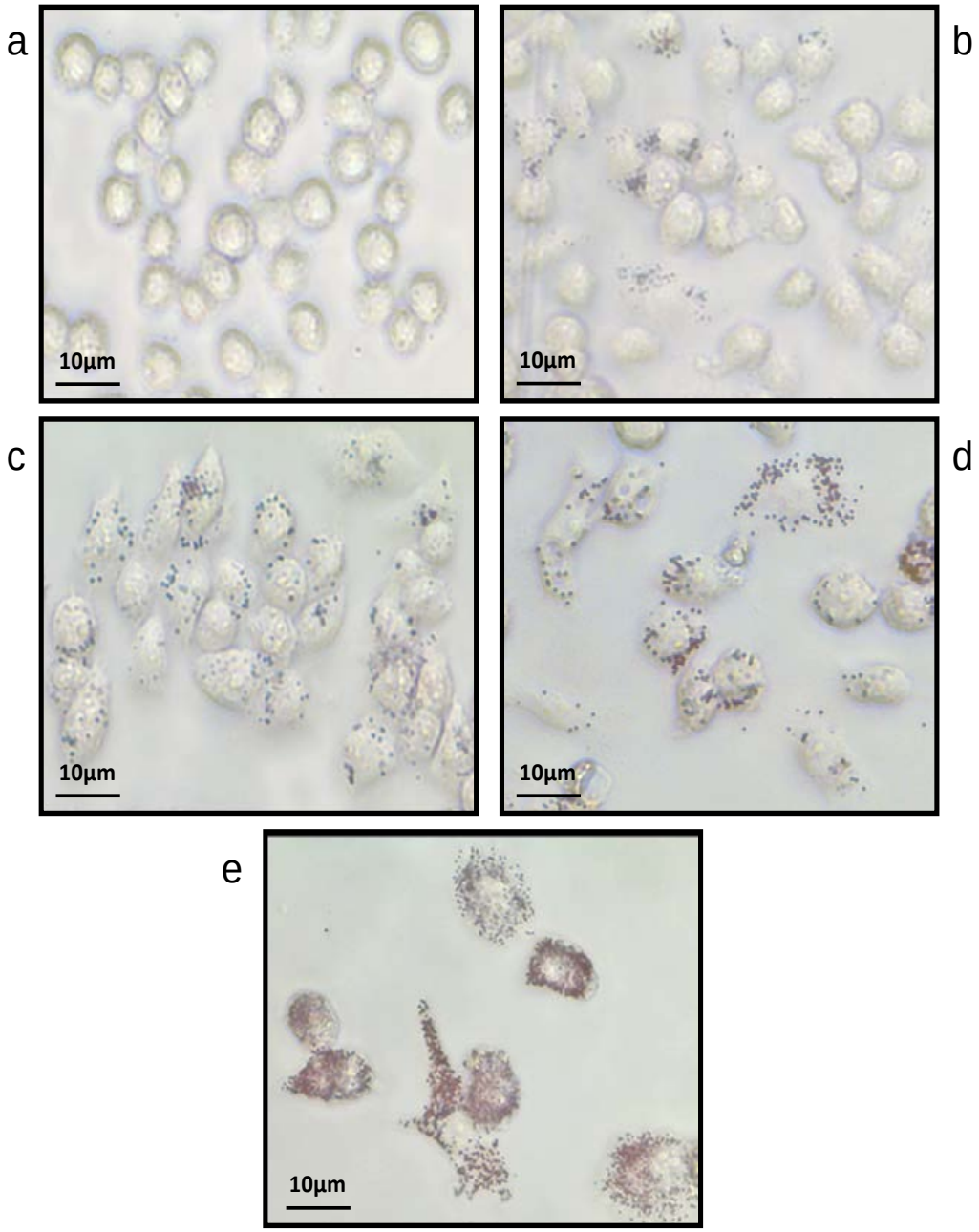

Figure 3.4. Kinetics of foam cell formation – Light microscopy.

Light microscopy (40x) of J774A.1 macrophages stained with Oil Red-O. The cells were challenged with 10^6 *E. coli* / ml without LDL supplementation for 0 h (a), 6 h (b), 24 h (c), 48 h (d), and 72 h (e).

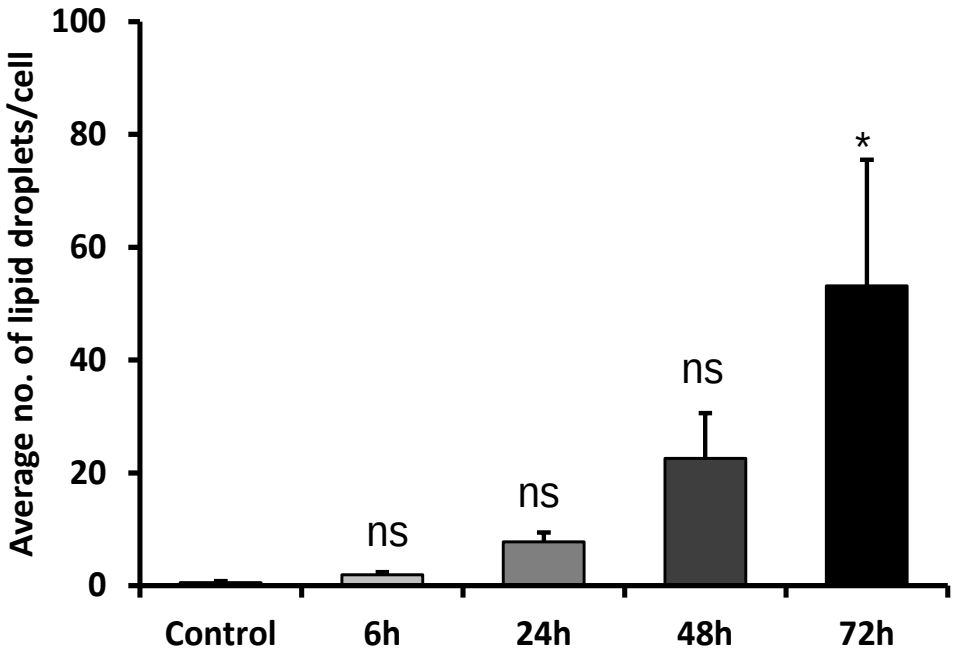

Figure 3.5. Kinetics of *E. coli*-induced foam cell formation.

J774A.1 macrophages were challenged with 10^6 *E. coli* / ml for the indicated time points. Foam cell formation was assessed by counting of Oil Red-O positive droplets per cell. Results are presented as the means ± SEM of three independent experiments. *$p < 0.05$ *vs*. control.

3.4. Lipoprotein dependence of bacteria-induced foam cell formation.

Foam cell quantification by counting was also performed on Oil Red-O-stained J774A.1 macrophages that were challenged for 24 hours with medium alone, nLDL, AcLDL (30 μg/ ml), or 10^6 *E. coli* / ml with or without nLDL supplementation. This time point was chosen to give a low background foam cell formation in *E. coli*-treated cells such that the effect of nLDL supplementation could be examined. The data are presented as average number of lipid droplets per cell for each treatment (Figure 3.6).

As previously observed by light microscopy (Figure 3.2), nLDL was less able to induce the formation of lipid droplets compared to AcLDL, as expected from the literature (Goldstein *et al.* 1979; Steinbrecher *et al.* 1984; Lee *et al.* 2008). Interestingly, *E. coli* alone was able to promote lipid droplet formation within 24 hours, although the average number of droplets per cell was lower compared to that obtained from AcLDL-treated cells (*E. coli* alone: 6 droplets/ cell *vs*. AcLDL: 18 droplets/ cell). This number was increased when *E. coli* was supplemented with nLDL, suggesting that although bacteria-induced foam cell formation does not require the presence of lipoproteins, the process of droplet formation might be partly regulated by LDL (*E. coli* + nLDL: 10 droplets/ cell *vs*. *E. coli* alone: 6 droplets/ cell).

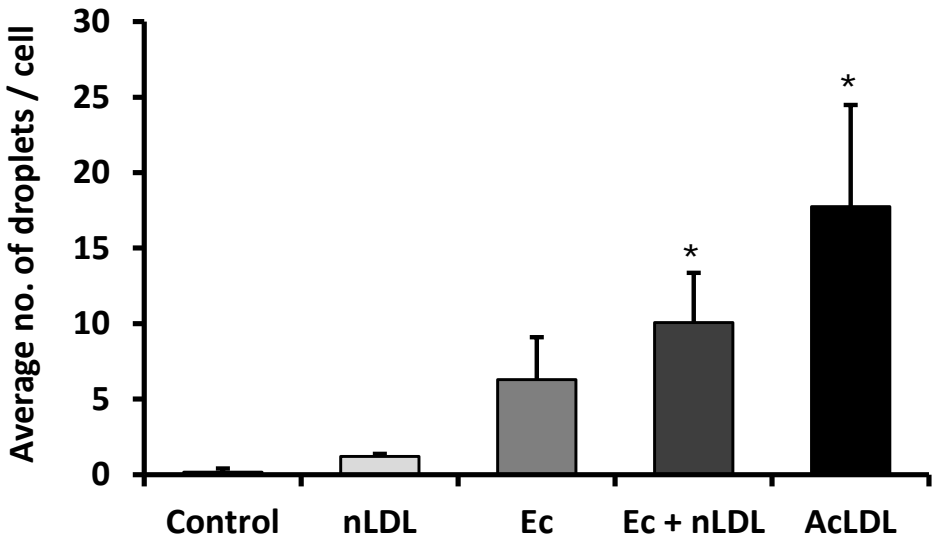

Figure 3.6. Lipoprotein dependence of bacteria-induced foam cell formation.

Foam cell formation was quantified in J774A.1 macrophages cultured with nLDL, *E. coli* in the presence or absence of nLDL, or AcLDL for 24 hours. Data is expressed as average number of lipid droplets per cell, and presented as the averages ± SD of three independent experiments. *$p < 0.05$ *vs.* control.

3.5. Examination of the diversity of bacteria capable of inducing foam cell formation.

A panel of nine bacteria (Table 2.1) representing those most frequently reported to be present in human atherosclerotic lesions (Ott *et al.* 2006; Erridge *et al.* 2008a; Renko *et al.* 2008) was examined for their capacity to promote lipid droplet formation in macrophages. J774A.1 macrophages challenged with heat-killed Gram-negative (10^5 bacteria/ ml) and Gram-positive (10^6 bacteria/ ml) bacteria for 24 hours were stained with Oil Red-O and examined under a light microscope.

All of the selected heat-killed bacteria were able to trigger the formation of lipid droplets in treated cells. Between treatments, there were no differences in the droplet size or their distribution in the cytoplasm. However, treatment with Gram-negative bacteria (Figure 3.7) resulted in more Oil Red-O positive cells per field, suggesting that Gram-negative bacteria exert a greater capacity to induce foam cell formation compared to Gram-positive bacteria (Figure 3.8).

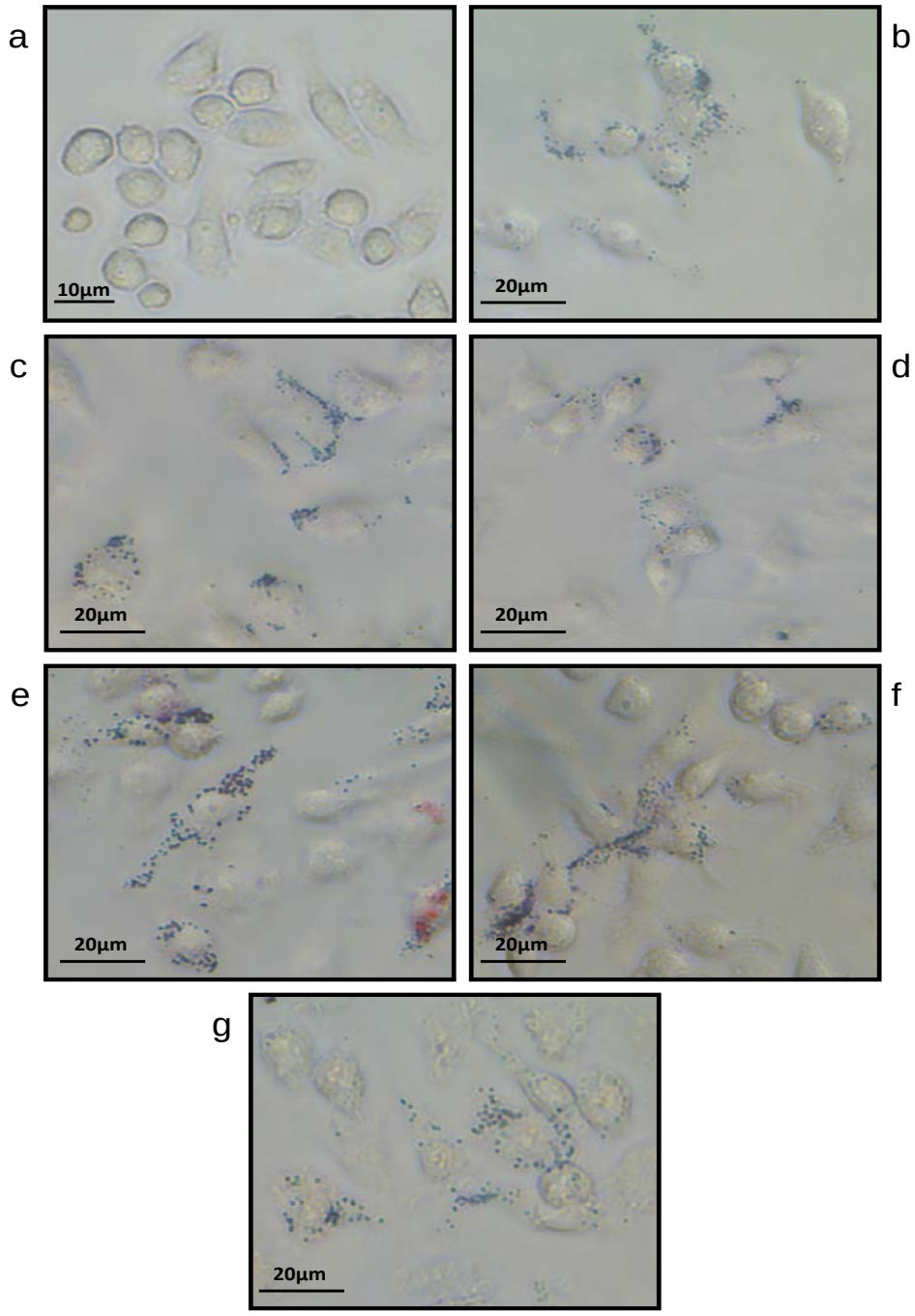

Figure 3.7. Gram-negative bacteria induce foam cell formation in J774A.1 macrophages.

Light microscopy (40x) of Oil Red-O stained J774A.1 macrophages challenged with 10^5 bacteria/ ml heat-killed Gram-negative bacteria for 24 hours. a) Control (medium alone), b) *Acinetobacter baumannii*, c) *Escherichia coli*, d) *Klebsiella pneumoniae*, e) *Proteus vulgaris*, f) *Pseudomonas aeruginosa*, g) *Pseudomonas diminuta*.

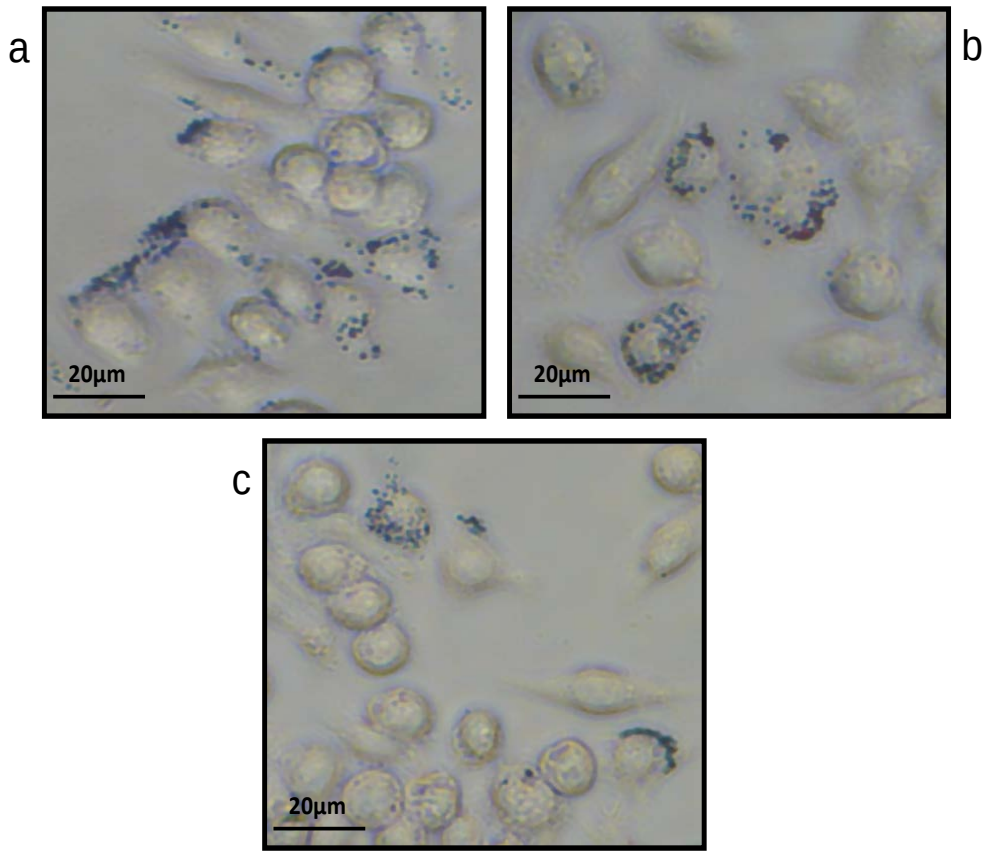

Figure 3.8. Gram-positive bacteria-induced foam cell formation in J774A.1 macrophages.

J774A.1 macrophages were challenged with 10^6 bacteria/ ml heat-killed Gram-positive bacteria for 24 hours. Foam cell formation was assessed by light microscopy (40x) of Oil Red-O stained cells. a) *Staphylococcus aureus*, b) *Staphylococcus epidermidis*, c) *Streptococcus salivarius.*

3.6. Foam cell quantification by flow cytometry.

Because foam cell quantification by light microscopy is a laborious and time-consuming process, we next examined the potential of flow cytometry of Nile Red-stained cells as an alternative method of foam cell quantification. The same panel of bacteria described above was used to challenge J774A.1 macrophages for 72 hours. On the basis of dose-ranging pilot experiments (data not shown), Gram-negative bacteria were used at 10^4 and 10^5 bacteria / ml, whereas Gram-positive bacteria were used at 10^5 and 10^6 bacteria / ml. Treated cells were stained with Nile Red, and analysed by flow cytometry. Control cells cultured in medium alone were assigned a 2% positivity threshold. During the course of the experiments, the flow cytometer developed a problem which rendered the measurement of the percentages of the positive cells unreliable, whereas mean fluorescence intensity always remained reliable. Therefore, the results obtained were expressed either as percentages of positive cells with fluorescence above the threshold or, in later experiments, as mean fluorescence intensity of non-treated and treated cells. Figure 3.9 illustrates the difference in the mean fluorescence intensity (ΔMFI) between control and *E. coli* treated macrophages, as revealed by the shift of the fluorescence peak produced by treated cells towards the right, this being indicative of foam cell formation.

Using this method, consistent with the results obtained by microscopy, all of the selected bacteria resulted in the formation of foam cells, as indicated by the increased percentages of positive cells in treated cells compared to non-treated cells, in a concentration-dependent manner (Figure 3.10).

Notably, Gram-negative bacteria consistently induced a higher percentage of foam cell formation than did Gram-positive bacteria even when used at concentrations lower than those used for the Gram-positive bacteria. Of note, only one bacterium per 10

macrophages was required for Gram-negative bacteria to promote foam cell formation, compared to at least one bacterium per macrophage required by Gram-positive bacteria.

In order to determine if the results obtained in these experiments were specific to the J774A.1 cell line examined, we next examined foam cell responses using the alternative murine macrophage cell line RAW 264.7. Similar results were obtained using this cell line. Treatment with Gram-negative bacteria at 10^5 bacteria/ ml or Gram-positive bacteria at 10^6 bacteria/ ml resulted in foam cell formation, as shown by the increase of mean fluorescence intensity in treated cells (Figure 3.11).

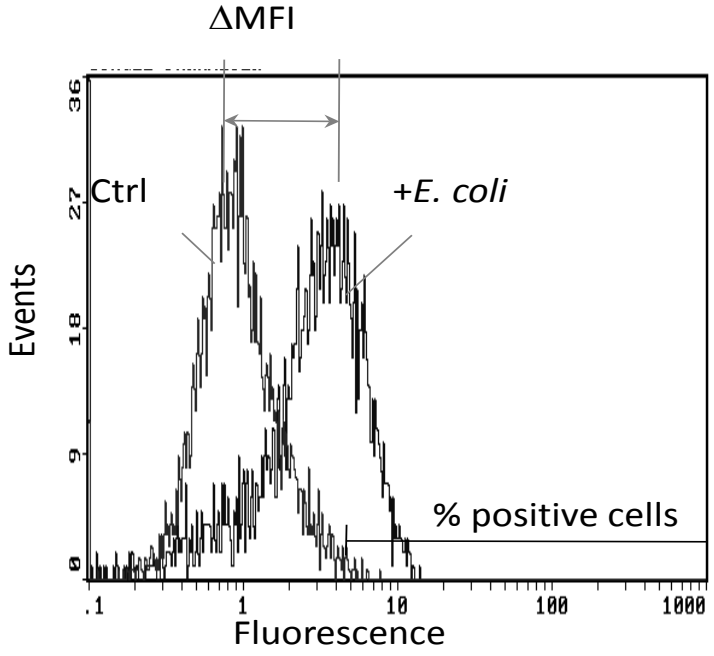

Figure 3.9. Flow cytometry histogram of control *vs. E. coli* treated macrophages. A shift of the fluorescence peak produced by *E. coli* treated J774A.1 cells to the right when compared to the peak produced by control cells (left) is indicative of the difference in fluorescence, and therefore cellular neutral lipid content, between the two samples (ΔMFI).

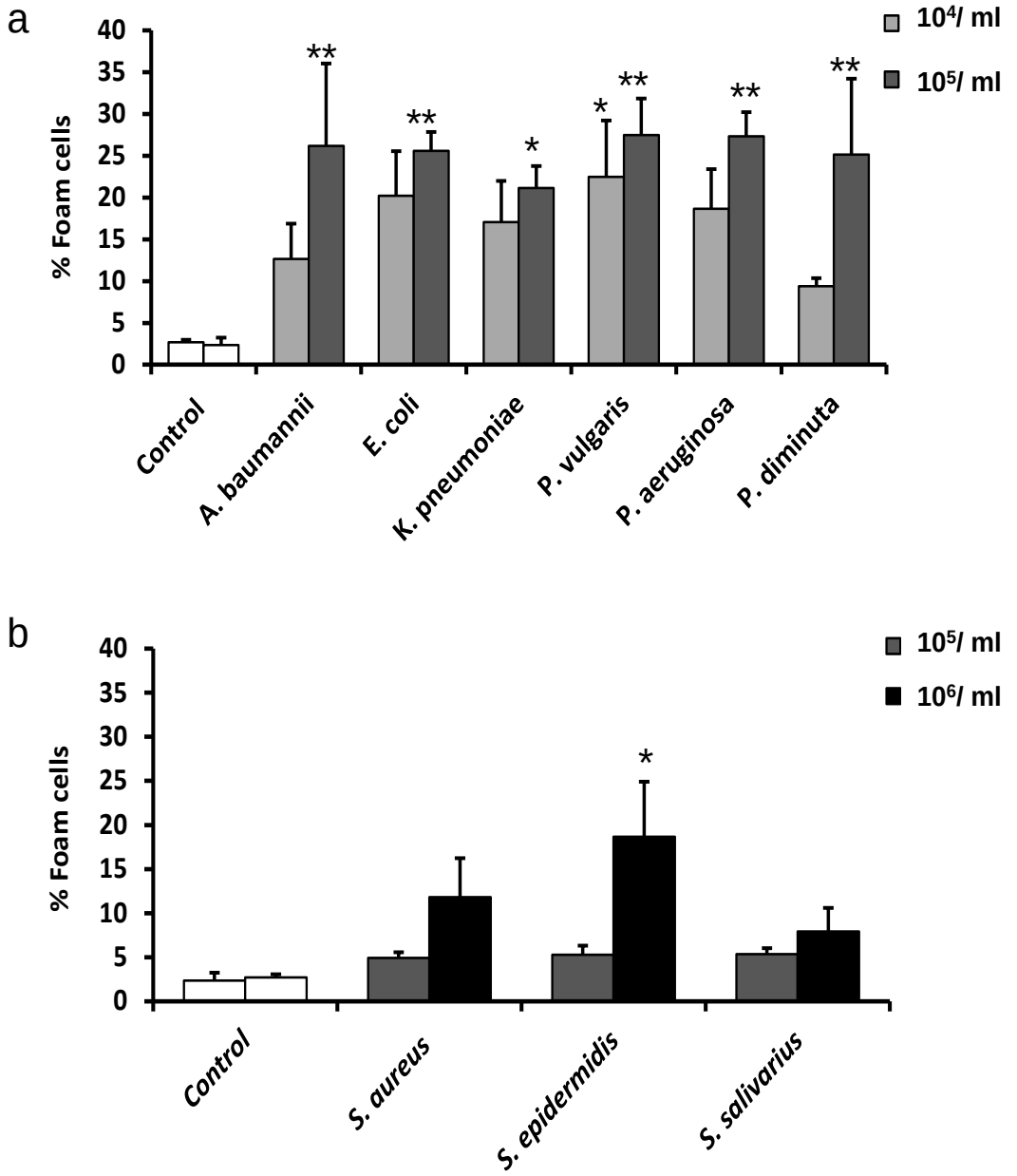

Figure 3.10. Quantification of bacteria-mediated foam cell formation by flow cytometry.

J774A.1 macrophages were treated with the indicated concentrations of Gram-negative (a) or Gram-positive bacteria (b) for 72 hours, and foam cell formation was assessed by flow cytometry of Nile Red stained cells. Results are presented as the means ± SEM of three (Gram-negative) and four (Gram-positive) independent experiments. *$p < 0.05$, **$p < 0.01$ *vs.* control.

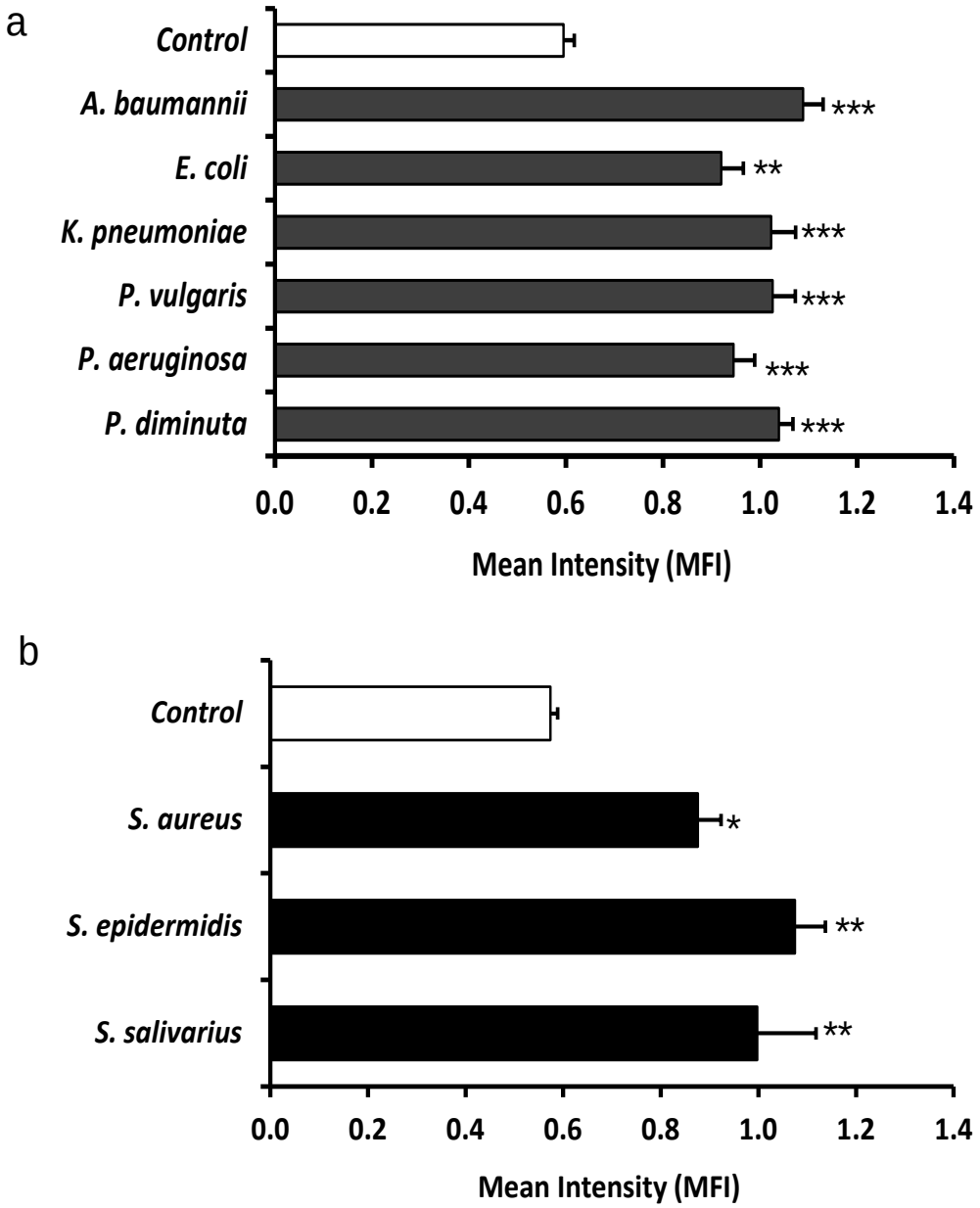

Figure 3.11. Quantification of bacteria-induced foam cell formation in RAW 264.7 macrophages.

RAW 264.7 macrophages were treated with Gram-negative (10^5 bacteria/ ml) (a) or Gram-positive bacteria (10^6 bacteria/ ml) (b) for 24 hours, and foam cell formation was assessed by flow cytometry of Nile Red stained cells. Results are presented as the means ± SEM of three independent experiments. *$p < 0.05$, **$p < 0.01$, ***$p < 0.001$ *vs.* control.

3.7. Cellular cholesterol content of bacteria-treated macrophages.

In order to add further confirmation to the data obtained by microscopy and flow cytometry, we performed a biochemical quantification of the cholesterol ester content of cells treated with bacteria. J774A.1 macrophages were treated for 48 hours with varying concentrations of *E. coli* (10^3 – 10^5 bacteria/ ml) supplemented with 30 μg/ ml of nLDL. Cholesterol ester (CE) content was measured from cellular lipid extracts using an enzyme-coupled reaction, and the results were presented as ng of cholesterol ester per μg of protein.

Cellular CE levels were shown to increase ~1.8 - 2.5 fold in a dose-dependent manner (Figure 3.12 - a). The highest increase was achieved when the cells were treated with 10^4 bacteria/ ml *E. coli* in the presence of nLDL (0.50 ng *vs*. control: 0.20 ng of CE per μg of protein; $p < 0.01$).

CE content was also measured in J774A.1 macrophages challenged with 10^6 heat-killed bacteria / ml and 50 μg/ ml nLDL for 24 hours [Research conducted by Dr. C. Erridge]. CE accumulation occurred in response to all treatments examined, increasing by ~5-10-fold over the baseline (Figure 3.12 - b). *S. epidermidis* was the strongest inducer of CE accumulation (3.02 ng *vs*. control: 0.30 ng of CE per μg of protein; $p < 0.01$), followed by *P. aeruginosa.*

Lipid extracts were also obtained from mouse primary BMDMs treated with 10^5 Gram–negative bacteria/ ml or 10^6 Gram-positive bacteria/ ml in the presence of 30 μg/ ml nLDL for 48 hours. As observed in J774A.1 macrophages, all of the selected bacteria induced a ~6 – 12-fold increase in cellular CE levels (Figure 3.13). Also consistent with the J774A.1 macrophage experiments, *P. aeruginosa* was the most potent inducer of CE accumulation in these cells (1.58 ng *vs*. control: 0.13 ng of CE per μg of protein; $p < 0.01$).

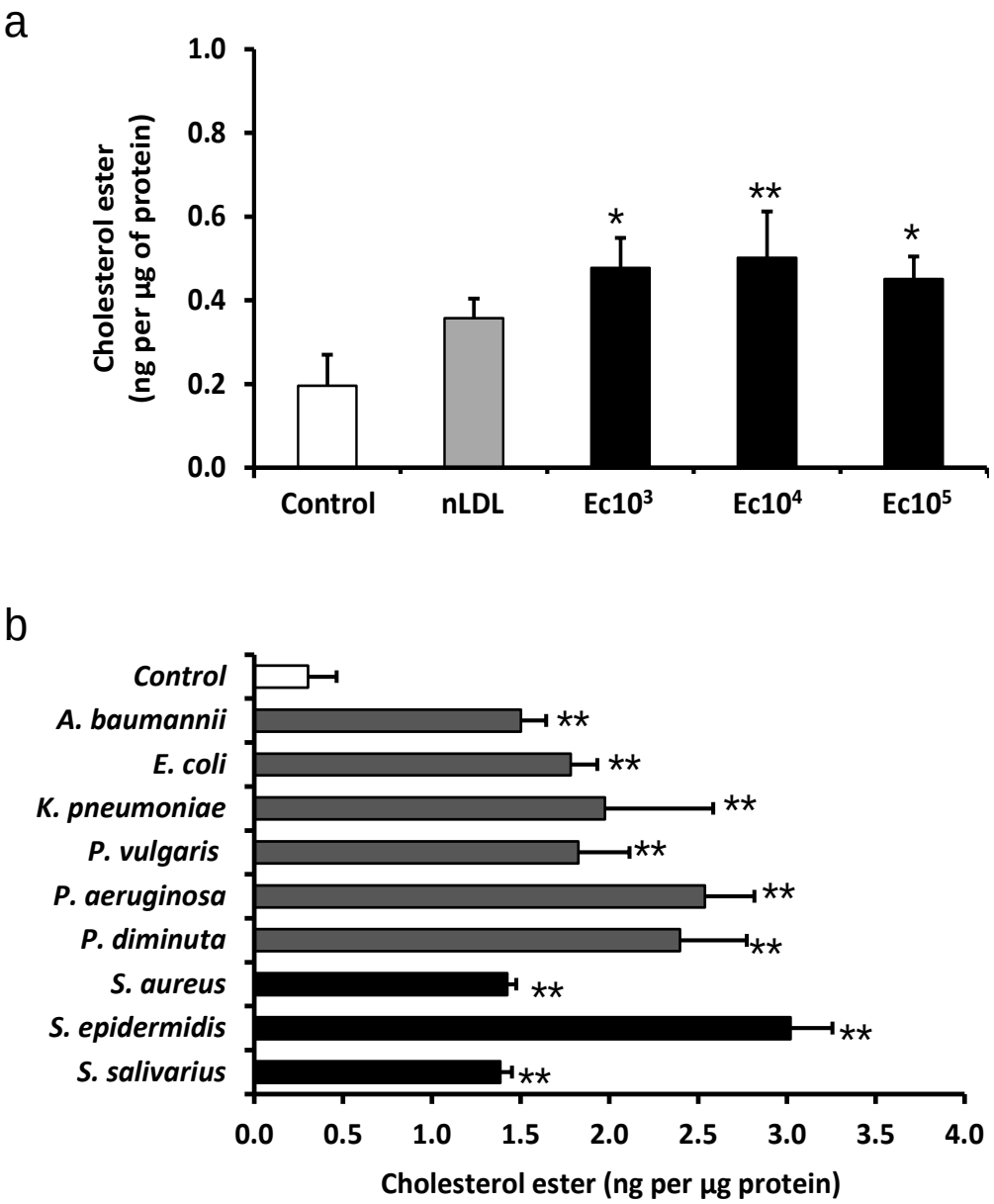

Figure 3.12. Bacteria-induced cholesterol ester accumulation in J774A.1 macrophages.

Cholesterol ester content was measured in lipid extracts obtained from J774A.1 macrophages treated with the indicated concentrations of *E. coli* in the presence of nLDL (30 μg/ ml) for 48 hours (a), or with 10^6 of each indicated bacteria/ ml and 50 μg/ ml nLDL for 24 hours (b). Results are presented as the means ± SEM (a) or means ± SD (b) of three independent experiments. *$p < 0.05$, **$p < 0.01$ *vs*. control.

Although the fold-induction of CE accumulation induced by bacteria relative to baseline was slightly higher in the primary cells, the absolute amounts of cholesterol ester accumulated intracellularly were lower than that observed in J774A.1 macrophages. Differences in the cell type might account for the variation observed in CE levels. We have previously shown that the process of lipid droplet formation in primary mouse BMDMs takes longer to occur than in J774A.1 cells (Figure 3.1). Also, as bacteria-mediated CE accumulation was shown to be enhanced by LDL supplementation, it can be suggested that the lower concentration of nLDL used in mouse BMDMs might have affected the results.

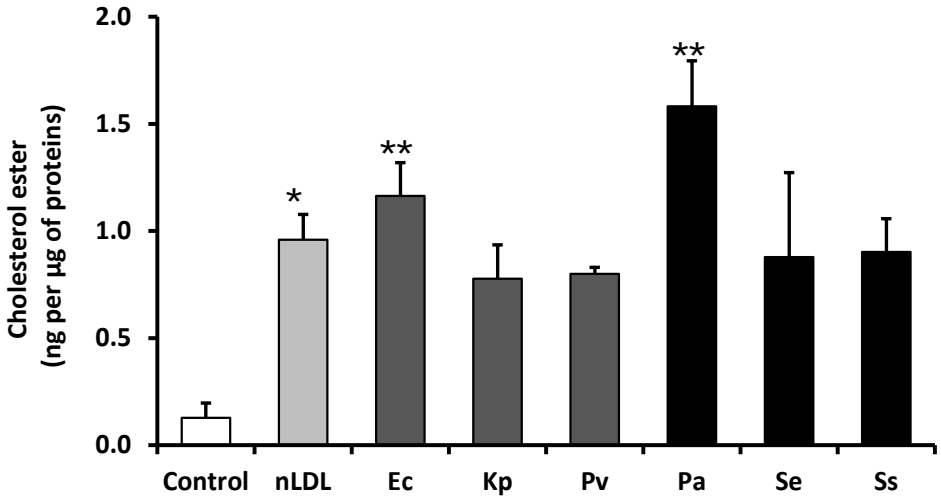

Figure 3.13. Cholesterol ester accumulation in mouse primary BMDMs.

Mouse BMDMs were treated with different heat-killed bacteria (10^5 bacteria / ml) in the presence of native LDL (30 μg/ ml) for 48 hours. Cholesterol ester accumulation was quantified by biochemical assay. Results are presented as the means ± SEM of three independent experiments. Abbreviations: *E. coli* (Ec), *K. pneumoniae* (Kp), *P. vulgaris* (Pv), *P. aeruginosa* (Pa), *S. epidermidis* (Sa), *S. salivarius* (Ss). *$p < 0.05$, **$p < 0.01$ *vs.* control.

3.8. Comparison of methods of quantification of foam cell formation.

It was important to compare the three methods used for foam cell quantification in order to establish how well results obtained by each of these methods correlate with each other. J774A.1 macrophages were treated for 48 hours with medium alone or *E. coli* at concentrations ranging from 10^3-10^5 bacteria/ ml, supplemented with nLDL (30 μg/ ml). Foam cell formation was assessed by droplet counting, flow cytometry, and a biochemical assay of CE accumulation.

The average number of lipid droplets per cell quantified by droplet counting strongly correlated with both the percentage of positive cells and the mean fluorescence intensity measured by flow cytometry ($r = 0.9$; $p < 0.001$) (Figure 3.14 – a, b). Similar results were obtained when the flow cytometry data was compared to that obtained from the quantification of the cellular cholesterol ester content of treated cells. The CE assay showed a strong, positive correlation with both the percentage of foam cells and the mean florescence intensity quantified by flow cytometry, although the correlation coefficient values obtained were slightly lower ($r = 0.7$) (Figure 3.14 – c, d). A positive correlation was also obtained when droplet counting was compared to CE accumulation ($r = 0.8$; $p < 0.05$) (Figure 3.14 - e). These observations indicate that all three methods can produce reliable results, and that the time-consuming method of droplet counting can be replaced with the more sensitive and higher throughput methods of flow cytometry or biochemical assays of CE accumulation.

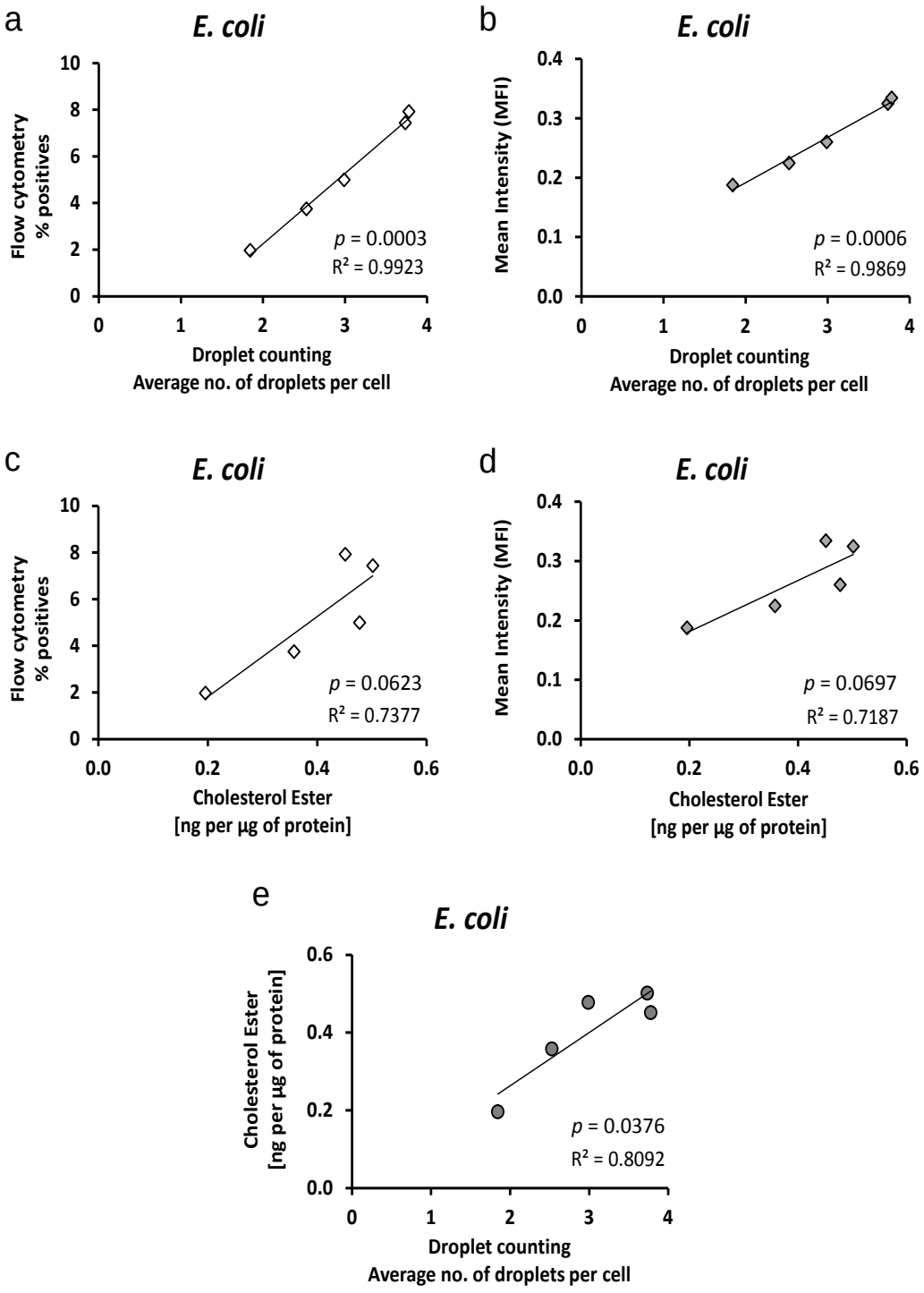

Figure 3.14. Correlation between droplet counting, flow cytometry and cholesterol ester biochemical assay.

All three methods used for foam cell quantification correlate well with each other, with correlation coefficient values ranging from 0.7 - 0.9.

Summary

The presented results have established that the exposure of macrophages to bacteria can lead to the accumulation of intracellular lipid and the formation of foam cells, and that this can be observed in both murine primary cells and murine cell lines. The process is not cell-line specific, as bacteria-induced foam cell formation was observed in both cell lines examined. The results also establish that foam cell formation can be assessed by a variety of methods which were shown to correlate well with each other, including microscopy of Oil Red-O-stained cells and droplet counting, fluorescence microscopy of Nile Red-stained cells, flow cytometry, and biochemical assays of cholesterol ester accumulation.

4. RESULTS - CONTRIBUTION OF TLR SIGNALLING TO BACTERIA-MEDIATED LIPID ACCUMULATION IN MACROPHAGES

Activation of an inflammatory response against microorganisms is initiated by Pattern Recognition Receptors (PRRs), which are important components of innate immunity. The Toll-like receptor family (TLR) of PRRs has been implicated in the initiation of the inflammatory response during atherosclerosis (Tobias and Curtiss 2007; Segers *et al.* 2008; Page *et al.* 2009). These receptors recognise bacteria-related products also known as pathogen-associated molecular patterns (PAMPs). Based on the results obtained in the previous chapter, we hypothesised that bacteria-induced foam cell formation might require the activation of Toll-like receptors (TLRs).

In this chapter, we aimed to investigate the contribution of TLR signalling to the process of macrophage lipid accumulation and foam cell formation mediated by bacteria. *K. pneumoniae* was used as a model organism in these experiments, since it is one of the most frequently observed Gram-negative organisms in human atherosclerotic plaques (Ott *et al.* 2006; Koren *et al.* 2011), and expresses ligands of both TLR2 and TLR4, the two TLRs shown to play a key role in murine models of atherosclerosis.

4.1. Effect of TLR inhibition on bacteria-induced foam cell formation.

J774A.1 macrophages were treated for 24 hours with 10^5 *K. pneumoniae*/ ml in the presence or absence of the selective TLR2 / TLR4 inhibitor oxidised 1-palmitoyl-2-arachidonyl-*sn*-glycero-3-phosphatidyl choline (OxPAPC) (30 μg/ ml), or the TLR4 inhibitors polymyxin B (PMB - 10 μg/ ml) or TAK-242 (1 μg/ ml), without LDL supplementation. Foam cell formation was assessed by flow cytometry, and results presented as averages of mean fluorescence intensities (MFI) (Figure 4.1).

As expected, treatment with *K. pneumoniae* resulted in an increase of the MFI in treated cells when compared to control cells (1.6-fold increase - *K pneumoniae* alone *vs.* control). Each of the selected TLR inhibitors significantly inhibited the formation of foam cells upon treatment with *K. pneumoniae*, as indicated by the differences in their MFIs (*K. pneumoniae* + OxPAPC MFI: 0.7 - $p < 0.01$; *K. pneumoniae* + PMB MFI: 0.7 – $p < 0.001$; *vs. K. pneumoniae* alone MFI: 0.8), with TAK-242 having the greatest effect (MFI: 0.6; $p < 0.001$). In the absence of *K. pneumoniae*, treatment with any of the inhibitors did not result in any increase of the MFIs in these cells, with levels remaining similar to those observed from control cells (in medium alone in the absence of both the bacterium and the inhibitors) (MFI ~ 0.5).

Alternatively, J774A.1 macrophages were treated for 72 hours with 10^5 *K. pneumoniae*/ ml without LDL supplementation in the presence of a blocking antibody against TLR2 (α-TLR2; 5 μg/ ml) or an isotype-matched control antibody targeting an unrelated irrelevant (Irr) epitope. Mean fluorescence intensity was recorded by flow cytometry (Figure 4.2).

As previously, higher MFI values were recorded for *K. pneumoniae*-treated cells compared to medium alone-treated cells. Inhibition of the TLR2 pathway in *K. pneumoniae*-treated cells resulted in a significant decrease in foam cell formation, as reflected by the lower MFI of these cells (*K. pneumoniae* + α-TLR2 MFI: 3.1 *vs*. *K. pneumoniae* + Irr. MFI: 4.4, $p < 0.05$). The isotype-matched control antibody failed to inhibit foam cell formation in *K. pneumoniae*-treated cells, further suggesting the involvement of TLR2 signalling in the process of foam cell formation.

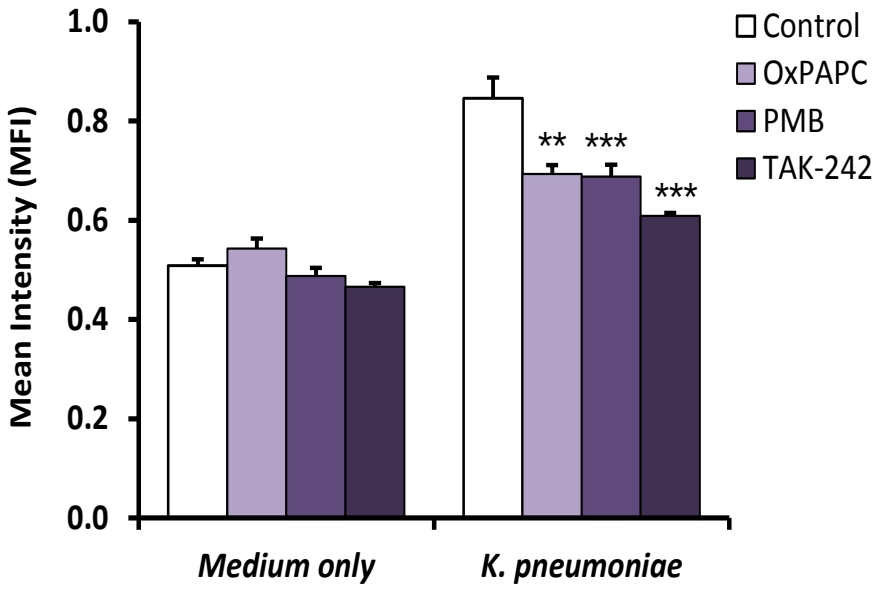

Figure 4.1. Effect of TLR inhibitors on *K. pneumoniae* - induced foam cell formation.

J774A.1 macrophages were cultured with 10^5 *K. pneumoniae*/ ml in the presence or absence of the indicated TLR inhibitors without LDL supplementation for 24 hours. Mean fluorescence intensity was measured by flow cytometry. Results are presented as the means ± SEM of three independent experiments. $^{**}p < 0.01$, $^{***}p < 0.001$ *vs.* cells cultured with *K. pneumoniae* alone.

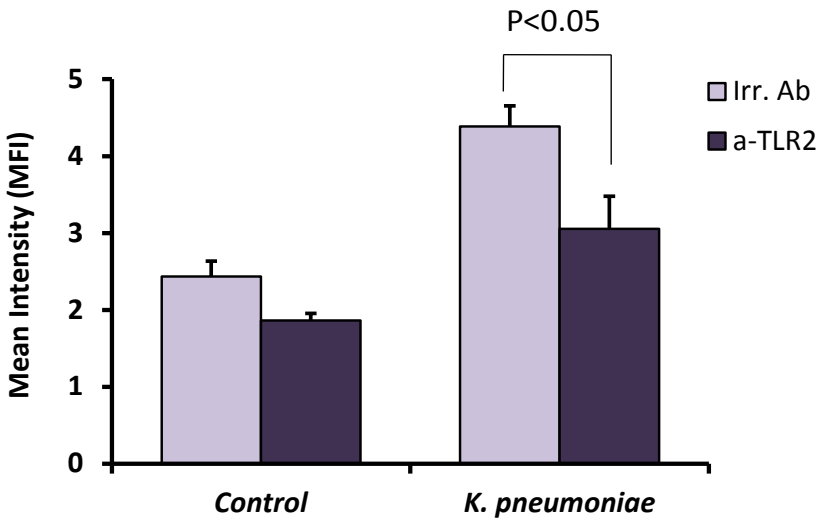

Figure 4.2. Effect of TLR2 antibody on *K. pneumoniae* – induced foam cell formation.

The effect of TLR inhibition on bacteria-induced foam cell formation was assessed in J774A.1 macrophages treated with 10^5 *K. pneumoniae/* ml with or without blocking antibody against TLR2 or an isotype-matched control antibody, without LDL supplementation for 72 hours. Mean fluorescence intensity was recorded by flow cytometry, and results are presented as the means ± SEM of three independent experiments.

A similar pattern was observed when the cholesterol ester content was measured in J774A.1 macrophages challenged for 24 hours with 10^5 *K. pneumoniae*/ ml supplemented with 50 μg/ ml of LDL with or without the above TLR inhibitors or antibodies (Figure 4.3 – a) [Research conducted by Dr. C. Erridge]. All three TLR inhibitors significantly blocked the accumulation of cholesterol ester in *K. pneumoniae*-treated cells. OxPAPC was the most potent inhibitor, resulting in a 4–fold reduction in CE accumulation when compared to cells treated with *K. pneumoniae* alone ($p < 0.01$). CE accumulation was also inhibited in *K. pneumoniae*-treated cells by the blocking α-TLR2 antibody (~1.5-fold reduction; $p < 0.05$) (Figure 4.3 – b).

Taken together, these results suggest a key role for TLR signalling, particularly via TLR2 and TLR4, in the process of bacteria-mediated CE accumulation and foam cell formation.

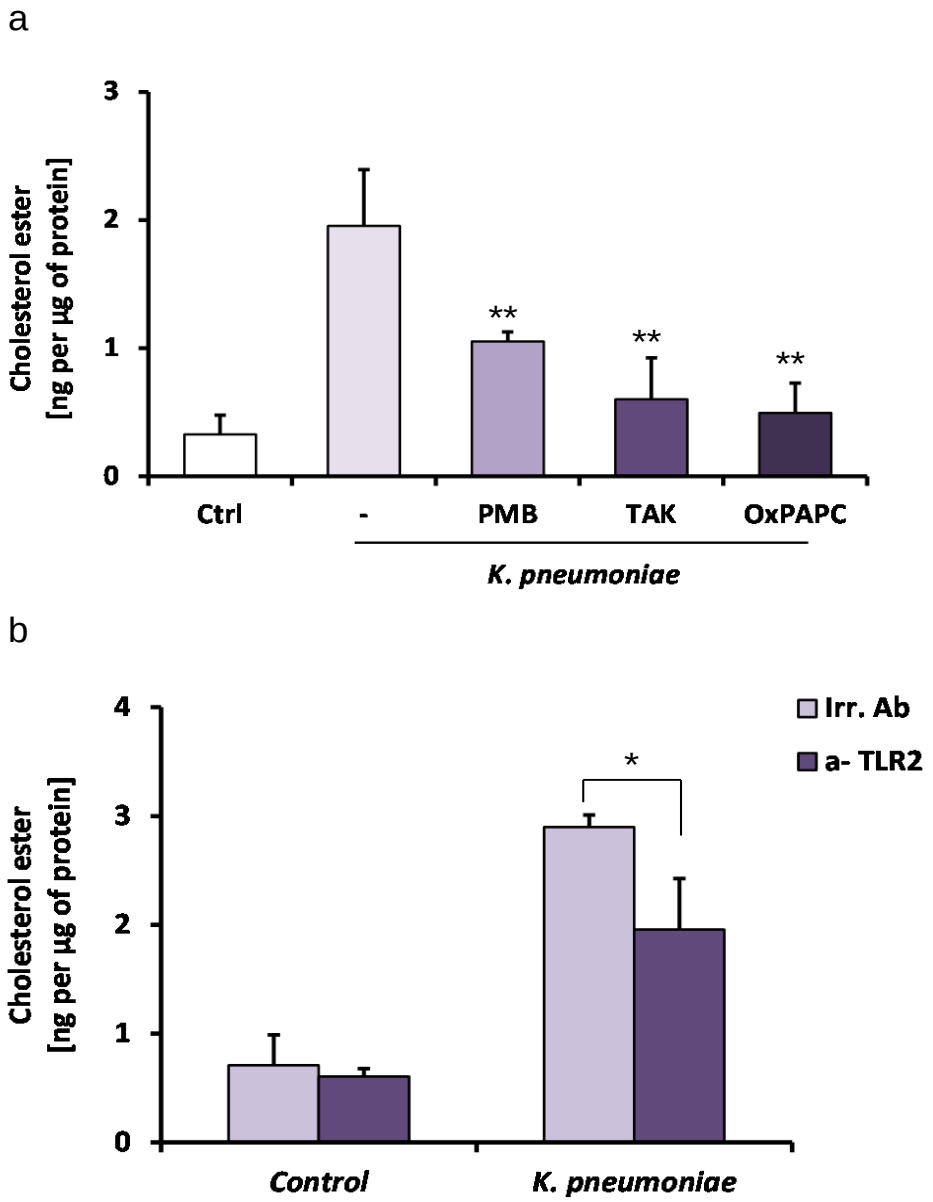

Figure 4.3. Effect of TLR inhibition on *K. pneumoniae* – induced cholesterol ester accumulation.

Cholesterol ester levels were measured in J774A.1 macrophages treated with 10^5 *K. pneumoniae*/ ml and 50 μg/ ml LDL for 24 hours, in the presence or absence of the indicated TLR inhibitors (a) or blocking antibodies against TLR2 (α-TLR2) or an isotype-matched control antibody (Irr. Ab) (b). Cholesterol ester levels were normalised to protein content. Results are presented as means ± SD of three independent experiments. *$p < 0.05$, **$p < 0.01$ *vs.* cells treated with *K. pneumoniae* only.

4.2. Bacteria - induced foam cell formation in TLR-deficient macrophages.

In order to further investigate a possible role of the TLR pathway in foam cell formation, TLR2 or TLR4 deficient mouse macrophage cell lines (each being immortalised lines from peritoneal macrophages derived from TLR2 or TLR4 deficient mice), were challenged for 72 hours with medium alone, 30 μg/ ml of nLDL, or 10^5 *E. coli*/ ml in the presence or absence of nLDL (30 μg/ ml). Foam cell formation was assessed by Oil Red-O staining and light microscopy, and quantification was performed by counting of Oil Red-O positive lipid droplets (Figure 4.4).

The percentages of foam cells obtained in TLR4-deficient cells were generally lower than those obtained from TLR2-deficient macrophages. When compared to TLR2-deficient macrophages, treatment with *E. coli* in the presence or absence of nLDL led to less foam cell formation in TLR4-deficient macrophages.

The results obtained from these cells were then compared to WT mouse BMDMs, where both TLR2 and TLR4 are expressed. Both TLR2 and TLR4-deficient cells had higher percentages of Oil Red-O staining at all treatments, even when treated with medium alone. The high background level of cellular lipid content recorded in TLR-deficient cells impeded further work using these cells, and could be the result of the viral transformation that these cells had undergone, which could have potentially changed their responsiveness to PAMPs.

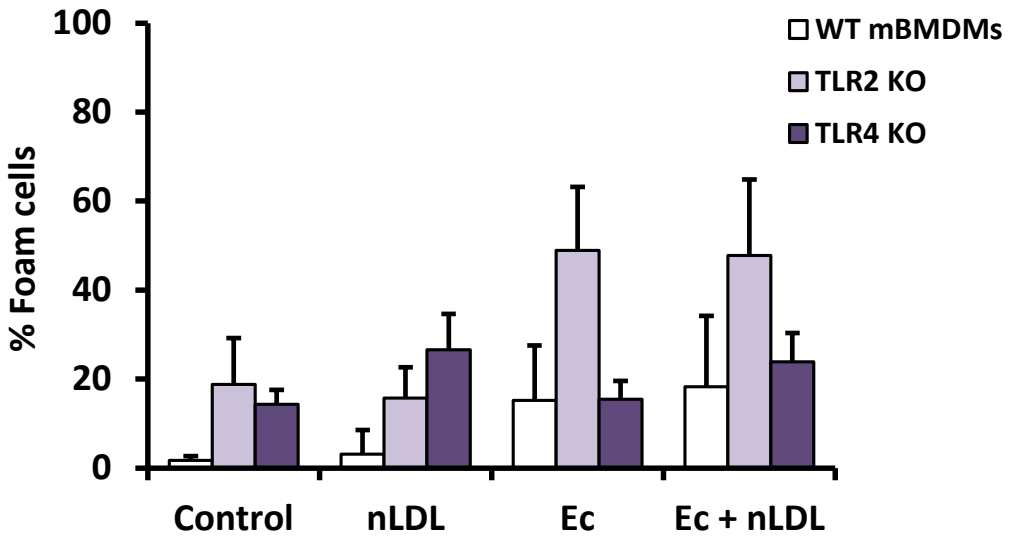

Figure 4.4. Bacteria – induced foam cell formation in TLR - deficient macrophages.

Macrophages deficient in TLR2 or TLR4 were treated for 72 hours with nLDL alone, or 10^5 *E. coli*/ ml in the presence or absence of nLDL. Results were compared to those obtained from WT mouse BMDMs, and are presented as the means ± SD of Oil Red-O positive cells.

4.3. Effects of TLR inhibitors on acetylated - LDL loading in macrophages.

Next, to rule out potential non-specific effects of the TLR-inhibitors examined on lipid uptake in macrophages, the effects of the inhibitors on acetylated-LDL (AcLDL) loading in macrophages were then examined. J774A.1 macrophages were treated for 24 hours with medium alone or 30 μg/ ml AcLDL in the presence or absence of the specific TLR4 inhibitors PMB (10 μg/ ml) or TAK-242 (1 μg/ ml), or 30 μg/ ml of the TLR2/TLR4 inhibitor OxPAPC. Flow cytometry was used to assess foam cell formation, and the results were representative of the averages of mean fluorescence intensities for each sample (Figure 4.5).

Foam cell formation induced by AcLDL is well established to be dependent on the uptake of modified LDL by scavenger receptors (Goldstein *et al.* 1979). As expected, treatment of cells with AcLDL resulted in a marked accumulation of intracellular lipid, as indicated by the 4.5–fold increase of mean fluorescence intensity in treated cells relative to control cells (AcLDL alone MFI: 0.9 *vs.* control MFI: 0.2). However, in contrast to the results obtained from *K. pneumoniae*-induced foam cell formation, inhibition of TLR signalling by specific TLR inhibitors did not block the formation of foam cells by AcLDL treatment, indicating that TLRs are not required in the process of AcLDL-induced foam cell formation.

Combined with the results obtained from *K. pneumoniae*-treated cells, and the earlier demonstration of no requirement for presence of either modified or unmodified lipoproteins (Figures 3.4 – 3.5), these data strongly suggest that the mechanisms by which bacteria, or TLR signalling, promote foam cell formation are quite distinct from those of the classical modified lipoprotein pathway.

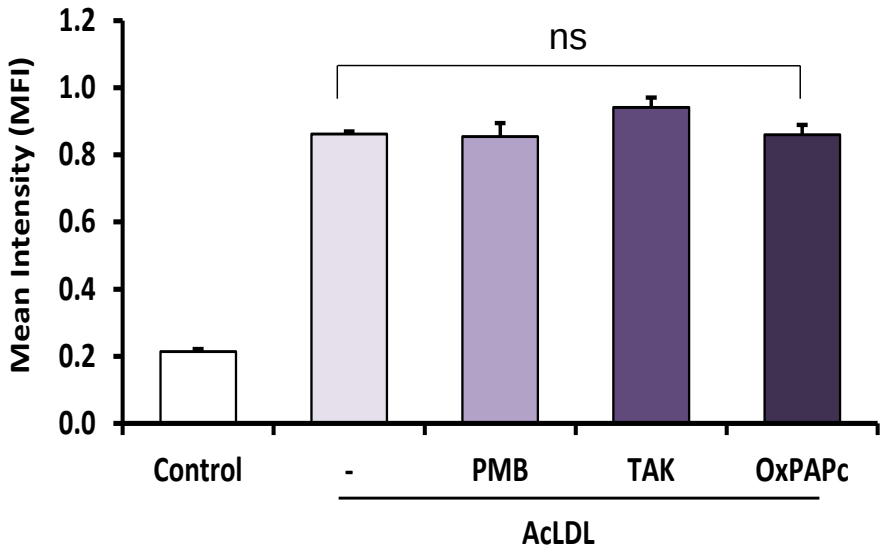

Figure 4.5. Effect of TLR inhibitors on AcLDL loading of J774A.1 macrophages.

The effect of selective TLR inhibitors was examined in J774A.1 macrophages cultured for 24 hours with AcLDL (30 μg/ ml) in the presence of the indicated TLR inhibitors. Mean fluorescence intensities were recorded by flow cytometry, and the results are presented as the means ± SEM of three independent experiments.

4.4. Effects of defined TLR stimulants on foam cell formation.

To test whether TLR signalling alone was sufficient to induce foam cell formation, a panel of six known TLR stimulants were tested for their ability to promote lipid accumulation in J774A.1 macrophages. Cells were challenged for 72 hours with medium alone or different concentrations (0.01 – 10,000 ng/ ml) of the selective TLR ligands Pam_3CSK_4 (TLR2/TLR1), FSL-1 (TLR2/TLR6), Poly I:C (TLR3), *E. coli* LPS (TLR4), *S. typhimurium* flagellin (TLR5), or bacterial CpG-containing DNA (TLR9) without LDL supplementation. Foam cell formation was assessed by light microscopy of Oil Red-O stained cells and droplet counting, as well as by flow cytometry of Nile Red stained cells.

All of the selected ligands induced the formation of lipid droplets, as observed by light microscopy (Figure 4.6). Cells treated with Pam_3CSK_4, FSL-1, and LPS had slightly larger cytoplasmic droplets compared to the cells treated with the other three TLR ligands. The average number of droplets per cell was also higher in response to those treatments.

Based on the definition of a foam cell containing ≥ 10 droplets per cell, all ligands induced the formation of foam cells in a dose-dependent manner, as indicated by droplet counting of Oil Red-O positive cells (Figure 4.7). The highest percentages were obtained from cells treated with LPS (56%), followed by Pam_3CSK_4 (52%) and FSL-1 (45%). CpG DNA treatment resulted in the lowest percentage of foam cells (13%) even at concentrations 10-times higher than the highest concentration used for the other PAMPs, suggesting that the cells might be hyporesponsive to CpG DNA stimulation.

Similar results were obtained by flow cytometry (Figure 4.8). PAMPs were used at concentrations where a clear induction of foam cell formation was observed by droplet

counting, and for the majority of the PAMPs these were lower compared to those used for light microscopy.

Similar to the results obtained by light microscopy quantification, the highest percentages of foam cells were observed in cells treated with Pam_3CSK_4 (22%), FSL-1 (22%) or LPS (20%). Both Poly I:C and CpG DNA failed to induce a strong response, with percentages at all tested concentrations remaining as low as that obtained from control cells (Poly I:C 4.2%; CpG DNA 4.8%). The fact that TLR3 and TLR9 are intracellular receptors might have affected the cell response to these ligands.

The percentages of foam cell formation obtained at the highest concentrations of PAMPs were slightly lower than the percentages obtained at the same concentrations by droplet counting. However, the percentages obtained at the lower concentrations were higher with this method, indicating that flow cytometry is more sensitive as a method when it comes to foam cell quantification.

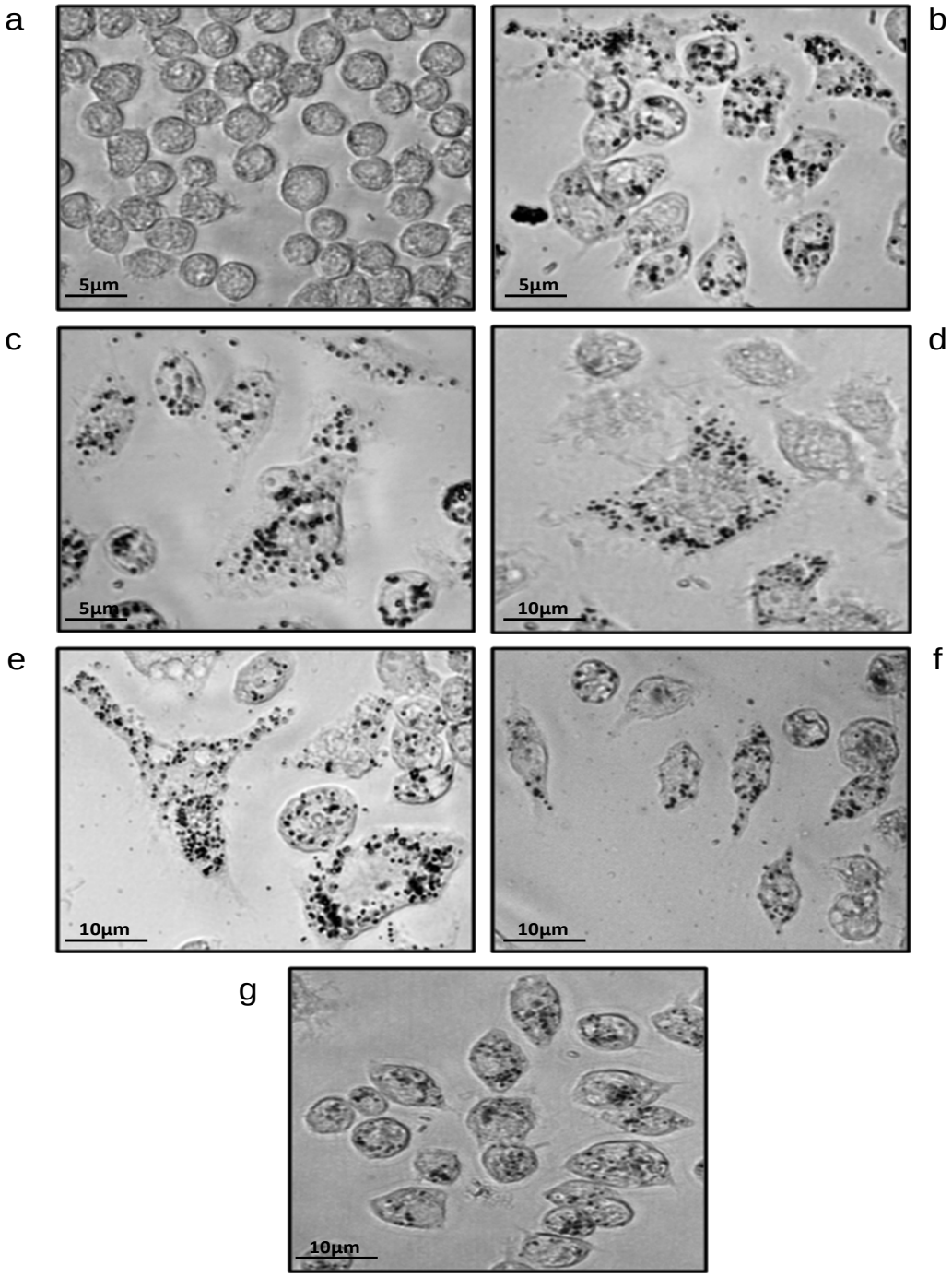

Figure 4.6. PAMP - induced foam cell formation in J774A.1 macrophages.

Light microscopy (40x) of Oil Red-O-stained J774A.1 macrophages treated for 72 hours with different TLR stimulants. a) Control (medium alone), b) Pam_3CSK_4 (1000 ng/ ml), c) FSL-1 (1000 ng/ ml), d) Poly I:C (100 ng/ml), e) LPS (1000 ng/ml), f) flagellin (1000 ng/ ml), g) CpG DNA (10,000 ng/ ml).

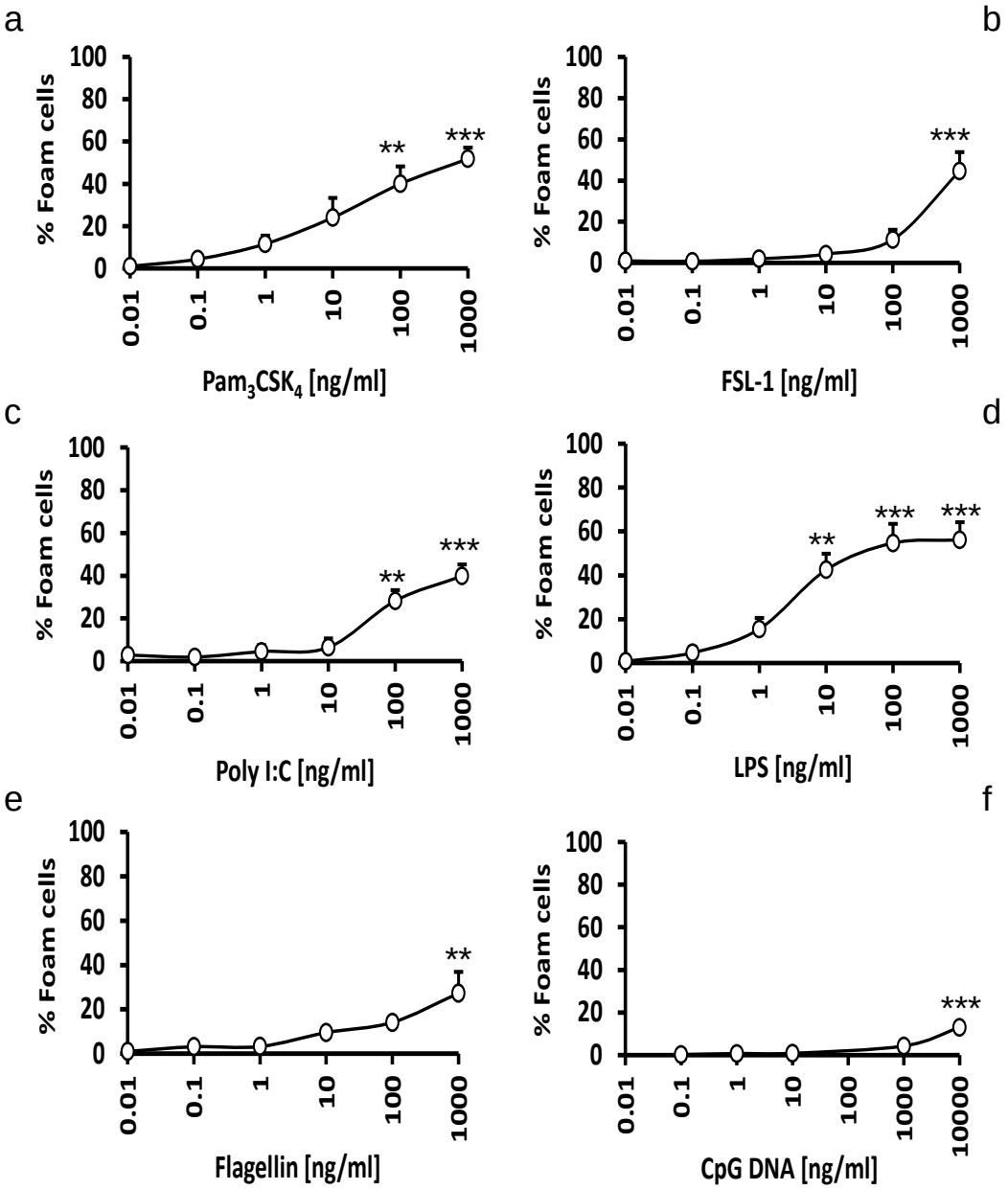

Figure 4.7. Quantification of PAMP – induced foam cell formation by droplet counting.

J774A.1 macrophages were cultured with defined TLR stimulants at different concentrations for 72 hours. Foam cell formation was quantified by light microscopy and droplet counting of Oil Red-O stained cells. Results are representative of the means ± SEM of three independent experiments. $^{**}p < 0.01$, $^{***}p < 0.001$ *vs.* cells cultured with PAMP at 0.01 ng/ ml.

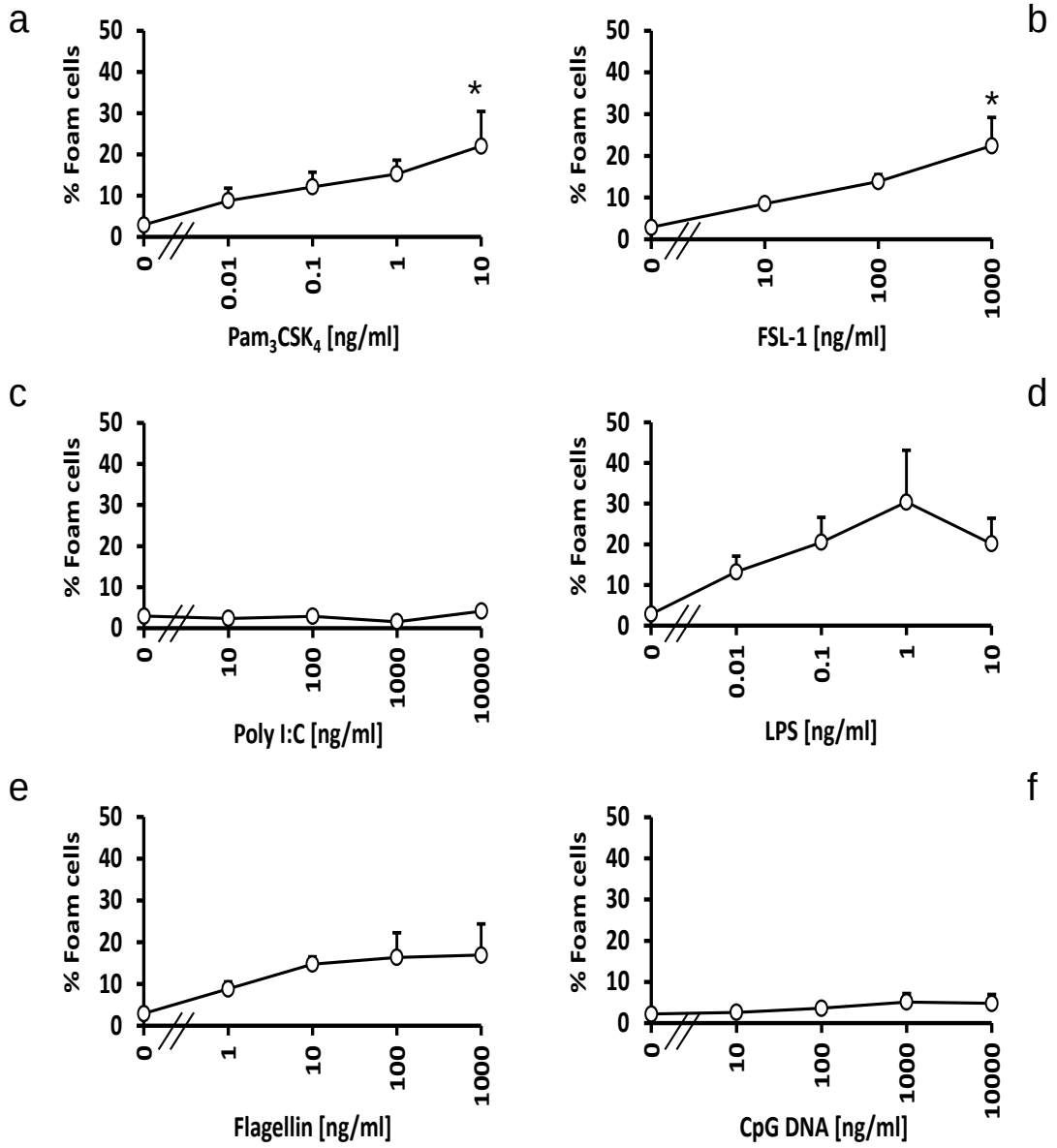

Figure 4.8. Quantification of PAMP – induced foam cell formation by flow cytometry.

Foam cell formation was assessed in J774A.1 macrophages treated for 72 hours with various TLR stimulants at different concentrations using flow cytometry. Results are presented as percentages of foam cells, and are representative of the means ± SEM of three independent experiments. *p <0.05 *vs.* control cells.

4.5. Effects of TLR stimulants on cellular cholesterol ester content.

PAMP-induced foam cell formation was also examined by biochemical quantification of cholesterol ester accumulation in J774A.1 macrophages treated with 1 μg/ ml of all the above TLR stimulants (except for Poly I:C used at 10 μg/ml), and 50 μg/ ml LDL for 24 hours [Research conducted by Dr. C. Erridge].

All tested PAMPs induced an increase in cellular cholesterol ester levels (Figure 4.9). FSL-1 had the most pronounced effect, resulting in a ~ 11-fold increase of CE levels above baseline, followed by Pam_3CSK_4 (~ 7-fold) (FSL-1: 4.30 ng, Pam_3CSK_4: 2.39 ng – $p < 0.01$; *vs*. control: 0.39 ng of CE/ μg of protein). Poly I:C and CpG DNA promoted the lowest increase in CE levels, confirming their low potency in inducing lipid droplet formation.

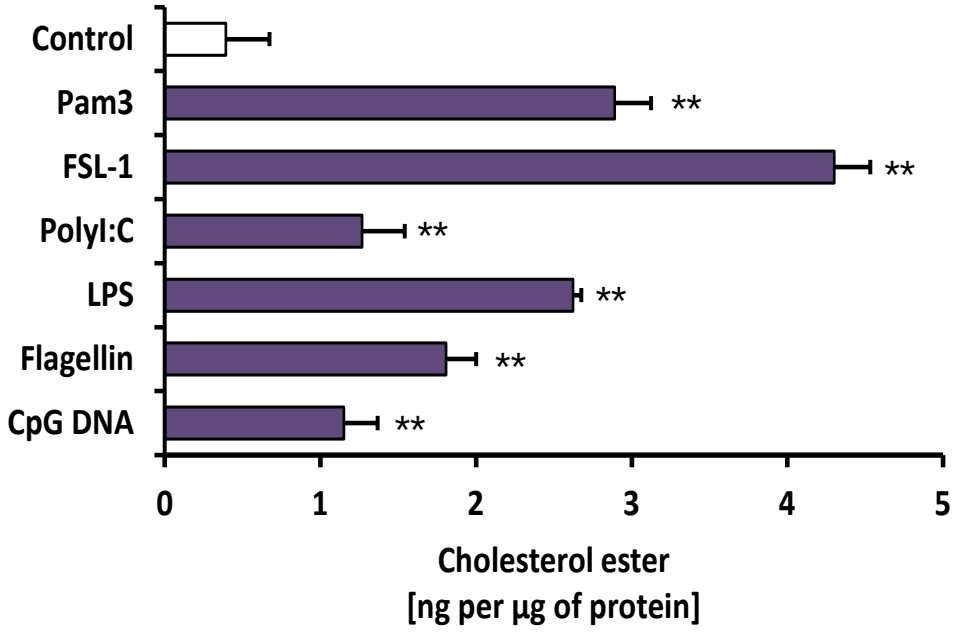

Figure 4.9. PAMP – induced cholesterol ester accumulation in J774A.1 macrophages.

J774A.1 macrophages were treated for 24 hours with 1 μg/ ml of the indicated TLR stimulants (except for Poly I:C, 10 μg/ ml) supplemented with 50 μg/ ml LDL. The measured cholesterol ester content was normalised to the protein content of the cells. Results are representative of the means ± SD of three different experiments. $^{**}p < 0.01$ *vs.* control cells.

4.6. Comparison of TLR-dependent foam cell quantification methods.

As in the previous chapter, we aimed to compare results obtained from PAMP challenge using the two main methods for foam cell quantification, to determine how well they may correlate with each other. The data used for the correlation charts were obtained by droplet counting and flow cytometry of J774A.1 macrophages challenged with Pam_3CSK_4, FSL-1, LPS and flagellin.

A strong correlation was obtained between droplet counting and flow cytometry for all the PAMPs tested (Pam_3CSK_4 r = 0.9; FSL-1 r = 0.9; LPS r = 0.8; flagellin r = 0.9; $p < 0.05$), adding further support to our conclusion that flow cytometry can be used as a reliable method for quantification of foam cells (Figure 4.10).

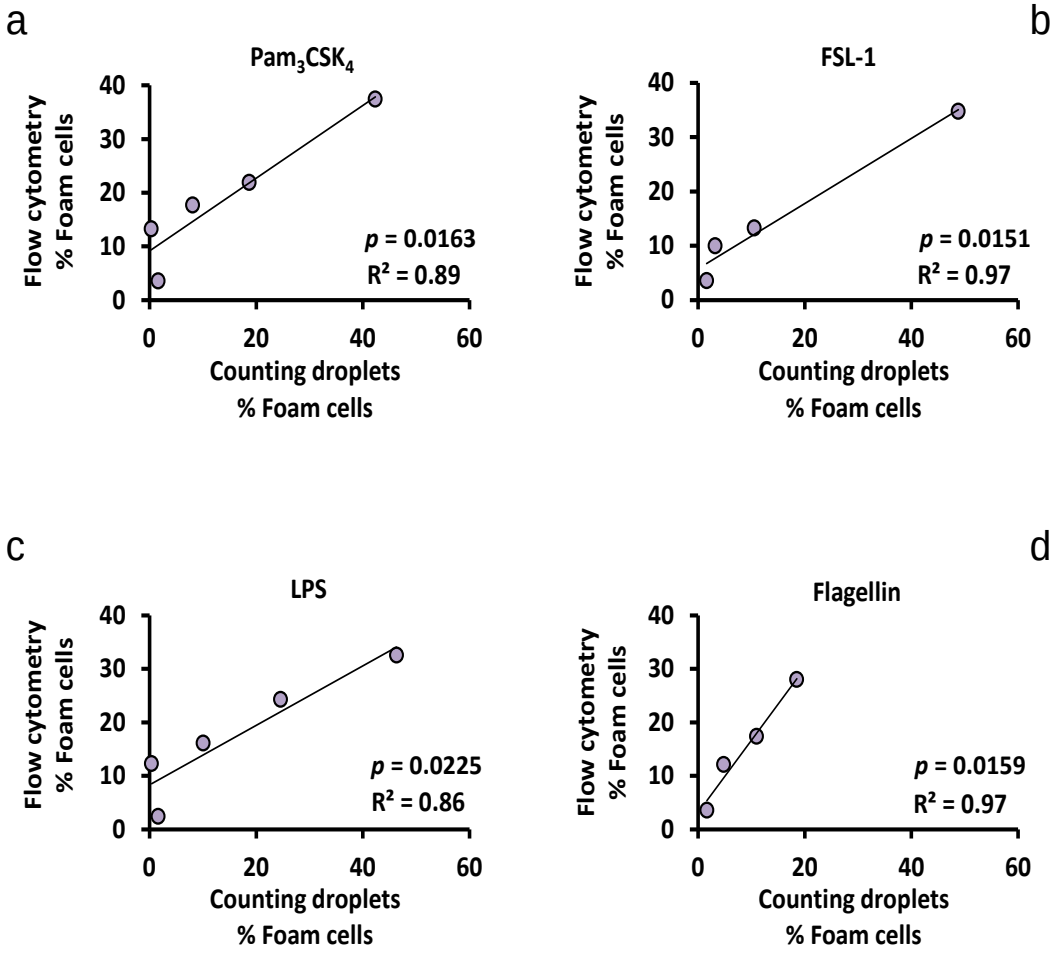

Figure 4.10. Correlation between droplet counting and flow cytometry.

4.7. Kinetics of LPS - induced foam cell formation.

In order to determine the kinetics of foam cell formation in response to PAMP treatment, a time-course experiment was carried out. LPS was used for this experiment, since it was shown to be one of the most potent inducers of foam cell formation both by droplet counting and flow cytometry. J774A.1 macrophages were treated with 100 ng/ml LPS for 0, 2, 6, 24, 48, and 72 hours, and foam cell formation was assessed by flow cytometry of Nile Red-stained cells. The data are presented as means of the percentages of positive cells at each time point (Figure 4.11).

Accumulation of cholesterol ester and foam cell formation was shown to occur by 24 hours after treatment, with the first signs of foam cell formation being observed at 6 hours, and increasing significantly over the next two days ($p < 0.05$ at 48 and 72 hours). These results were very similar to those obtained when J774A.1 macrophages were challenged with *E. coli* (section 3.3). Since LPS is a known TLR4 stimulant, the current results support the hypothesis of a contribution of TLR signalling in the process of foam cell formation.

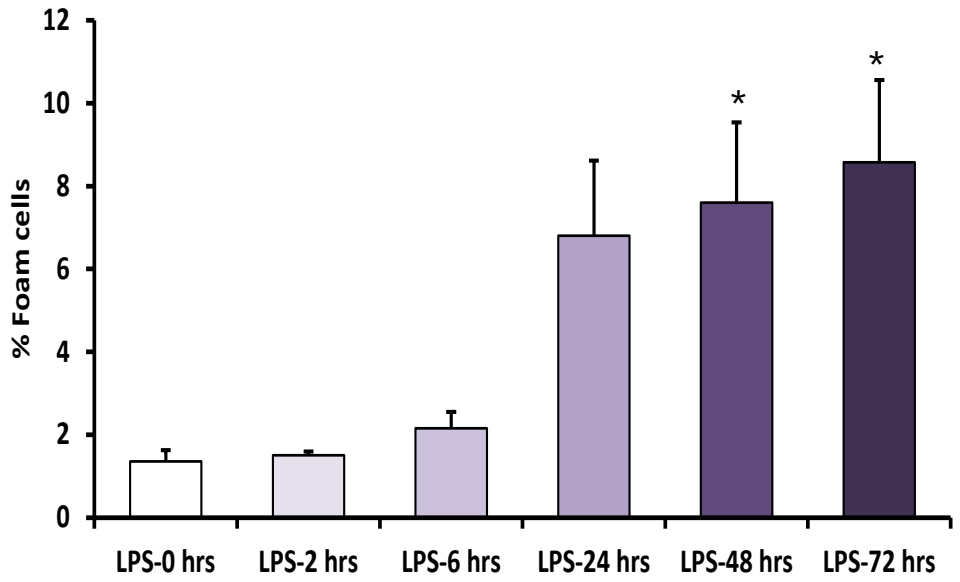

Figure 4.11. Kinetics of LPS – induced foam cell formation.

Foam cell formation in response to PAMP treatment was assessed in J774A.1 macrophages cultured for up to 72 hours with 100 ng/ ml LPS for the indicated time points. Percentages of positive cells were recorded by flow cytometry. The results are presented as the means ± SEM of three independent experiments. *$p < 0.05$ *vs.* LPS-treated cells at 0 hours.

4.8. TLR transfection assays.

In order to establish which types of TLR stimulants might be expressed by atheroma-associated bacteria, we performed a series of transfection assays. HEK-293 cells, which are TLR-deficient, were transfected with specific plasmids coding for human CD14, TLR2, TLR4/MD-2, and TLR5, along with an NF-κB-dependent reporter plasmid. 72 hours post-transfection the transfected cells were treated with 10^6 bacteria/ ml or 10 ng/ ml of Pam_3CSK_4, FSL-1, Poly I:C, LPS, flagellin or CpG DNA in triplicate, for 18 hours. Results are presented as fold-induction of the NF-κB-dependent promoter relative to control cells cultured in medium alone.

The results obtained show that the majority of the bacteria most commonly found in atherosclerotic plaques express stimulants of TLR2, TLR4 or TLR5, as indicated by the induction of the NF-κB-dependent promoter after treatment. TLR2 was activated by its known stimulants Pam_3CSK_4 and FSL-1, as well as both Gram-negative and the majority of Gram-positive bacteria, indicating that the majority of the bacteria tested express these two stimulants (Figure 4.12 - b).

In TLR4/MD-2-transfected cells, TLR4 signalling was, as expected, strongly induced by its selective ligand LPS. Activation of this receptor was also induced by the majority of the Gram-negative bacteria tested, as LPS is known to be a component of the outer wall of this type of bacteria (Figure 4.13 - c). *P. aeruginosa* and *P. diminuta* were less potent inducers of TLR4 signalling, consistent with the fact that that this genus expresses a penta-acylated LPS, which acts as an antagonist of human TLR4 (Hajjar *et al.* 2002).

Only *E. coli* and *P. aeruginosa* stimulated NF-κB signalling pathway in TLR5-transfected cells, consistent with the fact that flagellin is considered to be the only

stimulant of TLR5, and these were the only flagellated organisms in the panel tested (Figure 4.13 - d).

Of note, apart from LPS, none of the TLR stimulants used in this experiment induced the activation of TLR4 signalling in TLR4/MD-2-transfected cells, indicating that they were endotoxin-free, and therefore any effect exhibited by these stimulants in subsequent experiments is not due to LPS contamination.

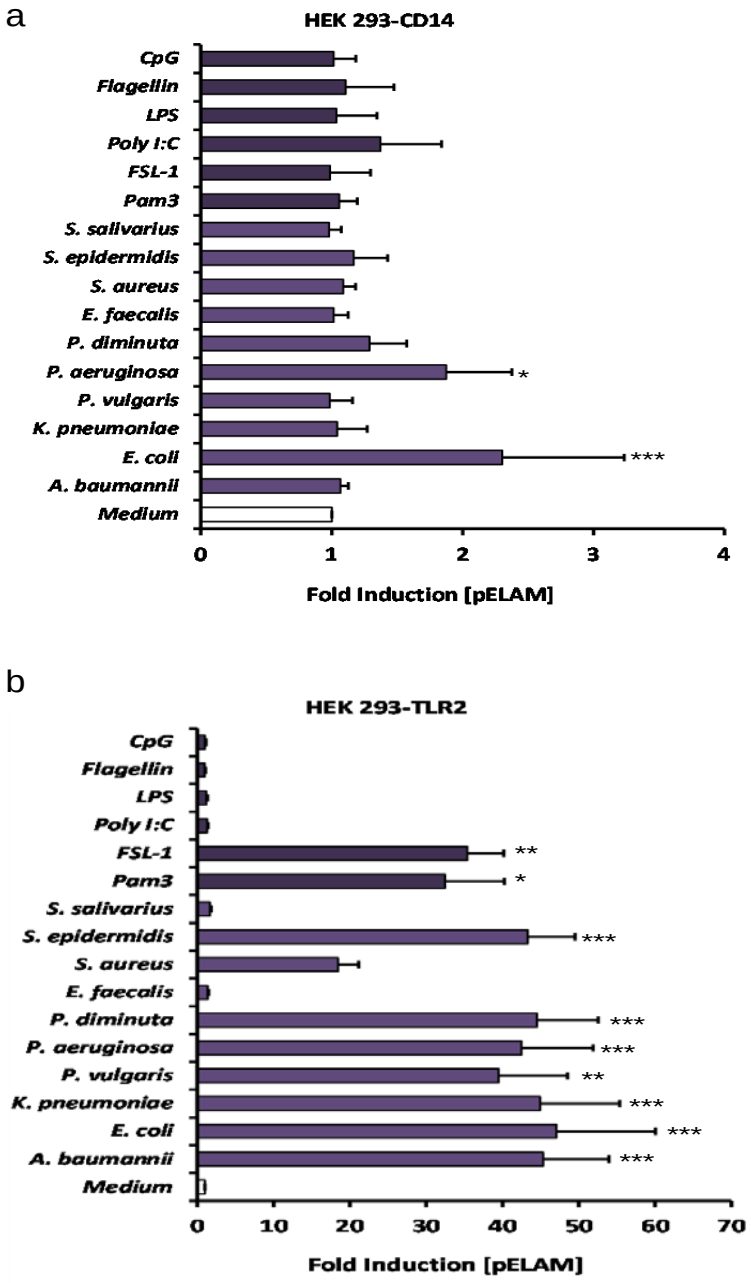

Figure 4.12. Atheroma – associated bacteria express TLR2 stimulants.

Transfection of TLR-deficient HEK-293 cells with CD14 (a), TLR2 (b) and NF-κB-dependent promoter. Transfected cells were then challenged with 10^6 bacteria/ ml or 10 ng/ ml of defined TLR stimulants for 18 hours. Data is presented as fold induction of the NF-κB-dependent reporter (pELAM) relative to control cells. Results are presented as the means ± SEM of three independent experiments. *$p < 0.05$, **$p < 0.01$, ***$p < 0.001$ *vs.* control cells in medium alone.

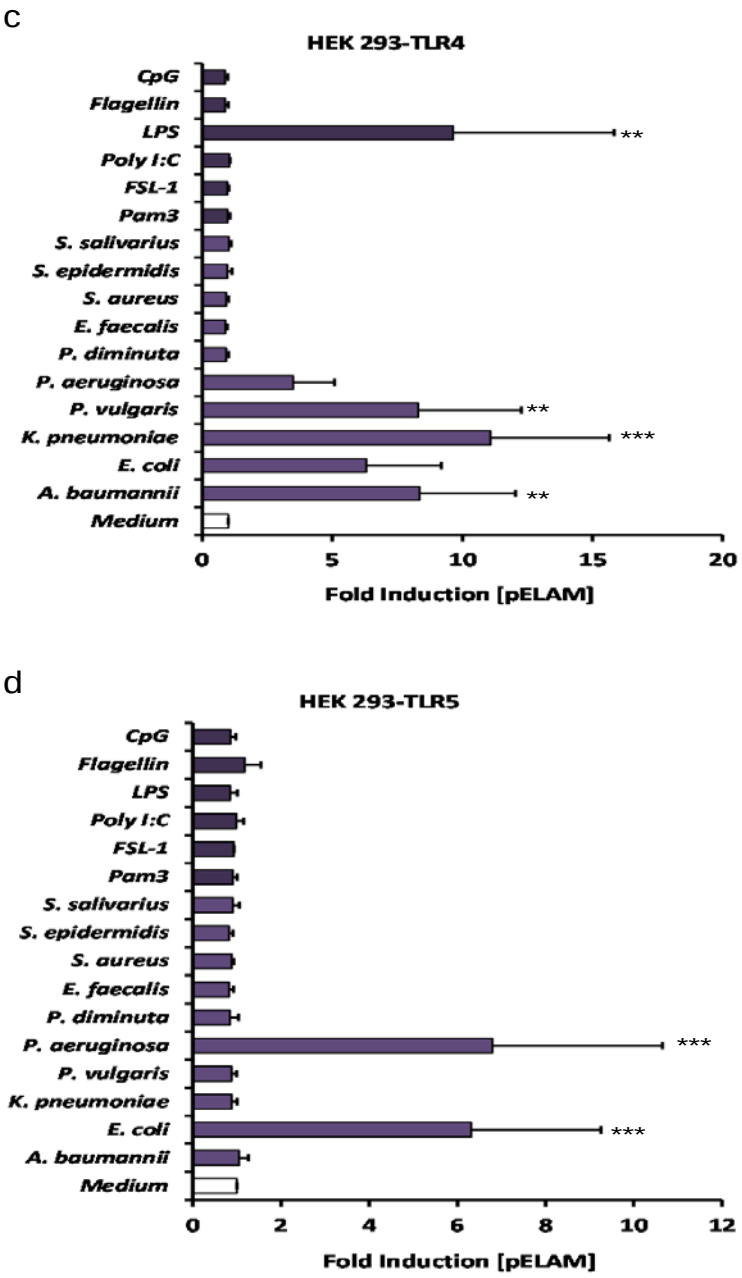

Figure 4.13. Atheroma – associated bacteria express TLR4 and TLR5 stimulants. HEK-293 cells were transfected with TLR4/MD-2 (c), TLR5 (d) and NF-κB-dependent promoter. Transfected cells were then challenged with 10^6 bacteria/ ml or 10 ng/ ml of defined TLR stimulants for 18 hours. Data is presented as fold induction of the NF-κB-dependent reporter (pELAM) relative to control cells. Results are presented as the means ± SEM of three independent experiments. *$p < 0.05$, **$p < 0.01$, ***$p < 0.001$ *vs.* control cells in medium alone.

Summary

The results presented in this chapter provide evidence that bacteria-induced foam cell formation is TLR-dependent, and specifically highlight key roles for TLR2 and TLR4 in this process. They also establish that TLR signalling is sufficient to induce the formation of foam cells, and that there is no requirement for modified or unmodified lipoproteins. Foam cell formation in response to bacteria, or other TLR stimulants, therefore appears to proceed via a mechanism distinct from the classical pathway, which requires the uptake of modified LDL by scavenger receptors.

5. RESULTS – LIPID ACCUMULATION IN PRIMARY CELLS AND *IN VIVO*

In vitro studies performed in recent years have helped in the understanding of several of the cellular and molecular mechanisms involved in the formation of foam cells (Lusis 2000). *In vivo* testing of hypotheses relating to mechanisms of foam cell formation generated from *in vitro* experimentation has been most frequently carried out through the use of gene-targeted or transgenic murine experimental models of atherogenesis, such as LDLr and Apo-E knock-out mice (Lusis 2000; McNeill *et al.* 2010). Both mouse models develop atherosclerotic lesions which are similar in many respects to those which develop in humans (Lusis 2000). However, as we did not have access to such models, and since it is always important to be able to reproduce *in vivo* what has been observed *in vitro*, we next aimed to establish whether or not exposure to PAMPs could modulate lipid accumulation in primary human monocytes in pure culture, in whole blood cultured *ex vivo* or in healthy volunteers *in vivo*.

5.1. Baseline lipid droplet formation in human monocytes and macrophages

In order to establish the best culture conditions that would enable us to culture human monocytes isolated from blood with a minimal background of cytoplasmic lipid body content, preliminary experiments were performed to determine the background levels of lipid accumulation of primary human monocytes isolated from blood of healthy human volunteers. The isolated monocytes were cultured in RPMI-1640 supplemented with 10% autologous serum. Cells were maintained in culture for 7 days to promote their differentiation into macrophages, and images of Oil Red-O-stained cells were taken daily (Figure 5.1).

To our surprise, human macrophages cultured in this way spontaneously formed foam cells, even in the absence of an exogenously delivered stimulus. The exact mechanism that triggers this transformation is not clear. We investigated the possibility that the autologous serum itself may contain a factor capable of triggering the spontaneous formation of foam cells in culture. However, similar observations were made when heat-treated serum or Gibco serum-free macrophage medium were used to culture the macrophages [Dr. C. Erridge; personal communication].

Monocyte isolation by adherence, after the purification of the PBMC fraction with Histopaque-1077, is one of the most commonly used methods to isolate monocytes. This procedure, although simple, yields a relatively high percentage of contamination with other cell types, most commonly lymphocytes (de Almeida *et al.* 2000). The isolation of monocytes using CD14 MACS beads is an alternative method used, which yields monocytes of a higher percentage purity and reduced contamination with other cell types. The use of this method, however, yielded similar results, as spontaneous droplet formation was still observed in monocytes prepared using this method (data not shown).

These observations led us to conclude that it was not feasible to use long-term cultured human macrophages for our studies of foam cell generation, as the level of spontaneous foam cell formation was too high.

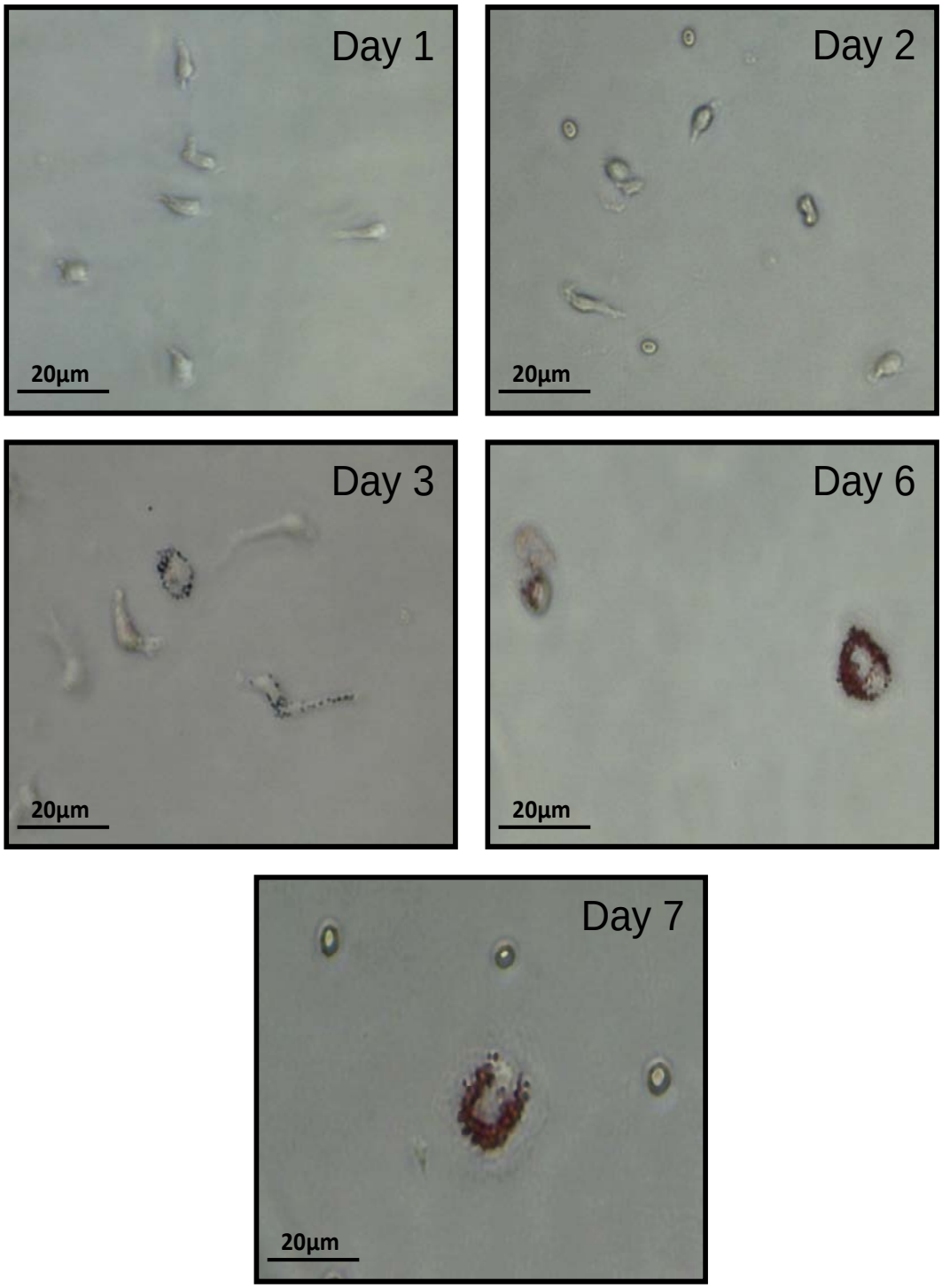

Figure 5.1. Spontaneous lipid droplet formation in human monocytes and macrophages

Light microscopy (40x) of Oil Red-O-stained monocytes and monocyte-derived macrophages maintained in autologous serum isolated from human blood.

5.2. Bacteria – mediated foam cell formation in human whole blood.

Since the use of human long-term cultured macrophages for foam cell studies proved to be confounded by issues with high levels of background lipid droplet formation, we attempted shorter-term experiments using whole blood, creating a model of transient bacteraemia which was intended to resemble real life conditions more closely than macrophages cultured in isolation.

For these experiments, whole blood collected from healthy donors was exposed to sterile PBS or 10^6 *K. pneumoniae* / ml or 10^6 *S. salivarius*/ ml, or 1 μg/ ml of the selective TLR ligands Pam_3CSK_4, FSL-1, Poly I:C, LPS, flagellin and CpG DNA for 30 minutes at 37 ˚C. *K. pneumoniae* and *S. salivarius* were chosen as model organisms to represent Gram-negative and Gram-positive bacteria, respectively. PBMCs were isolated by density gradient centrifugation on Histopaque-1077 separating solution, and the isolated monocytes were cultured in 10% autologous serum for 18 hours. Foam cell formation was assessed by light microscopy of Oil Red-O stained cells, followed by lipid droplet counting (Figure 5.2 – a-c).

Both types of bacteria induced the formation of large lipid droplets in treated cells. As with our previous observations, *K. pneumoniae* was a more potent inducer of foam cell formation than *S. salivarius*, as indicated by the higher average number of lipid droplets counted per cell (*K. pneumoniae*: mean 7 droplets/ cell *vs*. *S. salivarius*: 5 droplets/ cell; $p < 0.001$ *vs.* control) (Figure 5.2).

Similar results were obtained from PAMP-treated cells. All TLR stimulants examined were able to induce the formation of foam cells in human monocytes (Figure 5.3). The majority of PAMPs led to a significantly higher average number of droplets per cell when compared to control (Figure 5.4). Poly I:C led to droplet formation in treated cells, but the results obtained did not reach significance. Contrary to the results

obtained from J774A.1 macrophages, CpG DNA displayed the greatest potential to stimulate foam cell formation in human monocytes, suggesting that human monocytes might be more responsive to this treatment.

Compared to J774A.1 macrophages, the droplets observed in human monocytes were larger in size, and fewer in number. The results obtained provide evidence that foam cell formation in monocytes can occur within 24 hours if they have been exposed to bacteria or their products.

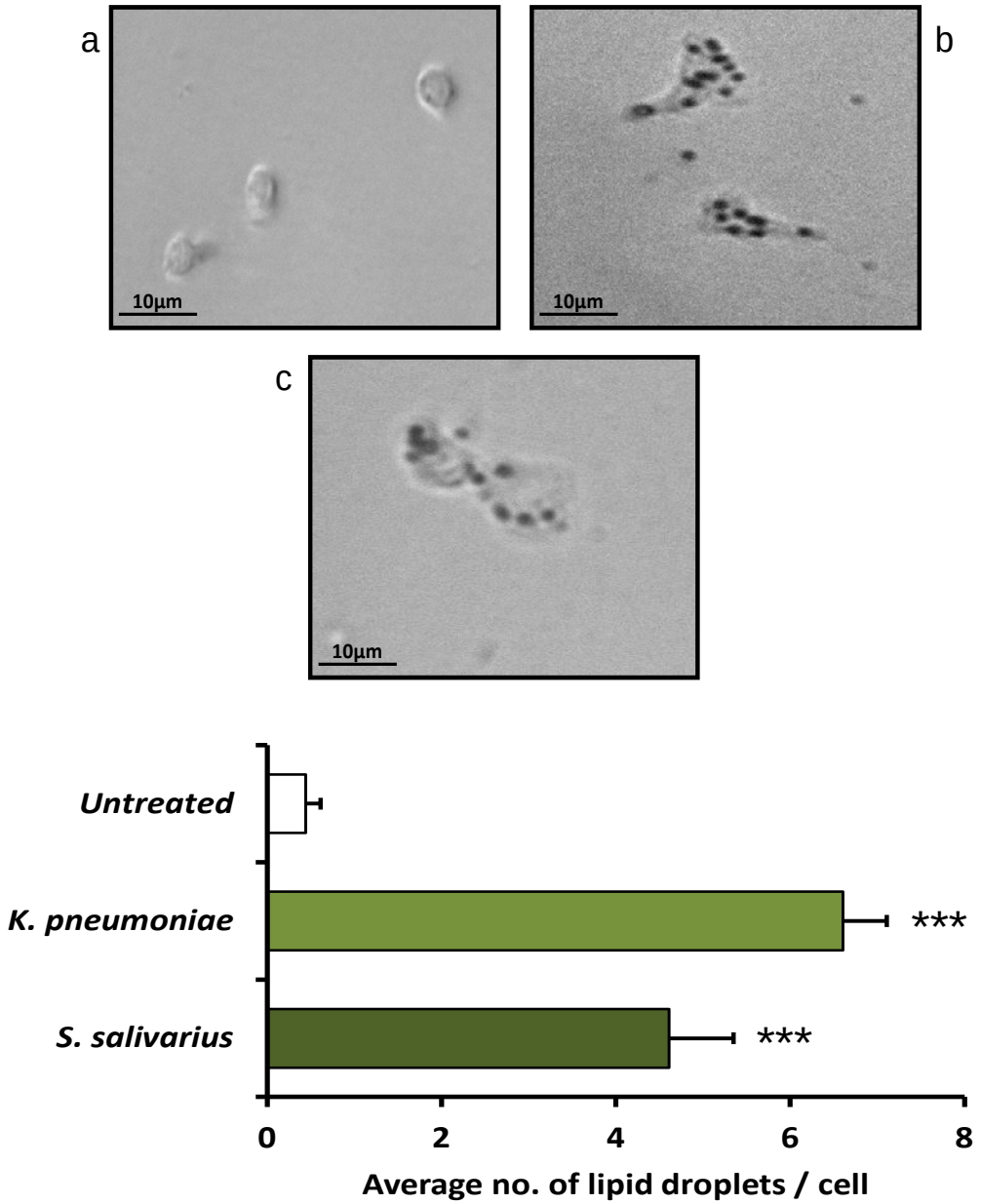

Figure 5.2. Bacteria-mediated lipid droplet formation in human monocytes

Whole blood was transiently exposed to 10^6 *K. pneumoniae* or *S. salivarius*/ ml for 30 minutes, and lipid droplet formation was assessed in isolated monocytes after 18 hours by light microscopy (40x) of Oil Red-O-stained cells (a) control, (b) *K. pneumoniae*, (c) *S. salivarius*. Foam cell quantification data is presented as the average no. of lipid droplets per cell ± SEM of five independent experiments. ***$p < 0.001$ *vs*. control.

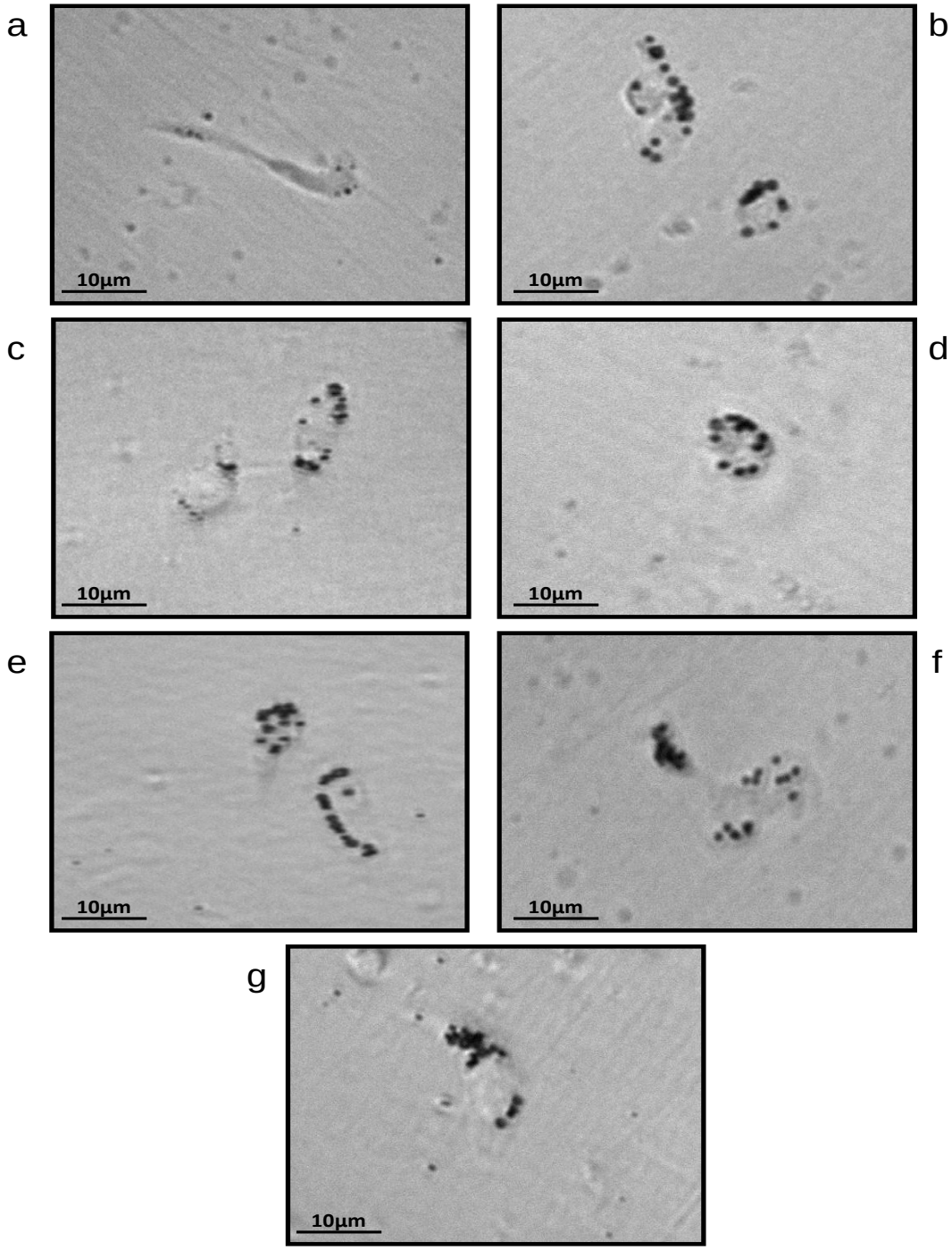

Figure 5.3. Human monocyte foam cell formation in a whole blood model of exposure to circulating PAMPs

Light microscopy of Oil Red-O stained human monocytes isolated from whole blood previously treated with PAMPs at 1 μg/ ml. (a) Control, (b) Pam_3CSK_4, (c) FSL-1, (d) Poly I:C, (e) LPS, (f) flagellin, (g) CpG DNA. Magnification: 40x

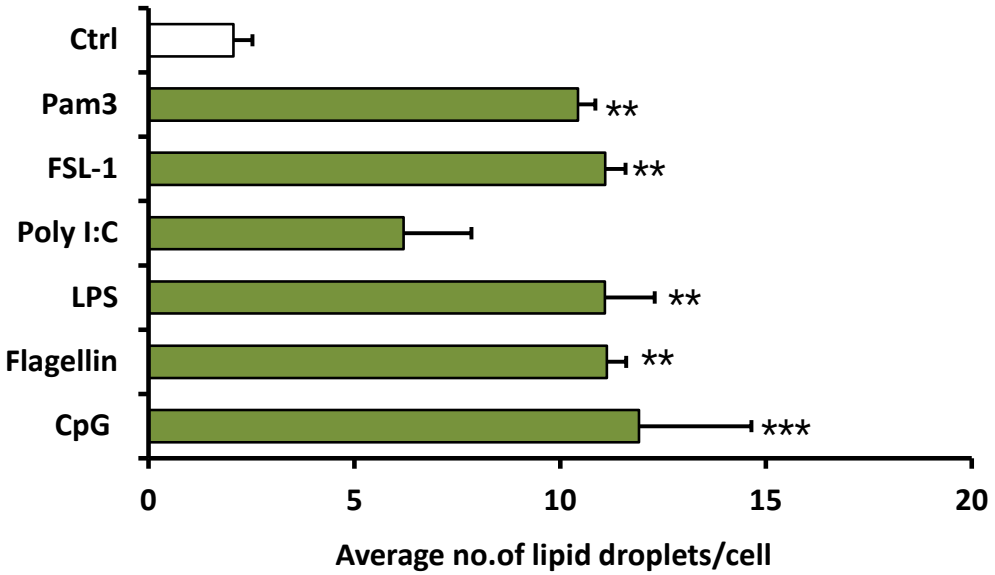

Figure 5.4. PAMP-mediated foam cell formation in human whole blood

Human whole blood was exposed for 30 minutes to TLR stimulants, and foam cell formation was quantified by droplet counting in Oil Red-O stained monocytes after 18 hours. Data is presented as the average no. of lipid droplets per cell ± SEM of three independent experiments. $^{**}p < 0.01$, $^{***}p < 0.001$ *vs*. control.

5.3. Kinetics of bacteria-induced foam cell formation in whole blood.

In previous time-course experiments performed using murine cell line cells, we were able to show that the process of bacteria or PAMP-mediated foam cell formation could be initiated as early as 6 hours post-treatment. It was therefore important to determine whether this could also be seen in human monocytes.

Whole blood collected from healthy individuals was treated with 10^6 *E. coli*/ ml for 0, 1, 2, 3, 4, and 5 hours at 37 ˚C. For this experiment, leukocytes were isolated after red blood cell lysis and were stained with Nile Red. Foam cell formation was assessed by flow cytometry, and gating on forward and side scatter was applied to ensure the assessment of the correct cell population.

The results obtained revealed that droplets formed quickly in human monocytes after bacterial challenge (Figure 5.5). An increase in fluorescence and the percentages of positive cells compared to control could be observed as early as 1 hour after treatment, and it continued to increase over time (average: 41.2 % at 5 hours *vs*. 2.2% at 0 hours; $p = 0.059$). The increase in fluorescence recorded for the treated cells was not a result of auto-fluorescence, since the fluorescence measured from unstained aliquots of the same samples remained low, an indication that any changes in fluorescence were lipid-specific.

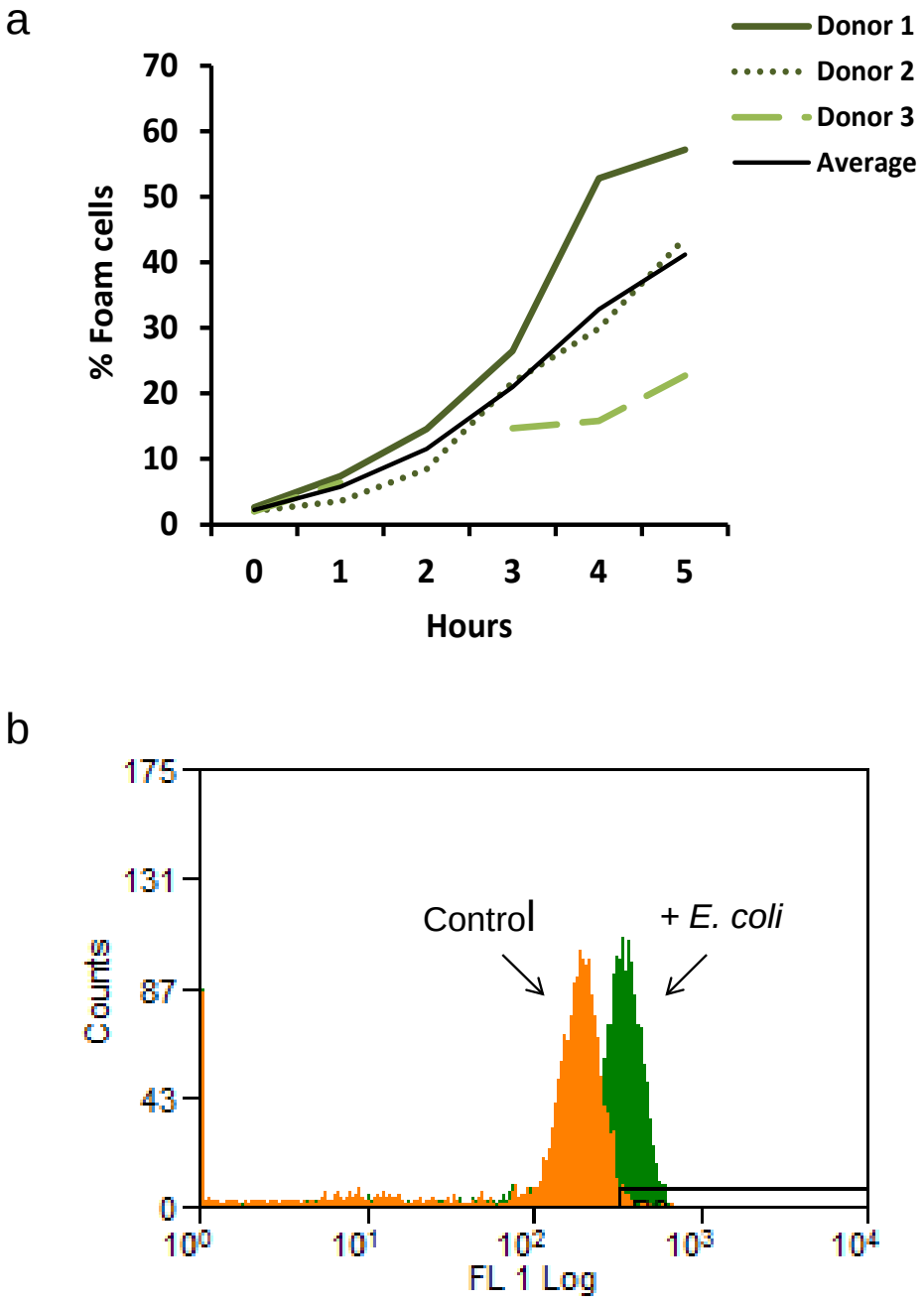

Figure 5.5. Kinetics of foam cell formation in human blood monocytes

Human whole blood was treated with 10^6 *E. coli* / ml for the indicated time points. Foam cell formation was assessed by flow cytometry of Nile Red-stained leukocytes (n=3). Data is presented as percentages of foam cell over time (a). The shift of the fluorescence peak to the right is indicative of foam cell formation in the assessed cells (b).

5.4. Monocyte lipid droplet formation during postprandial lipaemia

We next aimed to examine whether or not exposure to low doses of PAMPs could modulate lipid levels in circulating monocytes *in vivo*. The most commonly used model of endotoxaemia in human volunteers is bolus injection of *E. coli* LPS using typical doses of 2-4 ng/ kg (van Deventer *et al.* 1990). However, as this protocol can cause severe malaise, fever, nausea and vomiting, and is therefore a more severe inflammatory stimulus than the chronic low-grade stimulus thought to potentiate atherosclerosis, we elected for an alternative model of lower-grade endotoxaemia in human volunteers.

It is well established that consumption of a high-fat meal results in postprandial lipaemia. This phase is characterised by the accumulation of triglyceride-rich lipoproteins, such as chylomicrons and very low-density lipoproteins (VLDL) in the circulation (Hyson *et al.* 2002). However, post-prandial lipaemia is also characterised by a transient increase in circulating inflammatory markers (Poppitt *et al.* 2008). It was recently shown that this may be potentiated by the co-absorption of bacterial endotoxin from the gut with dietary fat (Erridge *et al.* 2007; Ghoshal *et al.* 2009). Studies have shown that the levels of circulating endotoxin increase by ~50-100% after the consumption of a high-fat meal, and that this increase was independent of the subjects' metabolic status (Erridge *et al.* 2007; Harte *et al.* 2012).

The increased concentration of endotoxin observed postprandially is the result of the transfer of endotoxin from the gastrointestinal tract into the circulation by one of the major groups of lipoproteins, the chylomicrons, which were shown to have a high affinity for endotoxin (Ghoshal *et al.* 2009). This can result in low-grade systemic inflammation, leading to the activation of leukocytes and the production of pro-inflammatory cytokines and other inflammatory markers (Cani *et al.* 2007; Erridge *et al.* 2007).

In our model of diet-induced endotoxaemia, whole blood was collected from healthy volunteers before and after a high fat meal (43 g fat, 705 kCal total). Foam cell formation in isolated leukocytes was assessed by flow cytometry. Leukocyte counts, temperature, blood pressure and pulse were also recorded before and after the meal for each individual.

Measurements of percentage positive staining of monocytes stained with Nile Red (or without dye treatment) in blood samples were made before (0 hours) and after (6 hours) the meal from each individual. A decrease in the percentage of positive cells was observed in the majority of the unstained samples at 6 hours, indicating that any possible changes in positive cell percentages in the stained samples at the same time point were lipid-specific and not due to monocyte auto-fluorescence (Figure 5.6 – a).

Analysis of the stained samples revealed an increase in the percentage of positive cells in three of the six donors, at 6 hours compared to 0 hours, as indicated by the increase in percentage positive cells in the postprandial phase ($p = 0.13$) (Figure 5.6 – b), and the shift of the fluorescence peak produced by postprandial samples to the right. This indicates that the lipid droplet content of monocytes of some volunteers increased postprandially.

Markers consistent with onset of low-grade inflammation were also seen in the majority of the volunteers. Total white blood cell (WBC), lymphocyte and monocyte counts were shown to be increased at 6 hours in some individuals (WBC: $p < 0.05$; lymphocytes: $p < 0.01$) (Figure 5.7). An increase was also observed in body temperature readings at the same time point, with the average increase being around 0.35 ˚C ($p < 0.05$) (Figure 5.9). Levels of the inflammatory cytokines IL-6, IL-1-β and TNF-α in plasma were below the limits of detection by standard sensitivity ELISA. As expected, no changes were observed with respect to non-inflammatory markers, such as red blood

cell (RBC) counts, haemoglobin concentrations, haematocrit, platelet counts, or procalcitonin (Figure 5.8). No major differences were observed between blood pressure or pulse measurements taken before or after the meal (Figure 5.9). It is possible that these observations indicate a low-grade inflammatory response induced by a systemic exposure to an inflammatory stimulus, although control meal experiments would be required to confirm this. Of interest, the individuals showing the biggest changes in inflammatory markers were also those who demonstrated the higher percentages of Nile Red positive cells in the post-prandial phase, suggesting that the two responses may be linked in some way.

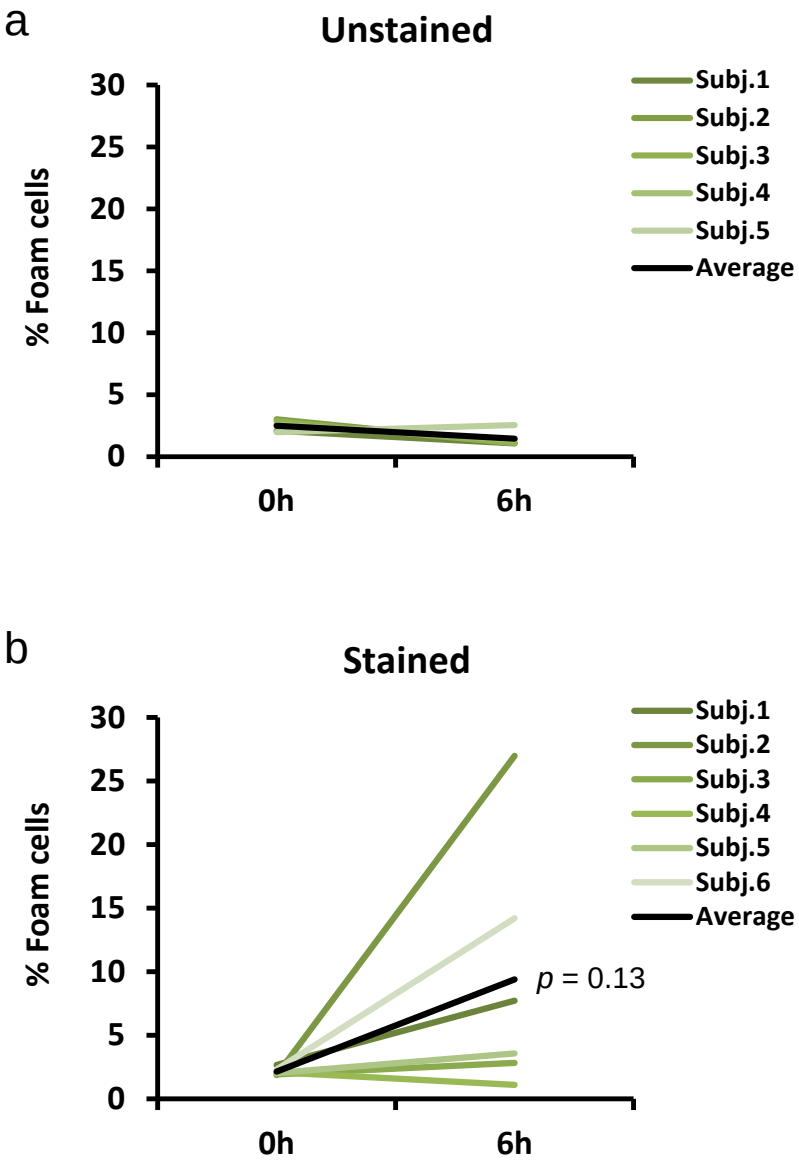

Figure 5.6. Foam cell formation in human monocytes in the postprandial phase

Quantification by flow cytometry of foam cell formation in unstained (a) and Nile Red-stained (b) samples collected from six volunteers before (0h) and after (6h) the consumption of a high-fat meal. Results are presented as percentages of foam cells.

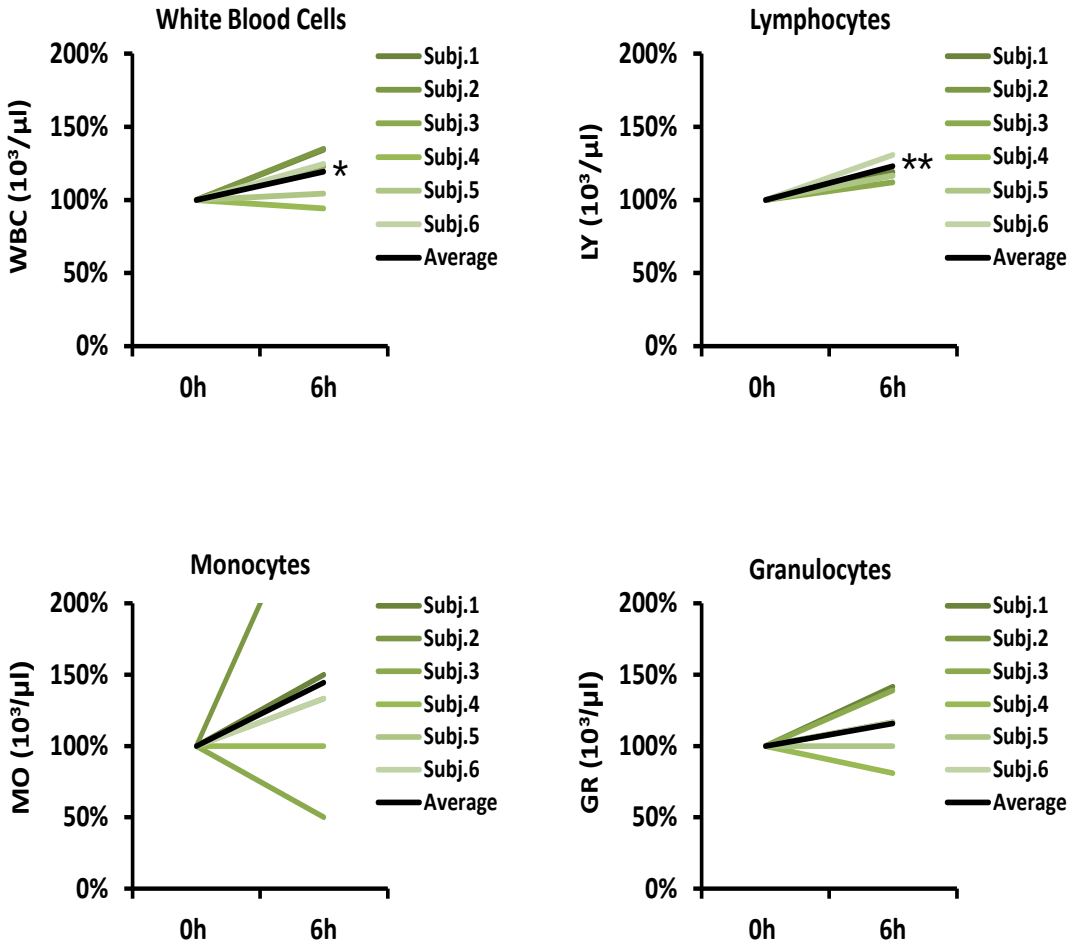

Figure 5.7. Postprandial changes in markers of systemic inflammation after a high-fat meal.

Markers of systemic inflammation, such as white blood cell, lymphocyte and monocyte counts increased postprandially (6h) after a high fat meal. Counts were obtained from whole blood samples from six volunteers. *$p < 0.05$, **$p < 0.01$ *vs.* before (0h) measurements.

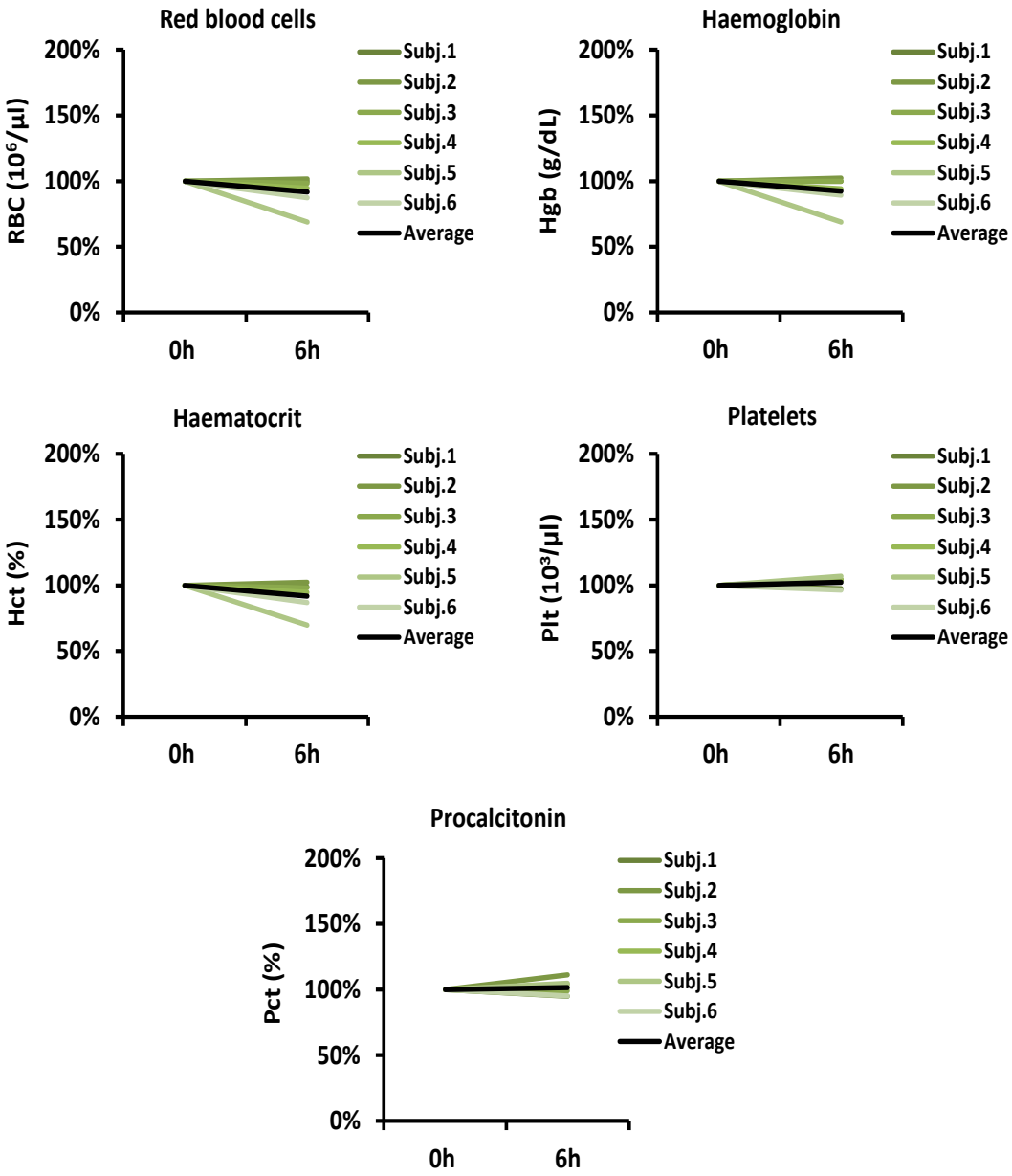

Figure 5.8. Effect of a high-fat meal on other haematological markers.

No postprandial changes were observed in red blood cell counts, haemoglobin concentration, haematocrit, platelet counts, or the calcitonin's peptide precursor, procalcitonin. Counts were obtained from whole blood samples from six volunteers.

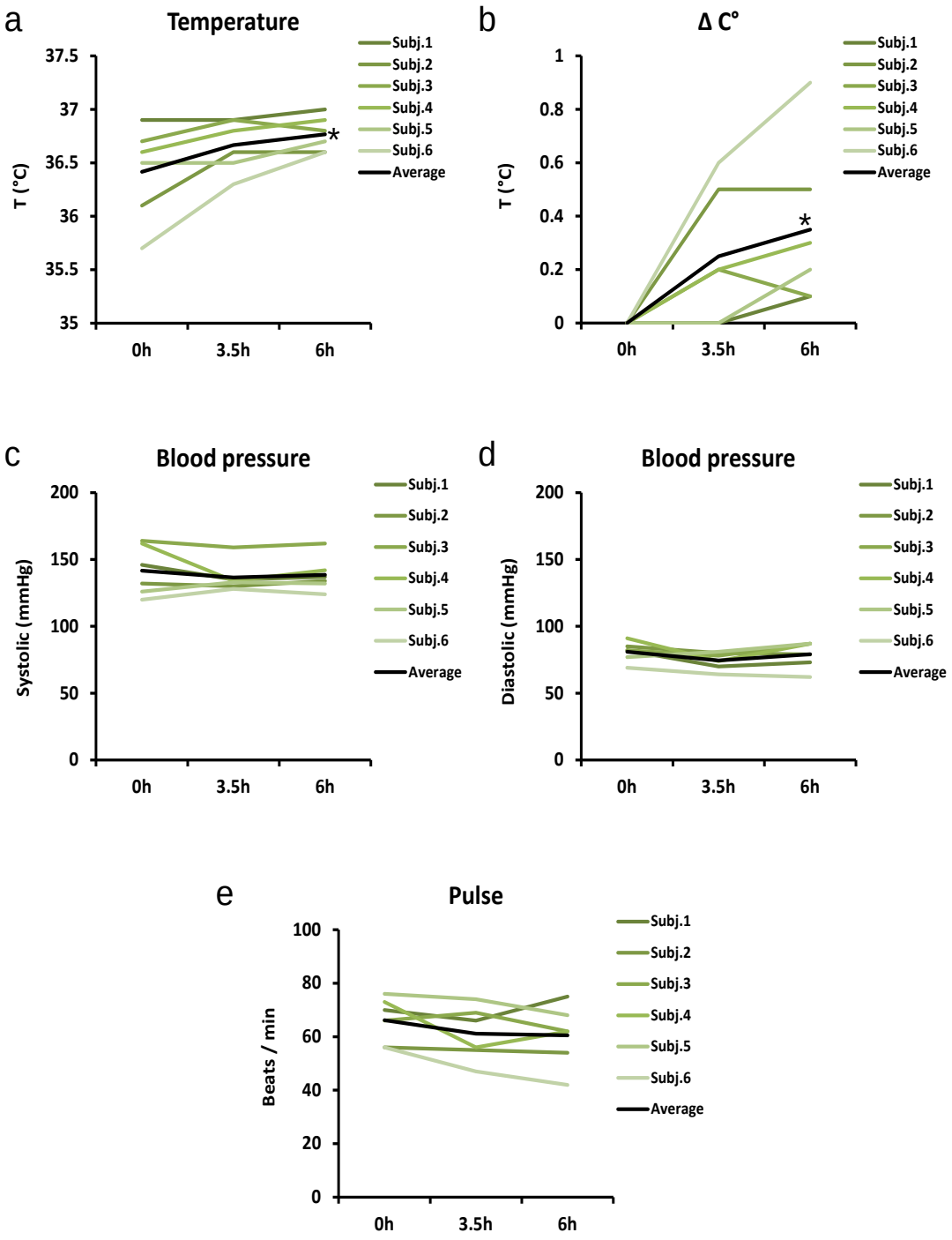

Figure 5.9. Effect of a high-fat meal on temperature, blood pressure and pulse rate.

Body temperature, blood pressure and pulse rate of each volunteer (n=6) were recorded before and after the consumption of a high-fat meal. *$p < 0.05$ *vs.* before (0h) measurements.

5.5. Production of IL-6 and TNF-*α* by TLR-stimulated leukocytes.

The chronic vascular inflammatory responses that characterise atherosclerosis are mediated by blood-derived inflammatory cells, with monocytes and monocyte-derived macrophages having an important role (Lusis 2000). Macrophage foam cells present in atherosclerotic plaques exhibit an inflammatory phenotype, further supporting the role these cells have in linking inflammation with atherosclerosis (Oiknine and Aviram 1992; Feingold *et al.* 2010). The activation of TLRs expressed in macrophages was shown to result in the production of pro-inflammatory mediators, such as cytokines, which play a key role in the process of atherogenesis (Drexler and Foxwell 2010; Verouti *et al.* 2011).

We therefore aimed to investigate what types of bacteria and what doses of TLR2 and TLR4 stimulants are required to stimulate the production of two key pro-inflammatory cytokines, IL-6 and TNF-*α* by leukocytes. Whole blood collected from healthy individuals was treated for 6 hours with a panel of heat-killed bacteria at 10^6 cells / ml, *K. pneumoniae* or *S. salivarius* at concentrations ranging from $10^2 – 10^6$ heat-killed bacteria/ ml, or with 0.01 – 1000 ng/ ml of Pam_3CSK_4 or LPS. Plasma from each sample was collected by centrifugation, and quantification of IL-6 and TNF-*α* was performed by ELISA.

All the Gram-negative bacteria examined (*E. coli*, *K. pneumoniae*, *P. aeruginosa*, *P. vulgaris*) promoted a significant increase in the production of both IL-6 and TNF-*α*. *P. aeruginosa* was the most potent inducer of IL-6 production (985 pg/ ml *vs.* control: 4 pg/ ml; $p < 0.001$) (Figure 5.10). *K. pneumoniae*, *P. aeruginosa*, and *P. vulgaris* induced similar levels of TNF-*α* (Figure 5.11). *E. coli* induced the lowest production of TNF-*α* when compared to the other Gram-negative bacteria tested. Contrary to treatment with Gram-negative bacteria, treatment with Gram-positive bacteria (*S.*

aureus, *S. epidermidis*, *S. salivarius*) did not induce a significant increase in the levels of the two cytokines (Figure 5.10, Figure 5.11).

Titration of heat-killed *K. pneumoniae* revealed that the production of both pro-inflammatory mediators can occur at concentrations as low as 100 bacteria per ml, and that the production is dose-dependent, as the levels of IL-6 and TNF-α at 10^6 bacteria/ ml were, respectively, 3.6-fold and 7.3-fold higher than the levels obtained at 10^2 bacteria/ ml (Figure 5.12 – a, Figure 5.13 – a). In general, the levels of TNF-α were lower compared to the levels of IL-6 measured at the same concentration of bacteria. In contrast to *K. pneumoniae*, *S. salivarius* induced a cytokine response only at the highest concentration used (10^6/ ml) (Figure 5.12 – b, Figure 5.13 – b).

Cytokine responses to LPS were also dose dependent (Figure 5.14 – b, Figure 5.15 – b). The levels of IL-6 produced at the highest concentration of LPS used (1,000 ng/ ml) were higher than the levels of TNF-α produced at the same LPS concentration (IL-6: 305 pg/ ml *vs.* TNF-α: 135 pg/ ml). Pam_3CSK_4 was able to induce the production of these cytokines only at the highest concentration used (1,000 ng/ ml) (Figure 5.14 – a, Figure 5.15 – a).

A trait that characterised all the results obtained was inter-individual variability. A wider inter-individual variability in the production of both inflammatory mediators was observed upon treatment with Gram-negative bacteria or the TLR4 stimulant LPS, where the individuals could be divided into high and low responders. Little variability was observed between individuals after Gram-positive bacterial treatment or treatment with the TLR2 stimulant Pam_3CSK_4.

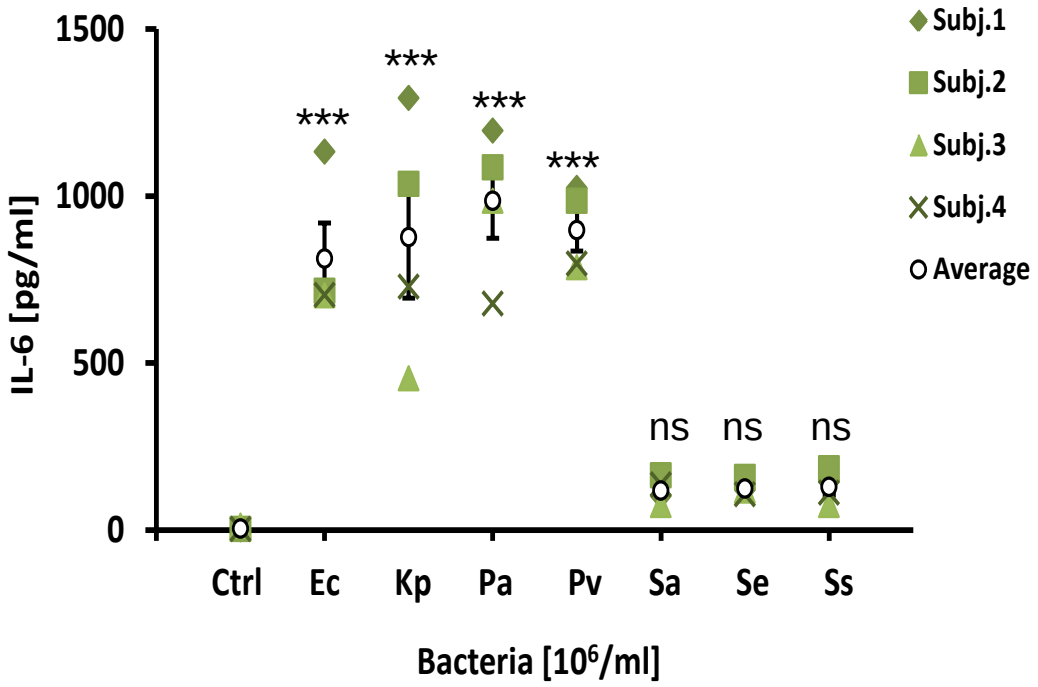

Figure 5.10. Whole blood IL-6 response to bacterial stimulation

Treatment of whole blood with 10^6 heat-killed Gram-negative or Gram-positive bacteria / ml led to the production of IL-6, the concentration of which was measured in the plasma fraction after 6 hours. Number of volunteers: four (4). Abbreviations: (Ctrl): control, (Ec): *E. coli*, (Kp): *K. pneumoniae*, (Pa): *P. aeruginosa*, (Pv): *P. vulgaris*, (Sa): *S. aureus*, (Se): *S. epidermidis*, (Ss): *S. salivarius*. ***$p < 0.001$ *vs*. control.

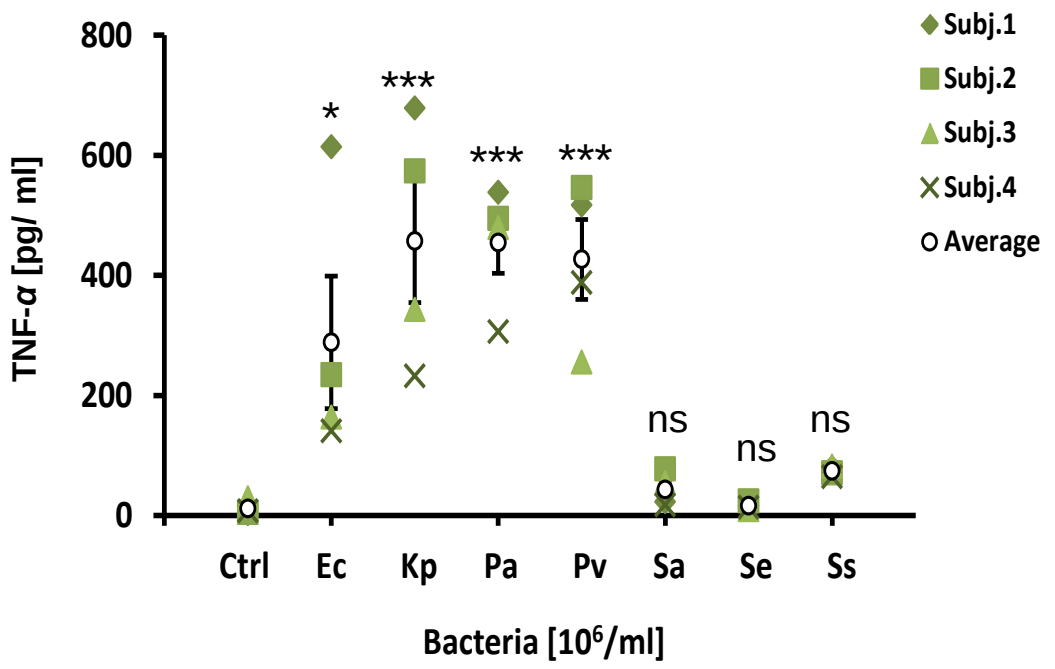

Figure 5.11. Whole blood TNF-*α* response to bacterial stimulation

TNF-*α* was quantified in plasma separated from whole blood after a 6 hour treatment with 10^6 heat-killed Gram-negative or Gram-positive bacteria/ ml. Number of volunteers: four (4). Abbreviations: (Ctrl): control, (Ec): *E. coli*, (Kp): *K. pneumoniae*, (Pa): *P. aeruginosa*, (Pv): *P. vulgaris*, (Sa): *S. aureus*, (Se): *S. epidermidis*, (Ss): *S. salivarius*. *p < 0.05, ***$p < 0.001$ *vs*. control.

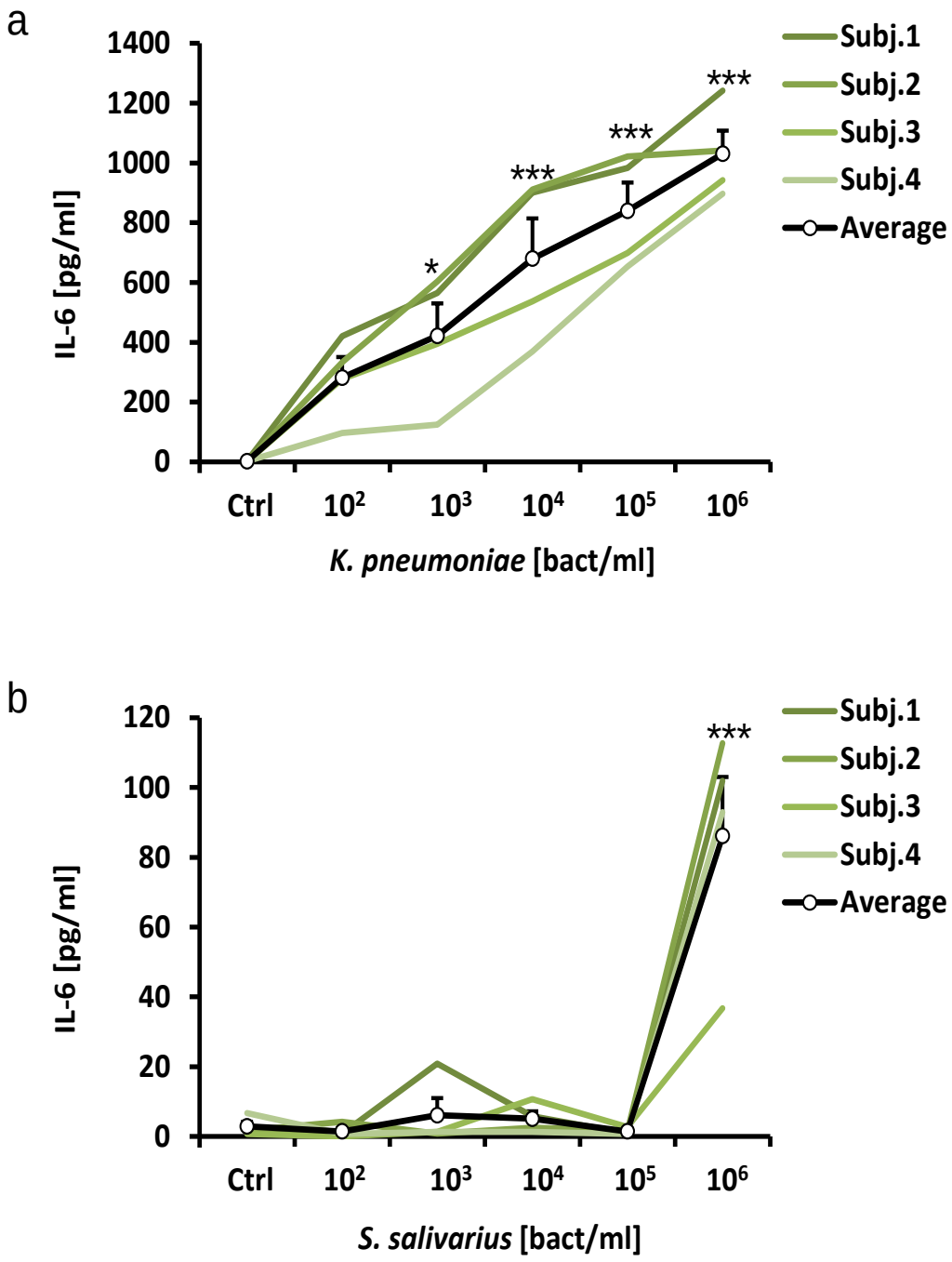

Figure 5.12. Effect of dose on whole blood IL-6 response to bacteria.

Whole blood was treated with varying concentrations of *K. pneumoniae* (a) or *S. salivarius* (b) (10^2 – 10^6 bacteria / ml) and IL-6 was measured in the collected plasma. Number of volunteers: four (4). *$p < 0.05$, ***$p < 0.001$ *vs*. control.

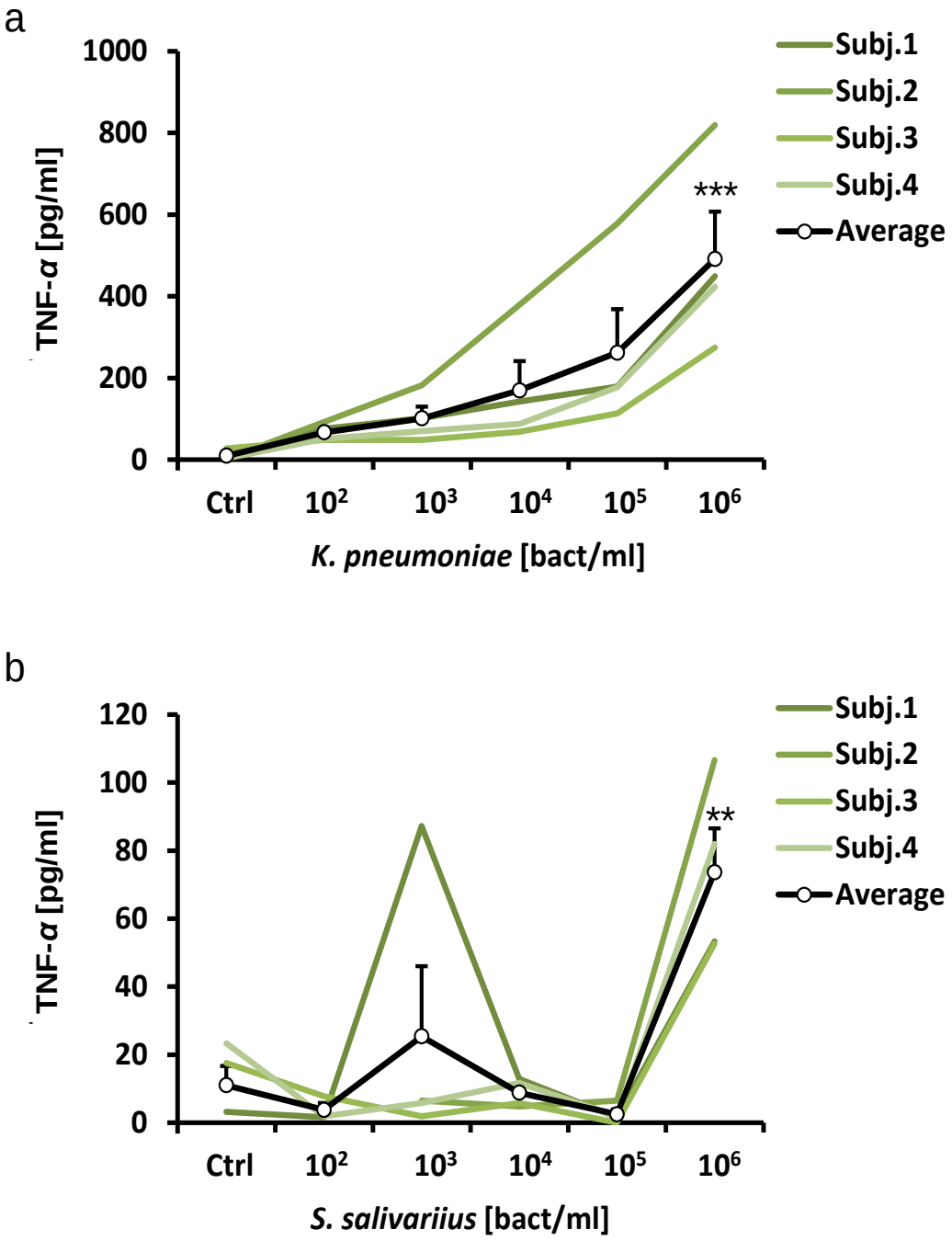

Figure 5.13. Effect of dose on whole blood TNF-α response to bacteria

Whole blood was treated with 10^2 – 10^6 *K. pneumoniae* (a) or *S. salivarius* (b) / ml for 6 hours, and TNF-α levels in plasma were quantified. Number of volunteers: four (4). $^{**}p < 0.01$, $^{***}p < 0.001$ *vs.* control.

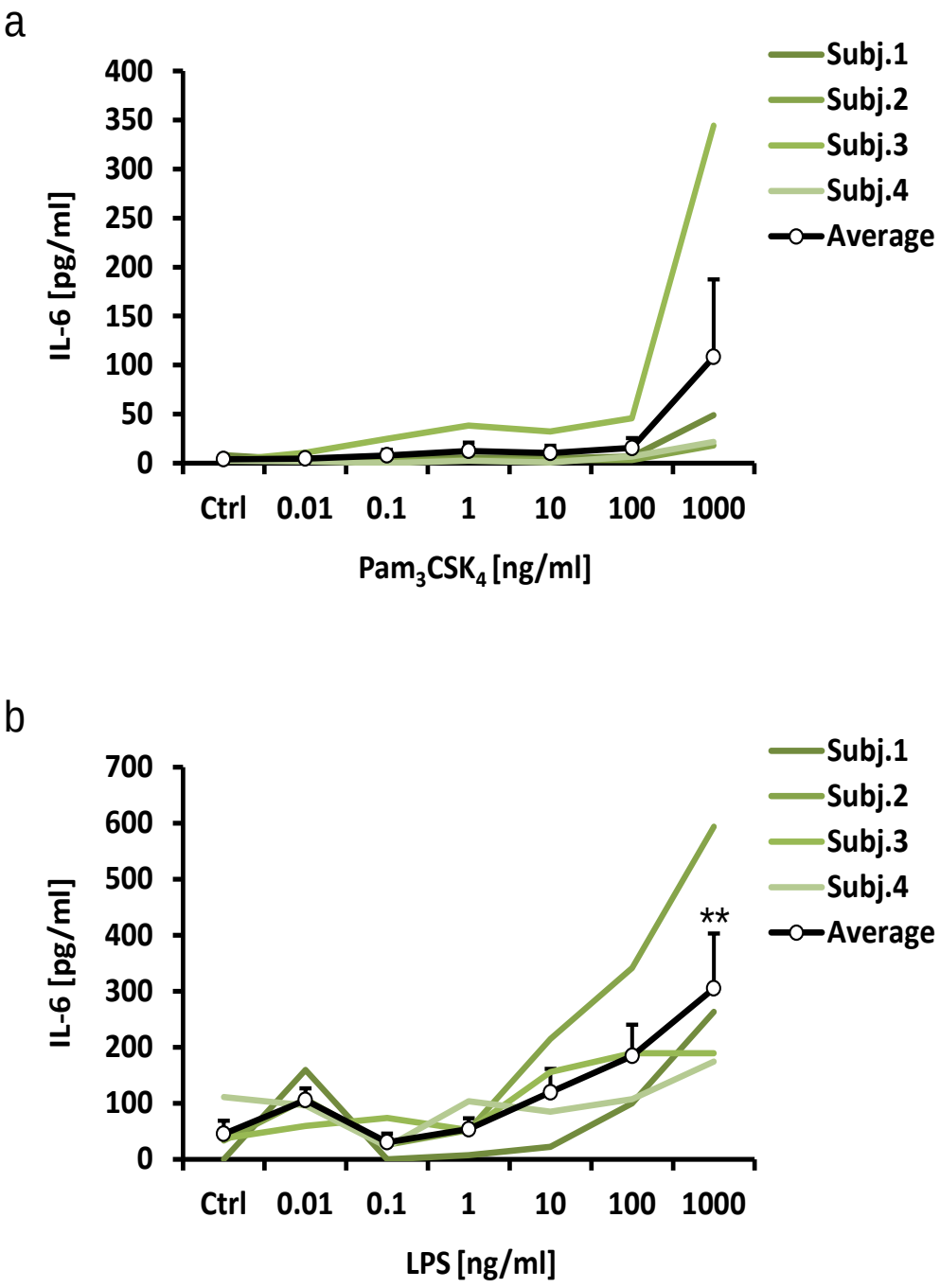

Figure 5.14. Whole blood IL-6 response to Pam_3CSK_4 and LPS.

IL-6 dose-response curves created after whole blood treatment with different concentrations of the TLR2 stimulant Pam_3CSK_4 (a) or the TLR4 stimulant LPS (b). IL-6 was measured in isolated plasma samples from four (4) volunteers. $^{**}p < 0.01$ *vs.* control.

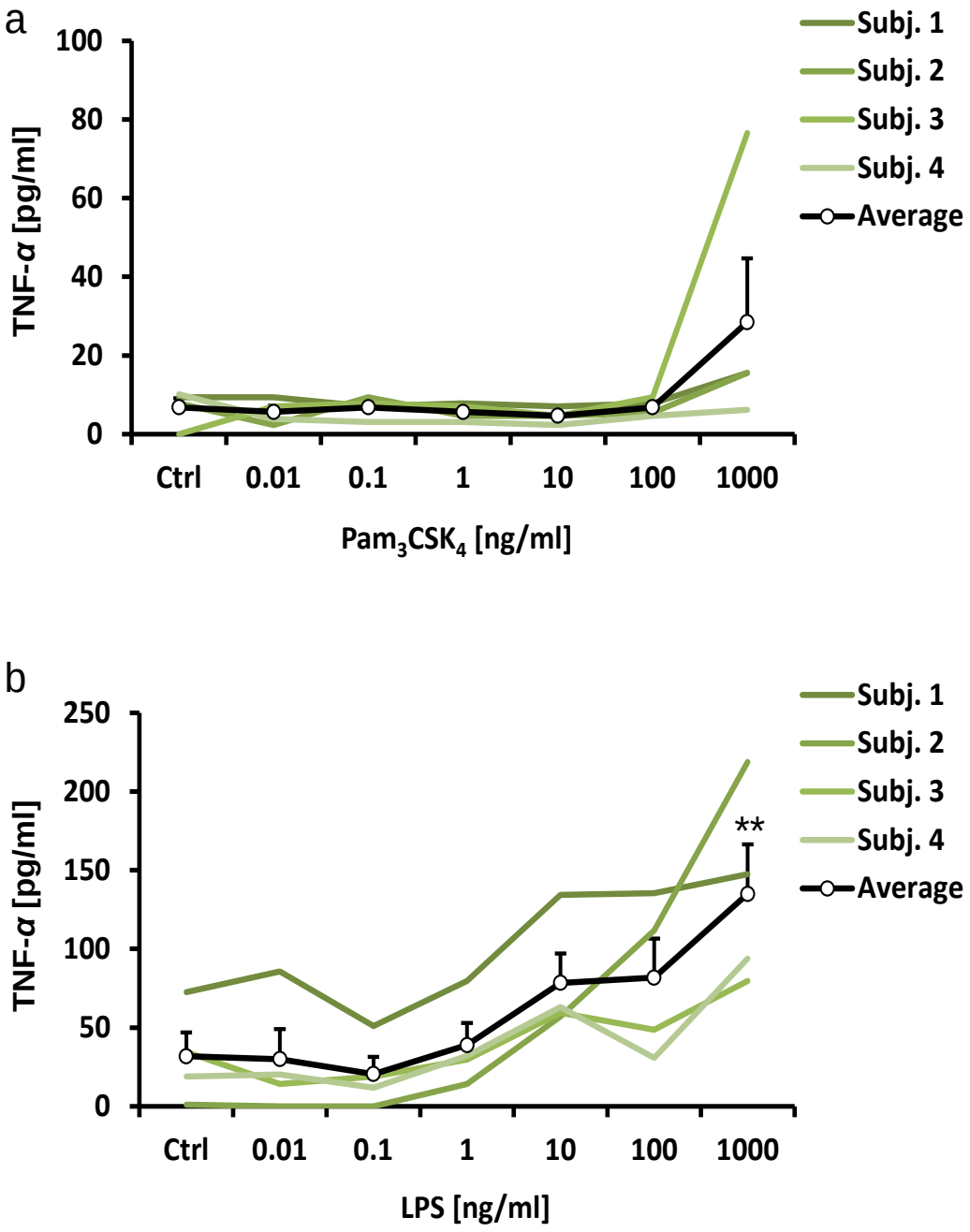

Figure 5.15. Whole blood TNF-α response to Pam_3CSK_4 and LPS

TNF-α production was measured in plasma samples after whole blood was treated for 6 hours with 10^2 – 10^6 / ml of the TLR stimulants Pam_3CSK_4 (a) or LPS (b). Number of volunteers: four (4). $^{**}p < 0.01$ *vs*. control.

Summary

Based on the results presented in this chapter, it can be concluded that bacteria or their related products are able to promote the formation of foam cells in primary human monocytes. Lipid accumulation in monocytes begins as early as one hour after exposure to PAMPs, and continues to increase over at least 5 h. Consumption of a meal high in fats also potentiates the accumulation of lipids in circulating monocytes, as indicated by flow cytometry. This process is accompanied by raised levels of markers that are consistent with the induction of a low-grade systemic inflammatory response, and this in turn is consistent with the hypothesis that a high-fat meal may promote post-prandial endotoxaemia.

6. RESULTS - MECHANISMS OF TLR-DEPENDENT LIPID DROPLET FORMATION IN MACROPHAGES

The results obtained from our previous experiments provide evidence that stimulation of TLRs is required for bacteria- or PAMP-mediated foam cell formation. However, the mechanisms connecting TLR signalling with regulation of cellular lipid content are not well understood. The series of experiments presented in this chapter aimed to identify the mechanisms that link TLR activation with pathways regulating lipid accumulation in macrophages.

6.1. Roles of lipoprotein oxidation and scavenger receptor-dependent uptake pathways in TLR-mediated foam cell formation.

It has been proposed that the activation of macrophages via TLR stimulation could lead to the release of reactive oxygen species (ROS), an event that could promote the oxidation of LDL and its subsequent uptake by scavenger receptors, eventually leading to the formation of foam cells (Witztum and Steinberg 1991; Jialal and Devaraj 1996; Steinberg 2005; Lee *et al.* 2008).

In order to investigate the potential roles of LDL oxidation and scavenger receptor uptake in the process of PAMP-mediated foam cell formation, J774A.1 macrophages were cultured for 72 hours with 10^4 *E. coli*/ ml or 10^6 *S. epidermidis*/ ml, or 1 ng/ ml of the TLR specific stimulants Pam_3CSK_4 or LPS in the presence or absence of the antioxidant butylated hydroxytoluene (BHT, 50 μM), or the scavenger receptor blocker polyinosinic acid (PIA, 20 μg/ ml). Foam cell formation was assessed by flow cytometry.

The antioxidant BHT did not inhibit the formation of foam cells in bacteria-treated cells, as indicated by the mean fluorescence intensity values which were similar to those

obtained from cells cultured with bacteria alone (*E. coli* + BHT MFI: 1.5 *vs. E. coli* alone MFI: 1.5 ; *S. epidermidis* + BHT MFI: 1.6 *vs. S. epidermidis* alone MFI: 1.7) (Figure 6.1). Similar results were observed in PAMP-treated cells (Pam_3CSK_4 + BHT MFI: 1.2 *vs.* Pam_3CSK_4 alone MFI: 1.2; LPS + BHT MFI: 1.4 *vs.* LPS alone MFI: 1.5) (Figure 6.2).

Similar to BHT, the scavenger receptor blocker PIA also failed to block foam cell formation in *E. coli* or *S. epidermidis*-treated cells (*E. coli* + PIA MFI: 1.4 *vs. E. coli* alone MFI: 1.5; *S. epidermidis* + PIA MFI: 2.0 *vs. S. epidermidis* alone MFI: 1.7) (Figure 6.1), as well as PAMP-treated cells (Pam_3CSK_4 + PIA MFI: 1.6 *vs.* Pam_3CSK_4 alone MFI: 1.2; LPS + PIA MFI: 1.4 *vs.* LPS alone MFI: 1.5) (Figure 6.2). The minor increase in MFI observed in *S. epidermidis* and Pam_3CSK_4-treated cells incubated with PIA could reflect a TLR3-dependent signal induced by this compound, as it is structurally similar to the canonical TLR3 agonist Poly I:C.

Overall, the results clearly indicate that oxidation of LDL is not required for bacteria or PAMP-dependent foam cell formation, and suggest the existence of an alternative pathway that is not scavenger receptor-dependent.

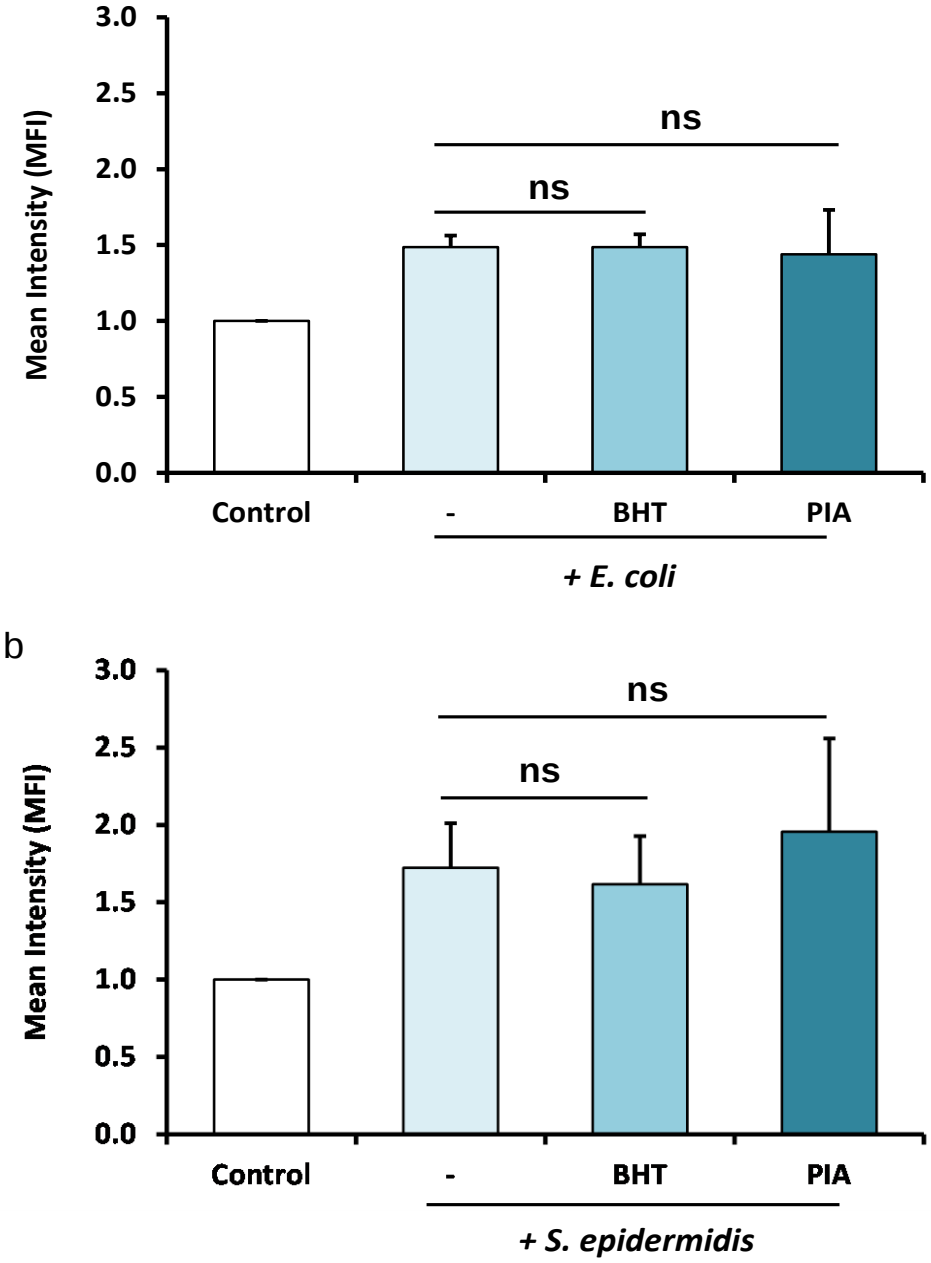

Figure 6.1. Effect of antioxidants and scavenger receptor blockers on bacteria-mediated foam cell formation.

Cells were cultured for 72 hours with 10^4 *E. coli*/ ml (a) or 10^6 *S. epidermidis*/ ml (b) in the presence or absence of the antioxidant butylated hydroxytoluene (BHT, 50 μM) or the scavenger receptor blocker polyinosinic acid (PIA, 20 μg/ ml), and mean fluorescence intensity was recorded by flow cytometry. Results are presented as the means ± SEM of four (*E. coli*) and three (*S. epidermidis*) independent experiments.

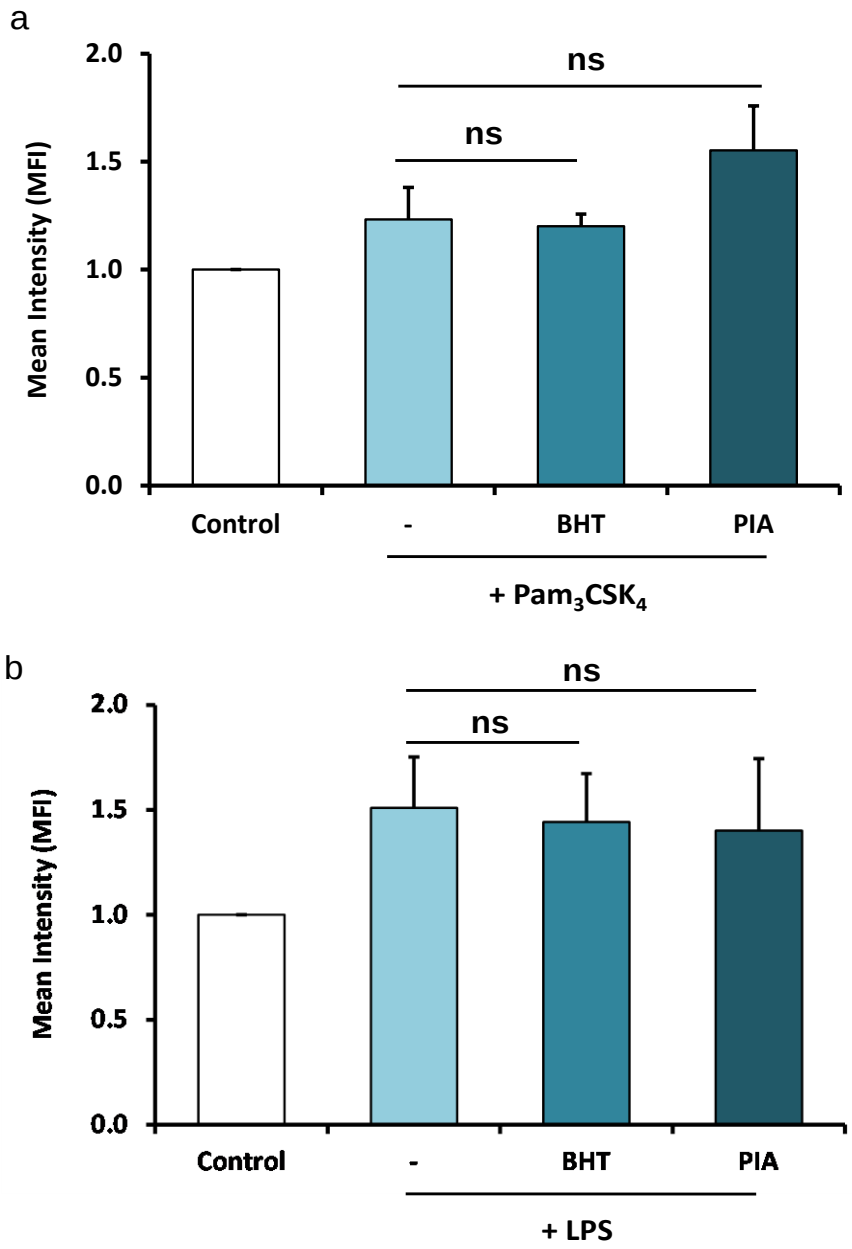

Figure 6.2. Effect of antioxidants and scavenger receptor blockers on foam cell formation mediated by PAMPs.

Cells were cultured for 72 hours with 1 ng/ ml of the selective TLR ligands Pam_3CSK_4 (a) or LPS (b) in the presence or absence of the antioxidant butylated hydroxytoluene (BHT, 50 μM) or the scavenger receptor blocker polyinosinic acid (PIA, 20 μg/ ml). Mean fluorescence intensity was recorded by flow cytometry. Results are presented as the means ± SEM of four independent experiments.

6.2. Role of LDL in TLR-mediated foam cell formation.

Since OxLDL is not required for bacteria-mediated foam cell formation, we next investigated the requirement for unmodified LDL (nLDL) in this process. J774A.1 macrophages were treated for 24 hours with 100 ng/ ml LPS in the presence of varying concentrations of nLDL (0, 5, 10, 30 μg/ ml), and foam cell formation was assessed by flow cytometry.

LPS in the absence of nLDL induced foam cell formation in treated cells as expected (Figure 6.3). However, there was in addition to this a dose-dependent increase in the recorded MFIs induced by nLDL, reaching significance at the highest concentration of nLDL used (LPS + nLDL at 30 μg/ ml MFI: 1.2 *vs.* LPS alone MFI: 1.0; $p < 0.05$).

These results therefore indicate that although LDL supplementation increases the ease of foam cell formation in a dose-dependent manner, LDL is not required for the process of foam cell formation induced by bacteria or PAMPs, as we have shown that, in both cases, it can occur in the absence of LDL. This partial regulation of foam cell formation by LDL concentrations could be of relevance to the observed association between elevated LDL levels and increased risk of cardiovascular disease.

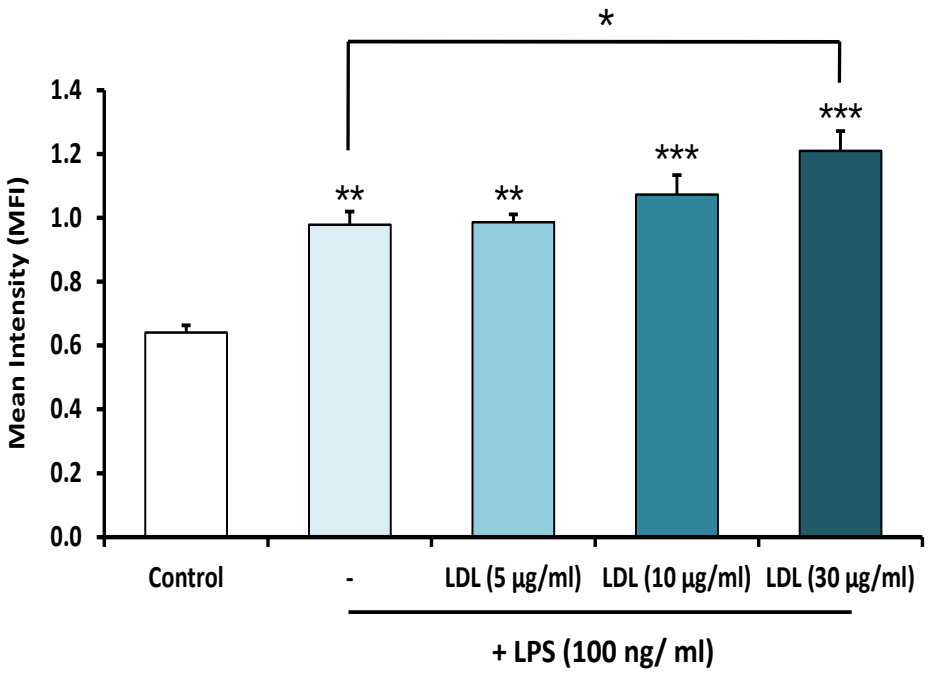

Figure 6.3. The role of native LDL in PAMP-mediated foam cell formation.

J774A.1 macrophages were treated for 24 hours with 100 ng/ ml of LPS with or without native LDL (5 – 30 μg/ ml), and foam cell formation was assessed by flow cytometry. Results are representative of the means ± SEM of three independent experiments. *p < 0.05 *vs*. LPS alone, **p < 0.01, ***p < 0.001 *vs*. medium alone.

6.3. Effect of PAMPs on macrophage uptake of LDL.

In order to further investigate the effects of PAMPs on pathways of LDL uptake, J774A.1 macrophages were challenged for 20 hours with 1 µg/ ml of Pam_3CSK_4 or LPS, and then incubated with DiI-LDL (20 μg/ ml) for 4 hours. Flow cytometry was used to assess foam cell formation in Nile Red-stained cells (Figure 6.4).

No significant increase in the uptake of DiI-LDL was observed in Pam_3CSK_4 or LPS-treated cells at the time point examined, suggesting that the LDL uptake pathway might not be affected by PAMPs. However, as we have shown in previous chapters that foam cell formation occurs within 24 hours and increases over the next two days, uptake of LDL might prove to be significant at later time points.

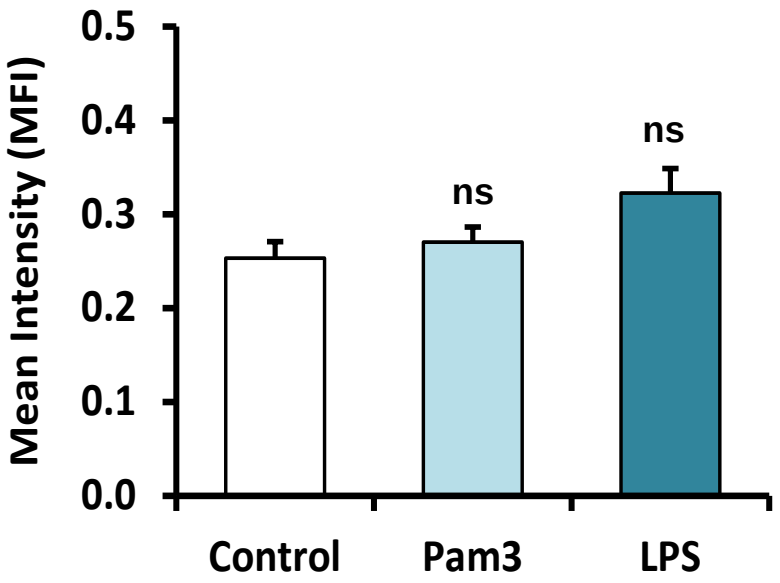

Figure 6.4. Effect of PAMPs on LDL uptake in macrophages.

Cells were challenged with 1 μg/ ml of the TLR stimulants Pam_3CSK_4 or LPS for 24 hours, and then incubated with 20 μg/ ml of DiI-LDL for another 4 hours. Mean fluorescence intensity was recorded by flow cytometry. Results are presented as the means ± SEM of three independent experiments.

6.4. Effects of PAMPs on macrophage cholesterol efflux pathways.

There is evidence that one of the cellular processes which is down-regulated during the process of foam cell formation is that of reverse cholesterol transport (RCT), which is responsible for the efflux of free cholesterol to HDL (Glomset 1968; Sviridov and Nestel 2002; Van Eck *et al.* 2005; Tsompanidi *et al.* 2010). We aimed to investigate the effect that selective PAMPs might have on this process by loading J774A.1 macrophages with ^{3}H-cholesterol (2 μCi/ ml) for 24 hours, and subsequently treating them with 1 μg/ ml Pam_3CSK_4 or LPS for a further 24 hours. Efflux to HDL particles was assessed by measuring the radioactivity in supernatants (this part of the experiment was conducted with assistance from Dr. V. Codd). Measurements were corrected to the amount of ^{3}H-cholesterol taken up by the cells and the amount effluxed by passive diffusion.

Treatment with the selective TLR stimulants significantly reduced cholesterol efflux as indicated by the reduced percentages of effluxed ^{3}H-cholesterol obtained from treated cells relative to control cells (Pam_3CSK_4-treated: 4.5% , $p < 0.01$; LPS-treated: 5.8%, $p < 0.05$; *vs.* control: 8.0%) (Figure 6.5).

Other workers have shown that activation of TLR4 via the IRF3 signalling pathway inhibits the process of cholesterol efflux in macrophages by reducing the expression of key components of the RCT process, such as the ABC transporter proteins (Cao *et al.* 2007; Lundberg and Hansson 2010). However, to date it has remained unknown what effect TLR2 activation might have on this process. We found that stimulation of TLR2 via Pam_3CK_4 treatment resulted in a greater reduction of cholesterol efflux than did stimulation of TLR4 via treatment with LPS, a novel observation which suggests the existence of a common intracellular mechanism downstream of both TLRs.

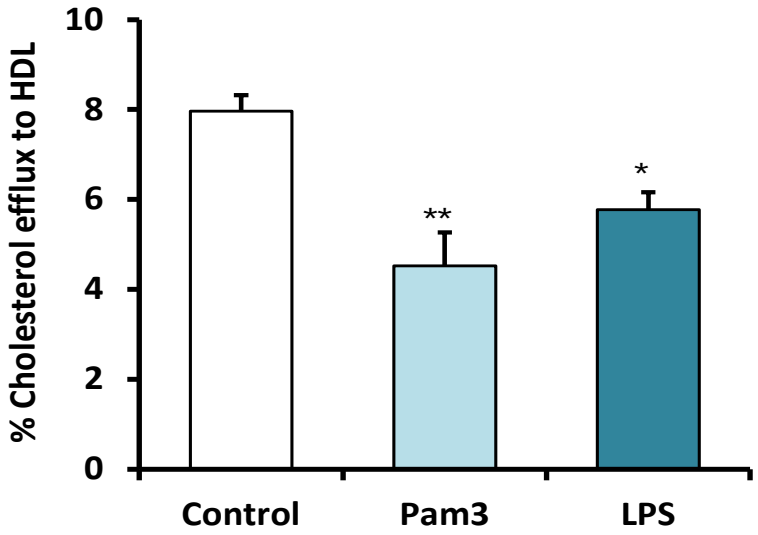

Figure 6.5. Regulation of the cholesterol efflux pathway by PAMPs.

J774A.1 macrophages were loaded with ^{3}H-cholesterol (2 μCi/ ml) for 24 hours, after which they were treated with Pam_3CSK_4 or LPS (1 μg/ ml) for a further 24 hours. Efflux of ^{3}H-cholesterol to HDL particles was quantified by measuring the radioactivity in supernatants, and adjusting to the amount of ^{3}H-cholesterol taken up by the cell and the amount of fractional efflux. Results are presented as the means ± SEM of three independent experiments. *$p < 0.05$, **$p < 0.01$ *vs.* control.

6.5. Effects of TLR stimulation on fluid-phase pinocytosis.

As fluid phase uptake of soluble molecules via pinocytosis could contribute to uptake of lipids or lipoprotein particles by activated macrophages, we next examined the potential of PAMPs and bacteria to modulate pinocytosis in TLR-stimulated macrophages. J774A.1 cells were treated for 6 hours with 10^6 bacteria/ ml or varying concentrations of the selective TLR stimulants Pam_3CSK_4 or LPS (0.1-1000 ng/ ml; 10-fold dilutions) in the presence of the pinocytosis marker HRP (200 μg/ ml). Cells were also treated for 6 hours with HRP alone in the absence of bacteria or PAMPs to assess the baseline pinocytic capacity of the cells. Absorbance was measured at 450 nm, and HRP uptake was normalised to the protein content of the samples.

The initial assay protocol incorporated 1% foetal calf serum (FCS) in the PBS diluent to deactivate SDS present in the sample lysates and thereby limit potential interference with the other components of the assay. When compared to samples diluted in PBS alone, however, FCS led to a slightly increased background signal (1% FCS/PBS OD: 0.247 *vs.* PBS OD: 0.241) (Figure 6.6 – a, b). This was an indication that deactivation of SDS by FCS was not required for optimal sensitivity, as it did not seem to interfere with any of the assay components when FCS was not used. The correlation coefficient of values obtained from standard curves produced from samples diluted in either 1% FCS in PBS or PBS alone were similar, with a slightly higher correlation coefficient value for PBS (FCS: r = 0.98; PBS: r = 0.99) (Figure 6.6 – c, d). This, combined with the lower background signal obtained when PBS alone was used, suggested that PBS without FCS was a better diluent for subsequent experiments.

Use of this protocol revealed that pinocytosis appeared to be a time-dependent, continuous process, as the HRP content of unchallenged cells was shown to increase significantly over time ($p < 0.05$ at 2 hours; $p < 0.001$ at 4 and 6 hours *vs.* 0 hours)

(Figure 6.7). The addition of bacteria though did not seem to have any effect on the process, as the levels of HRP that were taken up by treated cells were similar to those taken up by unchallenged cells (0.10-0.13 ng HRP per µg of protein in bacteria-treated cells *vs*. 0.14 ng HRP per µg of protein in untreated cells at 6 hours) (Figure 6.8).

PAMPs also had little impact on the pinocytic capacity of the cells (Figure 6.9). The levels of HRP taken up by cells did not change with different concentrations of Pam_3CSK_4. Peppelenbosch *et al.* (1999) reported that LPS was able to inhibit pinocytosis when used at low concentrations (0.1 - 100 ng/ ml), and that this could be reversed when higher concentrations were used (~ 10 μg/ ml). A similar pattern of inhibition at low LPS concentrations was observed in the current experiment, although the differences in HRP uptake at different concentrations did not reach significance.

Overall, compared to control cells, treatment with either bacteria or PAMPs led to a minor decrease in the levels of HRP taken up by the cells, but these differences did not reach statistical significance. Taken together, these results suggest that up-regulation of pinocytosis does not occur during, and therefore does not contribute to, TLR-stimulated foam cell formation.

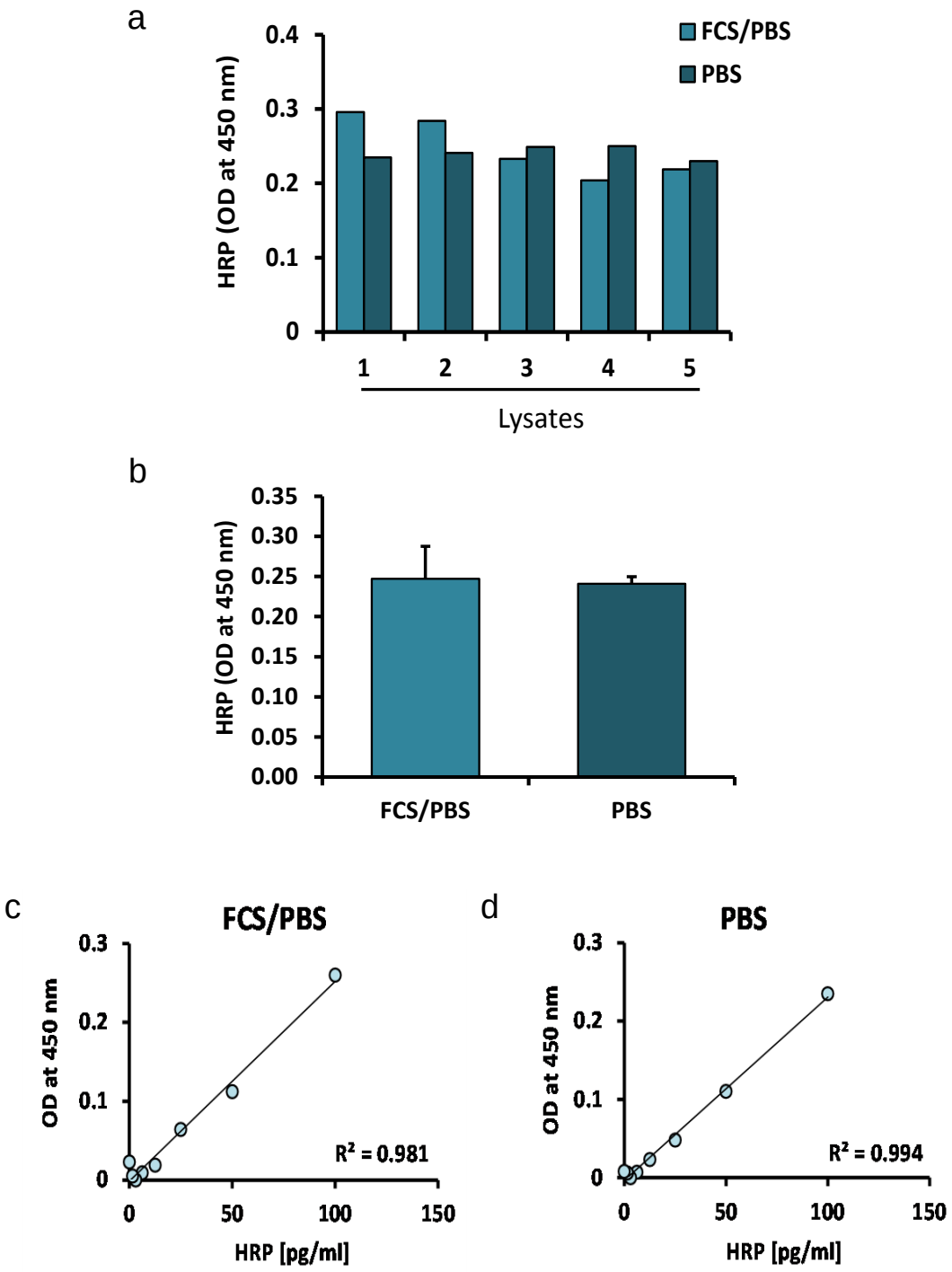

Figure 6.6. Pinocytosis assay method development.

Comparison of HRP absorbance values from lysates (1-5) diluted in PBS containing FCS (1%) or PBS alone (a). Average absorbance values represented in (b). Standard curves of HRP (starting at 100 pg/ ml) created by lysates diluted in 1% FCS/ PBS (c) or PBS alone (d).

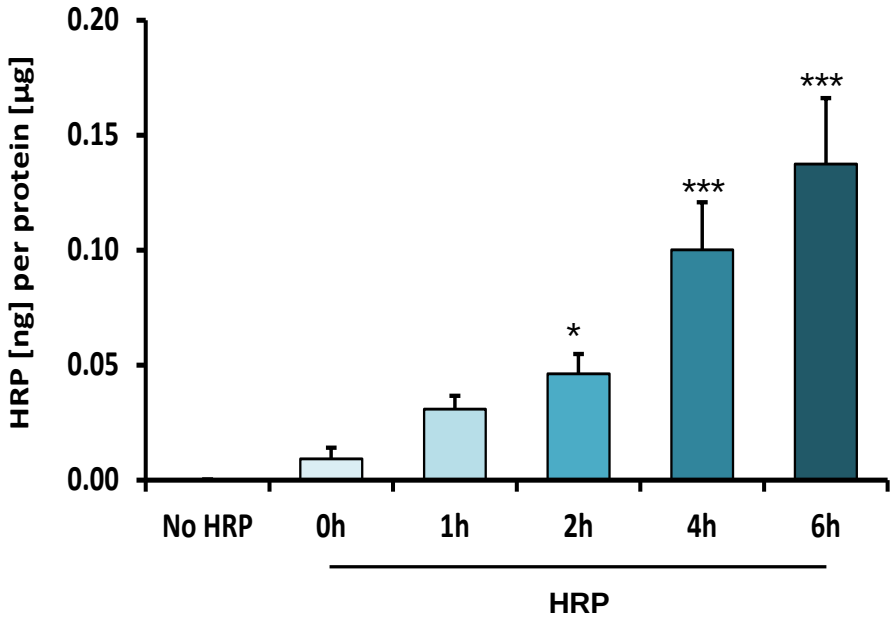

Figure 6.7. Pinocytosis rate in unchallenged cells.

The rate of pinocytosis was assessed in unchallenged J774A.1 macrophages incubated with HRP (200 μg/ ml) for a total of 6 hours. Absorbance was measured at 450 nm, and data was normalised to cellular protein content. Results are presented as the means ± SEM of four independent experiments. *$p < 0.05$, ***$p < 0.001$ *vs*. control (0 hours).

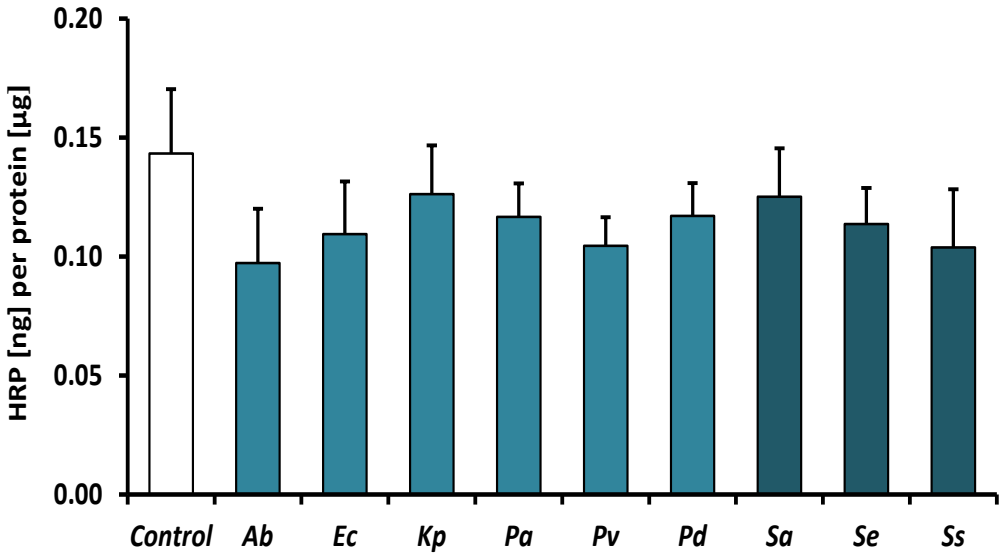

Figure 6.8. Effect of bacteria on the pinocytic capacity of macrophages.

J774A.1 macrophages were challenged with 10^6 bacteria/ ml in the presence of HRP (200 μg/ ml) for 6 hours, and absorbance was measured at 450 nm. Data was normalised to protein content. Results are presented as the means ± SEM of three independent experiments. Abbreviations: (Ab): *A. baumannii*, (Ec): *E. coli*, (Kp): *K. pneumoniae*, (Pa): *P. aeruginosa*, (Pv): *P. vulgaris*, (Sa): *S. aureus*, (Se): *S. epidermidis*, (Ss): *S. salivarius*.

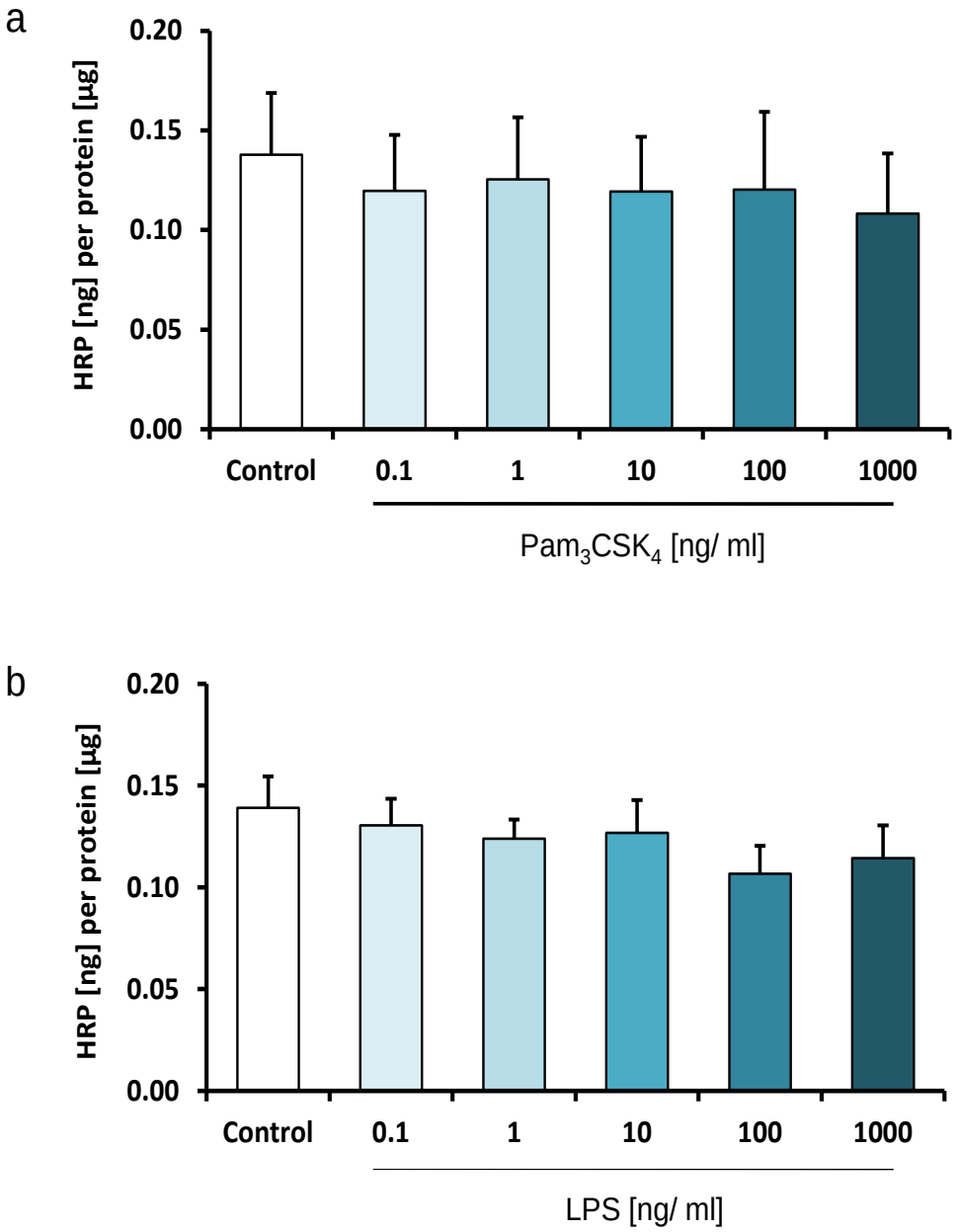

Figure 6.9. Effects of PAMP treatment on rate of pinocytosis.

The pinocytic capacity in response to PAMPs was measured in J774A.1 macrophages treated for 6 hours with different concentrations of the TLR ligands Pam_3CSK_4 (a) or LPS (b) in the presence of 200 μg HRP/ ml. Absorbance was measured at 450 nm and data was normalised to protein content. Results presented as the means ± SEM of three independent experiments.

6.6. Effects of PAMPs on *de novo* lipid synthesis.

Based on the results obtained so far, treatment of macrophages with bacteria or PAMPs were shown to have little impact on the receptor-dependent uptake of LDL or pinocytosis, thereby ruling out two major mechanisms that could, in theory, be responsible for increasing the lipid content of a cell. Given our observation that foam cell formation can occur even in the absence of LDL, we sought an alternative hypothesis for the origin of intracellular lipid droplets in PAMP-treated macrophages.

Another possible mechanism by which a cell can increase its lipid levels is by promoting the biosynthesis of new lipid, *i.e. de novo* lipid synthesis. To examine the effects of PAMPs on this pathway, J774A.1 macrophages were treated with 100 ng/ ml of Pam_3CSK_4 or LPS for 21 hours, and then incubated with 10 μCi/ ml of ^{14}C-acetate for 3 hours. For each treatment, lipid extracts in ethanol and protein lysates were collected. *De novo* lipid synthesis was then quantified by three different approaches.

In the first approach, ionising radiation was measured directly in aliquots of the unfractionated ethanol extracts, which contained the cellular lipids, and the results were recorded as counts per minute (CPM). The results were subsequently normalised first to protein content and then to measurements from cells cultured without PAMP treatment, which was set to an arbitrary value of 1.

Increased counts were obtained from ethanol extracts of both Pam_3CSK_4 and LPS-treated cells (mean CPM of extracts: control: 15758.08 CPM, Pam_3CSK_4: 41237.42 CPM, LPS: 26208.92 CPM), with the counts from the Pam_3CSK_4 extracts being significantly higher when compared to control cells treated in medium alone, when normalised to protein content and control (Pam_3CSK_4: 2.6 CPM, $p < 0.05$; *vs.* control: 1 CPM/ μg of protein) (Figure 6.10). These results suggest that an increase in *de novo*

lipid biosynthesis in challenged cells could have occurred at the examined time point, which could suggest a possible regulation of this pathway by PAMPs.

We next employed thin layer chromatography (TLC) to identify which lipid species were increased during the process of *de novo* lipid synthesis in PAMP-challenged cells. Separation of groups of lipids from a mixture on a silica gel plate is dependent on the solvent system used during the separation process. The separated lipids on the silica gel plates can be visualised after staining with 5% phosphomolybdic acid, which after being exposed to heat produces blue spots on a yellow background.

Before separating the lipid extracts obtained from the PAMP - ^{14}C-acetate – treated cells, we performed some preliminary experiments using standards for the three lipid groups of interest (cholesterol (1 mg/ ml), TAG (5 mg/ ml), CE (1 mg/ ml) in $CHCl_3$), as well as a mixture of the three. The solvent system used in these first experiments was composed of petroleum ether 60-80 ˚C and ethyl acetate in a 12:1 ratio. When the mixed standard was analysed, this solvent system led to a good separation of the TAG and CE groups, but not the cholesterol group, which could not be separated from the polar lipids group at the origin (Figure 6.11).

We then sought to improve resolution of cholesterol from the polar lipids by increasing the polarity of the mobile phase (solvent system), since doing so increases the mobility of the more polar compounds which interact strongly with the silica. This was achieved by changing the ratio between the two compounds of the solvent system. By increasing the levels of ethyl acetate, good separation of all three lipid groups was obtained. In particular, the cholesterol was successfully separated from the polar lipids, which remained at the origin (Figure 6.11).

Whereas single spots identified the cholesterol and TAG standards, three spots were visible in the CE standard lane. We presume that one corresponded to CE, and the other

two to degradation products, such as non-esterified fatty acids (Figure 6.12). Having identified the optimal solvent system to be composed of petroleum ether and ethyl acetate at 6:1 ratio, this mixture was used in all the subsequent TLC experiments.

Aliquots of the ethanol lipid extracts obtained from PAMP - ^{14}C-acetate-stimulated J774A.1 macrophages were separated by TLC using this protocol and plates were then placed in a radiography cassette with an X-ray film on top, and examined after two weeks.

Development of the X-ray film revealed the presence of bands of varying sizes and intensities in all the extracts tested (Figure 6.13). In addition to the expected bands corresponding to polar lipids, cholesterol, TAGs and CE, two further bands were observed between the cholesterol and the TAG bands. These bands were more intense in the extracts obtained from the PAMP-treated cells, and they were almost absent in the control samples. Based on earlier published work by other groups using similar solvent systems (Boren and Brindle 2012) these bands almost certainly correspond to diacyglycerides (DAGs) and free fatty acids (FFAs).

Densitometry was then performed on the developed X-ray films for the quantification of spot intensity (Figure 6.14). The data obtained was background-corrected and normalised to protein. Analysis of the results revealed that both PAMPs were able to induce changes in the lipid profiles of treated cells in most of the lipid groups tested, when compared to control. LPS was shown to stimulate greater changes in lipid biosynthesis when compared to Pam_3CSK_4, even though the differences observed in each lipid group were not significant.

Based on the band patterns observed on developed films, the silica gel plates were divided into six zones, each corresponding to the lipid groups identified by TLC. For each sample, the area of the band corresponding to each of the zones was carefully

scraped into vials containing scintillation fluid for the measurement of ionising radiation (CPM). High counts were obtained from Pam_3CSK_4-treated cells for all the zones tested, when compared to control (Figure 6.15). Counts obtained from LPS-treated cells were higher than the control for the majority of the zones. Both PAMPs led to a significant increase in DAGs when compared to control (Pam_3CSK_4: 3.7 CPM; LPS: 5.0 CPM *vs.* control: 1.0 CPM; $p < 0.05$ – normalised to protein content and control). For CE, there was no increase in the counts from LPS-treated samples when compared to control (LPS: 0.9 CPM *vs.* control: 1.0 CPM).

In general, the majority of the differences observed between control and challenged cells failed to reach statistical significance, but this could be attributed to the fact that the designation of the areas of the plate that needed to be scraped was based on the band pattern on the X-ray film and the spot pattern obtained by the standards, and as these were not always easily transposed to well-defined scraping areas could therefore have introduced some variation. The results do, however, suggest that TLR2 signalling might induce lipid biosynthesis to a greater extent than TLR4 signalling, as the highest counts were, in most cases, obtained from Pam_3CSK_4-treated samples. This could explain why TLR2 has a greater impact on atherosclerosis in mice than TLR4 (Mullick *et al.* 2005). Based on the observations that foam cell formation increases over time, it is also possible that the effects of TLR4 on lipid biosynthesis might be more evident at time points later than the 24 hour time point examined.

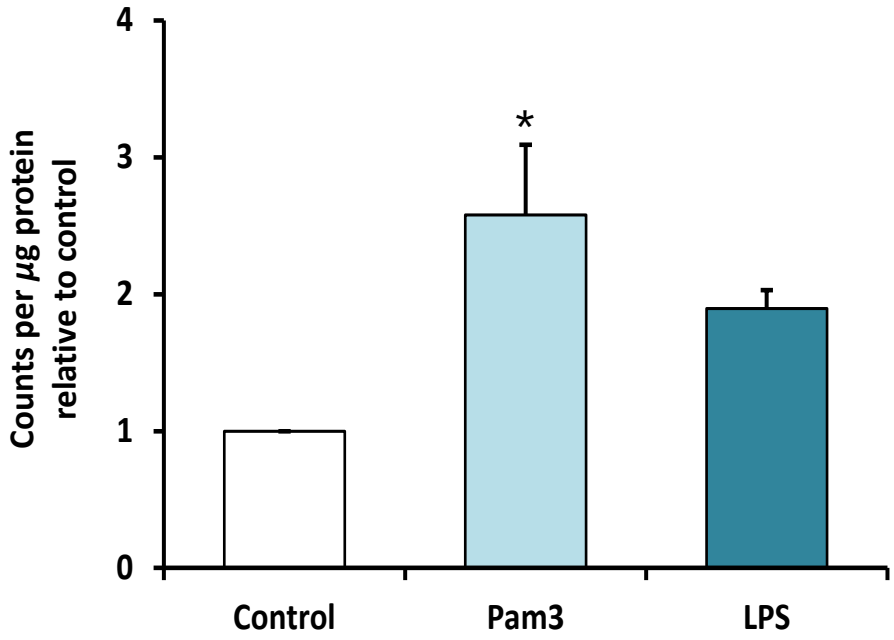

Figure 6.10. Effect of PAMPs on *de novo* lipid synthesis in macrophages.

J774A.1 macrophages were treated for 21 hours with 100 ng/ ml of the TLR stimulants Pam_3CSK_4 or LPS, after which they were incubated for 3 hours with ^{14}C-acetate (10 μCi/ ml). Lipids were extracted into ethanol and aliquots were transferred into scintillation fluid to measure radioactivity. Results were normalised first to protein content of each extract, and then to values obtained from control cells cultured in medium alone (set to 1), and presented as the means ± SEM of three independent experiments. *$p < 0.05$ *vs*. control.

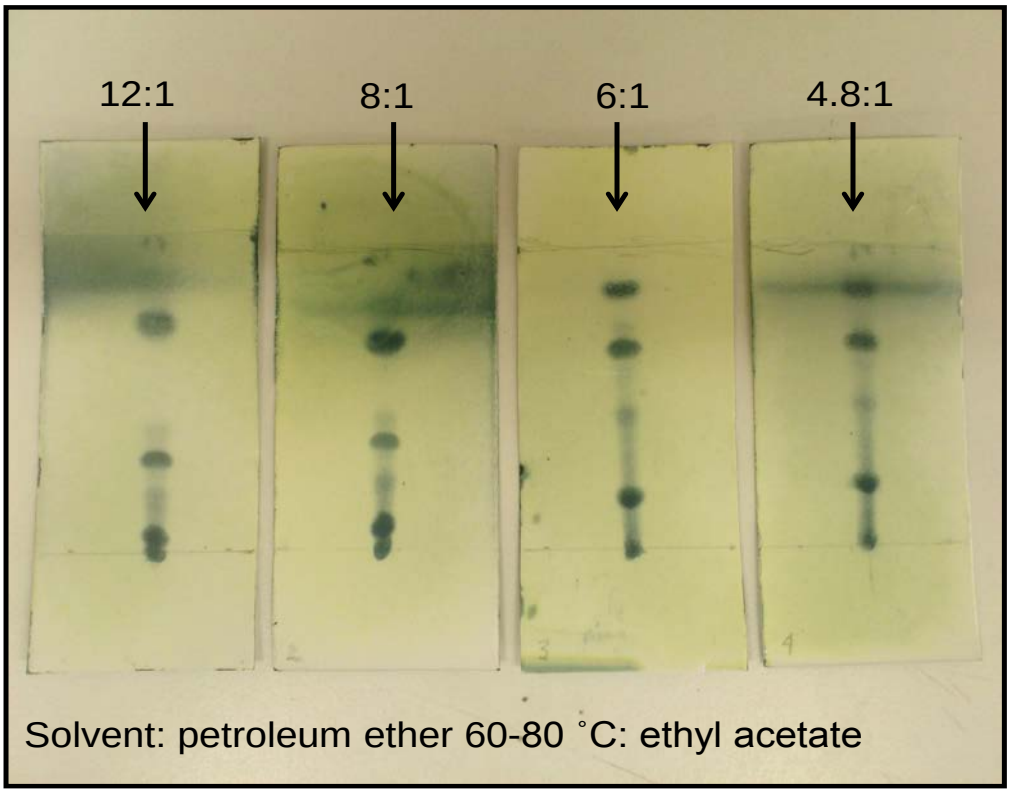

Figure 6.11. TLC method development.

A mixture composed of cholesterol, cholesterol ester and triglycerides was loaded onto TLC plates and the samples were analysed under different compositions of the separating solvent (petroleum ether 60-80 ˚C: ethyl acetate). Optimal separation of lipids was achieved when the separating solvent was used at a 6:1 or 4.8:1 ratio.

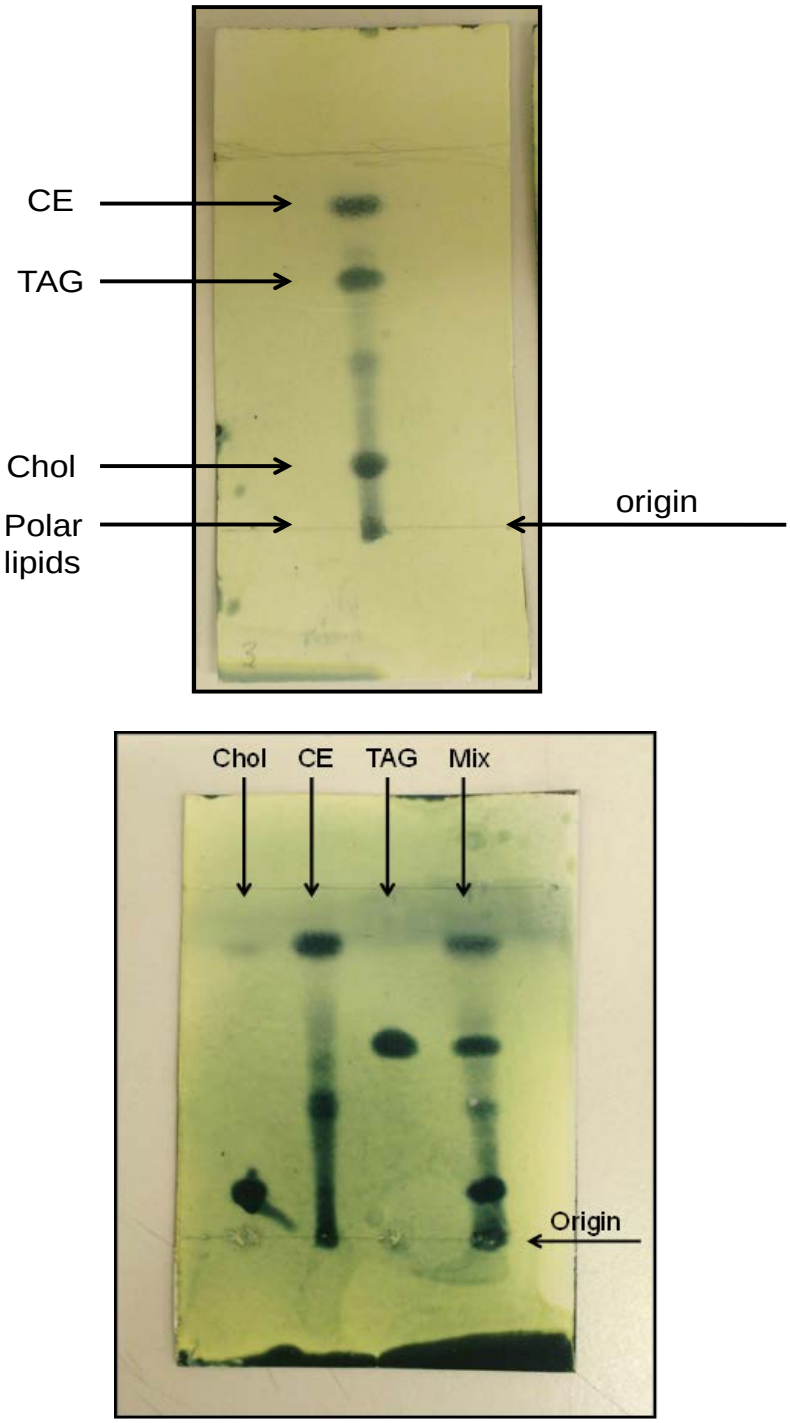

Figure 6.12. Optimised separation of lipid standards by TLC.

A mixture of lipid standards was separated into its constituents after the sample was analysed on a TLC plate using petroleum ether: ethyl acetate at a ratio of 6:1 as the separating solvent.

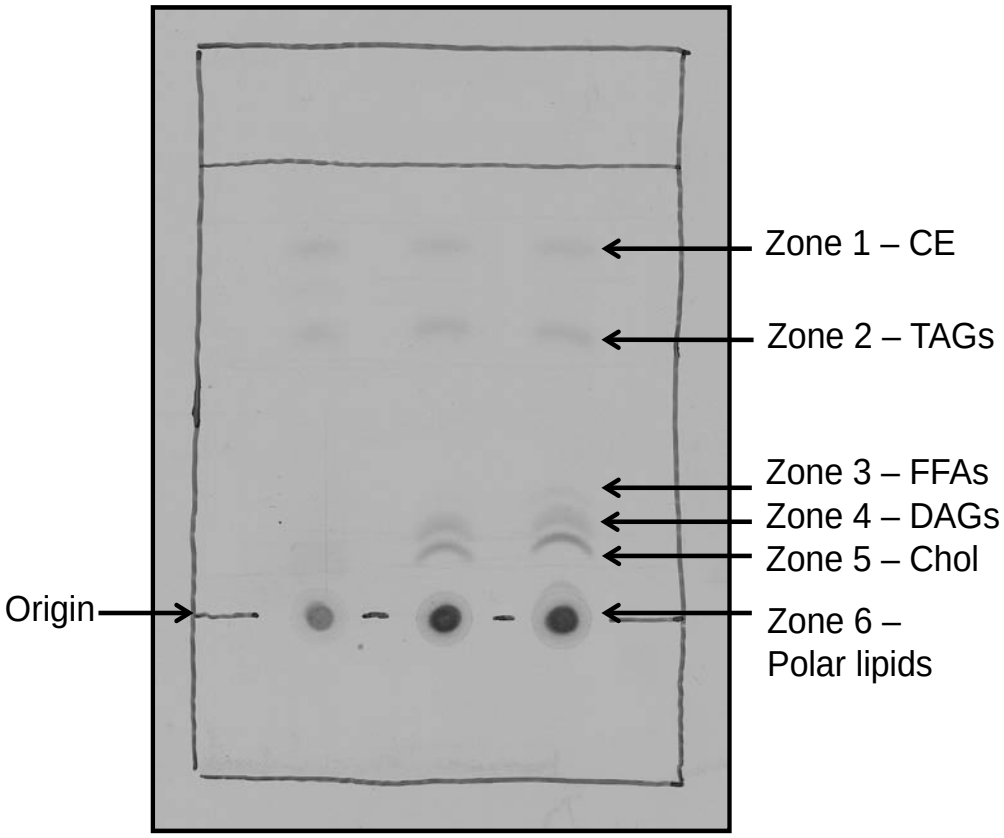

Figure 6.13. Autoradiography of cellular lipids separated by TLC.

Separation of cellular lipids was performed by TLC, and a representative X-ray film exposed to the TLC plate for two weeks is shown. The bands correspond to the position of the lipid groups on the TLC plate.

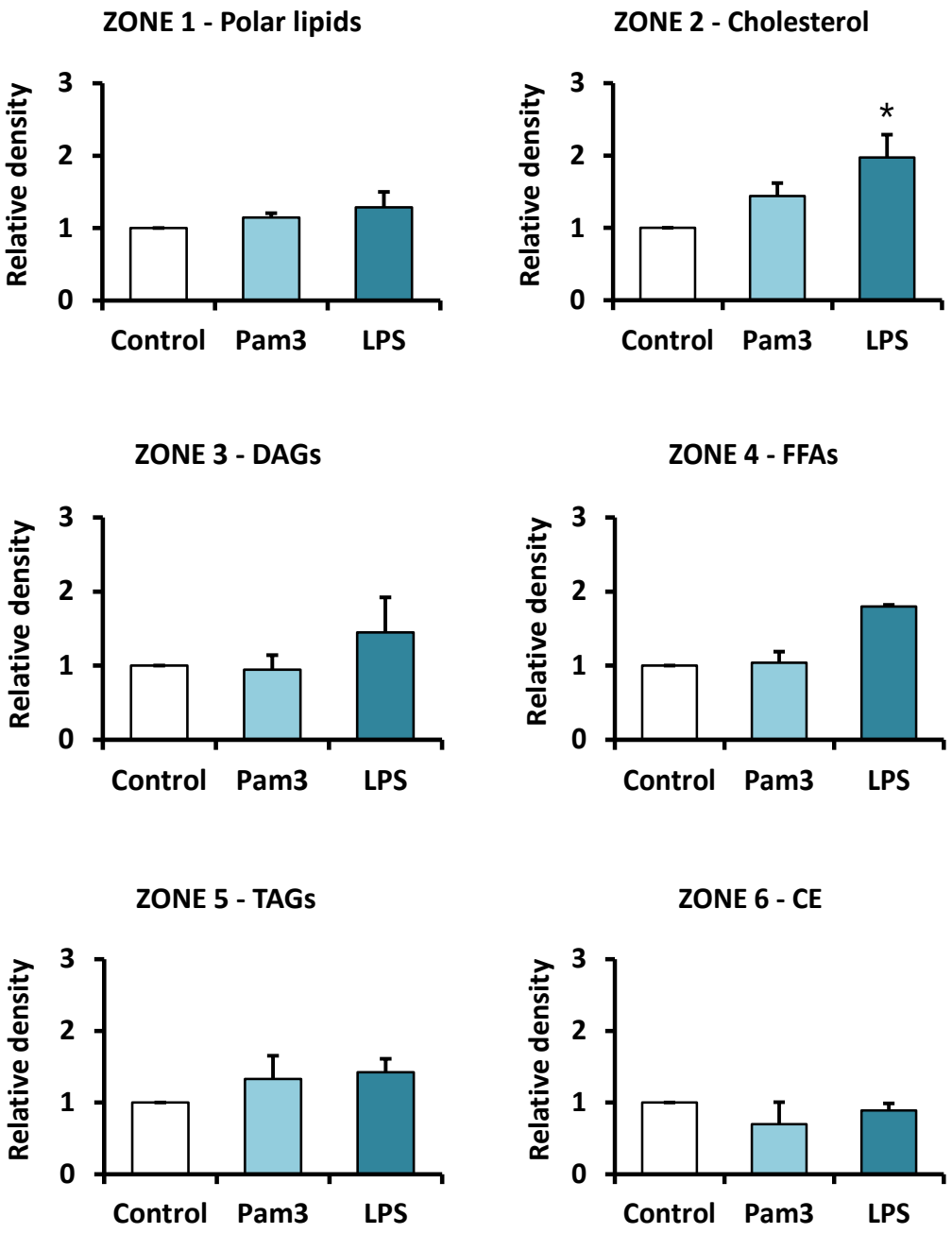

Figure 6.14. Densitometry of X-ray films exposed to TLC silica plates.

Densitometry was performed on the X-ray films that had been exposed for two weeks to the TLC silica gel plates used to separate cellular lipids. The obtained data was background-corrected and normalised to protein content and control (set to 1). Results are presented as the means ± SEM of three independent experiments. *$p < 0.05$ *vs.* control, as analysed by Kruskal-Wallis with Dunns post-test.

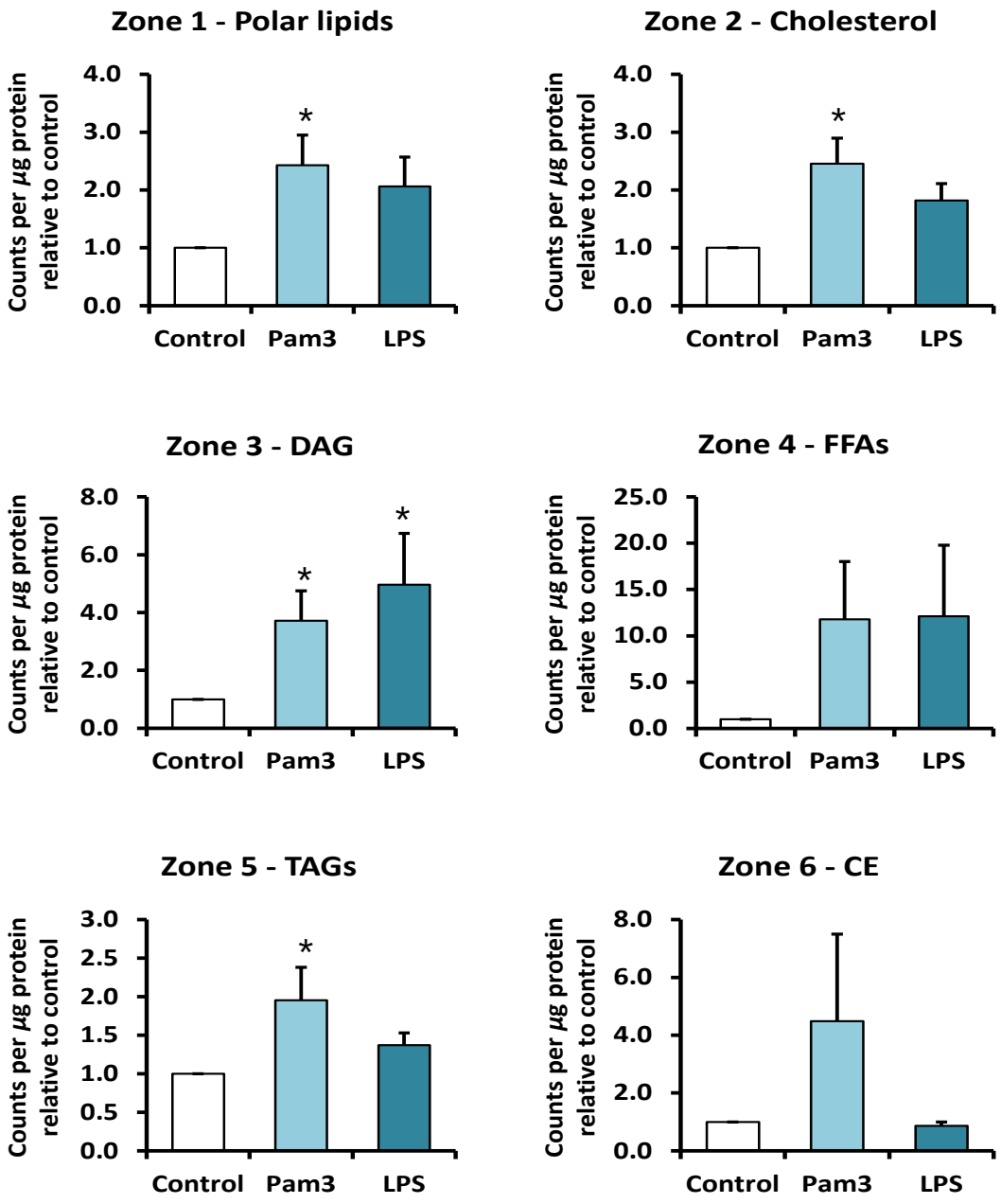

Figure 6.15. Quantification of radiolabel in scraped silica containing separated cellular lipid species.

Ethanol lipid extracts obtained from PAMP – ^{14}C-acetate – treated J774A.1 macrophages were separated by TLC, and the plates were incubated with an X-ray film for two weeks. Development of the film revealed bands corresponding to the different lipid groups on the silica plates. The zones containing each band were outlined with pencil and then scraped into vials containing scintillation fluid for measurement of

radioactivity of the samples (CPM). Results were normalised to protein content of each extract, and then to values obtained from control cells cultured in medium alone (set to 1), and presented as the means ± SEM of four independent experiments. *$p < 0.05$ *vs.* control, as analysed by Kruskal-Wallis with Dunns post-test.

6.7. Effect of PAMPs on expression of lipid metabolism genes in J774A.1 macrophages

The potential mechanisms for the observed increase in *de novo* lipid synthesis upon TLR activation were further investigated by analysing the expression of specific genes involved in lipid metabolism and regulation. For this purpose, J774A.1 macrophages were treated for 0, 6, 24 and 48 hours with medium alone or 1 µg/ ml of the TLR ligands Pam_3CSK_4 or LPS. The extracted mRNA was converted into cDNA, and RT-PCR (this last step conducted by Dr. C. Erridge) was then used to quantify the expression of selected genes.

As expected, PAMP treatment of cells resulted in significant induction of the interleukin 1-beta (*IL-1β*) gene at 6 hours ($p < 0.05$), with a gradual decrease at 24 and 48 hours. Both PAMPs down-regulated the expression of glucokinase (*Gck*) at 6 and 24 hours, with the change being significant at the later time point ($p < 0.05$). The expression of phosphoenolpyruvate carboxykinase (*Pck1*) was significantly up-regulated only by LPS at 48 hours ($p < 0.05$) (Figure 6.16).

Neither Pam_3CSK_4 nor LPS treatment affected the expression of the acyl-coenzyme A: cholesterol acyltransferase 1 (*Acat1*) gene responsible for esterification of cholesterol at any time point tested. The LDL receptor (*Lldr*) gene expression was shown to increase at 6 hours, and then decrease at the later time points in both Pam_3CSK_4 and LPS-treated cells, with the decrease reaching significance at both 24 and 48 hours Pam_3CSK_4-treated cells ($p < 0.05$) (Figure 6.17).

The expression of two of the main genes involved in the cholesterol efflux process during RCT was also examined (Figure 6.17). Both Pam_3CSK_4 and LPS were shown to significantly decrease the expression of the ATP-binding cassette transporter A-1 (*Abca1*) ($p < 0.05$), confirming the results obtained from the cholesterol efflux assays.

While Pam_3CSK_4 was shown to significantly decrease the expression of the other transporter, *Abcg1*, at 24 hours ($p < 0.05$), LPS had the opposite effect, suggesting that the two transporter proteins may be regulated differently by LPS.

Of the three lipid droplet regulatory proteins analysed, perilipin-A (*Plin1*) was the only protein to be significantly up-regulated by LPS at 48 hours ($p < 0.05$). Pam_3CSK_4 did not have any effect on the expression of this gene. The expression of adipophilin (*Plin2*) and tail interacting protein (TIP)-47 (*Plin3*) was shown to be down-regulated by both PAMPs, but the changes did not reach statistical significance at any time point tested (Figure 6.18).

Examination of genes involved in fatty acid metabolism revealed a significant down-regulation of peroxisome proliferator activated receptor-gamma (*Pparg*) mRNA in response to both PAMPs ($p < 0.05$ at 48 hours with Pam_3CSK_4 treatment; $p < 0.05$ at 6 and 24 hours with LPS treatment). On the contrary, hormone sensitive lipase (*Hsl-1*) was shown to be up-regulated at 6 hours ($p < 0.05$) in response to LPS. The same PAMP also induced significant up-regulation of fatty acid synthase (*Fasn*) and stearoyl-coenzyme A desaturase 1 (*Scd1*) at 48 hours ($p < 0.05$) (Figure 6.19).

Perhaps the most interesting finding from these experiments was the up-regulation of the 3-hydroxyl-3-methyl-glutaryl – coenzyme A reductase (*Hmgcr*) gene, which is a key rate-limiting enzyme involved in cholesterol biogenesis, by LPS (Figure 6.20). This up-regulation occurred at the late time point of 48 hours ($p < 0.05$), suggesting that *de novo* synthesis of lipid, particularly cholesterol, may become more obvious at later time points, such as 48 or 72 hours.

Taken together, the results suggest that the activation of TLR4, but not TLR2 in macrophages could lead to a late-phase transcriptional up-regulation of genes involved in *de novo* lipid synthesis.

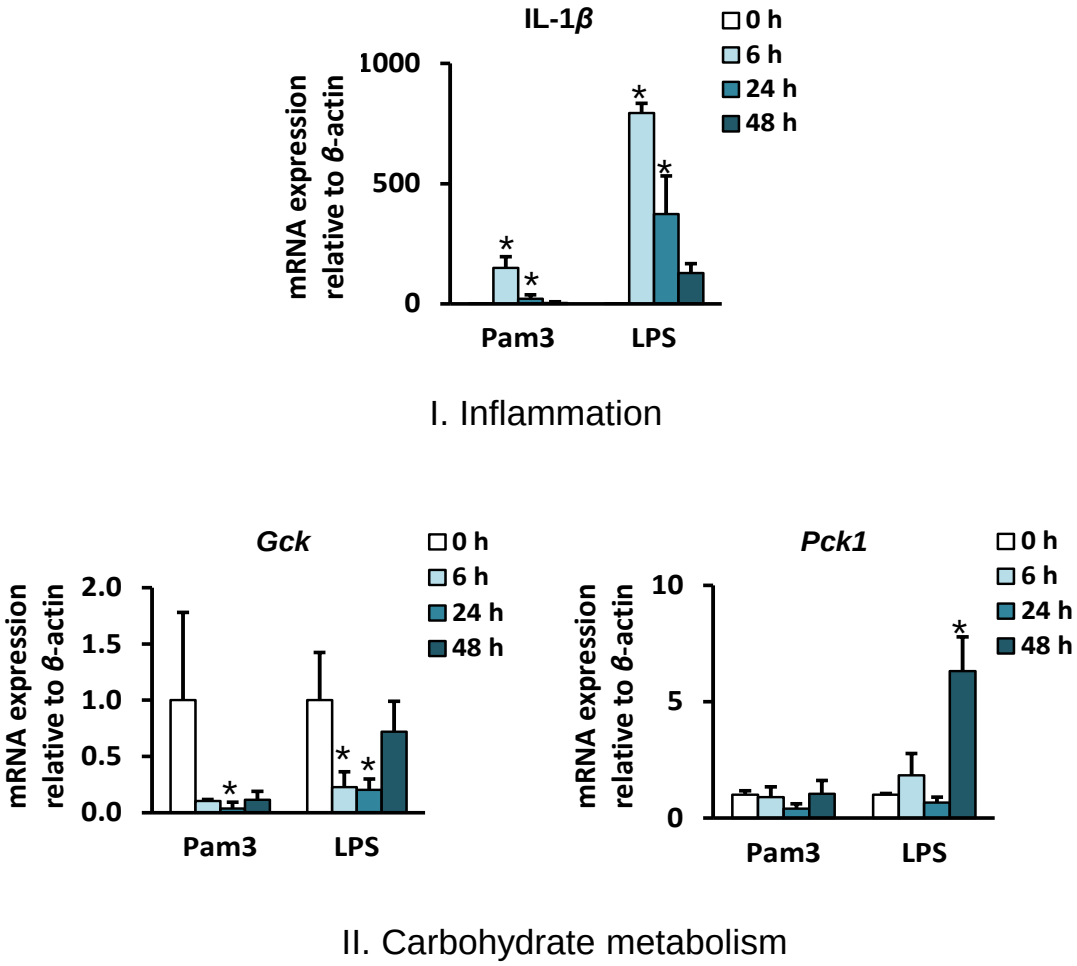

Figure 6.16. Effects of TLR2 and TLR4 stimulation on genes involved in inflammation and carbohydrate metabolism in J774A.1 macrophages

J774A.1 macrophages were treated with medium alone, Pam_3CSK_4 or LPS (1 μg/ ml) and the relative mRNA expression of genes involved in inflammation or carbohydrate metabolism was measured at 0, 6, 24, and 48 hours by RT-PCR. The results were normalised to β-actin and are presented as fold induction relative to control cells (medium alone) at each time point. Results are presented as the means ± SD of three independent experiments. *$p < 0.05$ *vs.* control at each time point. Abbreviations: interleukin-1beta (IL-1β), glucokinase (*Gck*), phosphoenolpyruvate carboxykinase (*Pck1*).

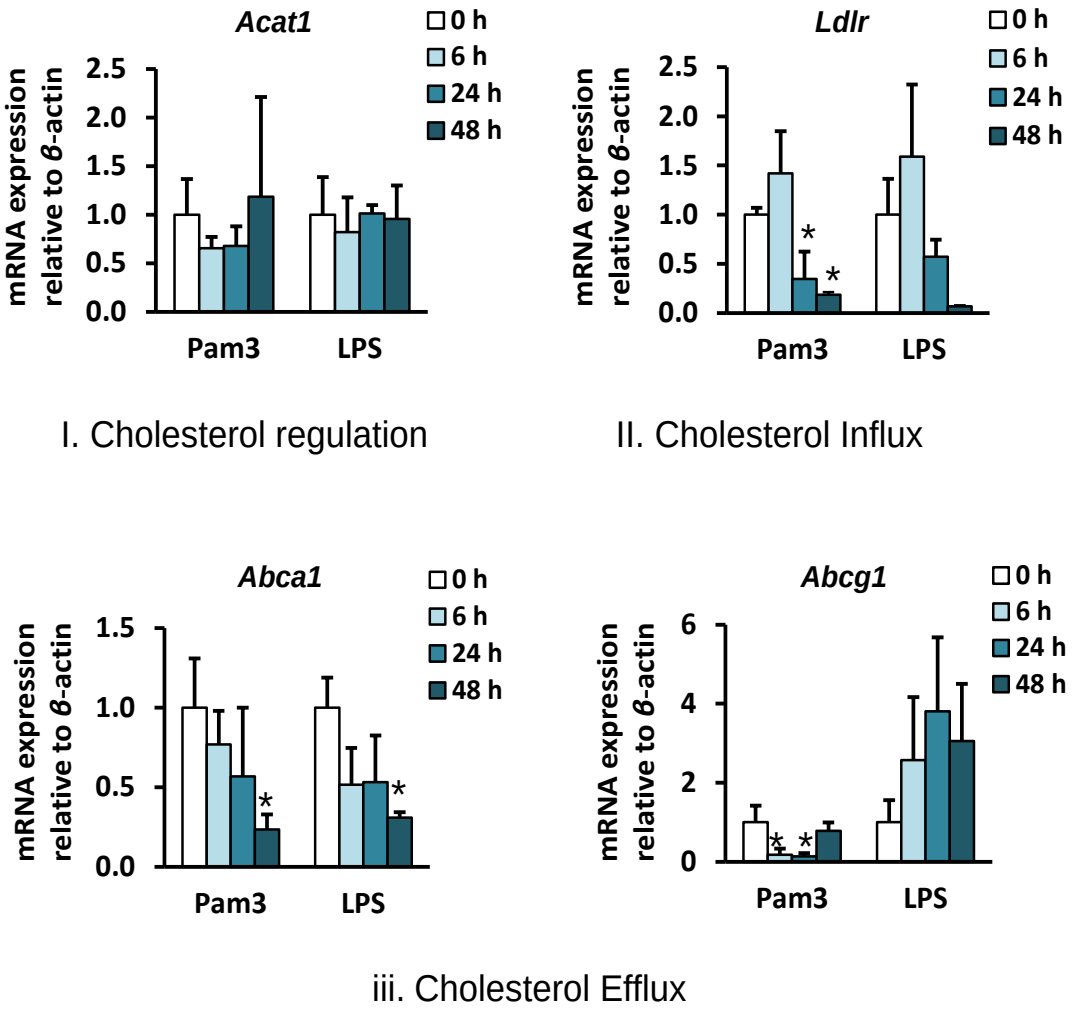

Figure 6.17. Effects of TLR2 and TLR4 stimulation on cholesterol metabolism regulating genes in J774A.1 macrophages

The expression levels of genes involved in cholesterol regulation, influx and efflux were measured in J774A.1 macrophages treated with medium alone, or 1 μg/ ml of Pam_3CSK_4 or LPS for 0, 6, 24, and 48 hours. Results were normalised to β-actin and are presented as means ± SD of three independent experiments. *$p < 0.05$ *vs*. control cells cultured in medium alone at each time point. Abbreviations: acyl coenzyme A: cholesterol acyltransferase (*Acat1*), low-density lipoprotein receptor (*Ldlr*), ATP-binding cassette A1 (*Abca1*), ATP-binding cassette G1 (*Abcg1*).

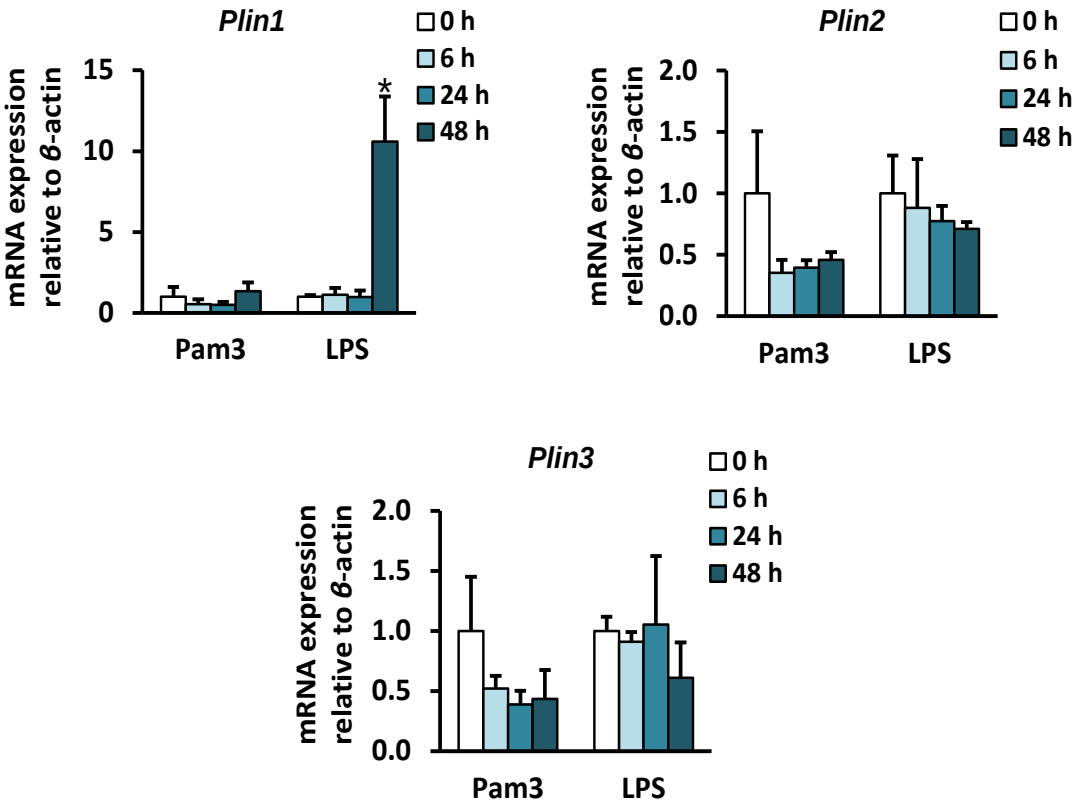

I. Lipid droplet regulatory proteins – PAT proteins

Figure 6.18. Effects of TLR2 and TLR4 stimulation on lipid droplet regulatory proteins in J774A.1 macrophages

Results were normalised to *β*-actin and are presented as means ± SD of three independent experiments. *$p < 0.05$ *vs*. control cells cultured in medium alone at each time point. Abbreviations: perilipin-A (*Plin1*), adipose differentiation-related protein (*Plin2*), tail-interacting protein (TIP)-47 (*Plin3*).

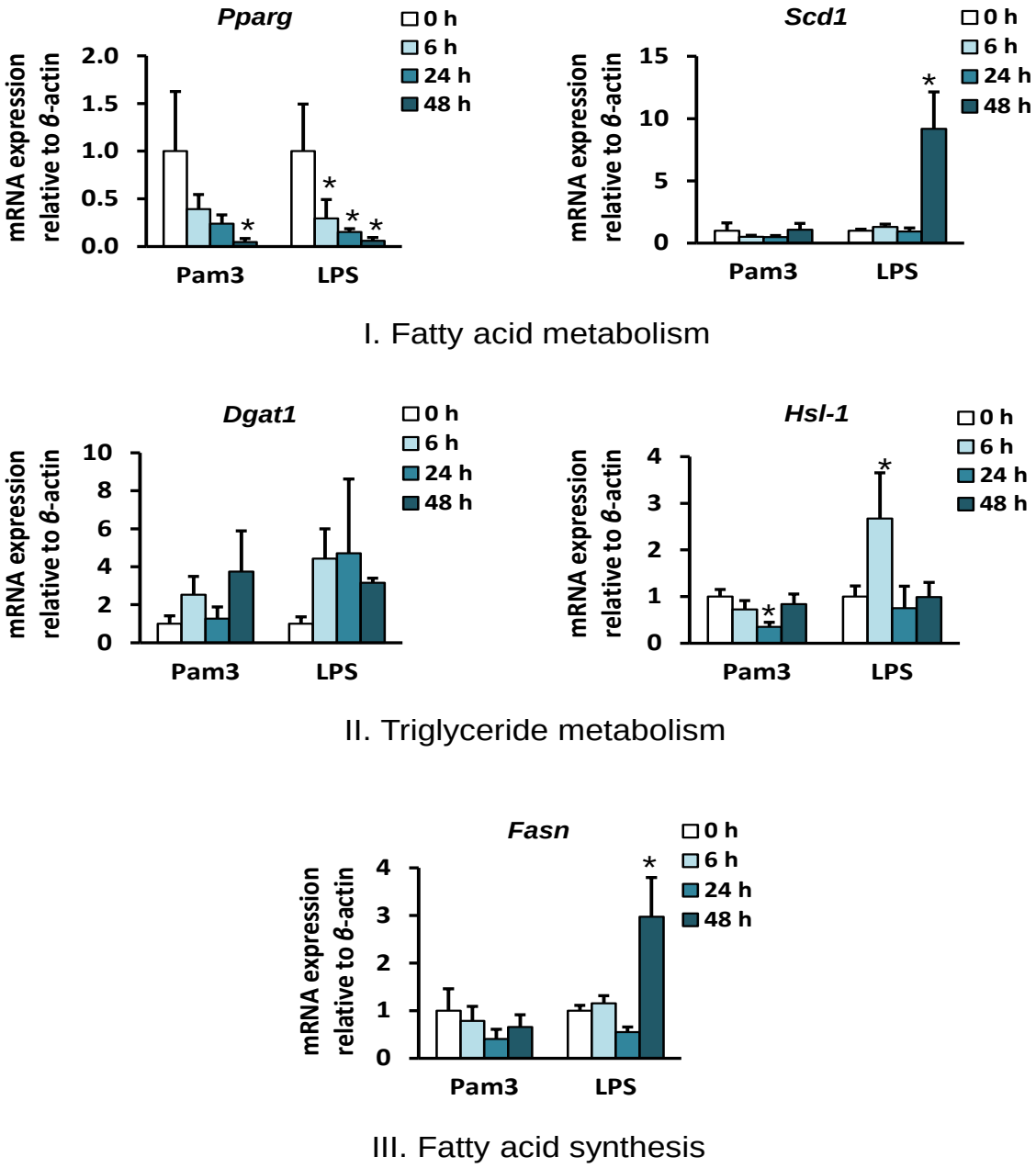

Figure 6.19. Effects of TLR2 and TLR4 stimulation on lipid metabolism genes in J774A.1 macrophages

Results were normalised to *β*-actin and are presented as means ± SD of three independent experiments. *$p < 0.05$ *vs*. control cells cultured in medium alone at each time point. Abbreviations: peroxisome proliferator activated receptor-*γ* (*Pparg*), stearoyl-coenzyme A desaturase (*Scd1*), diacylglycerol acyltransferase (*Dgat1*), hormone sensitive lipase (*Hsl-1*), fatty acid synthase (*Fasn*).

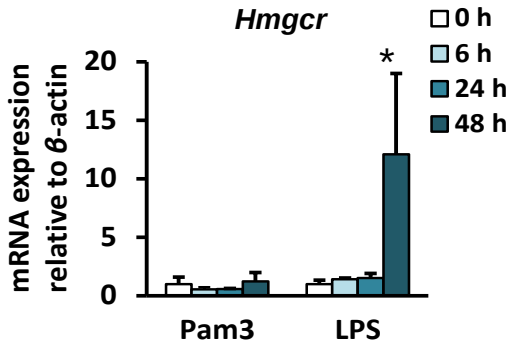

I. Cholesterol *de novo* synthesis

Figure 6.20. Effects of TLR2 and TLR4 stimulation on HMG-CoA reductase expression in J774A.1 macrophages

Results were normalised to β-actin and are presented as means ± SD of three independent experiments. *$p < 0.05$ *vs*. control cells cultured in medium alone at each time point. Abbreviations: 3-hydroxyl-3-methyl-glutaryl–coenzyme A reductase (*Hmgcr*).

6.8. Effect of PAMPs on expression of lipid metabolism genes in human monocytes

To add support to the data obtained from murine J774A.1 macrophages, human monocytes isolated from healthy individuals were grown for 7 days in autologous serum, after which they were treated with 100 ng/ ml of Pam_3CSK_4 or LPS for 24 and 48 hours. Total mRNA was extracted, reversed transcribed to cDNA, and gene expression analysis was performed using RT-PCR.

Similar to the results obtained from J774A.1 macrophages, stimulation of either TLR2 or TLR4 resulted in an increase in the expression of the inflammatory mediator IL-6 at 24 hours, which was followed by a decrease at 48 hours (Figure 6.21).

Expression of ABCA1 mRNA was shown to decrease at 48 hours in response to Pam_3CSK_4 treatment, supporting the results obtained from J774A.1 macrophage gene expression analysis and the cholesterol efflux assay (Figure 6.21). However, in contrast with the results obtained from J774A.1 macrophages, LPS treatment appeared to up-regulate the expression of this gene at the 48 hour time point. Expression of the LDL receptor (LDLR) gene was up-regulated at the two time points tested, with the expression increasing over time with both treatments (Figure 6.21).

A similar pattern of gene expression was observed for the sterol regulatory element-binding protein-2 (SREBP-2) gene, although the levels of expression in cells treated with LPS for 24 hours did not differ much from the levels obtained at 48 hours (Figure 6.21).

Of the genes involved in fatty acid metabolism, diacylglycerol acyltransferase (DGAT1) and fatty acid synthase (FASN) gene expression pattern was quite similar, with levels of expression being slightly lower at 48 hours compared to 24 hours in Pam_3CSK_4-treated cells. LPS was shown to up-regulate the expression of both genes in

a time-dependent manner (Figure 6.22). The stearoyl-coenzyme A desaturase-1 (SCD) gene was shown to be up-regulated at 24 hours by both PAMPs, and then down-regulated at the late time point of 48 hours (Figure 6.22).

Expression of the HMG-CoA reductase gene was shown to be down-regulated at 48 hours in response to Pam_3CSK_4, but up-regulated at 48 hours upon LPS treatment, a result that parallels the observations made in J774A.1 macrophages (Figure 6.22). However, expression of HMG-CoA reductase at this time point was slightly lower than measured in control cells or Pam_3CSK_4-treated cells at 24 hours.

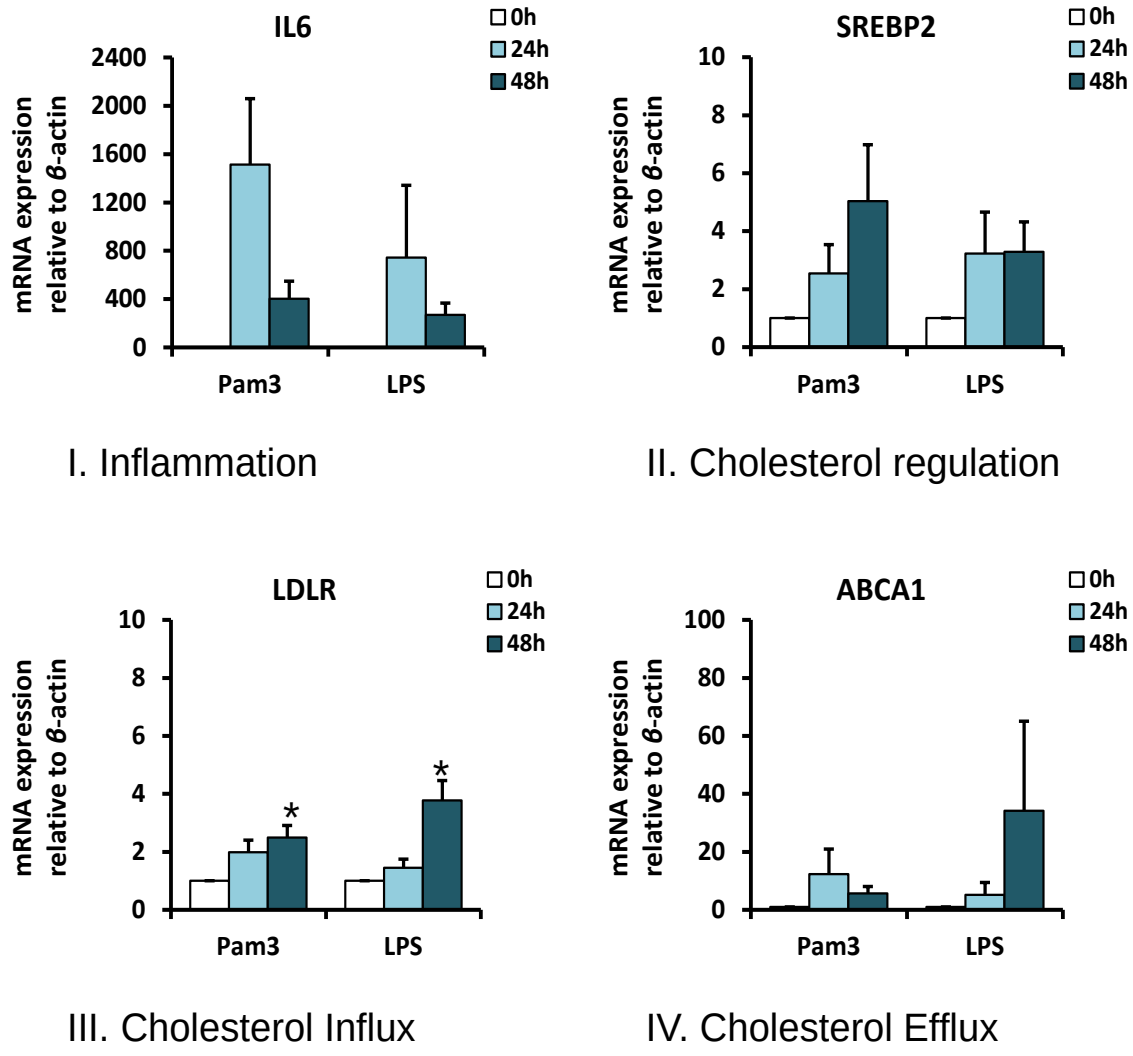

Figure 6.21. Effects of TLR2 and TLR4 stimulation on inflammation- and cholesterol-related genes in human macrophages

Human macrophages were challenged with medium alone, Pam_3CSK_4 or LPS (100 ng/ml) for 0, 24 and 48 hours. The expression of genes involved in inflammation or regulation of cholesterol influx or efflux pathways was assessed by RT-PCR. Results were normalised to *β*-actin, and are presented as means ± SEM of six independent experiments. Abbreviations: interleukin-6 (IL-6), sterol regulatory element-binding protein-2 (SREBP-2), low-density lipoprotein receptor (LDLR), ATP-binding cassette A-1 (ABCA1).

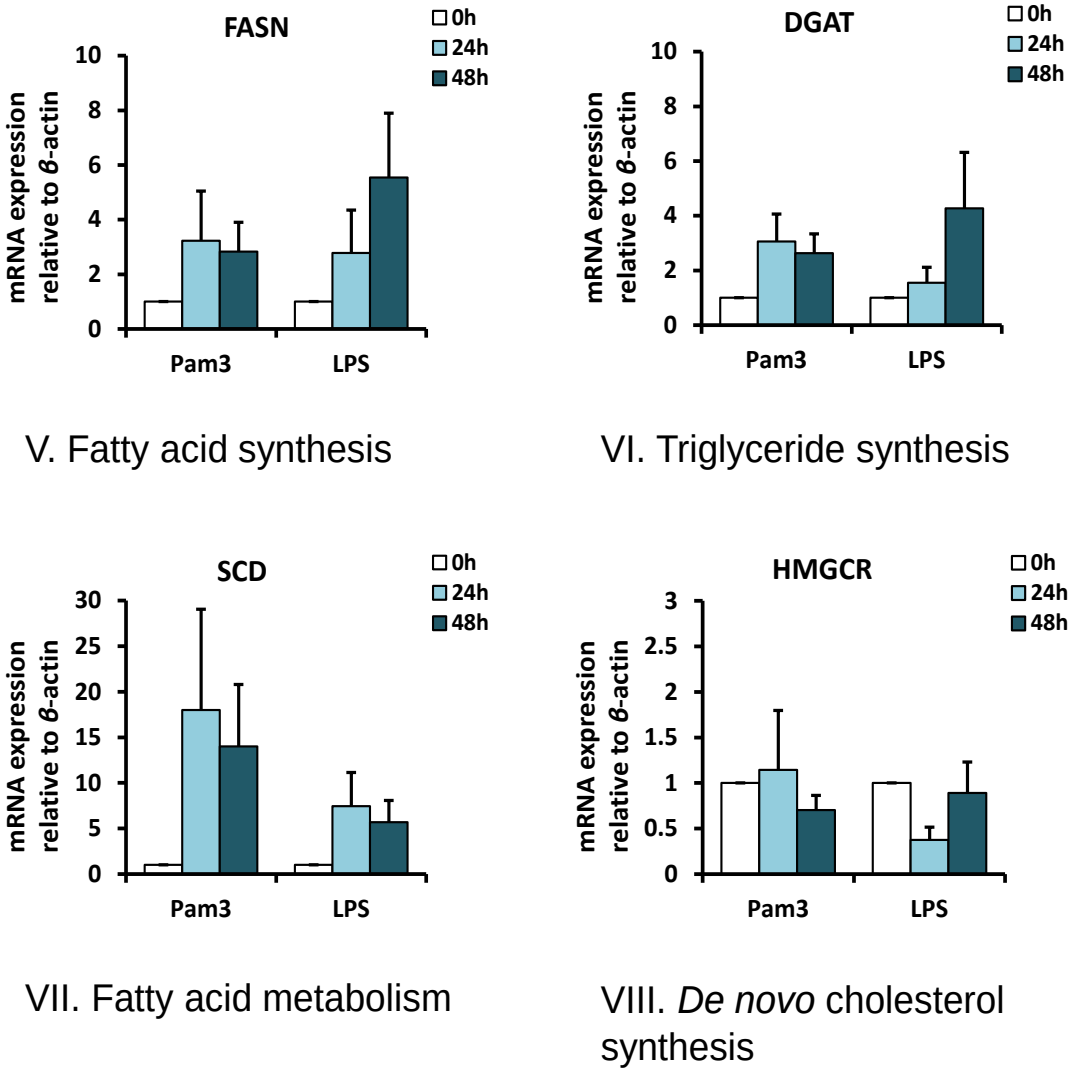

Figure 6.22. Effects of TLR2 and TLR4 stimulation on lipid metabolism and *de novo* cholesterol synthesis genes in human macrophages

Human macrophages were challenged with medium alone, Pam_3CSK_4 or LPS (100 ng/ml) for 0, 24 and 48 hours. The expression of genes involved in fatty acid and triglyceride metabolism, as well as *de novo* cholesterol synthesis was assessed by RT-PCR. Results were normalised to *β*-actin, and are presented as means ± SEM of six independent experiments. Abbreviations: fatty acid synthesis (FASN), diacylglycerol acyltransferase (DGAT), stearoyl-coenzyme A desaturase (SCD), 3-hydroxy-3-methyglutatyl-CoA reductase (HMGCR).

6.9. Effects of TLR4 stimulation on cellular levels of lipid regulatory proteins

It is important to check that the changes in the expression of a gene observed at the mRNA level are also observed at the protein level. Western blotting was performed to investigate the expression pattern of two key proteins involved in lipid metabolism whose mRNA levels were shown to be increased in J774A.1 or human macrophages upon PAMP stimulation, namely FASN and HMG-CoA reductase.

The lysates used in this experiment were collected from J774A.1 cells treated with LPS for 0, 2, 4, 6, 24, and 48 hours, separated by electrophoresis, transferred to membranes and probed with antibodies specific for the HMG-CoA reductase or FASN proteins.

Equal loading of protein in all wells was confirmed by Ponceau S Red staining of the blots (Figure 6.23 – a) after the protein transfer was completed, and also by probing for the house-keeping gene α-tubulin, each of which showed equal intensities (Figure 6.23 – b). Two bands were obtained when probing with antibody against HMG-CoA reductase, the upper band being between 70 and 80 kDa and the lower band, which presumably reflects a product of proteolysis, being ~60 kDa, much as expected from the antibody suppliers' product information (Figure 6.23 – b). HMG-CoA reductase staining intensity was shown to increase over time, becoming most intense at the latest time point tested (48 hours), thereby confirming the RT-PCR results that showed a significant increase of HMG-CoA reductase mRNA levels in cells treated with LPS at 48 hours.

A similar pattern was also obtained for FASN (Figure 6.23 – b). Two bands were obtained, with sizes slightly above and below 100 kDa. The expected size for full-length FASN product is around 273 kDa, and therefore, the bands obtained could reflect degradation products. The intensity of the signal was shown to increase over time, but

the difference in the signal intensity between time points was not as noticeable as in the HMG-CoA reductase blot. No positive staining was observed for FASN in the control sample, suggesting low expression of this protein in unchallenged cells.

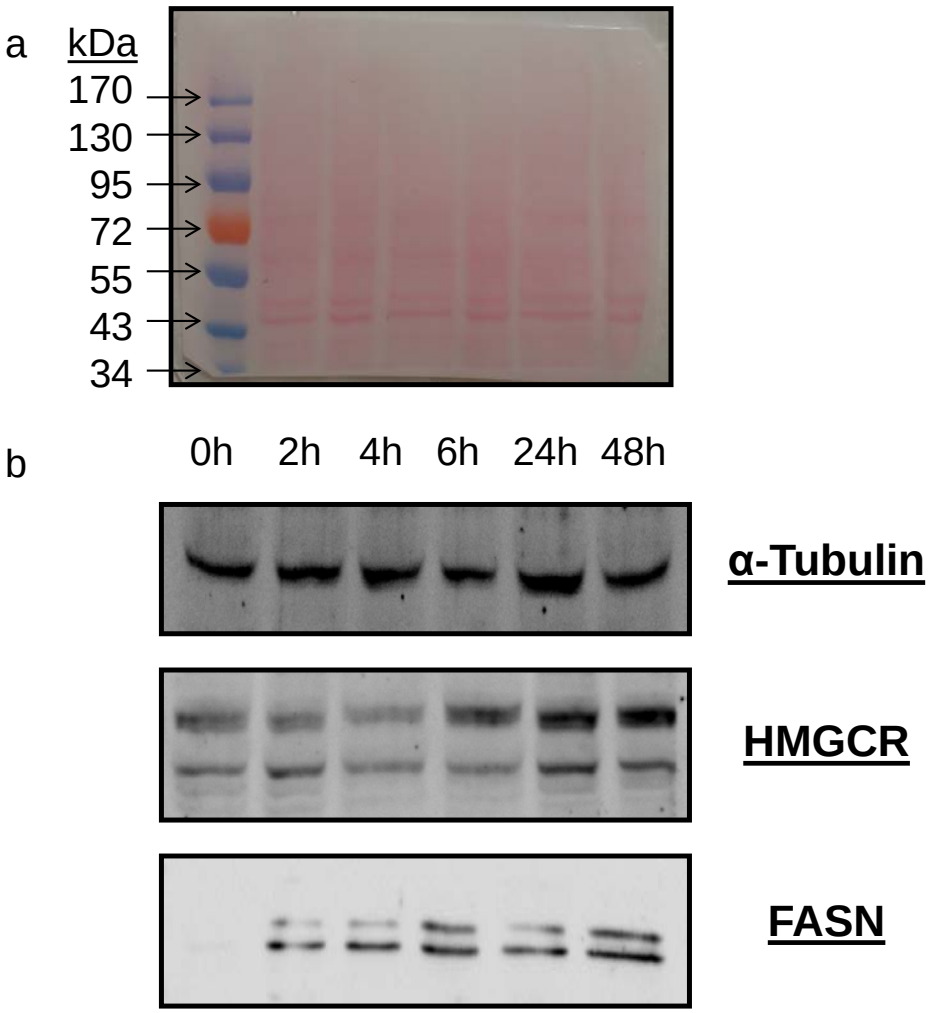

Figure 6.23. Western blots of lipid metabolism proteins in LPS-challenged J774A.1 macrophages.

Blots of lysates prepared from J774A.1 macrophages treated with LPS for the indicated time points. Ponceau S Red-stained blot (a) and blots probed for *α*-tubulin, HMG-CoA reductase, and FASN (b). Abbreviations: 3-hydroxy-3-methyglutatyl-CoA reductase (HMGCR), fatty acid synthesis (FASN).

6.10. Effect of HMG-CoA reductase inhibition on TLR2 and TLR4-dependent foam cell formation.

To further examine whether or not the accumulation of lipids during bacteria or PAMP-induced foam cell formation requires *de novo* lipid synthesis, we carried out experiments using the specific HMG-CoA reductase inhibitor simvastatin. Statins belong to a class of drugs that block the *de novo* synthesis of cholesterol by inhibiting the activity HMG-CoA reductase, an enzyme which plays a key role in *de novo* synthesis of cholesterol.

For these experiments, J774A.1 macrophages were challenged for 48 hours with medium alone, 100 ng/ ml of Pam_3CSK_4 or 100 ng/ ml LPS, in the presence of simvastatin (25 μM) or DMSO, which served as vehicle only control. Foam cell formation was assessed by flow cytometry of Nile Red-stained cells.

Treatment of cells with simvastatin in the presence of PAMPs led to a significant decrease in foam cell formation when compared to PAMP treatment in the presence of DMSO only (percentages of foam cell formation were: Pam_3CSK_4 + Sim: 1.08 *vs.* Pam_3CSK_4 + DMSO: 9.53, $p < 0.05$; LPS + Sim: 0.35 *vs.* LPS + DMSO: 12.28, $p < 0.05$) (Figure 6.24). The simvastatin-induced inhibition was more pronounced in LPS-treated cells, suggesting that cells treated with LPS might be more responsive to statin treatment. Simvastatin treatment was also able to reduce the basal level of foam cell formation in control cells (control – Sim: 0.25 *vs.* control – DMSO: 1.95, $p < 0.0001$).

These results clearly suggest a role for HMG-CoA reductase in the process of foam cell formation, and further confirm our hypothesis and our previous findings that *de novo* lipid biosynthesis might be one of the major mechanisms involved in bacteria or PAMP-induced foam cell formation upon TLR activation.

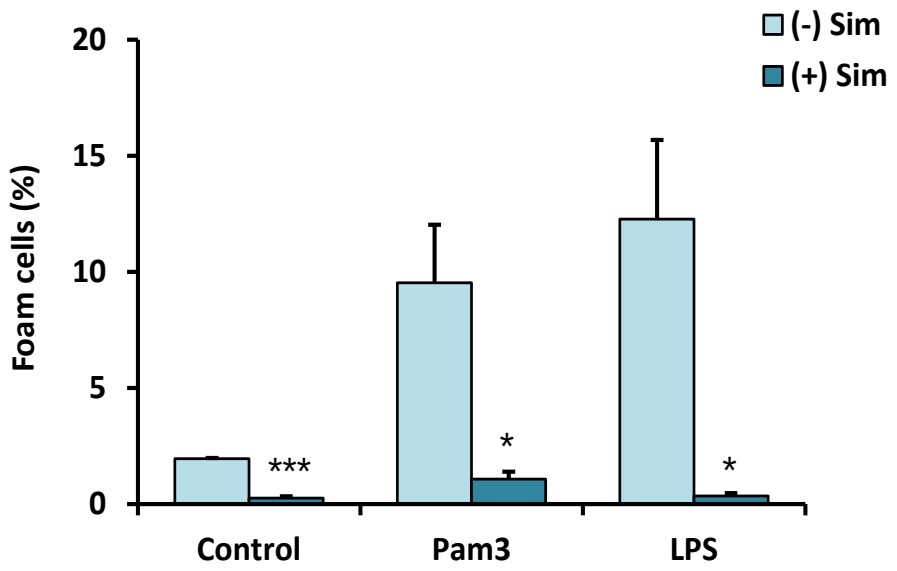

Figure 6.24. Effect of HMG-CoA reductase inhibition on TLR-dependent foam cell formation.

J774A.1 macrophages were treated for 48 hours with 100 ng/ ml of Pam_3CSK_4 or LPS in the presence of DMSO or Simvastatin (25 μM). Foam cell formation was assessed by flow cytometry. Results are presented as the means ± SEM of four independent experiments. *$p < 0.05$, ***$p < 0.001$ *vs.* cells in DMSO (-Sim).

7. DISCUSSION

Can common, atheroma-associated bacteria modify macrophage lipid metabolism?

One of the key steps during atherogenesis is the formation and accumulation of LDs in macrophages and their subsequent transformation into foam cells. It has been traditionally thought that this process is largely dependent on the oxidation of LDL in the vessel wall and its subsequent uptake by macrophage scavenger receptors (Kruth *et al.* 2002; Larigauderie *et al.* 2006). However, recent evidence has emerged from a variety of sources that challenges this view. For example, mice genetically deficient in both CD36 and SR-A show no deficit in foam cell formation when bred onto an atherosclerosis-prone background (Moore *et al.* 2005; Steinberg 2005; Kuchibhotla *et al.* 2008; Manning-Tobin *et al.* 2009), and humans genetically deficient in CD36 have increased, rather than decreased, cardiovascular risk (Masuda *et al.* 2009; Yuasa-Kawase *et al.* 2012). Large, placebo-controlled clinical trials of antioxidant supplements in man have also failed to reduce cardiovascular risk (Steinberg and Witztum 2002; Steinberg 2005; Dotan *et al.* 2009). Mice deficient in pro-oxidant gene products, such as NADPH oxidase or myeloperoxidase, show either no change in or increased susceptibility to atherosclerosis (Kirk *et al.* 2000; Brennan *et al.* 2001). Taken together, these findings argue against a prominent role for the OxLDL / scavenger receptor uptake mechanism in atherogenesis, and have renewed interest in identifying alternative potential mechanisms of macrophage foam cell formation.

This project set out to examine the potential of bacteria, and their related molecules, to promote macrophage foam cell formation for three main reasons. First, a consensus is beginning to emerge that human atheromatous plaques contain large quantities of bacterial DNA, although notably, not living organisms, whereas healthy artery does not (Meijer *et al.* 2000; Laman *et al.* 2002; Liu and Waters 2005; Ott *et al.* 2006; Renko *et*

al. 2008). Second, it has been reported that exposure of macrophages to the bacterium *C. pneumoniae* results in cellular lipid accumulation *in vitro* (Cao *et al.* 2007; D'Avila *et al.* 2008; Chen *et al.* 2009). Third, cumulative lifetime exposure to bacterial infections is associated with increased cardiovascular risk in man (Boekholdt *et al.* 2003; Ott *et al.* 2006; Lockhart *et al.* 2008; Vikatmaa *et al.* 2009), and increased rate of lesion formation in experimentally inoculated rodent models of atherosclerosis (Lehr *et al.* 2001; Mullick *et al.* 2005; Westerterp *et al.* 2007; Madan and Amar 2008).

The panel of bacteria examined in this study was selected to reflect the Gram-positive and Gram-negative bacterial DNA signatures most frequently identified in human atheromatous tissues from various studies using broad-range 16S rDNA gene PCR (Br-PCR) (Ott *et al.* 2006; Erridge *et al.* 2008a; Renko *et al.* 2008; Koren *et al.* 2011). These organisms represent known human pathogens involved in various common infections, such as skin infections (*S. aureus*), respiratory infections (*K. pneumoniae*), gastrointestinal or urinary tract infections (*E. coli, P. vulgaris*), hospital-acquired infections (*Acinetobacter* species, *P. aeruginosa*), and also commensal bacteria such as those found on the skin (*S. epidermidis*) or in the oral cavity (*S. salivarius*). The notion that commensal organisms may contribute to the accumulation of bacterial DNA in atheroma is supported by the study of Koren *et al.* (2010), which showed that several microbial communities are shared between atherosclerotic plaques and the gut, as well as the oral cavities. Previous studies suggest that a major mechanism by which such diverse bacteria reach the plaque is by delivery of killed organisms within recruited macrophages, further supporting the notion that many plaque macrophages may be exposed to bacteria before their recruitment to the growing lesion (Castrillo *et al.* 2003; Kazemi *et al.* 2005; He *et al.* 2009; Wiesner *et al.* 2010).

We found that while OxLDL and acetylated-LDL caused foam cell formation in primary mouse macrophages within 24 hours as expected (Goldstein *et al.* 1979; Henriksen *et al.* 1981; Kita *et al.* 1990; Robenek *et al.* 2006; Buers *et al.* 2009), co-culture with *E. coli* did not do so until at least 72 hours. By contrast, we found that human primary macrophages spontaneously accumulated lipid droplets, even in the absence of stimulus, when cultured beyond 48 hours *in vitro*. The J774A.1 macrophage cell line was therefore chosen for subsequent experiments because it displayed an intermediate phenotype, *i.e.* somewhere between human and mouse primary macrophages in terms of propensity to bacteria-induced foam cell formation, and was suitable for high-throughput experimentation. It is tempting to speculate that these differences may contribute to the much greater susceptibility of man to atherogenesis, relative to mice (Keyel *et al.* 2012), and that the late kinetics of the mouse macrophage response may partly explain the limited discussion of bacteria-mediated foam cell formation in the literature to date.

As the quantification of lipid droplets in macrophages by light microscopy of Oil Red-O stained macrophages was found to be laborious, and is potentially open to operator bias, we sought to develop a novel, higher throughput, unbiased assay of foam cell formation using flow cytometry of macrophages stained with the fluorescent dye Nile Red. This dye was chosen because it exhibits high affinity, specificity and sensitivity for neutral lipids, which promote yellow fluorescence of the dye (Tavian and Colombo 2007; Diaz *et al.* 2008). Also, unlike Oil Red-O, Nile Red staining does not cause deformation of LDs (Fukumoto and Fujimoto 2002; Nan *et al.* 2003). This assay yielded not only higher sensitivity, but also much higher throughput and unbiased, reproducible quantification of foam cell formation. The results of the Nile Red flow cytometry assays correlated well not only with manual counting of Oil Red-O stained

droplets by light microscopy, but also with biochemical measurements of cellular cholesterol ester content, and therefore represents a useful new method for the field.

Using these assays, we made the novel discovery that any of the diverse panel of bacteria examined promoted foam cell formation in J774A.1 macrophages in a dose-dependent manner. Interestingly, Gram-negative bacteria were more potent inducers of foam cell formation than Gram-positive bacteria, promoting foam cell formation even when less than 1 bacterium was present per macrophage.

Role of TLR signalling in bacteria-mediated foam cell formation

Because bacteria contain abundant stimulants of TLR signalling (Pålsson-McDermott and O'Neill 2004; Schoneveld *et al.* 2005; Tobias and Curtiss 2007; Gu *et al.* 2010), we first sought to examine the potential role of TLRs in bacteria-mediated foam cell formation. Inhibition of TLR2 with antibody, TLR4 with polymyxin B or TAK-242 (Kawamoto *et al.* 2008; Takashima *et al.* 2009), or both TLR2 and TLR4 with OxPAPC (Erridge *et al.* 2008b), all reduced foam cell formation caused by the model organism *K. pneumoniae*. Supporting this, PAMPs specific for any of the cell-surface TLRs (TLRs 1, 2, 4, 5, 6), promoted lipid accumulation in macrophages in a dose-dependent manner, as measured by microscopy, flow cytometry, and biochemical assay. We confirmed that almost all of the bacteria studied stimulated either TLR2, TLR4 or TLR5, suggesting that macrophages in atheroma containing DNA signatures of such organisms may have historically received a signal via these receptors. This finding is consistent with the marked up-regulation of these receptors observed in human atheroma relative to healthy artery (Schoneveld *et al.* 2005; Cao *et al.* 2007; Erridge *et al.* 2008a; Lee *et al.* 2008; Lundberg and Hansson 2010).

Our results are also consistent with earlier studies which showed that LPS and Pam_3CSK_4 can promote lipid accumulation, particularly CE and TG, in cultured

macrophages (Funk *et al.* 1993; Lee *et al.* 2008; Ye *et al.* 2009; Feingold *et al.* 2010). Contrary to these PAMPs, other PAMPs such as Poly I:C and CpG DNA, known to stimulate intracellular TLRs, did not lead to significant accumulation of CEs, and this was in agreement with results from earlier studies (Kazemi *et al.* 2005). The limited lipid droplet induction by Poly I:C, which signals via TLR3, relative to other PAMPS, offers potentially useful mechanistic insight, as TLR3 utilises the signalling adaptor TRIF, but not MyD88, which is used by other TLRs. It also suggests that the enhanced responses observed to LPS, in terms of both foam cell formation and cytokine synthesis, are not due solely to the fact that TLR4 also utilises TRIF. Taken together, our findings and those of other workers suggest that the IRF signalling pathways downstream of TRIF are unlikely to be the major mediators of lipid accumulation in these models, and that mediators downstream of MyD88-dependent pathways are more likely to be the relevant signalling mechanisms.

Our demonstration that stimulants of TLR2 and TLR4 are the most potent inducers of foam cell formation among the TLRs is also consistent with results of atherogenesis experiments in TLR-deficient murine models. Genetic deficiency in TLR4 results in a modest reduction in lesion formation (Michelsen *et al.* 2004b; den Dekker *et al.* 2010), and TLR2 deficiency results in a dramatic reduction in lesion formation, as reported by several independent groups (Mullick *et al.* 2005; Schoneveld *et al.* 2005). Notably, MyD88 deficiency also results in reduced atherogenesis in Apo-$E^{-/-}$ mice, adding further weight to a potential role of this pathway in foam cell formation (Björkbacka *et al.* 2004; Michelsen *et al.* 2004b; Schoneveld *et al.* 2005).

Relevance of TLR-mediated foam cell formation in primary cells and *in vivo.*

We next considered two potential mechanisms by which human monocytes may be exposed to TLR stimulants *in vivo*. First, it has been shown that transient, low-grade

bacteraemias are more common in healthy subjects than previously appreciated. For example, bacteria derived from the oral microbiota are detectable in the bloodstream for up to 30 minutes after tooth brushing in subjects with gum disease (Bhanji *et al.* 2002; Lockhart *et al.* 2008). Gum disease itself is a proposed risk factor for atherosclerosis in man (Ott *et al.* 2006). We discovered that even brief exposure (30 minutes) of primary human monocytes to any of the studied bacteria caused obvious LD formation within 24 hours, and this was also caused by diverse TLR stimulants. We next applied this to a whole blood model of low-grade bacteraemia, finding that significant lipid accumulation began to occur in human blood monocytes, but not other leukocytes, from as early as 2 hours post-stimulation.

To determine if such accumulation of lipids could occur in circulating monocytes *in vivo*, we considered various means of modelling low-grade TLR stimulation in man. The model chosen was low-grade endotoxaemia induced by a high fat meal, which has been reported to occur within hours after ingestion of a fatty test meal in healthy subjects (Erridge *et al.* 2007; Ghoshal *et al.* 2009; Harte *et al.* 2012). Earlier studies have shown that fatty meals cause translocation of LPS from the microbiota into the circulation via incorporation in chylomicrons with dietary fat (Ghoshal *et al.* 2009; Ghanim *et al.* 2010; Wiesner *et al.* 2010; Harte *et al.* 2012). Leukocyte activation and cytokine production consistent with exposure to low levels of LPS also occurs after ingestion of fatty meals (Cani *et al.* 2007; Erridge *et al.* 2007; Jackson *et al.* 2012).

We found that cellular lipid content did indeed increase in monocytes of 4 out of 6 subjects studied following a standardised high fat test meal. This was not due to changes in auto-fluorescence, as the increase was observed only in Nile Red-stained cells. Increased monocyte and granulocyte counts relative to baseline are considered to be an early indicator of acute, low-grade systemic inflammation in man (Herieka and Erridge

2013), and these measures were increased in the same donors which showed a cellular lipid response.

These findings are potentially of much relevance to potential mechanisms of atherosclerosis, as it has been traditionally assumed that the process of lipid accumulation in macrophages occurs only in the vessel wall, after monocyte-derived macrophages have been recruited into the intima (Choi *et al.* 2009). The concept that lipid accumulation may begin in the circulating monocyte before entry into the vessel wall is quite new, but has some support from studies reported by other workers. For example, VLDL lipolysis products were shown to induce lipid droplet formation in monocytes *in vitro*, as well as in primary postprandial monocytes isolated from whole blood (den Hartigh *et al.* 2010; Gower *et al.* 2011). In a study conducted by Choi *et al.* (2009), circulating peripheral blood monocytes from $LDLr^{-/-}$ mice were shown to accumulate lipids under hyperlipidaemic conditions before entering the vessel wall. Wu *et al.* (2009) also reported that $CD11c^{+}$ circulating monocytes from $Apo\text{-}E^{-/-}$ mice contained cytoplasmic lipid inclusions when animals were fed a high fat diet. Taken together, these observations suggest that the accumulation of lipids and the subsequent formation of LDs can occur *in vivo* in the circulation.

It is not clear whether the formation of foam cells we observed in the circulation of some donors after the high fat meal was mediated by increased levels of circulating triglyceride-rich lipoproteins, or their lipolysis products, or by the exposure of circulating monocytes to endotoxin. Future studies will be required to investigate which of these potential mechanisms may be involved by repeating the study with inclusion of a low fat meal control arm, and possibly some inhibitor of intestinal LPS translocation or signalling. It would also be interesting to determine in follow-up studies if the responder phenotype, *i.e.* those subjects who readily accumulate lipid in monocytes

postprandially, are at increased risk of developing CVD, and whether or not this assay could offer a useful tool for risk prediction. The high variability we observed in cytokine responses to different bacteria and TLR stimulants between donors could also be examined in the same way.

Mechanisms connecting TLR signalling with macrophage lipid metabolism

We next sought potential mechanisms to connect TLR signalling with pathways of lipid metabolism in macrophages. Our first consideration was that the most likely mechanism was via increased production of reactive oxygen species causing oxidation of LDL, and its subsequent uptake via scavenger receptors. Indeed, it has been proposed that *C. pneumoniae*-induced foam cell formation could be mediated via oxidation of LDL by activated macrophages, followed by the up-regulation of scavenger receptors and the uptake of OxLDL (Cao *et al.* 2007). However, we found that neither the antioxidant BHT, nor the scavenger receptor blocker PIA, inhibited foam cell formation induced by bacteria or TLR stimulants. These findings are supported by earlier studies showing that BHT also failed to inhibit lipid accumulation caused by *C. pneumoniae* or LPS (Oiknine and Aviram 1992; Kalayoglu and Byrne 1998). Other antioxidants, including nodihydroguaiaretic acid (NGDA) or l-ascorbic acid, also failed to prevent the formation of foam cells in RAW 264.7 macrophages after LPS stimulation (Funk *et al.* 1993). Ye *et al.* (2009) furthermore reported that PIA did not reduce the accumulation of lipids in THP-1 macrophages treated with LPS in the presence of LDL.

Remarkably, we found that LPS-induced foam cell formation occurred even in the complete absence of LDL. This finding is supported by the earlier observation of Funk *et al.* (1993) that cellular TG levels increased in macrophages incubated with LPS in the absence of lipoproteins. However, we found that the addition of LDL to LPS-treated macrophages dose-dependently increased cellular lipid accumulation. The latter

observation could offer some mechanism to reconcile the lipoprotein-independent foam cell pathway with the long understood association between high levels of LDL-cholesterol in the blood and increased cardiovascular risk (Perk *et al.* 2012). Indeed, Ye *et al.* (2009) suggested that the accumulation of lipids observed upon LPS stimulation could be the result of an LPS-induced up-regulation of the SCAP-SREBP-2 pathway, which could lead to the up-regulation of the LDL receptor and the subsequent uptake of native LDL. Kalayoglu and Byrne (1998) also reported that heparin, a known LDL receptor inhibitor, reduced the formation of foam cells induced by *C. pneumoniae*. However, we saw little impact of TLR2 or TLR4 stimulants on LDL uptake in our experiments.

It has also been proposed that macrophage foam cell formation may be promoted by increased rate of pinocytosis. For example, Choi *et al.* (2009) proposed that activation of TLR4 by LPS or mmLDL could enhance the uptake of soluble molecules via macropinocytosis. However, we found that treatment of J774A.1 macrophages with TLR2 or TLR4 ligands, or with heat-killed bacteria, did not result in increased pinocytosis rate, as measured by HRP uptake. The effects of LPS on fluid-phase pinocytosis were also studied by other groups. Activation of cells with IFN-γ or LPS was shown to decrease the rate of constitutive pinocytosis, pinosome formation and membrane trafficking compared to non-activated cells (Tsang *et al.* 2000). In our studies, LPS at low concentrations inhibited pinocytosis while higher concentrations reversed this effect. This concentration-dependent regulation of pinocytosis by LPS is in agreement with previous studies. Peppelenbosch *et al.* (1999) reported that low concentrations of LPS (0.1-10 ng/ ml) decreased the pinocytosis rate in both monocytes and macrophages, whereas higher concentrations of LPS (> 10 ng/ ml) stimulated pinocytosis.

We next examined the potential of TLR stimulants to modify macrophage reverse cholesterol transport (RCT), since mouse models indicate that this pathway plays a key role in atherosclerosis (Sviridov and Nestel 2002; Van Eck *et al.* 2005; Yvan-Charvet *et al.* 2010; Khera *et al.* 2011). We found that while LPS reduced cholesterol efflux to HDL by ~30%, an equal concentration of Pam_3CSK_4 reduced cholesterol efflux by almost 50%, suggesting that TLR2 signalling may be a more potent inhibitor of this pathway than TLR4 signalling. Our mRNA expression studies indicated that both TLR2 and TLR4 stimulants reduced expression of ABCA1 mRNA in J774A.1 macrophages. However, TLR2 stimulation, unlike TLR4 stimulation, also down-regulated the expression of the alternative cholesterol efflux mediator ABCG1, offering a potential explanation for the more potent inhibition of RCT by TLR2 stimulants.

Our finding of reduced cholesterol efflux in response to LPS is supported by other workers. For example, several studies showed that LPS dose-dependently inhibited the HDL-mediated cholesterol efflux pathway, via the down-regulation of both ABCA1 and SR-B1 (Baranova *et al.* 2002; Chen *et al.* 2009; Maitra *et al.* 2009; Feingold *et al.* 2010). Cytokines, such as IL-1*β* which shares a similar signalling pathway to TLR4, were also shown to down-regulate the expression of ABCA1 in a variety of cells, through mechanisms involving both LXR-dependent and independent pathways, at the transcriptional and post-transcriptional levels (Chen *et al.* 2007; Persson *et al.* 2008). Such pathways may also be relevant *in vivo*, as experimental endotoxaemia inhibits RCT in mice (McGillicuddy *et al.* 2009), and evidence suggests that RCT is impaired during the acute phase response, as a result of decreased expression of several proteins of the RCT pathway, such as ACAT-1, CETP, PTP, SR-B1, HDL and enzymes implicated in the catabolism of cholesterol (Persson *et al.* 2008; McGillicuddy *et al.* 2009; Feingold and Grunfeld 2010).

With respect to potential mechanisms connecting TLR signalling to RCT mediator expression, there is evidence suggesting the existence of interactions between TLR signalling and both PPAR and LXR signalling pathways, influencing one another bi-directionally (Chen *et al.* 2007; Chen *et al.* 2009). The process of cholesterol efflux mediated by LXRs was initially shown to be inhibited by TLR activation through the MyD88-independent or late-response IRF3 pathway (Castrillo *et al.* 2003; Lundberg and Hansson 2010). Chen *et al.* (2008) reported that *C. pneumoniae*-induced foam cell formation was a result of the activation of both TLR2 and TLR4, and that the IRF3/MyD88-independent pathway was responsible for the down-regulation of LXR target genes and the inhibition of cholesterol efflux. This process was shown to be reversed by the activation of LXR (Chen *et al.* 2009; Maitra *et al.* 2009). Later studies documented that this process could also be inhibited by the activation of the canonical NF-κB pathway (Cao *et al.* 2007; Maitra *et al.* 2009; Lundberg and Hansson 2010). Different mechanisms regarding the TLR-mediated inhibition of the LXR pathway have been proposed, and include enhanced activation of IRF3 by TBK-1, a kinase participating in the MyD88-independent pathway, the competition of IRF3 and LXR for a common co-activator, and the IRAK-1-mediated suppression of LXR via inhibition of the nuclear export of LXR and RXR (Castrillo *et al.* 2003; Maitra *et al.* 2009). Majdalawieh and Ro (2009) suggested that the effects of LPS on cholesterol efflux might be the result of the LPS-induced up-regulation of adipocyte enhancer-binding protein-1 (AEBP-1), a transcriptional repressor that was shown to up-regulate the expression of NF-κB and subsequently, down-regulate the expression of both nuclear transcription factors LXR-α and PPAR-γ. It could be possible that Pam_3CSK_4 might mediate its effects via a similar mechanism.

We finally examined the potential of TLR stimulants to regulate *de novo* lipid synthesis. Treatment of macrophages with Pam_3CSK_4 or LPS resulted in significantly increased cellular total lipid synthesis, as determined by scintillation counting of cellular lipid extracts. In keeping with results from the earlier experiments, Pam_3CSK_4 more potently induced lipid synthesis than did LPS, further supporting the notion that TLR2 may more extensively regulate macrophage lipid metabolism than TLR4.

Thin layer chromatography revealed that stimulation via TLR2 or TLR4 resulted in increased synthesis of all major groups of cellular lipids. Although densitometry of autoradiography films exposed to TLC plates proved to be quite variable and difficult to draw conclusions from, scintillation counting of bands scraped from TLC plates revealed useful information regarding which lipid species were up-regulated by TLR stimulants. These experiments revealed that TLR2 was a more potent inducer of synthesis of polar lipids, cholesterol, CE, FFAs and TAG than TLR4.

To explore potential mechanisms connecting TLR signalling to *de novo* lipid synthesis, mRNA expression analysis of key candidate lipid regulatory genes was performed. This analysis revealed that many genes involved in lipid metabolism were altered by TLR2 or TLR4 stimulation in murine J774A.1 macrophages. For example, the cholesterol efflux mediators ABCA1 and ABCG1 were down-regulated by both PAMPs or by Pam_3CSK_4 alone, respectively, within 24 hours. This could explain the reduced efflux capacity exhibited by Pam_3CSK_4-treated cells when compared to LPS-treated cells. A significant increase in the expression of perilipin-A was observed 48 hours after treatment with LPS, which is in accordance with the fact that the expression of perilipin-A occurs after the initiation of LD formation, as it is mostly associated with larger droplets (Wolins *et al.* 2005). PPAR-γ expression was significantly down-regulated by both PAMPs. This may reflect the fact that there is a negative cross-talk

between the NF-κB and the PPAR pathways; activation of NF-κB was shown to reduce the expression of PPAR-γ, and *vice versa* (Castrillo *et al.* 2003; Almeida *et al.* 2009). The down-regulation of PPAR-γ is associated with reduced expression of LXR, which is known to be one of its target genes (Chawla *et al.* 2001b). This, in turn, could explain the decreased expression of ABCA1 and ABCG1 seen after PAMP treatment.

The most interesting finding from these experiments was the up-regulation of HMG-CoA reductase, the key enzyme of cholesterol *de novo* synthesis, by LPS. Although HMG-CoA reductase mRNA expression was not increased until at least 48 hours post-treatment, this likely remains relevant in the context of atherogenesis, since macrophages are long-lived cells in atherosclerotic plaques (Ley *et al.* 2011). As most previous studies of LPS-induced transcriptional programmes have used terminal time points of 24 hours, this could explain why this effect has not been reported previously. Notably, while Pam_3CSK_4 did not alter expression of HMG-CoA reductase mRNA, it still caused increased synthesis of cholesterol at early time points. Post-transcriptional and/or post-translational regulation of HMG-CoA reductase activity could be a possible explanation for this finding.

When these experiments were repeated in human primary macrophages, different sets of lipid regulatory genes were found to be altered by TLR2 and TLR4 stimulants compared to those observed in the J774A.1 macrophage cell line. Notably, genes involved in LDL uptake (LDL receptor), and fatty acid or triglyceride synthesis (FASN, DGAT, SCD-1), were all up-regulated by TLR2 or TLR4. However, HMG-CoA reductase expression was not induced and, paradoxically, ABCA1 was actually up-regulated by TLR stimulants. The differing results obtained between human and mouse macrophages likely reflect species-specific differences in the mechanisms connecting TLR signalling to lipid metabolism.

The statin family of drugs is currently the most widely used and effective therapy for the reduction of cardiovascular risk (Van Eck *et al.* 2005; Segers *et al.* 2008; den Dekker *et al.* 2010; Dennis *et al.* 2010). As the key enzyme targeted by statins is HMG-CoA reductase, the rate-limiting enzyme during *de novo* cholesterol synthesis, we therefore investigated if TLR-induced foam cell formation could be modulated by statin treatment. Treatment of macrophages with simvastatin resulted in complete inhibition of foam cell formation induced by Pam_3CSK_4 or LPS treatment.

It is likely that either of two possible mechanisms explains this finding. First, it could simply be due to direct inhibition of HMG-CoA reductase, as statins were shown to inhibit cholesterol synthesis in macrophages, both *in vivo* and *in vitro*, in ways similar to those observed in hepatocytes (Vaughan *et al.* 1996). The second possibility is that simvastatin acts as an inhibitor of intracellular TLR signalling. Supportive of this notion, statins were shown to inhibit the responses of arterial endothelial cells to LPS by disrupting the geranylgeranylation and RhoA signalling pathways (Rice *et al.* 2003), or perhaps via inhibition of NF-κB (den Dekker *et al.* 2010). Anti-inflammatory effects associated with statin therapy are becoming more apparent, and include increased production of endothelial NOS and preservation of endothelial function, reduced leukocyte attachment to the endothelium, changes in the balance between Th1 and Th2 lymphocytes, and inhibition of SMC proliferation (Vaughan *et al.* 1996; Bellosta *et al.* 2000; Libby *et al.* 2002; Segers *et al.* 2008).

It has been reported, however, that the concentration of simvastatin achieved in human plasma after the administration of the drug at 40 mg is in the 10 - 100 nM range (Corsini and Bellosta 2007; Björkhem-Bergman *et al.* 2011). This concentration is ~1,000-fold lower than the concentration used in our *in vitro* studies (25 μM). To gain more insight into the potential effects of statins on monocyte lipid droplet regulation in

humans *in vivo*, it would be important to examine the effects of statins *in vitro* at concentrations similar to those observed in the plasma of individuals undergoing statin treatment.

Clinical implications

The key findings of this study with respect to potential clinical relevance are that (i) any of a diverse range of bacteria may promote macrophage foam cell formation, (ii) TLR2 or TLR4 may represent useful therapeutic targets for the prevention of foam cell formation and hence, atherosclerosis and (iii) a key target of the statins may be not the liver, as currently thought, but in fact the circulating monocyte.

The implications of the first observation are that the bacterial signatures commonly observed in atheroma, which were previously considered innocuous, may actually contribute to lipid accumulation in macrophages and therefore, increased risk of formation of lipid-rich necrotic cores which are associated with an unstable plaque phenotype. Because every type of organism examined, including commensals, promoted foam cell formation independently of bacterial viability, it also suggests that it will not be possible to develop any simple antibiotic therapy that targets one group of organisms for the prevention or treatment of atherosclerosis. This is supported by the failure of recent antibiotic trials aimed at eradication of *Chlamydia* species to reduce cardiovascular risk (Liu and Waters 2005; Segers *et al.* 2008; Wang *et al.* 2011). Nevertheless, it remains possible that generalised methods for the reduction of transient bacteraemias and endotoxaemias could be developed into novel therapeutic approaches to reduce cardiovascular risk.

The findings also warrant future studies of the therapeutic potential of targeting TLR2 and TLR4 with specific inhibitors. Such approaches are likely to be safe, since mice genetically deficient in these receptors, or key TLR signalling adaptors, show no

obvious deleterious phenotype, and are protected from lesion formation (Björkbacka *et al.* 2004; Michelsen *et al.* 2004b; Mullick *et al.* 2005; Schoneveld *et al.* 2005). Moreover, a small number of human patients carry mutations resulting in the complete absence of functional MyD88 or IRAK-1, both of which are essential transducers of signalling from cell-surface TLRs. While such patients suffer from increased risk of severe bacterial infections in childhood, they do not display immunodeficiency or increased risk of infection in adulthood because the adaptive immune system has by that time evolved sufficient memory to deal with infectious threats (Picard *et al.* 2010; von Bernuth *et al.* 2012). It is also possible that the statins, currently used to reduce cardiovascular risk, inhibit TLR signalling on the basis of *in vitro* experiments using concentrations relevant to those observed at therapeutic doses (Rice *et al.* 2003), and the reduction in CRP levels and other inflammatory markers observed in subjects receiving statin therapy (Ridker *et al.* 2009). Statin family molecules could perhaps be developed to target TLR signalling more specifically or aggressively.

The final major clinically relevant finding is that lipid accumulation and foam cell formation may begin in circulating monocytes, long before their entry into the vessel wall, and that this may be at least partly dependent on *de novo* cholesterol synthesis. The sensitive flow cytometric assay we have developed for monocyte lipid droplet content could potentially be used to screen for individuals at increased risk of foam cell formation as part of a simple blood test. Appropriate therapies, *i.e.* personalised medicines, could then be administered. As we found that simvastatin efficiently blocked TLR-induced foam cell formation *in vitro*, it will also be useful to determine if such effects are observed in monocytes of patients receiving statins at therapeutic doses. Furthermore, should it be identified in follow-up studies that the circulating monocyte,

rather than the liver, is the key target of statins, this may enable the development of novel statin analogues to more efficiently target circulating leukocytes.

Future work.

It would be interesting to conduct a number of further studies based on the results obtained from this project. First, it will be useful to confirm in a larger cohort, and then establish the mechanism of the increased monocyte lipid droplet content observed in healthy volunteers following a fatty meal. In particular, experiments should be performed to determine if the lipid accumulation is TLR-dependent, or if it is merely due to increased circulating concentrations of triglyceride-rich lipoproteins in the postprandial phase. Since there are currently no specific TLR inhibitors commercially available for human use, such studies could instead address this question by experimental induction of low-grade endotoxaemia by bolus injection of 1 ng/ kg *E. coli* LPS, as commonly used to model low-grade systemic inflammatory signalling in healthy volunteers (van Deventer *et al.* 1990).

It would also be interesting to measure the contribution made by macrophage-specific TLR signalling during foam cell formation in murine atherosclerosis. Preliminary experiments using bone marrow-derived macrophages from mice deficient in specific TLRs, or downstream signalling adaptors, would help further delineate mechanisms of TLR-mediated foam cell formation. Apo-$E^{-/-}$ or $LDLr^{-/-}$ mice could then be crossed with mice lacking TLRs specifically in macrophages, created by Cre-Lox deletion of TLRs driven by the macrophage-specific CD68 promoter, to test the main hypothesis that macrophage-specific TLR signalling promotes foam cell formation. Should orally-available drugs targeting TLR2 or TLR4 become available, these should also be tested in murine models of atherosclerosis.

Finally, it will be very useful to establish whether or not *de novo* lipid synthesis by macrophages themselves may contribute to atherosclerosis. This could be tested initially using a murine model of atherosclerosis, such as Apo-$E^{-/-}$ mice, in which specific components of lipid biosynthetic pathways are genetically deleted. Key genes to be examined in this way would be fatty acid synthase (to investigate *de novo* triglyceride synthesis) and HMG-CoA reductase (to investigate *de novo* cholesterol synthesis). As HMG-CoA reductase deficiency is embryonic lethal, a conditional knockout would need to be generated. As described above, such a conditional knockout could be generated by Cre-Lox recombination driven by the CD68 promoter, perhaps in tandem with drug-induced (e.g. tamoxifen) gene deletion, to generate lines in which HMG-CoA reductase is only knocked out in macrophages.

In summary, this project has made a number of novel discoveries which challenge existing concepts of atherogenesis and advance understanding of the underlying mechanisms connecting infection with innate immunity, foam cell formation and atherosclerosis. The findings reported in this thesis should be useful to workers in the fields of macrophage lipid metabolism and atherosclerosis research. Using this information to drive the development of novel therapeutic approaches for atherosclerosis should remain the key ambition of studies intended to follow this one.

A P P E N D I X

The following published articles have been removed from the Appendix (pp. 266-284) of the electronic version of this thesis due to copyright restrictions:

Nicolaou, G., Erridge, C. (2010) Toll-like receptor-dependent lipid body formation in macrophage foam cell formation. *Current Opinion in Lipidology*, 21(5), pp. 427– 433. http://dx.doi.org/10.1097/MOL.0b013e32833cacd5

Nicolaou, G., Goodall, A.H., Erridge, C. (2012) Diverse bacteria promote macrophage foam cell formation via Toll-like receptor-dependent lipid body biosynthesis. *Journal of Atherosclerosis and Thrombosis*, 19(2), pp. 137-148. http://dx.doi.org/10.5551/jat.10249

The unabridged version can be consulted at the University of Leicester Library.

BIBLIOGRAPHY

Adachi O, Kawai T, Takeda K, *et al.* (1998) Targeted disruption of the MyD88 gene results in loss of IL-1- and IL-18-mediated function. Immunity 9:143–150.

Almeida PE, Silva AR, Maya-Monteiro CM, *et al.* (2009) Mycobacterium bovis bacillus Calmette-Guérin infection induces TLR2-dependent peroxisome proliferator-activated receptor gamma expression and activation: Functions in inflammation, lipid metabolism, and pathogenesis. The Journal of immunology 183:1337–1345.

Anzinger JJ, Chang J, Xu Q, *et al.* (2010) Native low-density lipoprotein uptake by macrophage colony-stimulating factor-differentiated human macrophages is mediated by macropinocytosis and micropinocytosis. Arteriosclerosis, thrombosis, and vascular biology 30:2022–2231.

Ashida K, Miyazaki K, Takayama E, *et al.* (2005) Characterization of the expression of TLR2 (Toll-like Receptor 2) and TLR4 on circulating monocytes in coronary artery disease. Journal of atherosclerosis and thrombosis 12:53–60.

Ball RY, Stowers EC, Burton JH, *et al.* (1995) Evidence that the death of macrophage foam cells contributes to the lipid core of atheroma. Atherosclerosis 114:45–54.

Baranova I, Vishnyakova T, Bocharov A, *et al.* (2002) Lipopolysaccharide Down Regulates Both Scavenger Receptor B1 and ATP Binding Cassette Transporter A1 in RAW Cells. Infection and Immunity 70:2995–3003.

Bellosta S, Ferri N, Arnaboldi L, *et al.* (2000) Pleiotropic effects of statins in atherosclerosis and diabetes. Diabetes care 23 Suppl 2:B72–78.

Berg JM, Tymoczko JL, Stryer L (2007) Biochemistry, Sixth. W. H. Freeman & co., New York

Berk BC, Weintraub WS, Alexander RW (1990) Elevation of C-reactive protein in "active" coronary artery disease. The American journal of cardiology 65:168–172.

Beutler B, Jiang Z, Georgel P, *et al.* (2006) Genetic analysis of host resistance: Toll-like receptor signaling and immunity at large. The Annual Review of Immunology 24:353–389.

Bhanji S, Williams B, Sheller B, *et al.* (2002) Transient bacteremia induced by toothbrushing: a comparison of the Sonicare toothbrush with a conventional toothbrush. Pediatric dentistry 24:295–299.

Binder CJ, Hörkkö S, Dewan A, *et al.* (2003) Pneumococcal vaccination decreases atherosclerotic lesion formation: molecular mimicry between Streptococcus pneumoniae and oxidized LDL. Nature medicine 9:736–743.

Björkbacka H, Kunjathoor VV, Moore KJ, *et al.* (2004) Reduced atherosclerosis in MyD88-null mice links elevated serum cholesterol levels to activation of innate immunity signaling pathways. Nature medicine 10:416–421.

Björkhem-Bergman L, Lindh JD, Bergman P (2011) What is a relevant statin concentration in cell experiments claiming pleiotropic effects? British journal of clinical pharmacology 72:164–165.

Blessing E, Campbell LA, Rosenfeld ME, *et al.* (2001) Chlamydia pneumoniae infection accelerates hyperlipidemia induced atherosclerotic lesion development in C57BL/6J mice. Atherosclerosis 158:13–17.

Boekholdt SM, Agema WRP, Peters RJG, *et al.* (2003) Variants of Toll-like receptor 4 modify the efficacy of statin therapy and the risk of cardiovascular events. Circulation 107:2416–2421.

Boekholdt SM, Peters RJG, Hack CE, *et al.* (2004) IL-8 plasma concentrations and the risk of future coronary artery disease in apparently healthy men and women: the EPIC-Norfolk prospective population study. Arteriosclerosis, thrombosis, and vascular biology 24:1503–1508.

Boren J, Brindle KM (2012) Apoptosis-induced mitochondrial dysfunction causes cytoplasmic lipid droplet formation. Cell death and differentiation 19:1561–1570.

Boring L, Gosling J, Cleary M, Charo IF (1998) Decreased lesion formation in CCR2−/− mice reveals a role for chemokines in the initiation of atherosclerosis. Nature 394:894–897.

Bozza PT, Magalhães KG, Weller PF (2009) Leukocyte lipid bodies - Biogenesis and functions in inflammation. Biochimica et biophysica acta 1791:540–551.

Bozza PT, Melo RCN, Bandeira-Melo C (2007) Leukocyte lipid bodies regulation and function: contribution to allergy and host defense. Pharmacology & therapeutics 113:30–49.

Brånén L, Hovgaard L, Nitulescu M, *et al.* (2004) Inhibition of Tumor Necrosis Factor-alpha reduces atherosclerosis in apolipoprotein E knockout mice. Arteriosclerosis, thrombosis, and vascular biology 24:2137–2142.

Brennan MLL, Anderson MMM, Shih DMM, *et al.* (2001) Increased atherosclerosis in myeloperoxidase-deficient mice. The Journal of clinical investigation 107:419–30.

Brochériou I, Maouche S, Durand H, *et al.* (2011) Antagonistic regulation of macrophage phenotype by M-CSF and GM-CSF: Implication in atherosclerosis. Atherosclerosis 214:316–324.

Brown MS, Ho YK, Goldstein JL (1980) The Cholesteryl Ester Cycle in Macrophage Foam Cells. The Journal of Biological Chemistry 255:9344–9352.

Buers I, Robenek H, Lorkowski S, *et al.* (2009) TIP47, a lipid cargo protein involved in macrophage triglyceride metabolism. Arteriosclerosis, thrombosis, and vascular biology 29:767–773.

Bulut Y, Faure E, Thomas L (2002) Chlamydial heat shock protein 60 activates macrophages and endothelial cells through Toll-like receptor 4 and MD2 in a MyD88-dependent pathway. The Journal of immunology 168:1435–1440.

Buono C, Li Y, Waldo SW, Kruth HS (2007) Liver X receptors inhibit human monocyte-derived macrophage foam cell formation by inhibiting fluid-phase pinocytosis of LDL. Journal of lipid research 48:2411–2418.

Burger PC, Wagner DD (2003) Platelet P-selectin facilitates atherosclerotic lesion development. Blood 101:2661–2666.

Cani PD, Amar J, Iglesias MA, *et al.* (2007) Metabolic endotoxemia initiates obesity and insulin resistance. Diabetes 56:1761–1772.

Cao F, Castrillo A, Tontonoz P, *et al.* (2007) Chlamydia pneumoniae-induced macrophage foam cell formation is mediated by Toll-like receptor 2. Infection and immunity 75:753–759.

Castrillo A, Joseph SB, Vaidya SA, *et al.* (2003) Crosstalk between LXR and Toll-like receptor signaling mediates bacterial and viral antagonism of cholesterol metabolism. Molecular cell 12:805–816.

Chang M-K, Binder CJ, Miller YI, *et al.* (2004) Apoptotic cells with oxidation-specific epitopes are immunogenic and proinflammatory. The Journal of experimental medicine 200:1359–70.

Chang M-K, Binder CJ, Torzewski M, Witztum JL (2002) C-reactive protein binds to both oxidized LDL and apoptotic cells through recognition of a common ligand: Phosphorylcholine of oxidized phospholipids. Proceedings of the National Academy of Sciences of the United States of America 99:13043–13048.

Chávez-Sánchez L, Madrid-Miller A, Chávez-Rueda K, *et al.* (2010) Activation of TLR2 and TLR4 by minimally modified low-density lipoprotein in human macrophages and monocytes triggers the inflammatory response. Human immunology 71:737–744.

Chawla A, Barak Y, Nagy L, *et al.* (2001a) PPAR-gamma dependent and independent effects on macrophage-gene expression in lipid metabolism and inflammation. Nature medicine 7:48–52.

Chawla A, Boisvert WA, Lee C-H, *et al.* (2001b) A PPAR gamma-LXR-ABCA1 pathway in macrophages is involved in cholesterol efflux and atherogenesis. Molecular cell 7:161–171.

Chen M, Li W, Wang N, *et al.* (2007) ROS and NF-kappa B but not LXR mediate IL-1 beta signaling for the downregulation of ATP-binding cassette transporter A1. American Journal of Physiology - Cell Physiology 292:1493–1501.

Chen S, Sorrentino R, Shimada K, *et al.* (2009) Chlamydia pneumoniae-induced foam cell formation requires Myd88 dependent and independent signaling and is reciprocally modulated by LXR activation. Journal of Immunology 181:7186–7193.

Chi H, Messas E, Levine RA, *et al.* (2004) Interleukin-1 receptor signaling mediates atherosclerosis associated with bacterial exposure and/or a high-fat diet in a murine apolipoprotein E heterozygote model: Pharmacotherapeutic implications. Circulation 110:1678–1685.

Chinetti G, Fruchart JC, Staels B (2006) Transcriptional regulation of macrophage cholesterol trafficking by PPAR-alpha and LXR. Biochemical Society transactions 34:1128–1131.

Chinetti G, Lestavel S, Fruchart J-C, *et al.* (2003) Peroxisome Proliferator-Activated Receptor alpha Reduces Cholesterol Esterification in Macrophages. Circulation Research 92:212–217.

Chinetti-Gbaguidi G, Staels B (2009) Lipid ligand-activated transcription factors regulating lipid storage and release in human macrophages. Biochimica et biophysica acta 1791:486–493.

Choi S-H, Harkewicz R, Lee JH, *et al.* (2009) Lipoprotein accumulation in macrophages via Toll-like receptor-4 - dependent fluid phase uptake. Circulation research 104:1355–1363.

Cignarella A (2011) Targeting interleukin-1 beta hampers atherosclerosis progression - Is there great promise? Atherosclerosis 217:64–66.

Collins RG, Velji R, Guevara NV, *et al.* (2000) P-Selectin or Intercellular Adhesion Molecule (ICAM)-1 deficiency substantially protects against atherosclerosis in apolipoprotein E-deficient mice. The Journal of experimental medicine 191:189–194.

Constantineau J, Greason E, West M, *et al.* (2010) A synonymous variant in scavenger receptor, class B, type I gene is associated with lower SR-BI protein expression and function. Atherosclerosis 210:177–182.

Corsini A, Bellosta S (2007) Farmaci ipolipemizzanti: metabolismo ed interazioni clinicamente rilevanti. Prevenzione & Terapia dell'Aterosclerosi 4:27–44.

D'Avila H, Maya-Monteiro CM, Bozza PT (2008) Lipid bodies in innate immune response to bacterial and parasite infections. International immunopharmacology 8:1308–1315.

D'Avila H, Melo RCN, Parreira GG, *et al.* (2006) Mycobacterium bovis Bacillus Calmette-Guerin induces TLR2-Mediated Formation of Lipid Bodies: Intracellular Domains for Eicosanoid Synthesis In Vivo. The Journal of Immunology 176:3087–3097.

Dalpke AH, Lehner MD, Hartung T, Heeg K (2005) Differential effects of CpG-DNA in Toll-like receptor-2/-4/-9 tolerance and cross-tolerance. Immunology 116:203–12.

Daniels TF, Killinger KM, Michal JJ, *et al.* (2009) Lipoproteins, cholesterol homeostasis and cardiac health. International journal of biological sciences 5:474–488.

Dansky HM, Barlow CB, Lominska C, *et al.* (2001) Adhesion of Monocytes to Arterial Endothelium and Initiation of Atherosclerosis Are Critically Dependent on Vascular Cell Adhesion Molecule-1 Gene Dosage. Arteriosclerosis, Thrombosis, and Vascular Biology 21:1662–1667.

Dasu MR, Devaraj S, Zhao L, *et al.* (2008) High Glucose Induces Toll-Like Receptor Expression in human monocytes - Mechanism of Activation. Diabetes 57:3090–3098.

Dasu MR, Park S, Devaraj S, Jialal I (2009) Pioglitazone inhibits Toll-like receptor expression and activity in human monocytes and db/db mice. Endocrinology 150:3457–3464.

Davies MJ, Gordon JL (1993) The expression of the adhesion molecules ICAM-1, VCAM-1, PECAM, and E-selectin in human atherosclerosis. The Journal of Pathology 171:223–229.

De Almeida MC, Silva AC, Barral A, Netto MB (2000) A Simple Method for Human Peripheral Blood Monocyte Isolation. Memórias do Instituto Oswaldo Cruz 95:221–223.

De la Llera-Moya M, Drazul-Schrader D, Asztalos BF, *et al.* (2010) The ability to promote efflux via ABCA1 determines the capacity of serum specimens with similar high-density lipoprotein cholesterol to remove cholesterol from macrophages. Arteriosclerosis, thrombosis, and vascular biology 30:796–801.

De Nardo D, Nguyen T, Hamilton JA, Scholz GM (2009) Down-regulation of IRAK-4 is a component of LPS- and CpG DNA-induced tolerance in macrophages. Cellular signalling 21:246–252.

De Souza LF, Jardim FR, Sauter IP, *et al.* (2008) High glucose increases RAW 264.7 macrophages activation by lipoteichoic acid from Staphylococcus aureus. Clinica chimica acta; international journal of clinical chemistry 398:130–133.

De Villiers WJ, Smart EJ (1999) Macrophage scavenger receptors and foam cell formation. Journal of leukocyte biology 66:740–746.

De Villiers WJS, Smith JD, Miyata M, *et al.* (1998) Macrophage Phenotype in Mice Deficient in Both Macrophage-Colony Stimulating Factor (Op) and Apolipoprotein E. Arteriosclerosis, Thrombosis, and Vascular Biology 18:631–640.

Den Dekker WK, Cheng C, Pasterkamp G, Duckers HJ (2010) Toll like receptor 4 in atherosclerosis and plaque destabilization. Atherosclerosis 209:314–320.

Den Hartigh LJ, Connolly-Rohrbach JE, Fore S, *et al.* (2010) Fatty acids from very low-density lipoprotein lipolysis products induce lipid droplet accumulation in human monocytes. Journal of Immunology 184:3927–3936.

Dennis EA, Deems RA, Harkewicz R, *et al.* (2010) A mouse macrophage lipidome. The Journal of biological chemistry 285:39976–39985.

Diaz G, Melis M, Batetta B, *et al.* (2008) Hydrophobic characterization of intracellular lipids in situ by Nile Red red/yellow emission ratio. Micron 39:819–824.

Dotan Y, Pinchuk I, Lichtenberg D, Leshno M (2009) Decision analysis supports the paradigm that indiscriminate supplementation of vitamin E does more harm than good. Arteriosclerosis, thrombosis, and vascular biology 29:1304–1309.

Drexler SK, Foxwell BM (2010) The role of Toll-like receptors in chronic inflammation. The International Journal of Biochemistry & Cell Biology 42:506–518.

Edfeldt K, Swedenborg J, Hansson GK, Yan Z (2002) Expression of Toll-like receptors in human atherosclerotic lesions: A possible pathway for plaque activation. Circulation 105:1158–1161.

Engelmann MG, Redl CV, Pelisek J, *et al.* (2006) Chronic perivascular inoculation with Chlamydophila pneumoniae results in plaque formation in vivo. Laboratory investigation 86:467–476.

Erridge C (2008) The Roles of Pathogen-Associated Molecular Patterns in Atherosclerosis. Trends in cardiovascular medicine 18:52–56.

Erridge C (2009) The Roles of Toll-Like Receptors in Atherosclerosis. Journal of Innate Immunity 1:340–349.

Erridge C (2010) Endogenous ligands of TLR2 and TLR4: agonists or assistants? Journal of leukocyte biology 87:989–999.

Erridge C, Attina T, Spickett CM, Webb DJ (2007) A high-fat meal induces low-grade endotoxemia: evidence of a novel mechanism of postprandial inflammation. The American journal of clinical nutrition 86:1286–1292.

Erridge C, Burdess A, Jackson AJ, *et al.* (2008a) Vascular cell responsiveness to Toll-like receptor ligands in carotid atheroma. European journal of clinical investigation 38:713–720.

Erridge C, Kennedy S, Spickett CM, Webb DJ (2008b) Oxidized phospholipid inhibition of Toll-like receptor (TLR) signaling is restricted to TLR2 and TLR4: Roles for CD14, LPS-binding protein, and MD2 as targets for specificity of inhibition. The Journal of biological chemistry 283:24748–24759.

Feingold KR, Grunfeld C (2010) The acute phase response inhibits reverse cholesterol transport. Journal of lipid research 51:682–684.

Feingold KR, Kazemi MR, Magra AL, *et al.* (2010) ADRP/ADFP and Mal1 expression are increased in macrophages treated with TLR agonists. Atherosclerosis 209:81–88.

Feng X, Zhang Y, Xu R, *et al.* (2010) Lipopolysaccharide up-regulates the expression of Fc alpha/mu receptor and promotes the binding of oxidized low-density lipoprotein and its IgM antibody complex to activated human macrophages. Atherosclerosis 208:396–405.

Ferreira V, van Dijk KW, Groen AK, *et al.* (2007) Macrophage-specific inhibition of NF-kappa B activation reduces foam-cell formation. Atherosclerosis 192:283–290.

Flegel WA, Baumstark MW, Weinstock C, *et al.* (1993) Prevention of endotoxin-induced monokine release by human low- and high-density lipoproteins and by apolipoprotein A-I. Infection and immunity 61:5140–5146.

Forcheron F, Legedz L, Chinetti G, *et al.* (2005) Genes of cholesterol metabolism in human atheroma: Overexpression of perilipin and genes promoting cholesterol storage and repression of ABCA1 expression. Arteriosclerosis, thrombosis, and vascular biology 25:1711–1717.

Fuchs B, Süss R, Teuber K, *et al.* (2011) Lipid analysis by thin-layer chromatography--a review of the current state. Journal of chromatography A 1218:2754–2774.

Fukumoto S, Fujimoto T (2002) Deformation of lipid droplets in fixed samples. Histochemistry and Cell Biology 118:423–428.

Funk JL, Feingold KR, Moser AH, Grunfeld C (1993) Lipopolysaccharide stimulation of RAW 264.7 macrophages induces lipid accumulation and foam cell formation. Atherosclerosis 98:67–82.

Geissmann F, Jung S, Littman DR (2003) Blood monocytes consist of two principal subsets with distinct migratory properties. Immunity 19:71–82.

Ghanim H, Sia CL, Upadhyay M, *et al.* (2010) Orange juice neutralizes the proinflammatory effect of a high-fat, high-carbohydrate meal and prevents endotoxin increase and Toll-like receptor expression. The American Journal of Clinical Nutrition 91:940–949.

Ghoshal S, Witta J, Zhong J, *et al.* (2009) Chylomicrons promote intestinal absorption of lipopolysaccharides. Journal of lipid research 50:90–97.

Glomset JA (1968) The plasma lecithins: cholesterol acyltransferase reaction. Journal of lipid research 9:155–167.

Goldstein JL, Ho YK, Basu SK, Brown MS (1979) Binding site on macrophages that mediates uptake and degradation of acetylated low density lipoprotein, producing massive cholesterol deposition. Proceedings of the National Academy of Sciences of the United States of America 76:333–337.

Gordon S, Taylor PR (2005) Monocyte and macrophage heterogeneity. Nature Reviews Immunology 5:953–964.

Gower RM, Wu H, Foster GA, *et al.* (2011) CD11c/CD18 expression is upregulated on blood monocytes during hypertriglyceridemia and enhances adhesion to Vascular Cell Adhesion Molecule-1. Arteriosclerosis, thrombosis, and vascular biology 31:160–166.

Greaves D., Channon KM (2002) Inflammation and immune responses in atherosclerosis. Trends in immunology 23:535–541.

Gu J-Q, Wang D-F, Yan X-G, *et al.* (2010) A Toll-like receptor 9-mediated pathway stimulates perilipin 3 (TIP47) expression and induces lipid accumulation in macrophages. American journal of physiology - Endocrinology and metabolism 299:E593–600.

Guilherme A, Virbasius JV, Puri V, Czech MP (2008) Adipocyte dysfunctions linking obesity to insulin resistance and type 2 diabetes. Nature reviews - Molecular cell biology 9:367–377.

Hajjar AM, Ernst RK, Tsai JH, *et al.* (2002) Human Toll-like receptor 4 recognizes host-specific LPS modifications. Nature immunology 3:354–359.

Haraguchi G, Kobayashi Y, Brown ML, *et al.* (2003) PPAR-alpha and PPAR-gamma activators suppress the monocyte-macrophage apoB-48 receptor. Journal of lipid research 44:1224–31.

Harte AL, Varma MC, Tripathi G, *et al.* (2012) High fat intake leads to acute postprandial exposure to circulating endotoxin in type 2 diabetic subjects. Diabetes care 35:375–382.

He P, Mei C, Cheng B, *et al.* (2009) Chlamydia pneumoniae induces macrophage-derived foam cell formation by up-regulating acyl-coenzyme A: cholesterol acyltransferase 1. Microbes and infection 11:157–163.

Hektoen L (1896) The vascular chages of tuberculous meningitis especially the tuberculous endarteritis. Journal of Experimental Medicine 1:112–163.

Henriksen T, Mahoney EM, Steinberg D (1981) Enhanced macrophage degradation of low density lipoprotein previously incubated with cultured endothelial cells: recognition by receptors for acetylated low density lipoproteins. Proceedings of the National Academy of Sciences of the United States of America 78:6499–6503.

Herieka M, Erridge C (2013) High-fat meal induced post-prandial inflammation. Molecular Nutrition & Food Research (in press).

Hodgkinson CP, Ye S (2003) Microarray analysis of peroxisome proliferator-activated receptor-gamma induced changes in gene expression in macrophages. Biochemical and Biophysical Research Communications 308:505–510.

Hoshino K, Takeuchi O, Kawai T, *et al.* (2010) Cutting edge: Toll-like receptor 4 (TLR4)-deficient mice are hyporesponsive to Lipopolysaccharide: Evidence for TLR4 as the Lps gene product. The Journal of Immunology 162:3749–3752.

Hsu H-Y, Twu Y-C (2000) Tumor Necrosis Factor-alpha -mediated protein kinases in regulation of scavenger receptor and foam cell formation on macrophage. The Journal of biological chemistry 275:41035–41048.

Hyson DA, Paglieroni TG, Wun T, Rutledge JC (2002) Postprandial lipemia is associated with platelet and monocyte activation and increased monocyte cytokine expression in normolipemic men. Clinical and applied trhombosis/hemostasis 8:147–155.

Ihendyane N, Sparrelid E, Wretlind B, *et al.* (2004) Viridans streptococcal septicaemia in neutropenic patients: Role of proinflammatory cytokines. Bone marrow transplantation 33:79–85.

Ishiyama J, Taguchi R, Yamamoto A, Murakami K (2010) Palmitic acid enhances lectin-like oxidized LDL receptor (LOX-1) expression and promotes uptake of oxidized LDL in macrophage cells. Atherosclerosis 209:118–124.

Jackson KG, Poppitt SD, Minihane AM (2012) Postprandial lipemia and cardiovascular disease risk: Interrelationships between dietary, physiological and genetic determinants. Atherosclerosis 220:22–33.

Ji A, Meyer JM, Cai L, *et al.* (2011) Scavenger receptor SR-BI in macrophage lipid metabolism. Atherosclerosis 217:106–112.

Jialal I, Devaraj S (1996) The Role of Oxidized Low Density Lipoprotein in atherogenesis. The journal of nutrition 126:1053–1057.

Kadl A, Meher AK, Sharma PR, *et al.* (2011) Identification of a novel macrophage phenotype that develops in response to atherogenic phospholipids via Nrf2. Circulation Research 107:737–746.

Kalayoglu MV, Byrne GI (1998) Induction of macrophage foam cell formation by Chlamydia pneumoniae. The Journal of infectious diseases 177:725–729.

Kawamoto T, Ii M, Kitazaki T, *et al.* (2008) TAK-242 selectively suppresses Toll-like receptor 4-signaling mediated by the intracellular domain. European journal of pharmacology 584:40–48.

Kazemi MR, McDonald CM, Shigenaga JK, *et al.* (2005) Adipocyte fatty acid-binding protein expression and lipid accumulation are increased during activation of murine macrophages by Toll-like receptor agonists. Arteriosclerosis, thrombosis, and vascular biology 25:1220–1224.

Keyel PA, Tkacheva OA, Larregina AT, Salter RD (2012) Coordinate stimulation of macrophages by microparticles and TLR ligands induces foam cell formation. Journal of Immunology 189:4621–4629.

Khera AV, Cuchel M, de la Llera-Moya M, *et al.* (2011) Cholesterol efflux capacity, high-density lipoprotein function, and atherosclerosis. The New England journal of medicine 364:127–135.

Khoo JC, Miller E, McLoughlin P, Steinberg D (1988) Enhanced macrophage uptake of low density lipoprotein after self- aggregation. Arteriosclerosis, Thrombosis, and Vascular Biology 8:348–358.

Khovidhunkit W, Moser AH, Shigenaga JK, *et al.* (2003) Endotoxin down-regulates ABCG5 and ABCG8 in mouse liver and ABCA1 and ABCG1 in J774 murine macrophages: differential role of LXR. Journal of lipid research 44:1728–1736.

Kiechl S, Egger G, Mayr M, *et al.* (2001) Chronic infections and the risk of carotid atherosclerosis: prospective results from a large population study. Circulation 103:1064–1070.

Kim J-S, Park D-W, Lee H-K, *et al.* (2009) Early growth response-1 is involved in foam cell formation and is upregulated by the TLR9-MyD88-ERK1/2 pathway. Biochemical and biophysical research communications 390:196–200.

Kindt TJ, Kuby J (2007) Kuby Immunology, 6th ed. W. H. Freeman & co.

Kirk EA, Dinauer MC, Rosen H, *et al.* (2000) Impaired Superoxide Production Due to a Deficiency in Phagocyte NADPH Oxidase Fails to Inhibit Atherosclerosis in Mice. Arteriosclerosis, Thrombosis, and Vascular Biology 20:1529–1535.

Kita T, Ishii K, Yokode M, *et al.* (1990) The role of oxidized low density lipoprotein in the pathogenesis of atherosclerosis. European heart journal 11 Suppl E:122–7.

Kleemann R, Zadelaar S, Kooistra T (2008) Cytokines and atherosclerosis: a comprehensive review of studies in mice. Cardiovascular research 79:360–376.

Kollipara RK, Perumal NB (2010) Motif prediction to distinguish LPS-stimulated pro-inflammatory vs. antibacterial macrophage genes. Immunome research 6:5–16.

Koren O, Spor A, Felin J, *et al.* (2011) Human oral, gut, and plaque microbiota in patients with atherosclerosis. Proceedings of the National Academy of Sciences of the United States of America 108 Suppl:4592–4598.

Kotzka J, Knebel B, Avci H, *et al.* (2010) Phosphorylation of sterol regulatory element-binding protein (SREBP)-1a links growth hormone action to lipid metabolism in hepatocytes. Atherosclerosis 213:156–165.

Kruth HS, Huang W, Ishii I, Zhang W-Y (2002) Macrophage foam cell formation with native low density lipoprotein. The Journal of biological chemistry 277:34573–34580.

Kuchibhotla S, Vanegas D, Kennedy DJ, *et al.* (2008) Absence of CD36 protects against atherosclerosis in ApoE knock-out mice with no additional protection provided by absence of scavenger receptor A I/II. Cardiovascular research 78:185–196.

Kumagai Y, Takeuchi O, Akira S (2008) TLR9 as a key receptor for the recognition of DNA. Advanced drug delivery reviews 60:795–804.

Kuo CC, Shor A, Campbell LA, *et al.* (1993) Demonstration of Chlamydia pneumoniae in atherosclerotic lesions of coronary arteries. The Journal of infectious diseases 167:841–849.

Kutuzova GD, Albrecht RM, Erickson CM, Qureshi N (2001) Diphosphoryl Lipid A from Rhodobacter sphaeroides blocks the binding and internalization of lipopolysaccharide in RAW264.7 cells. The Journal of Immunology 167:482–489.

Kuwahata S, Fujita S, Orihara K, *et al.* (2010) High expression level of Toll-like receptor 2 on monocytes is an important risk factor for arteriosclerotic disease. Atherosclerosis 209:248–254.

Laman JD, Schoneveld AH, Moll FL, *et al.* (2002) Significance of peptidoglycan, a proinflammatory bacterial antigen in atherosclerotic arteries and its association with vulnerable plaques. The American journal of cardiology 90:119–123.

Lammers B, Out R, Hildebrand RB, *et al.* (2009) Independent protective roles for macrophage Abcg1 and Apoe in the atherosclerotic lesion development. Atherosclerosis 205:420–426.

Larigauderie G, Cuaz-Pérolin C, Younes AB, *et al.* (2006) Adipophilin increases triglyceride storage in human macrophages by stimulation of biosynthesis and inhibition of beta-oxidation. The FEBS journal 273:3498–3510.

Larigauderie G, Furman C, Jaye M, *et al.* (2004) Adipophilin enhances lipid accumulation and prevents lipid efflux from THP-1 macrophages: potential role in atherogenesis. Arteriosclerosis, thrombosis, and vascular biology 24:504–510.

Le Brun AP, Clifton LA, Halbert CE, *et al.* (2013) Structural Characterization of a Model Gram-Negative Bacterial Surface Using Lipopolysaccharides from Rough Strains of Escherichia coli. Biomacromolecules 14:2014–2022.

Le Goff W, Dallinga-Thie GM (2011) ABCG1: not as good as expected? Atherosclerosis 219:393–394.

Lee J-G, Lim E-J, Park D-W, *et al.* (2008) A combination of Lox-1 and Nox1 regulates TLR9-mediated foam cell formation. Cellular signalling 20:2266–75.

Lee JY, Sohn KH, Rhee SH, Hwang D (2001) Saturated fatty acids, but not unsaturated fatty acids, induce the expression of cyclooxygenase-2 mediated through Toll-like receptor 4. The Journal of biological chemistry 276:16683–16689.

Lee S-H, Park D-W, Park SC, *et al.* (2009) Calcium-independent phospholipase A2 beta-Akt signaling is involved in lipopolysaccharide-induced NADPH oxidase 1 expression and foam cell formation. Journal of immunology (Baltimore, Md : 1950) 183:7497–7504.

Lehr H-A, Sagban TA, Ihling C, *et al.* (2001) Immunopathogenesis of Atherosclerosis: Endotoxin Accelerates Atherosclerosis in Rabbits on Hypercholesterolemic Diet. Circulation 104:914–920.

Ley K, Miller YI, Hedrick CC (2011) Monocyte and macrophage dynamics during atherogenesis. Arteriosclerosis, thrombosis, and vascular biology 31:1506–1516.

Li AC, Glass CK (2002) The macrophage foam cell as a target for therapeutic intervention. Nature medicine 8:1235–1242.

Libby P, Ridker PM, Maseri A (2002) Inflammation and Atherosclerosis. Circulation 105:1135–1143.

Lin E, Freedman JE, Beaulieu LM (2010) Innate immunity and Toll-like receptor antagonists: A potential role in the Treatment of Cardiovascular Diseases. Cardiovascular Therapy 27:117–123.

Liu C, Waters DD (2005) Chlamydia Pneumoniae and Atherosclerosis: From Koch Postulates to Clinical Trials. Progress in Cardiovascular Diseases 47:230–239.

Lockhart PB, Brennan MT, Sasser HC, *et al.* (2008) Bacteremia Associated With Toothbrushing and Dental Extraction. Circulation 117:3118–3125.

Lohmann KL, Vandenplas ML, Barton MH, *et al.* (2007) The equine TLR4/MD-2 complex mediates recognition of lipopolysaccharide from Rhodobacter sphaeroides as an agonist. Journal of endotoxin research 13:235–242.

Loppnow H, Libby P, Freudenberg M, *et al.* (1990) Cytokine induction by lipopolysaccharide (LPS) corresponds to lethal toxicity and is inhibited by nontoxic Rhodobacter capsulatus LPS. Infection and immunity 58:3743–3750.

Lorenz E, Patel DD, Hartung T, Schwartz DA (2002) Toll-Like Receptor 4 (TLR4) - Deficient Murine Macrophage Cell Line as an In Vitro Assay System To Show TLR4-Independent Signaling of Bacteroides fragilis Lipopolysaccharide. Infection and immunity 70:4892–4896.

Lu H, Daugherty A (2009) Atherosclerosis: cell biology and lipoproteins. Current Opinion in Lipidology 20:528–529.

Lundberg AM, Hansson GK (2010) Innate immune signals in atherosclerosis. Clinical immunology 134:5–24.

Lusis AJ (2000) Atherosclerosis. Nature 407:233–241.

Lynn WA, Golenbock DT (1992) Lipopolysaccharide antagonists. Immunology today 13:271–276.

Ma J, Chen T, Mandelin J, *et al.* (2003) Regulation of macrophage activation. Cellular and molecular life sciences 60:2334–2346.

Madan M, Amar S (2008) Toll-like receptor-2 mediates diet and/or pathogen associated atherosclerosis: proteomic findings. PloS one 3:e3204.

Maitra U, Parks JS, Li L (2009) An innate immunity signaling process suppresses macrophage ABCA1 expression through IRAK-1-mediated downregulation of retinoic acid receptor alpha and NFATc2. Molecular and cellular biology 29:5989–5997.

Manning-Tobin JJ, Moore KJ, Seimon TA, *et al.* (2009) Loss of SR-A and CD36 activity reduces atherosclerotic lesion complexity without abrogating foam cell formation in hyperlipidemic mice. Arteriosclerosis, thrombosis, and vascular biology 29:19–26.

Martin S, Parton RG (2006) Lipid droplets: a unified view of a dynamic organelle. Nature Reviews - Molecular Cell Biology 7:373–378.

Masuda D, Hirano K, Oku H, *et al.* (2009) Chylomicron remnants are increased in the postprandial state in CD36 deficiency. Journal of lipid research 50:999–1011.

Mattos KA, D'Avila H, Rodrigues LS, *et al.* (2010) Lipid droplet formation in leprosy: Toll-like receptor-regulated organelles involved in eicosanoid formation and Mycobacterium leprae pathogenesis. Journal of leukocyte biology 87:371–384.

Mayr M, Kiechl S, Willeit J, *et al.* (2000) Infections, Immunity, and Atherosclerosis : Associations of Antibodies to Chlamydia pneumoniae, Helicobacter pylori, and Cytomegalovirus With Immune Reactions to Heat-Shock Protein 60 and Carotid or Femoral Atherosclerosis. Circulation 102:833–839.

McGillicuddy FC, de la Llera Moya M, Hinkle CC, *et al.* (2009) Inflammation impairs reverse cholesterol transport in vivo. Circulation 119:1135–1145.

McNeill E, Channon KM, Greaves DR (2010) Inflammatory cell recruitment in cardiovascular disease: murine models and potential clinical applications. Clinical science 118:641–655.

Meadows JW, Pitzer B, Brockman DE, Myatt L (2005) Expression and localization of Adipophilin and Perilipin in human fetal membranes: Association with lipid bodies and enzymes involved in prostaglandin synthesis. The Journal of clinical endocrinology and metabolism 90:2344–2350.

Medzhitov R, Preston-Hurlburt P, Janeway CA (1997) A human homologue of the Drosophila Toll protein signals activation of adaptive immunity. Nature 388:6–9.

Meijer A, Roholl PJM, Gielis-Proper SK, *et al.* (2000) Chlamydia pneumoniae in vitro and in vivo : A critical evaluation of in situ detection methods. Journal of clinical pathology 53:904–910.

Methe H, Kim J-O, Kofler S, *et al.* (2005) Expansion of circulating Toll-like receptor 4-positive monocytes in patients with acute coronary syndrome. Circulation 111:2654–2661.

Michelsen KS, Doherty TM, Shah PK, Arditi M (2004a) TLR signaling: an emerging bridge from innate immunity to atherogenesis. The Journal of Immunology 173:5901–5907.

Michelsen KS, Wong MH, Shah PK, *et al.* (2004b) Lack of Toll-like receptor 4 or myeloid differentiation factor 88 reduces atherosclerosis and alters plaque phenotype in mice deficient in apolipoprotein E. Proceedings of the National Academy of Sciences of the United States of America 101:10679–10684.

Miller YI, Choi S-H, Wiesner P, *et al.* (2011) Oxidation-specific epitopes are danger-associated molecular patterns recognized by pattern recognition receptors of innate immunity. Circulation research 108:235–248.

Monaco C, Gregan SM, Navin TJ, *et al.* (2009) Toll-like receptor-2 mediates inflammation and matrix degradation in human atherosclerosis. Circulation 120:2462–2469.

Moore KJ, Kunjathoor VV, Koehn SL, *et al.* (2005) Loss of receptor-mediated lipid uptake via scavenger receptor A or CD36 pathways does not ameliorate atherosclerosis in hyperlipidemic mice. The Journal of clinical investigation 115:2192–2201.

Muhlestein JB, Anderson JL, Hammond EH, *et al.* (1998) Infection With Chlamydia pneumoniae Accelerates the Development of Atherosclerosis and Treatment With Azithromycin Prevents It in a Rabbit Model. Circulation 97:633–636.

Mullick AE, Tobias PS, Curtiss LK (2005) Modulation of atherosclerosis in mice by Toll-like receptor 2. The Journal of clinical investigation 115:3149–3156.

Nan X, Cheng J-X, Xie XS (2003) Vibrational imaging of lipid droplets in live fibroblast cells with coherent anti-Stokes Raman scattering microscopy. Journal of lipid research 44:2202–2208.

Ni Z, Zhao S, Wu Z (2007) ABCG1--a potential therapeutic target for atherosclerosis. Medical hypotheses 69:214–217.

Nicolaou G, Goodall AH, Erridge C (2012) Diverse bacteria promote macrophage foam cell formation via Toll-like receptor-dependent lipid body biosynthesis. Journal of atherosclerosis and thrombosis 19:137–148.

Oiknine J, Aviram M (1992) Increased susceptibility to activation and increased uptake of low density lipoprotein by cholesterol-loaded macrophages. Arteriosclerosis, thrombosis, and vascular biology 12:745–753.

Okazaki H, Igarashi M, Nishi M, *et al.* (2008) Identification of Neutral Cholesterol Ester hydrolase, a key enzyme removing cholesterol from macrophages. The Journal of biological chemistry 283:33357–33364.

Ott SJ, El Mokhtari NE, Musfeldt M, *et al.* (2006) Detection of diverse bacterial signatures in atherosclerotic lesions of patients with coronary heart disease. Circulation 113:929–937.

Pacheco P, Bozza FA, Gomes RN, *et al.* (2002) Lipopolysaccharide-induced leukocyte lipid body formation in vivo: Innate immunity elicited intracellular loci involved in eicosanoid metabolism. The Journal of Immunology 169:6498–6506.

Page TH, Smolinska M, Gillespie J, *et al.* (2009) Tyrosine kinases and inflammatory signalling. Current molecular medicine 9:69–85.

Pålsson-McDermott EM, O'Neill LAJ (2004) Signal transduction by the lipopolysaccharide receptor, Toll-like receptor-4. Immunology 113:153–162.

Parker TS, Levine DM, Chang JC, *et al.* (1995) Reconstituted high-density lipoprotein neutralizes Gram-negative bacterial lipopolysaccharides in human whole blood. Infection and immunity 63:253–258.

Pasterkamp G, van Keulen JK, de Kleijn DPV (2004) Role of Toll-like receptor 4 in the initiation and progression of atherosclerotic disease. European journal of Clinical Investigation 34:328–334.

Patole PS, Pawar RD, Lech M, *et al.* (2006) Expression and regulation of Toll-like receptors in lupus-like immune complex glomerulonephritis of MRL-Fas(lpr) mice. Nephrology, dialysis, transplantation 21:3062–3073.

Paul A, Chang B.-J, Li L, *et al.* (2008) Deficiency of Adipose Differentiation-Related Protein impairs foam cell formation and protects against atherosclerosis. Circulation research 102:1492–1501.

Perk J, De Backer G, Gohlke H, *et al.* (2012) European Guidelines on cardiovascular disease prevention in clinical practice (version 2012). European heart journal 33:1635–1701.

Persson J, Nilsson J, Lindholm MW (2008) Interleukin-1 beta and Tumour Necrosis Factor-alpha impede neutral lipid turnover in macrophage-derived foam cells. BMC immunology 9:70–80.

Picard C, von Bernuth H, Ghandil P, *et al.* (2010) Clinical features and outcome of patients with IRAK-4 and MyD88 deficiency. Medicine 89:403–425.

Poppitt SD, Keogh GF, Lithander FE, *et al.* (2008) Postprandial response of adiponectin, Interleukin-6, Tumor Necrosis Factor-alpha, and C-reactive protein to a high-fat dietary load. Nutrition 24:322–329.

Pussinen PJ, Tuomisto K, Jousilahti P, *et al.* (2007) Endotoxemia, immune response to periodontal pathogens, and systemic inflammation associate with incident cardiovascular disease events. Arteriosclerosis, thrombosis, and vascular biology 27:1433–1439.

Rahaman SO, Lennon DJ, Febbraio M, *et al.* (2006) A CD36-dependent signaling cascade is necessary for macrophage foam cell formation. Cell metabolism 4:211–221.

Rajavashisth T, Qiao JH, Tripathi S, *et al.* (1998) Heterozygous osteopetrotic (op) mutation reduces atherosclerosis in LDL receptor- deficient mice. The Journal of clinical investigation 101:2702–2710.

Randolph GJ (2008) Emigration of monocyte-derived cells to lymph nodes during resolution of inflammation and its failure in atherosclerosis. Current opinion in lipidology 19:462–468.

Renko J, Lepp PW, Oksala N, *et al.* (2008) Bacterial signatures in atherosclerotic lesions represent human commensals and pathogens. Atherosclerosis 201:192–197.

Ricardo SD, van Goor H, Eddy AA (2008) Macrophage diversity in renal injury and repair. The Journal of clinical investigation 118:3522–3530.

Rice JB, Stoll LL, Li W-G, *et al.* (2003) Low-level endotoxin induces potent inflammatory activation of human blood vessels: Inhibition by statins. Arteriosclerosis, thrombosis, and vascular biology 23:1576–1582.

Ridker PM, Danielson E, Fonseca FA, *et al.* (2009) Reduction in C-reactive protein and LDL cholesterol and cardiovascular event rates after initiation of rosuvastatin: A prospective study of the JUPITER trial. Lancet 373:1175–1182.

Rigamonti E, Chinetti-Gbaguidi G, Staels B (2008) Regulation of macrophage functions by PPAR-alpha, PPAR-gamma, and LXRs in mice and men. Arteriosclerosis, thrombosis, and vascular biology 28:1050–1059.

Robenek H, Hofnagel O, Buers I, *et al.* (2006) Adipophilin-enriched domains in the ER membrane are sites of lipid droplet biogenesis. Journal of cell science 119:4215–4224.

Rocha VZ, Libby P (2009) Obesity, inflammation, and atherosclerosis. Nature reviews Cardiology 6:399–409.

Rohde LE, Lee RT, Rivero J, *et al.* (1998) Circulating Cell Adhesion Molecules Are Correlated With Ultrasound-Based Assessment of Carotid Atherosclerosis. Arteriosclerosis, Thrombosis, and Vascular Biology 18:1765–1770.

Rose JR, Christ WJ, Bristol JR, *et al.* (1995) Agonistic and antagonistic activities of bacterially derived Rhodobacter sphaeroides Lipid A: comparison with activities of synthetic material of the proposed structure and analogs. Infection and immunity 63:833–839.

Rosenblat M, Volkova N, Roqueta-Rivera M, *et al.* (2010) Increased macrophage cholesterol biosynthesis and decreased cellular paraoxonase 2 (PON2) expression in Delta 6-desaturase knockout (6-DS KO) mice: beneficial effects of arachidonic acid. Atherosclerosis 210:414–421.

Saikku P, Leinonen M, Mattila K, *et al.* (1988) Serological evidence of an association of a novel Chlamydia, TWAR, with chronic coronary heart disease and acute myocardial infarction. Lancet 2:983–6.

Saitoh S, Akashi S, Yamada T, *et al.* (2004) Lipid A antagonist, lipid IVa, is distinct from lipid A in interaction with Toll-like receptor 4 (TLR4)-MD-2 and ligand-induced TLR4 oligomerization. International immunology 16:961–969.

Schmitz G, Grandl M (2009) Endolysosomal phospholipidosis and cytosolic lipid droplet storage and release in macrophages. Biochimica et biophysica acta 1791:524–539.

Schoneveld AH, Oude Nijhuis MM, van Middelaar B, *et al.* (2005) Toll-like receptor 2 stimulation induces intimal hyperplasia and atherosclerotic lesion development. Cardiovascular research 66:162–169.

Schoneveld AH, Oude Nijhuis MM, van Middelaar B, *et al.* (2008) Atherosclerotic lesion development and Toll like receptor 2 and 4 responsiveness. Atherosclerosis 197:95–104.

Schuh TJ (2002) An introduction to lipid analysis in the cell biology laboratory. The American biology teacher 64:122–129.

Segers D, Garcia-Garcia HM, Cheng C, *et al.* (2008) A primer on the immune system in the pathogenesis and treatment of atherosclerosis. EuroIntervention 4:378–390.

Sekiya M, Osuga J-I, Nagashima S, *et al.* (2009) Ablation of Neutral Cholesterol Ester hydrolase 1 accelerates atherosclerosis. Cell metabolism 10:219–228.

Serri O, Li L, Maingrette F, *et al.* (2004) Enhanced Lipoprotein Lipase Secretion and Foam Cell Formation by Macrophages of Patients with Growth Hormone Deficiency: Possible Contribution to Increased Risk of Atherogenesis? Journal of Clinical Endocrinology & Metabolism 89:979–985.

Shaw PX, Hörkkö S, Chang MK, *et al.* (2000) Natural antibodies with the T15 idiotype may act in atherosclerosis, apoptotic clearance, and protective immunity. The Journal of clinical investigation 105:1731–1740.

Sorrentino R, Morello S, Chen S, *et al.* (2010) The activation of Liver X Receptors inhibits Toll-like receptor-9-induced foam cell formation. Journal of cellular physiology 223:158–167.

Steinberg D (2005) The LDL modification hypothesis of atherogenesis: An update. Journal of lipid research 1–25.

Steinberg D, Witztum JL (2002) Is the Oxidative Modification Hypothesis Relevant to Human Atherosclerosis?: Do the Antioxidant Trials Conducted to Date Refute the Hypothesis? Circulation 105:2107–2111.

Steinbrecher UP, Parthasarathy S, Leake DS, *et al.* (1984) Modification of low density lipoprotein by endothelial cells involves lipid peroxidation and degradation of low density lipoprotein phospholipids. Proceedings of the National Academy of Sciences of the United States of America 81:3883–3887.

Stewart CR, Stuart LM, Wilkinson K, *et al.* (2010) CD36 ligands promote sterile inflammation through assembly of a Toll-like receptor 4 and 6 heterodimer. Nature immunology 11:155–161.

Sviridov D, Nestel P (2002) Dynamics of reverse cholesterol transport: protection against atherosclerosis. Atherosclerosis 161:245–254.

Tabas I (2010) Macrophage death and defective inflammation resolution in atherosclerosis. Nature reviews - Immunology 10:36–46.

Takashima K, Matsunaga N, Yoshimatsu M, *et al.* (2009) Analysis of binding site for the novel small-molecule TLR4 signal transduction inhibitor TAK-242 and its therapeutic effect on mouse sepsis model. British journal of pharmacology 157:1250–1262.

Takeuchi O, Hoshino K, Akira S (2000) Cutting edge: TLR2-deficient and MyD88-deficient mice are highly susceptible to Staphylococcus aureus infection. Journal of immunology 165:5392–5396.

Takeuchi O, Hoshino K, Kawai T, *et al.* (1999) Differential roles of TLR2 and TLR4 in recognition of Gram-negative and Gram-positive bacterial cell wall components. Immunity 11:443–451.

Takeuchi O, Kawai T, Mühlradt PF, *et al.* (2001) Discrimination of bacterial lipoproteins by Toll-like receptor 6. International immunology 13:933–940.

Tall AR, Yvan-Charvet L, Terasaka N, *et al.* (2008) HDL, ABC transporters, and cholesterol efflux: Implications for the treatment of atherosclerosis. Cell metabolism 7:365–375.

Tanigawa K, Suzuki K, Nakamura K, *et al.* (2008) Expression of adipose differentiation-related protein (ADRP) and perilipin in macrophages infected with Mycobacterium leprae. FEMS microbiology letters 289:72–79.

Tavian D, Colombo R (2007) Improved cytochemical method for detecting Jordans' bodies in neutral lipid storage diseases. Journal of clinical pathology 60:956–958.

Tobias PS, Curtiss LK (2007) Toll-like receptors in atherosclerosis. Biochemical Society transactions 35:1453–1455.

Tobias PS, Curtiss LK (2005) Paying the price for pathogen protection: Toll receptors in atherogenesis. Journal of lipid research 46:404–411.

Tsang AW, Oestergaard K, Myers JT, Swanson JA (2000) Altered membrane trafficking in activated bone marrow- derived macrophages. Journal of leukocyte biology 68:487–494.

Tsompanidi EM, Brinkmeier MS, Fotiadou EH, *et al.* (2010) HDL biogenesis and functions: Role of HDL quality and quantity in atherosclerosis. Atherosclerosis 208:3–9.

Van Deventer SJ, Büller HR, ten Cate JW, *et al.* (1990) Experimental endotoxemia in humans: Analysis of cytokine release and coagulation, fibrinolytic, and complement pathways. Blood 76:2520–2526.

Van Eck M, Pennings M, Hoekstra M, *et al.* (2005) Scavenger receptor BI and ATP-binding cassette transporter A1 in reverse cholesterol transport and atherosclerosis. Current opinion in lipidology 16:307–315.

Van Tits LJH, Stienstra R, van Lent PL, *et al.* (2011) Oxidized LDL enhances pro-inflammatory responses of alternatively activated M2 macrophages: A crucial role for Krüppel-like factor 2. Atherosclerosis 214:345–349.

Vaughan CJ, Murphy MB, Buckley BM (1996) Statins do more than just lower cholesterol. Lancet 348:1079–1082.

Verouti SN, Fragopoulou E, Karantonis HC, *et al.* (2011) PAF effects on MCP-1 and IL-6 secretion in U-937 monocytes in comparison with oxLDL and IL-1 beta effects. Atherosclerosis 219:519–525.

Vikatmaa P, Lajunen T, Ikonen TS, *et al.* (2009) Chlamydial lipopolysaccharide (cLPS) is present in atherosclerotic and aneurysmal arterial wall- cLPS levels depend on disease manifestation. Cardiovascular pathology 19:48–54.

Voight BF, Peloso GM, Orho-Melander M, *et al.* (2012) Experimental and natural infections in MyD88- and IRAK-4-deficient mice and humans. Lancet 380:572–580.

Von Bernuth H, Picard C, Puel A, Casanova J-L (2012) Experimental and natural infections in MyD88- and IRAK-4-deficient mice and humans. European journal of immunology 42:3126–3135.

Von Hodenberg E, Khoo JC, Jensen D, *et al.* (2010) Mobilization of stored triglycerides from macrophages as free fatty acids. Arteriosclerosis 4:630–635.

Vreugdenhil AC, Snoek AM, van 't Veer C, *et al.* (2001) LPS-binding protein circulates in association with apoB-containing lipoproteins and enhances endotoxin-LDL/VLDL interaction. The Journal of clinical investigation 107:225–234.

Wan H-C, Melo RCN, Jin Z, *et al.* (2007) Roles and origins of leukocyte lipid bodies: proteomic and ultrastructural studies. FASEB journal 21:167–178.

Wang X, Reape TJ, Li X, *et al.* (1999) Induced expression of adipophilin mRNA in human macrophages stimulated with oxidized low-density lipoprotein and in atherosclerotic lesions. FEBS letters 462:145–150.

Wang X, Sato R, Brown MS, *et al.* (1994) SREBP-1, a membrane-bound transcription factor released by sterol-regulated proteolysis. Cell 77:53–62.

Wang Z, Klipfell E, Bennett BJ, *et al.* (2011) Gut flora metabolism of phosphatidylcholine promotes cardiovascular disease. Nature 472:57–63.

Watson AD, Leitinger N, Navab M, *et al.* (1997) Structural identification by mass spectrometry of oxidized phospholipids in minimally oxidized low density lipoprotein that induce monocyte/endothelial interactions and evidence for their presence in vivo. The Journal of biological chemistry 272:13597–13607.

Weischenfeldt J, Porse B (2008) Bone Marrow-Derived Macrophages (BMM): Isolation and Applications. Cold Spring Harbor Protocols.

Westerterp M, Berbée JFP, Pires NMM, *et al.* (2007) Apolipoprotein C-I is crucially involved in lipopolysaccharide-induced atherosclerosis development in apolipoprotein E-knockout mice. Circulation 116:2173–2181.

Wiedermann CJ, Kiechl S, Dunzendorfer S, *et al.* (1999) Association of endotoxemia with carotid atherosclerosis and cardiovascular disease: Prospective results from the Bruneck Study. Journal of the American College of Cardiology 34:1975–1981.

Wiesner P, Choi S-H, Almazan F, *et al.* (2010) Low doses of lipopolysaccharide and minimally oxidized low-density lipoprotein cooperatively activate macrophages via Nuclear Factor-kappa B and activator protein-1. Circulation research 107:56–65.

Witztum JL, Steinberg D (1991) Role of Oxidized Low Density Lipoprotein in atherogenesis. The Journal of clinical investigation 88:1785–1792.

Wolins NE, Quaynor BK, Skinner JR, *et al.* (2005) S3-12, Adipophilin, and TIP47 package lipid in adipocytes. The Journal of biological chemistry 280:19146–19155.

Wong HR, Odoms K, Sakthivel B (2008) Divergence of canonical danger signals: The genome-level expression patterns of human mononuclear cells subjected to heat shock or lipopolysaccharide. BMC immunology 9:24–41.

Wright SD, Burton C, Hernandez M, *et al.* (2000) Infectious agents are not necessary for murine atherogenesis. The Journal of experimental medicine 191:1437–1442.

Xu S, Huang Y, Xie Y, *et al.* (2010) Evaluation of foam cell formation in cultured macrophages: an improved method with Oil Red O staining and DiI-oxLDL uptake. Cytotechnology 62:473–481.

Xu XH, Shah PK, Faure E, Equils O (2001) Toll-like receptor-4 is expressed by macrophages in murine and human lipid-rich atherosclerotic plaques and upregulated by oxidized LDL. Circulation 104:3103–3108.

Xue J, Yuan Z, Wu Y, *et al.* (2010) High glucose promotes intracellular lipid accumulation in vascular smooth muscle cells by impairing cholesterol influx and efflux balance. Cardiovascular research 86:141–150.

Yang IA, Holloway JW, Ye S (2003) TLR4 Asp299Gly polymorphism is not associated with coronary artery stenosis. Atherosclerosis 170:187–190.

Ye Q, Chen Y, Lei H, *et al.* (2009) Inflammatory stress increases unmodified LDL uptake via LDL receptor: An alternative pathway for macrophage foam-cell formation. Inflammation research 58:809–818.

Yu W-H, Hu H, Zhou Q, *et al.* (2010) Bioinformatics analysis of macrophages exposed to Porphyromonas gingivalis: Implications in acute vs. chronic infections. PloS one 5:e15613.

Yuan X-M, Osman E, Miah S, *et al.* (2010) P53 Expression in Human Carotid Atheroma Is Significantly Related To Plaque Instability and Clinical Manifestations. Atherosclerosis 210:392–399.

Yuasa-Kawase M, Masuda D, Yamashita T, *et al.* (2012) Patients with CD36 Deficiency Are Associated with Enhanced Atherosclerotic Cardiovascular Diseases. Journal of atherosclerosis and thrombosis 19:263–275.

Yvan-Charvet L, Wang N, Tall AR (2010) Role of HDL, ABCA1, and ABCG1 transporters in cholesterol efflux and immune responses. Arteriosclerosis, thrombosis, and vascular biology 30:139–143.

Zhou M, Wu R, Dong W, *et al.* (2008) Endotoxin downregulates peroxisome proliferator-activated receptor-gamma via the increase in TNF-alpha release. American journal of physiology Regulatory, integrative and comparative physiology 294:84–92.

WEBSITES

http://www.who.int/mediacentre/factsheets/fs317/en/index.html

http://en.wikipedia.org/wiki/Atherosclerosis

http://www.framinghamheartstudy.org

http://www.cellsignal.com

http://www.cellsignal.com/products/4139.html

http://www.ohsu.edu/xd/health/services/doernbecher/research-education/research/research-labs/steiner-lab-current-projects.cfm

http://www.ej2hosting.com/gilmarcomuniones.es/cholesterol-esterification

http://pathmicro.med.sc.edu/pcr/realtime-home.htm

http://www.rndsystems.com/product_detail_objectname_quantikineelisaassayprinciple.aspx